Imperial College London

VALUE OF ENERGY STORAGE COORDINATION: MANAGING RENEWABLES UNCERTAINTY AND THE MAXIMIZATION OF PROFITABILITY

A thesis submitted to
Imperial College London
for the degree of Doctor of Philosophy

by

TIAGO ANDRÉ DA MOTA JESUS RODRIGUES

Control & Power Group
Department of Electrical and Electronic Engineering
Imperial College London

May 2018

© Tiago Rodrigues, 2018

Declaration of Originality

I hereby declare that the work developed in this thesis is entirely based on my own research and that, to the best of my knowledge and belief, it contains no material published or written by another person. The ideas, work and any diagrams or visuals developed by other writers is duly referenced and acknowledged in every instance. I also certify that this thesis was not and will not be submitted to any other university or institution for the purpose of fulfilling another degree.

Tiago Rodrigues

The copyright of this thesis rests with the author and is made available under a Creative Commons Attribution Non-Commercial No Derivatives licence. Researchers are free to copy, distribute or transmit the thesis on the condition that they attribute it, that they do not use it for commercial purposes and that they do not alter, transform or build upon it. For any reuse or redistribution, researchers must make clear to others the licence terms of this work.

London, United Kingdom, May 2018

Abstract

Aggressive carbon emissions reduction targets in electricity industry lead to the large-scale penetration of intermittent renewables. Renewables' uncertain and volatile nature, however, negatively impacts power systems operation by increasing the need for larger volumes of operating reserve and flexible, ideally carbon-free, generation technologies for ensuring a cost-effective operation. Energy storage systems are widely agreed to be the key for integrating renewables due to their flexibly and quick response. However, poor regulation and lack of long-term economic incentives have lead to a slow deployment of this technology.

This research analyses and models how renewable generation and energy storage coordination create value by managing uncertainty and maximizing profitability. A novel large-scale two-stage stochastic mixed-integer linear programming investment and operational model is proposed. The model allows considering different levels of risk aversion for a renewable producer that looks to determine the optimal size of an energy storage system and bidding strategy to maximize profit. Profit maximization is achieved by managing renewable generation imbalances and by offering ancillary services. In order to minimize the renewable operator's exposure to low profit outcomes, the Conditional Value-at-Risk of the expected profit is included in the problem's formulation. Computational tractability and efficiency is achieved by using the Progressive Hedging Algorithm decomposition technique to decompose the large-scale investment problem into smaller, easier to solve and scenario-specific sub-problems.

A series of case studies not only provide evidence of the significant benefits that energy storage system brings to a risk-averse renewables' operator, but also shows how energy storage allows storing cheap energy that otherwise would need to be curtailed to improve ancillary services provision.

Finally, the developed models can be of help for market participants to make more informed decisions, and also provides regulators and system operators with flexible solutions to mitigate the operational challenges of future low-carbon power systems.

List of Publications

The ideas and/or figures presented in this Thesis have appeared in the following publications:

JOURNAL PAPERS

1. T. Rodrigues, P. J. Ramírez and G. Strbac, "Risk-averse bidding of energy and spinning reserve by wind farms with on-site energy storage," in IET Renewable Power Generation, vol. 12, no. 2, pp. 165-173, 2018.

CONFERENCE PAPERS

1. T. Rodrigues, P. Ramírez, G. Strbac, "The Value of Storage for a Wind Farm Offering Energy and Spinning Reserve", *5th IET International Conference on Renewable Power Generation (RPG) 2016*, London, 2016, pp. 1-6.

2. T. Rodrigues, R. Moreira, G. Strbac, "Coordinated Operation of Distributed Energy Storage in Low Carbon Networks", *2017 IEEE Power and Energy Society General Meeting (PESGM)*, Chicago, IL, 2017, pp. 1-5.

Acknowledgements

After an intensive period of 4 years of both professional and personal development, I would like to reflect on the people whose contributions helped shape this Doctorate and making these 4 years a reality.

Firstly, I would like to appreciate not only the unwavering support, motivation, guidance and expertise my supervisor, Professor Goran Strbac, provided during the completion of this research but also the challenges and brilliant ideas he presented me in order for me to succeed in this endeavour. It is, without a doubt, an immense privilege to work and learn under him. A special thanks also needs to go to Professor Vladimiro Miranda at INESC TEC for the opportunity he provided for me to meet Professor Strbac.

My sincere gratitude and admiration for Dr. Pedro Ramírez and Dr. Roberto Moreira for all the supervision, companionship and friendship throughout these 4 years. No amount of words can be used to express the impact that they had on my life and their expertise in solving the challenges of this research. My life going forward wouldn't the same if I hadn't met them.

I would like to thank my examiners, Professor David Angeli and Professor Aleksandar Mijatović, for providing an interesting and productive critique of this work during my viva examination and for their valuable contributions for improving this Thesis.

I would also like to extend my thanks to everyone from the Control and Power research group for the support, great moments and for enriching my cultural experience. A special mention to Alex, Ankur, Antonio, Bulat, Efstratios, George, Giuseppe, Himadri, Hossein, Inma, Javier, Muhammad Ali and Vincenzo for all the laughs and thoughtful discussions.

I would like to express my deepest gratitude to Miguel, Sam, João, Patrícia, Marcos, Tam, Rafael and Diana for easing my move to the UK and making me feel at home away from home. I would also like to thank my great friends Afonso, Carlos, João, Jorge, Ricardo and Tiago for their support, friendship and the great moments we shared in Porto.

My special thanks to my father and mother their unending love and encouragement for me to pursue my dreams, to my brother and his girlfriend for their ever present companionship and support despite the distance. I would also like to thank the rest of my family for their love.

There are no amount of words that I could use to thank the person who supported me the most and gave me the strength and confidence to face the biggest challenge in my life. From the bottom of my heart, thank your for all your patience and support in the most difficult part of my life. You'll always be the sun and centre of the universe in my life, I love you Joana!

Lastly, I thank every person who helped shape me into the person I am now, all of whom are still with me, those who unfortunately are not and those whose work and philosophies influenced me the most.

"Will we ever know what the answer to life really is?
Can you really tell me what life is?
Maybe all the things that you know that are precious to you,
Could be swept away by fate's own hand."

Iron Maiden

Contents

Abstract 5

List of Publications 7

Acknowledgements 9

List of Figures 21

List of Tables 23

Acronyms & Abbreviations 25

1 Introduction 27
- 1.1 The Impacts of Renewable Generation Integration . . . 27
- 1.2 Motivation and Research Questions . . . 28
  - 1.2.1 The case for Coordinating ESS . . . 28
  - 1.2.2 Research Questions . . . 29
- 1.3 Proposed Research Scope and Methodologies . . . 31
  - 1.3.1 Research Proposal and Scope . . . 31
  - 1.3.2 Methodologies . . . 32
- 1.4 Summary of Research Contributions . . . 32
- 1.5 Thesis Structure . . . 33

2 Deterministic Business Models for Energy Storage Systems 35
- 2.1 Nomenclature . . . 35
  - 2.1.1 Indices, Sets and Sub-Sets . . . 35
  - 2.1.2 Parameters . . . 35
  - 2.1.3 Binary Variables . . . 36
  - 2.1.4 Continuous Variables . . . 36
- 2.2 Introduction . . . 37
  - 2.2.1 Literature Review . . . 37
  - 2.2.2 An ESS Business Model . . . 37
- 2.3 Mathematical Formulation . . . 38
  - 2.3.1 Key properties and assumptions . . . 38
  - 2.3.2 Objective function . . . 39

2.3.3 Model Constraints . . . 39
2.3.3.1 Energy market operation . . . 39
2.3.3.2 AS market operation . . . 40
2.3.3.3 Energy and Balancing Services Bids . . . 41
2.3.3.4 Variables types . . . 42
2.4 Case Studies . . . 42
2.4.1 Input Data . . . 42
2.4.2 Value of providing ancillary services . . . 44
2.4.3 Performance against uncertainty . . . 46
2.5 Chapter Conclusions . . . 48

3 Risk-Neutral Wind Generation and Energy Storage Coordination Strategies 49
3.1 Wind-ESS Model Nomenclature . . . 49
3.1.1 Indices, Sets and Sub-Sets . . . 49
3.1.2 Parameters . . . 50
3.1.3 Binary Variables . . . 50
3.1.4 Continuous Variables . . . 50
3.2 Wind-PHSP Model Nomenclature . . . 51
3.2.1 Indices, Sets and Sub-Sets . . . 51
3.2.2 Parameters . . . 52
3.2.3 Binary Variables . . . 52
3.2.4 Integer Variables . . . 53
3.2.5 Continuous Variables . . . 53
3.3 Introduction . . . 54
3.3.1 Literature Review . . . 54
3.3.2 Joint Energy and SPR Bidding Strategies for WF and ESS . . . 55
3.4 Stochastic Wind and Generic ESS Model . . . 57
3.4.1 Key Properties and Assumptions . . . 57
3.4.2 Objective Function . . . 57
3.4.2.1 Non-Linear Objective Function . . . 57
3.4.2.2 Linearisation of Absolute Value Functions . . . 58
3.4.3 Model Constraints . . . 59
3.4.3.1 Generation and Energy Limits . . . 59
3.4.3.2 SPR Provision . . . 59
3.4.3.3 Service Deliverability Constraints . . . 60
3.4.3.4 Bid Limits . . . 61
3.4.3.5 Variable Types . . . 61
3.5 Wind and PHSP Model . . . 62
3.5.1 Key Properties and Assumptions . . . 62
3.5.2 Objective Function . . . 62
3.5.2.1 Non-Linear Objective Function . . . 62
3.5.2.2 Tight Reformulation for absolute value function linearisation . . . 63
3.5.3 Model Constraints . . . 64

3.5.3.1 Reservoir Constraints . . . 64
3.5.3.2 Operating Mode State Equations . . . 65
3.5.3.3 Operational Limits . . . 65
3.5.3.4 Wind Power and Reserve Limits . . . 66
3.5.3.5 Service Deliverability Constraints . . . 66
3.5.3.6 Bid Limits . . . 68
3.5.3.7 Other Bounds . . . 68
3.5.3.8 Variables Type and Sign Constrains . . . 68
3.6 The Value of an ESS for a WF . . . 68
3.6.1 Input data . . . 68
3.6.2 The benefit of WF-ESS coordination . . . 69
3.6.3 Impact of WF-ESS coordination on generation uncertainty . . . 71
3.7 Joint Bidding Strategies for Combined WF and PHSP . . . 73
3.7.1 Input data . . . 74
3.7.1.1 WF and PHSP Parameters . . . 74
3.7.1.2 Day-ahead Wind Power Availability and Price Forecasts . . . 74
3.7.2 The value of PHSP for enhancing the offering of a WF . . . 75
3.7.2.1 Day 1 . . . 75
3.7.2.2 Day 2 . . . 77
3.7.3 Impact of SU and SD Costs on Energy and SPR Provision . . . 78
3.7.3.1 Omission of the SU and SD Costs for SPR Provision . . . 78
3.7.3.2 Fixed-speed vs Variable-speed Pump-turbine units . . . 79
3.7.4 Constrained Wind Energy Use . . . 81
3.7.4.1 Case A . . . 81
3.7.4.2 Case B . . . 82
3.7.5 Influence of WF and PHSP Capacities on the JBS Benefit . . . 82
3.7.6 Assessment of the Computational Performance . . . 83
3.8 Chapter Conclusions . . . 84

4 Risk-Averse Coordination Strategies 87
4.1 Nomenclature . . . 87
4.1.1 Indices, Sets and Sub-Sets . . . 87
4.1.2 Parameters . . . 88
4.1.3 Continuous Variables . . . 88
4.2 Introduction . . . 88
4.2.1 Literature Review . . . 88
4.2.2 Risk-averse Joint Bidding Strategies for WF and ESS . . . 89
4.3 Risk-averse JBS Model . . . 90
4.3.1 Key Properties and Assumptions . . . 90
4.3.2 CVaR measure . . . 91
4.3.3 Objective Function and Additional Constraints . . . 92
4.4 Case Studies . . . 93
4.4.1 Expected Profit Risk Management . . . 93

4.4.1.1 Day 1 . . . 93
4.4.1.2 Day 2 . . . 94
4.4.1.3 Day 3 . . . 96
4.4.2 The impact of risk aversion on the management of imbalances . . . 97
4.5 Chapter Conclusions . . . 99

5 Energy Storage Investment for Risk-averse Wind Farm Operators 101
5.1 Nomenclature . . . 102
5.1.1 Indices, Sets and Sub-Sets . . . 102
5.1.2 Parameters . . . 102
5.1.3 Binary Variables . . . 103
5.1.4 Continuous Variables . . . 103
5.1.4.1 First-Stage Variables . . . 103
5.1.4.2 Second-Stage Variables . . . 103
5.1.5 Parameters and Auxiliary Variables for the Progressive Hedging Algorithm . . . 104
5.2 Introduction . . . 105
5.2.1 Literature Review . . . 105
5.2.2 Risk-averse Investment in ESS . . . 107
5.3 Risk-averse ESS Investment Problem . . . 108
5.3.1 Key Properties and Assumptions . . . 108
5.3.2 Objective Function . . . 108
5.3.3 Model Constraints . . . 111
5.3.3.1 Generation and Energy Limits . . . 111
5.3.3.2 Provision of SPR and FR Services . . . 111
5.3.3.3 SPR Service Deliverability Constraints . . . 112
5.3.3.4 FR Service Deliverability Constraints . . . 113
5.3.3.5 Bid Limits . . . 114
5.3.3.6 Sized ESS Parameters' Limits . . . 115
5.3.3.7 Variable Types . . . 115
5.4 Achieving Computational Tractability . . . 115
5.4.1 Representative weeks . . . 115
5.4.1.1 Objective Function with Representative Weeks . . . 116
5.4.1.2 Model Constraints with Representative Weeks . . . 116
5.4.2 Decomposition Techniques – Progressive Hedging Algorithm . . . 117
5.4.2.1 Implementation of the PHA . . . 118
5.4.2.2 Choice of Penalty factors $\lambda_{d,h}^{(.)(i)}$, $\lambda^{K,P/E(i)}$ and $\lambda^{\zeta,(.)(i)}$ . . . 120
5.4.2.3 Convergence Criteria . . . 121
5.4.2.4 Other Approximations . . . 121
5.4.2.5 Algorithm and Parallel Computing Implementation . . . 122
5.5 Performance assessment of the PHA against Stochastic Models . . . 124
5.5.1 Input Data . . . 124
5.5.2 15 Scenarios . . . 126
5.5.3 30 Scenarios . . . 128

5.5.4 270 Scenarios . . . 129
5.6 Profitability of ESS investments . . . 131
5.6.1 270 Scenarios Performance Test . . . 131
5.6.2 Impact of larger capacities and higher investment costs . . . 132
5.7 Chapter Conclusions . . . 134

6 Coordinated Residential Energy Trading and Service Provision 135
6.1 Nomenclature . . . 135
6.1.1 Indices, Sets and Sub-Sets . . . 135
6.1.2 Parameters . . . 135
6.1.3 Binary Variables . . . 136
6.1.4 Continuous Variables . . . 136
6.2 Introduction . . . 137
6.2.1 Literature Review . . . 137
6.2.2 Coordinated P2P Energy Trading and Services Provision . . . 138
6.3 Coordinated Storage Operation in Low Carbon Communities . . . 139
6.3.1 Key Properties and Assumptions . . . 139
6.3.2 Objective Function . . . 139
6.3.3 Household Constraints . . . 139
6.3.4 ESS Operational Constraints . . . 140
6.3.5 Services Constraints . . . 141
6.3.6 Network Constraints . . . 142
6.4 Case Studies . . . 142
6.4.1 Input Data for UK studies . . . 142
6.4.2 The Value of Coordinating Residential ESS Operation . . . 144
6.4.3 Influence of different PV and ESS Penetration levels . . . 145
6.5 Chapter Conclusions . . . 146

7 Conclusion and Future Work 147
7.1 Conclusions . . . 147
7.1.1 Response to the research questions . . . 148
7.1.2 Contributions of this research . . . 153
7.2 Future Work . . . 154
7.2.1 Impact of a risk-averse WF-ESS participant in market outcomes . . . 154
7.2.2 Optimize the participation of a risk-averse WF-ESS operator in the energy and AS markets considering competition from other strategic WF-ESS participants . . . 155
7.2.3 The maximization of the benefit of the ESS for a WF that participates in intra-day trading . . . 155
7.2.4 Decentralized approach to the coordinated residential energy trading and service provision strategy . . . 155

Bibliography 169

Appendix A Assessment Model for Deterministic Bids **171**
A.1 Nomenclature . . . 171
A.1.1 Indices, Sets and Sub-Sets . . . 171
A.1.2 Parameters . . . 171
A.1.3 Binary Variables . . . 172
A.1.4 Continuous Variables . . . 172
A.2 Mathematical Formulation . . . 173
A.2.1 Keys properties and assumptions . . . 173
A.2.2 Objective function . . . 174
A.2.3 Model Constraints . . . 174
A.2.3.1 Energy and AS market operation . . . 174
A.2.3.2 Energy and AS Bids . . . 176
A.2.3.3 Variables types . . . 176

Appendix B Full List of Expressions used in the Progressive Hedging Algorithm **177**
B.1 Aggregation of Decision Variables . . . 177
B.2 Calculation of Lagrange multipliers . . . 178
B.3 Choice of Penalty factors $\lambda_{d,h}^{(.)(i)}$, $\lambda^{K,P/E(i)}$ and $\lambda^{\zeta,(.)(i)}$ . . . 179
B.4 Stopping Criteria . . . 180
B.5 Piecewise Linear Approximation for the Square Proximal Term . . . 180
B.5.1 Day-ahead bids . . . 180
B.5.2 Power and Energy Capacities of the ESS . . . 181
B.5.3 Profit VaR . . . 182

Appendix C Pricing and Wind Power Availability Scenarios for Case Studies in Chapter 5 **185**
C.1 Energy Price Forecasts . . . 186
C.2 SPR Price Forecasts . . . 187
C.3 FR Price Forecasts . . . 188
C.4 Wind Power Availability Forecasts . . . 189
C.4.1 5 Forecasts . . . 189
C.4.2 10 Forecasts . . . 190

List of Figures

2.1 Different services that ESS can provide to the several sectors of the energy system [1]. . 38
2.2 Day-ahead wind power availability forecasts for all days. 43
2.3 Day-ahead energy and AS market prices. 43
2.4 Expected energy profits for the three days for the ESS (left) and the WF (right). 44
2.5 Expected energy and AS profits for the three days for the ESS (left) and the WF (right). . 44
2.6 Deterministic day-ahead energy and AS bids for the ESS (left) and the WF (right). 45
2.7 Stored energy levels for the scheduled operation during the 3 days. 46
2.8 ESS profit distribution when exposed to uncertainty for all days. 47
2.9 WF profit distribution when exposed to uncertainty for all days. 47

3.1 Graphical representation of the difference between the Uncoordinated (red) and the Joint (blue) Bidding Strategies. 56
3.2 Reduction of the solution space for the positive energy imbalances due to the proposed tight formulation. 63
3.3 Summary of benefit of the JBS in expected profits and imbalance costs over the stochastic UBS and deterministic UBS. 70
3.4 Resulting bids for the EN-SPR Sto.UBS for all days. 70
3.5 Resulting bids for the EN-SPR JBS for all days. 71
3.6 Comparison of the injected power (black dots) and energy bid (red line) for all scenarios of the Sto.UBS (up) and the JBS (down) for day 1. 72
3.7 Comparison of the injected power (black dots) and energy bid (red line) for all scenarios of the Sto.UBS (up) and the JBS (down) for day 2. 72
3.8 Comparison of the injected power (black dots) and energy bid (red line) for all scenarios of the Sto.UBS (up) and the JBS (down) for day 3. 73
3.9 Day-ahead wind generation and energy price scenarios for both days. 74
3.10 Benefits of the JBS in expected profit and imbalance costs for Day 1. 76
3.11 Resulting bids for the EN-SPR bidding strategies for Day 1. 76
3.12 Benefits of the JBS in expected profit and imbalance costs for Day 2. 77
3.13 Resulting bids for the EN-SPR bidding strategies for Day 2. 78
3.14 Relative profit increase achieved with the JBS for EN (left) and for the EN-SPR (right) bidding strategies. 83
3.15 Execution time comparison for different number of scenarios and formulations. 84

4.1 VaR and CVaR for a day-ahead WF profit distribution. 91

4.2 Risk-neutral (left) and risk-averse (right) total profit distributions for the UBS (top) and the JBS (bottom) for day 1. . . . 94
4.3 Comparison of CVaR, expected profit and STD for the UBS (red) and the JBS (blue) for day 1 (a) Efficient frontier, (b) Profit STD. . . . 94
4.4 Risk-neutral (left) and risk-averse (right) total profit distributions for the UBS (top) and the JBS (bottom) for day 2. . . . 95
4.5 Comparison of CVaR, expected profit and STD for the UBS (red) and the JBS (blue) for day 2 (a) Efficient frontier, (b) Profit STD. . . . 95
4.6 Risk-neutral (left) and risk-averse (right) total profit distributions for the UBS (top) and the JBS (bottom) for day 3. . . . 96
4.7 Comparison of CVaR, expected profit and STD for the UBS (red) and the JBS (blue) for day 3 (a) Efficient frontier, (b) Profit STD. . . . 97
4.8 Comparison of the injected power (black dots) and energy bid (red line) for all scenarios of the risk-averse UBS (up) and the JBS (down) for day 1. . . . 98
4.9 Comparison of the injected power (black dots) and energy bid (red line) for all scenarios of the risk-averse UBS (up) and the JBS (down) for day 2. . . . 98
4.10 Comparison of the injected power (black dots) and energy bid (red line) for all scenarios of the risk-averse UBS (up) and the JBS (down) for day 3. . . . 99

5.1 Decomposition of the two-stage stochastic problem for the planning horizon. . . . 117
5.2 Decomposition of the first-stage decision variables. . . . 118
5.3 Sequential vs Parallel Implementation of the PHA. . . . 123
5.4 Structure of the solution algorithm for the risk-averse investment problem. . . . 124
5.5 Variation of the convergence gap for the PHA, risk-neutral simulation (left) and risk-averse simulations (right). . . . 127
5.6 Variation of the convergence gap for the PHA, risk-neutral simulation (left) and risk-averse simulations (right). . . . 128
5.7 Variation of the convergence gap for the PHA, risk-neutral simulation (left) and risk-averse simulations (right). . . . 130
5.8 Variation of performance of the PHA and Stochastic models in terms of execution time (left) and objective function (right). . . . 130
5.9 Efficient frontier for the WF only and WF+ESS configurations. . . . 132
5.10 Yearly breakdown of profits, total VaR and CVaR for all three configurations. . . . 133

6.1 Schematic diagram differentiating the proposed coordinated energy trading and service provision strategy. . . . 138
6.2 WF profit distribution when exposed to uncertainty for all days. . . . 143
6.3 Rooftop PV profile for the considered week. . . . 144
6.4 Breakdown of costs and revenues for the community across all operating strategies. . . . 144
6.5 Yearly value of the Coordinated & Services Strategy. . . . 145
6.6 Value of the Coordinated & Services Strategy depending on the ESS and PV penetration. 145

C.1 Energy price forecasts for the 5 representative weeks (24 hour resolution). . . . 186
C.2 SPR price forecasts for the 5 representative weeks (24 hour resolution). . . . 187

C.3 FR price forecasts for the 5 representative weeks (24 hour resolution). 188
C.4 5 Wind power availability forecasts for the 5 representative weeks (24 hour resolution). . 189
C.5 10 Wind power availability forecasts for the 5 representative weeks (24 hour resolution). 190

List of Tables

2.1 WF and ESS parameters . . . 43
2.2 Profit variation (%) between both market participations for both installations . . . 44
2.3 Performance of the deterministic bids against uncertainty . . . 46

3.1 Economic results for each EN bidding strategy (£). . . . 69
3.2 Economic results for each EN-SPR bidding strategy (£). . . . 69
3.3 AVG and STD of the energy imbalances for all days in MW. . . . 72
3.4 Pump-Turbine Unit Specifications . . . 74
3.5 Expected Day 1 Profit Breakdown for the EN Participation (£) . . . 75
3.6 Expected Day 1 Profit Breakdown for the EN-SPR Participation (£) . . . 76
3.7 Expected Day 2 Profit Breakdown for EN Participation (£) . . . 77
3.8 Expected Day 2 Profit Breakdown for the EN-SPR Participation (£) . . . 77
3.9 Expected Profits for both cases (£) . . . 79
3.10 AVG and STD of SU and SD Events . . . 79
3.11 Expected Total Profit Breakdown for both cases (£) . . . 80
3.12 AVG of SU and SD Events for both cases . . . 80
3.13 Economic Results for Case A . . . 81
3.14 Economic Results for Case B . . . 82
3.15 Sensitivity Analysis Parameters . . . 82

4.1 AVG and STD of the energy imbalances for all days in MW. . . . 98

5.1 Number of decision variables for each problem as a function of the number of scenarios 125
5.2 Number of constraints for each problem as a function of the number of scenarios . . . 125
5.3 Representative Weeks definition and Weight factors in weeks/year . . . 125
5.4 Technical and Economic Specifications of the ESS . . . 126
5.5 Performance of the PHA and Stochastic Models with 15 Scenarios . . . 127
5.6 Performance of the PHA and Stochastic Models with 30 Scenarios . . . 128
5.7 Performance of the PHA with 270 Scenarios . . . 129
5.8 Economic Results of the WF and WF+ESS operation in £ . . . 131
5.9 Technical and Economic Specifications of the larger ESS . . . 132

6.1 ESS and PV Capacities and level of penetration . . . 143
6.2 Distribution of the number households for each demand profile . . . 143

Acronyms & Abbreviations

AS	Ancillary service(s)
AVG	Average value
BV	Binary Variables
CAES	Compressed Air Energy Storage
CV	Continuous Variables
CVaR	Conditional Value-at-Risk
DoD	Depth-of-Discharge
DNO	Distribution Network Operator
ESS	Energy Storage System(s)
EV	Electric Vehicles
FR	Frequency Response
FS	Fixed-speed
IRR	Internal Rate of Return
JBS	Joint Bidding Strategy
MILP	Mixed-Integer Linear Programming
MINLP	Mixed-Integer Non Linear Programming
P2P	Peer-to-Peer
PHA	Progressive Hedging Algorithm
PHSP	Pumped-hydro Storage Plant(s)
PV	Photovoltaics
ROI	Return on investment
SCV	Semi-continuous Variables
SD	Shut-down
SoC	State-of-charge
SOS1	Special-order-set type 1
SPR	Spinning Reserve
STD	Standard Deviation

SU	Start-up
TSO	Transmission System Operator
UBS	Uncoordinated Bidding Strategy
V2G	Vehicle-to-grid
VaR	Value-at-Risk
VS	Variable-speed
WF	Wind farm(s)

Chapter 1

Introduction

This chapter serves as a preamble for the research work carried out in and summarized in this Thesis. The chapter starts with an overview of the techno-economical challenges that power systems' operators are facing as a result of the large-scale integration of intermittent renewable generation, and how Energy Storage Systems (ESS) are considered to have a key role in mitigating these challenges, to then describe the motivation of this thesis, research questions and related objectives. The last two sections of this Chapter summarize the key research contributions and the Thesis' structure.

1.1 The Impacts of Renewable Generation Integration

Increasing environmental and climate change concerns have translated into dramatic changes in the power system's landscape over the course of the last few decades. Many governments worldwide have responded to these concerns with goals to reduce the emission of greenhouse gases from electricity generation [2–4]. In order to achieve these goals, old carbon-intensive generation plants, such as coal-fired power plants, are being decommissioned and replaced with inflexible carbon-free generation technologies such as nuclear power, carbon capture and storage, and large-scale intermittent renewable generation. On the other hand, the electrification of the transport and heat sectors is also expected to play a key role in achieving carbon emission reduction targets and, thus, create further challenges for power system operations [5, 6].

The deployment of renewable generation technology, such as wind and solar photovoltaics (PV), plays in many countries a key role for reducing carbon emissions, such as the UK's where the installed wind generation capacity is expected to double by 2030 [7]. Furthermore, renewable generation costs are expected to continue decreasing [8], becoming on the same level of the lower end of the fossil-fuel cost range by 2020. Despite the ability to produce cheap and carbon-free energy, wind generation's intermittency and stochastic nature complicates its widespread integration due to operational and economic challenges. From the operational perspective, the power injections of wind generation contribute to increase the variability and uncertainty of net-demand and are characterized by unique and seasonal patterns, in which periods of high demand do not align with periods of high renewable energy output [9]. Product of the increased volatility and uncertainty of net-demand, larger volumes of operating reserves and new sources of flexibility are required in order to ensure the cost-effective balance of demand and supply. On the other hand, conventional thermal generators are negatively impacted by net-demand's increased variability and uncertainty due to the increased cycling and ramping requirements, leading to

losses in generation efficiency, lifespan and to increases O&M costs due to the larger thermal stress to which they are exposed to [10, 11].

From the economic point of view, renewable generation's variability directly influences market prices. In periods of high renewable output, conventional generation is displaced given the marginal costs of renewable energy resources being very low, zero or even negative [11], resulting in low energy prices. In contrast, low renewable output results in higher prices as costlier generators having to respond to sharp decreases in generation. For renewable producers, additional costs associated with balancing forecasted and real-time generation are incurred, while power systems which lack the appropriate means to cope with uncertainty and variability are faced with generation curtailment as common practice to stabilize net-demand and avoid thermal stress build-up in conventional generation. Renewable energy curtailment is an undesirable practice, not only because cheap carbon-free energy is wasted, but also due to the fact that renewable investments become less efficient and potential investors turn away from this business due to the increased risks of not recovering investment costs [12].

As indicated previously, increased demand-supply imbalances caused by renewable generation variability translates into the need for larger volumes of operational reserve. Traditionally, operating reserves have been provided by quick-start conventional generation, such as gas and oil-fired power plants, or hydropower plants subject to water inflow availability [11]. However, with the exception of hydropower plants, traditional reserve procurement is not aligned with governments goals for carbon emission reductions. Thus, market signals need to be created in order to incentivize the deployment of new and carbon-free resources for the provision of reserve and flexibility to keep in line with stricter carbon emission limits. [13] identifies new sources of carbon-free flexibility in the form of demand response, ESS and plug-in Electric Vehicles (EV), while [14] provides evidence for the benefits of smart grid systems in integrating renewables. Recognizing that future power systems will comprise of large shares of renewable generation, [15, 16] investigate the benefits of having wind generation providing Ancillary Services (AS) such as reserve and [17] demonstrates a methodology to incorporate Frequency Response (FR) support from Wind Farms (WF).

Flexibility is key for future power systems with large-scale intermittent renewable generation. The following section presents this research's approach to the aforementioned challenges and the research questions that looks to answer.

1.2 Motivation and Research Questions

1.2.1 The case for Coordinating ESS

ESS are currently one of the most popular solutions to the problem of integrating large-scales of intermittent renewable generation [18, 19]. This is largely due to the ESS's flexibility and exceptional ability to provide multiple services to the different sectors of the electricity industry [1]. These benefits for the UK power system can be translated in cost savings of up to £2.4bn per year through efficient ESS deployment, even achieving savings up to £7bn per year through market-driven approaches [20]. This report also recommends that coordination between renewables and ESS is key for decreasing the investment cost payback period.

Current literature shows how ESS can bring significant benefits to the several sectors of the electricity industry [21–23]. The transmission system can be positively impacted by network expansion deferral

[24] and the level of renewables integration can reach 90% [25] with optimal ESS investment. WF operators can obtain higher daily profits through coordination with Pumped-Hydro Power Plants (PHSP) and minimization of imbalance penalties, i.e. deviations between submitted day-ahead energy market bids and real-time operation, as illustrated by the stochastic optimization model proposed in [26]. On the one hand, [27] argues that energy arbitrage actions bring higher benefits to the transmission system than the distribution system, while on the other hand, [28–30] present strategies for improving the benefits of ESS in the distribution system. From a whole-systems perspective, [31] analyses the value of distributed and bulk ESS deployment against flexible generation, interconnection reinforcement and demand-side response. Although the proposed approach allows determining which sectors benefit the most from the different services that ESS can provide, further work is required to understand how ESS investors can be rewarded as it is not captured by the adopted centralized cost minimization. Lastly, [32, 33] illustrated the system reliability improvements through system-wide coordination of ESS.

Despite the diverse set of benefits that ESS can bring to power systems, there are certain economic, legal and regulatory barriers that hinder the large-scale deployment of this technology. Economic barriers such as unclear business models, unvalued benefits and lack of appropriate compensation for AS are identified in [34, 35]. Although PHSP have been widely adopted for load management, resource availability and capital intensiveness still limit their development. This is mainly due to the fact that the risk of failing to recover the high investment costs is too high for investors in the absence of long-term incentives. [36, 37] argue that failure to recover investment costs is mainly due to insufficient revenue from conventional generation price arbitrage, payment of grid fees for transmission line usage during consumption periods and payment of high water utilization fees. [38, 39] provide insights into the main regulatory barriers to the deployment of ESS such as regulation complexity and prescriptive conditions for different services, short contract lengths or incomprehension regarding network connection and charging. A proper and clear market participation framework is then key for allowing for ESS to aggregate different revenue streams and, consequently, to achieve a profitable business case.

The benefits that ESS can bring to power systems and barriers to its widespread deployment identified in the previous paragraph give rise to the need of developing clear and profitable business models. Although several business models [1, 40, 41] and optimal ESS investment models [42–45] have been proposed in literature, there is still a lack in understanding how to build a profitable business model for risk-averse renewable producers who are looking to reduce their exposure to low profits by investing in ESS.

1.2.2 Research Questions

Within the issues identified in the previous Section and the gap in literature that this research looks to address, the following research questions and related objectives are posed:

Question 1: How to maximize the value of an ESS in facilitating an efficient integration of variable renewable generation and minimize the impacts of intermittent generation uncertainty? How can uncertainty be reduced and revenue maximized?

As previously mentioned, intermittent renewable generation, such as wind power, negatively impacts power systems operations given its stochastic nature. This, in turn, translates into increasing requirements for operating reserves and new sources of flexibility. ESS are currently viewed as a solution to either the management of intermittent renewable generation uncertainty or to provide energy arbitrage and reserve

services. In this context, it is necessary to develop a business model that incorporates both ESS's ability to manage uncertainty and provide AS to maximize revenue. Such a model must include an accurate representation of the uncertainty inherent to intermittent renewable generation and capture the full set of ESS operation modes in the provision of AS. This research question is investigated in Chapter 3 and the objectives for it are:

Q1.a) Develop an optimization framework in order to investigate the value of ESS and wind generation coordination in providing energy and AS.

Q1.b) Model day-ahead resource availability and pricing uncertainty and optimize the operation strategy for both facilities in order to maximize revenue with a two-stage stochastic formulation.

Q1.c) Investigate how a wind producer benefits from coordinating with a specific ESS technology, such as PHSP.

Q1.d) Demonstrate the economic and non-economic value of coordination for both the wind-ESS producer and system operator through case studies.

Question 2: How can the exposure to risk of experiencing low profits be mitigated through the operation of combined WF-ESS facilities in the day-ahead markets? Does the mitigation of the probability of experiencing low profits interfere with ESS's ability to manage wind generation uncertainty?

The mitigation of exposure to low profits is key to potential investors in renewable generation. In order to do so, risk measures are often included in the profit maximization problems. This research question, which is analysed in Chapter 4, seeks to provide a risk-averse formulation for the optimization of renewable generation and ESS's participation in the day-ahead markets developed in Chapter 3. In other words, this new formulation seeks to address the impact of risk aversion on the provision of AS and how to optimize the management of generation uncertainty while minimizing the risk of experiencing low profits. The objectives of this research question are:

Q2.a) Expand the model developed in Chapter 3 in order to allow the consideration of different degrees of risk aversion when optimizing the day-ahead bidding strategy of WF and ESS.

Q2.b) Investigate the impact of risk aversion on the provision of AS.

Q2.c) Understand how minimizing the exposure to low profits conflict with wind generation uncertainty.

Question 3: Is it economically feasible for a risk-averse wind producer to invest in an ESS system in order minimize the impact of uncertainty and to provide ancillary services? How can the benefits of wind-ESS coordination be efficiently modelled for long-term horizons and maximized for recovery of investment costs?

One of the biggest barriers to the widespread deployment of ESS is the recovery of their capital costs [34, 35]. Considering a renewable producer's fluctuating and uncertain revenue from the operation in the day-ahead markets, it's necessary to investigate the profitability of ESS investments to enhance the offerings from renewable energy resources. Therefore, an operational model which considers the long-term impact of generation and pricing uncertainty must be developed and, in order to achieve profitability, the business models developed in the previous chapters must be expanded to provide additional services

to generate sufficient revenue. Long-term stochastic models, however, can become very difficult to solve in reasonable execution times due to the high number of scenarios that need to be used to accurately represent the evolution of uncertainty over time. Consequently, techniques such as scenario reduction algorithms, representative weeks or problem decomposition, are often utilized to reduce the problem size and achieve tractability. Furthermore, incorporating risk associated with investment decisions is a key aspect for prospective ESS investors. Such a computationally efficient ESS investment model would allow strategic renewable producers to determine the optimal ESS size under different levels of risk aversion. Chapter 5 investigates this research question which addresses the following objectives:

Q3.a) Expand the business model for WF and ESS to provide several AS and to optimize the bidding strategy for long-term horizons.

Q3.b) Develop an ESS investment model for risk-averse WF operators to determine the optimal power and energy capacities of the ESS that maximize profitability and minimize risk.

Q3.c) Implement a problem decomposition technique to achieve computational tractability.

Q3.d) Demonstrate how WF operators seeking to invest in ESS investment can achieve profitability through carefully designed case studies.

Question 4: Considering the proliferation of low carbon generation technologies in the residential sector, how can the procurement of flexibility be extended to end-users? Which type of services can be provided to network operators by coordinated households with ESS and how can the community itself benefit from these technologies?

Besides its current deployment at the transmission level, low-carbon generation technologies such as solar PV and battery ESS are also proliferating at the consumers level. As such, the flexibility that smart end-users can provide to the system operator and mitigate the challenges of integrating renewables needs to be investigated. This objective may, however, conflict with the consumers' main interest to reduce their energy bills. Therefore, a strategy needs to be developed that manages to minimize consumers energy procurements costs and to provide flexibility services such as peak demand reduction, provision of reserve and FR to the system operator. Chapter 6 presents the work developed to answer this question, in which the objectives are:

Q4.a) Establish a coordinated energy procurement arrangement that allows consumers to procure energy from their neighbours with excess generation resources.

Q4.b) Develop a multi-service business model in order to provide flexibility to the system operator.

Q4.c) Analyse the value of coordinated intra-neighbourhood energy trading and service provision and support the business case for low carbon communities to support the integration of renewables.

1.3 Proposed Research Scope and Methodologies

1.3.1 Research Proposal and Scope

For the purpose of tackling the issues identified in previous sections and answer the proposed research questions, this thesis proposes a novel ESS investment and operation model that allows risk-averse renewable producers to manage their offerings' uncertainty and procure additional sources of revenue

through the provision of AS. The operational modelling features a detailed coordinated bidding strategy for the operation of renewable technologies, such as wind generation, and an ESS. This coordinated approach combines ESS's flexibility to respond to unexpected generation variation and provision of services, such as FR and spinning reserve (SPR), with renewables' cheap and carbon-free energy. The provision of AS on top of uncertainty management allows for profitability to be increased and, therefore, incentivizes the procurement of flexibility in the form of ESS and renewables coordination.

The models developed and conclusions provided in this thesis will present prospective renewable producers seeking to invest in ESS with a clear business model to maximize the Return On Investment (ROI). The analysis and results from the case studies illustrated here have the objective of detailing the economic and non-economic benefits of coordinating renewables and ESS operation to renewable producers, system operators and regulators. It is also expected that this work will contribute to promote the role of ESS in integrating renewables and thus, complying with governments' targets to reduce carbon emissions.

1.3.2 Methodologies

In order to develop an investment model for risk-averse renewable producers to enhance their bidding strategies through coordination with ESS, three essential objectives must be ensured:

- The operation of energy systems for the management of wind uncertainty and provision of AS must be precisely modelled.
- Wind generation and energy and AS pricing uncertainty must be adequately modelled.
- The resulting investment model must be computationally efficient for the purpose of considering long-term assessment horizons under a reasonable number of scenarios.

These three objectives are addressed by means of the following methodologies: Mixed-Integer Linear Programming (MILP); two-stage stochastic programming; Progressive Hedging Algorithm (PHA). MILP was used to develop all models presented in this thesis in order to capture ESS's two states of operation, i.e. either consuming or generating, and the discontinuities related to the provision of AS such as ensuring sufficient energy is available when called upon to provide and minimum provision levels. Two-stage stochastic programming [46, 47] is one of the most popular methods for dealing with uncertainty. First-stage decisions include actions that need to be decided before the outcome of the uncertain parameters is known, while second-stage decisions are related to the recourse actions made after the reveal of the outcome of the uncertain parameters. A set of scenarios is used to model the different values that the uncertain parameters (wind generation and prices) in order to capture uncertainty. In order to make the resulting model computationally efficient, the main problem is decomposed into smaller, easier to solve sub-problems using the PHA [48, 49] while minimizing the sub-optimality of the solution.

1.4 Summary of Research Contributions

The work developed in order to answer the research questions presented in Section 1.2.2 lead to the following original contributions:

- The development of an optimization framework for Wind Farms and Energy Storage Systems to coordinate their operation for the provision of energy and ancillary services. Resource availability, stored energy limitations and the provision of ancillary services through the full set of storage operation modes are incorporated in the formulation of the bidding strategy.

- The proposal of a stochastic formulation in order to represent how generation and provision of ancillary services are affected by day-ahead wind generation and prices uncertainty. This has allowed to better understand how wind imbalance management impacts the revenue generated from providing ancillary services, and vice-versa. It is also shown how the proposed coordinated bidding strategy mitigates the conflict between imbalance management and provision of services.

- The development of a novel two-stage stochastic mathematical programming model that allows considering different degrees of risk aversion when optimising the day-ahead energy and ancillary services bidding strategy of a Wind Farm with an on-site Energy Storage System. As a result, risk-averse wind producers will have an improved position in the day-ahead markets due to the reduced offer uncertainty.

- The linearization of absolute value functions through a tight formulation using Special Ordered-Set Type 1 (SOS1) and integer variables to dynamically enforce bounds for positive and negative values of energy and ancillary services imbalances that allows reducing the solutions' searching space and computational time.

- The development of a model that allows considering additional pump-turbine unit start-up (SU) and shut-down (SD) costs of a Pumped-Hydro Storage Plant due to the provision of SPR. The modelling of these additional costs allowed for, on the one hand, more informed Pumped-Hydro Storage Plant commitment decisions to be made which improve the operational lifespan of the pump-turbine units. On the other hand, it provides better insight into how wind generation variability impacts the benefit of variable-speed (VS) over fixed-speed (FS) pump-turbine technology.

- The development of a risk-averse formulation for the Energy Storage System investment problem for wind coordination and provision of ancillary services and the successful application of the Progressive Hedging Algorithm to this formulation in order to achieve computational tractability.

- Establishing a MILP model to minimize energy procurement costs through a coordinated intra-neighbourhood energy trading and multi-service business model.

1.5 Thesis Structure

This thesis is divided into seven chapters.

Chapter 2 provides an overview of the application of ESS in current literature. The objective of this chapter is to present a modelling basis for ESS from which the next chapters' models will be built upon. Concretely, a deterministic ESS model for the provision of energy arbitrage and a generic AS will be presented.

Chapter 3 expands the modelling presented in Chapter (2) by formulating a two-stage stochastic problem for the operation of ESS. In order to realize the potential of ESS in low-carbon power systems, a

coordinated bidding strategy is proposed for combined WF and ESS. The proposed coordination strategy involves the management of wind generation imbalances and the provision of SPR for day-ahead energy and SPR markets. The application of this strategy to a specific ESS technology such as PHSP is also presented. A novel tight reformulation for the calculation of the absolute value of imbalances specific to the operation of PHSP is proposed and demonstrated.

Chapter 4 continues the development of the coordinated bidding strategy presented in Chapter 3 by introducing risk measures. The new formulation allows for considering several degrees of risk aversion when optimizing the day-ahead bidding strategy for combined WF and ESS. This formulation is assessed through two case studies to determine the benefit of wind and ESS coordination in the management of expected profit risk, and in the management of wind generation uncertainty.

Chapter 5 concludes the development of the risk-averse coordinated bidding strategy presented in the previous chapters. Improvements include the provision of additional AS such as the provision of FR and expanding the assessment horizon from one day to one year. These improvements allowed to formulate an ESS investment model for risk-averse wind producers. As such, the resulting two-stage stochastic MILP model became too complex to solve within desirable execution times. In order to overcome this hurdle, the PHA is used to decompose the problem by scenario and achieve computational tractability.

Chapter 6 investigates how low-carbon residential communities with rooftop PV and ESS can improve power systems' flexibility. A coordinated operation strategy is presented in which households look to minimize energy procurement costs by sharing energy resources in a peer-to-peer (P2P) arrangement, providing flexibility services to the system operator and reducing peak demand at the distribution network level.

Chapter 7 concludes this thesis by presenting the main conclusions and key messages from this work. This chapter also identifies new areas of interest regarding renewable generation and ESS coordination and recommendations for future research.

Chapter 2

Deterministic Business Models for Energy Storage Systems

This chapter introduces the modelling of ESS operation with the objective of detailing the first modelling building block from which the following models were developed in this work. This chapter begins with a literature overview concerning the deterministic modelling of the operation of this technology and the types of AS it can provide.

The case studies in this chapter illustrate the economic value of the ESS providing multiple services. Although deterministic modelling sufficiently captures ESS response to pricing uncertainty, mitigating unexpected variations caused by renewable generation requires a more precise modelling of the uncertain parameters. Therefore, operational models need to evolve to be able to cope with increased net-demand volatility and uncertainty caused by the increasing integration of intermittent renewable resources.

2.1 Nomenclature

2.1.1 Indices, Sets and Sub-Sets

$e \in S^{\mathrm{E}}$	Day-ahead energy price forecasts.
$a \in S^{\mathrm{A}}$	Day-ahead AS price forecasts.
$w \in S^{\mathrm{W}}$	Day-ahead available wind power forecasts.
$h \in H$	Time periods.
Ω^{BV}	Set of all binary decision variables.
Ω^{CV}	Set of all continuous decision variables.
$\Omega^{\mathrm{CV^+}}$	Set of all positive continuous decision variables.
$\Omega^{\mathrm{SCV^+}}$	Set of all positive semi-continuous decision variables.
$\Omega^{\mathrm{CV^{SOS1}}}$	Set of all positive SOS1 continuous decision variables.

2.1.2 Parameters

K^{W}	WF generation capacity [MW].
$\mathrm{P}^{\mathrm{AV}}_{w,h}$	Wind power availability for forecast w and time period h [p.u.].

η Roundtrip efficiency of the ESS [p.u.].

$\overline{\mathrm{P}}$ Maximum charge/discharge rate of the ESS [MW].

$\overline{\mathrm{E}}$ Energy capacity of the ESS [MWh].

$\mathrm{E}^{\mathrm{Min/Max}}$ Minimum/Maximum stored energy level in the ESS [p.u.].

$\pi^{\mathrm{En}}_{e,h}$ Energy market price at forecast e and time period h [£/MWh].

$\pi^{\mathrm{AS,Up}}_{a,h}$ Upward AS market price at forecast a and time period h [£/MW/h].

$\pi^{\mathrm{AS,Dw}}_{a,h}$ Downward AS market price at forecast a and time period h [£/MW/h].

τ^{AS} Maximum duration of AS requirement [h].

$\underline{\mathrm{AS}}^{\mathrm{Up/Dw}}$ Minimum level for upward/downward AS provision [MW].

ρ_e, ρ_a, ρ_w Probability of each forecast e, a and w [p.u.].

M Large number for constraint relaxation.

2.1.3 Binary Variables

$Q^{\mathrm{Up,D/C}}_h$ Commitment of upward AS in discharging/charging mode at time period h.

$Q^{\mathrm{Dw,D/C}}_h$ Commitment of downward AS in discharging/charging mode at time period h.

2.1.4 Continuous Variables

e_h Energy stored in the ESS at time period h [MWh].

p^{C}_h Power charged by the ESS at time period h [MW].

p^{D}_h Power generated by the ESS at time period h [MW].

p^{W}_h Power output of the WF at time period h [MW].

$r^{\mathrm{Up,D}}_h$ Upward AS contribution by the ESS during discharging at time period h [MW].

$r^{\mathrm{Dw,D}}_h$ Downward AS contribution by the ESS during discharging at time period h [MW].

$r^{\mathrm{Up,C}}_h$ Upward AS contribution by the ESS during charging at time period h [MW].

$r^{\mathrm{Dw,C}}_h$ Downward AS contribution by the ESS during charging at time period h [MW].

$r^{\mathrm{Up,ESS}}_h$ Total Upward AS contribution by the ESS during time period h [MW].

$r^{\mathrm{Dw,ESS}}_h$ Total Downward AS contribution by the ESS during time period h [MW].

$r^{\mathrm{Up,W}}_h$ Upward AS contribution of the WF at time period h [MW].

$r^{\mathrm{Dw,W}}_h$ Downward AS contribution of the WF at time period h [MW].

$x^{\mathrm{En,ESS}}_h$ Day-ahead energy bid for the ESS for time period h [MWh].

$x^{\mathrm{AS\text{-}Up,ESS}}_h$ Day-ahead upward AS bid for the ESS for time period h [MW].

$x^{\mathrm{AS\text{-}Dw,ESS}}_h$ Day-ahead downward AS bid for the ESS for time period h [MW].

$x^{\mathrm{En,W}}_h$ Day-ahead energy bid for the WF for time period h [MWh].

$x^{\mathrm{AS\text{-}Up,W}}_h$ Day-ahead upward AS bid for the WF for time period h [MW].

$x^{\mathrm{AS\text{-}Dw,W}}_h$ Day-ahead downward AS bid for the WF for time period h [MW].

2.2 Introduction

2.2.1 Literature Review

As previously stated, barriers to the deployment of ESS, such as failure to recover investment costs and regulation complexity, give rise to the need to develop strategies to achieve profitability [20, 50, 51]. Bradbury et al. compare in [51] several ESS technologies and their ability of achieving an economically efficient internal rate of return (IRR). It is also concluded that technological characteristics and capital costs greatly influence IRR, while market price volatility increases IRR, and that PHSP and compressed air energy storage (CAES) systems are more attractive than flywheels, capacitors and chemical-based ESSs. The authors of [50] argue that besides the New York state's electricity market benefiting from the arbitrage decisions from ESS, other opportunities such as voltage regulation, provision of frequency regulation services and deferment of system upgrades provide great value for this technology. As such, several authors have investigated the wide range of services that ESS can bring to the different sectors of the energy system [18, 22, 24, 31, 32].

[52] concludes that AS market revenues can become the main source of profit for ESS as the scale of renewable technology deployment increases, while [53] demonstrates that ESS technologies such as ultra-capacitors and flywheels are more suitable for providing frequency regulation services, while lithium-ion and lead acid batteries are more suitable for peak-shaving. The authors also note that, at the time of publication, merely providing contingency reserves was insufficient in order to earn positive net profits. Despite understanding how ESS can benefit from supporting other sectors of the energy system, current literature points towards a need for bundling multiple services in order to build a profitable business case.

Maximizing ESS revenue by providing reserve services in addition to price arbitrage has been investigated in [54, 55] through self-scheduling PHSP and battery ESS operations. [56] estimates that VS PHSP can generate more revenue in the secondary regulation market. Business models for aggregating the revenue from the provision of multiple services are proposed in [40, 41]. On one hand, [41] presents a model consisting of a series of auctions for the utilization rights for the ESS in order to maximize ROI, while ensuring non-conflicting usage by different auction participants. On the other hand, Moreno et al. propose in [40] an ESS-centric profit maximisation model to co-optimize the provision of several services (price arbitrage, regulation and reserve, and reactive power control) from ESS, and later in [57] expand the business model to consider corrective network support capabilities. Modelling-wise, the latter models consider disjunctive constraints for ensuring sufficient stored energy to provide committed reserve services, but do not take into account any source of uncertainty, simplify the modelling of operation modes during provision of reserve services, and disregard discharging efficiency in which these services are provided. The planning of short-term operations in the Chilean Northern Interconnected Power System can be improved greatly by deploying ESS as evidenced in [58].

2.2.2 An ESS Business Model

As referenced in subsection 1.2.1, ESS can provide several services to different sectors of the energy system. Fig. 2.1 summarizes the types of services that ESSs can provide to different sectors. From this illustration it is possible to construct a business model comprised of different services such as: energy arbitrage in the wholesale market, provision of FR and reserve services, voltage support and congestion

management. However, an optimal business model must take into account ESS limitations and service requirements to avoid possible service conflict in order to maximize revenue.

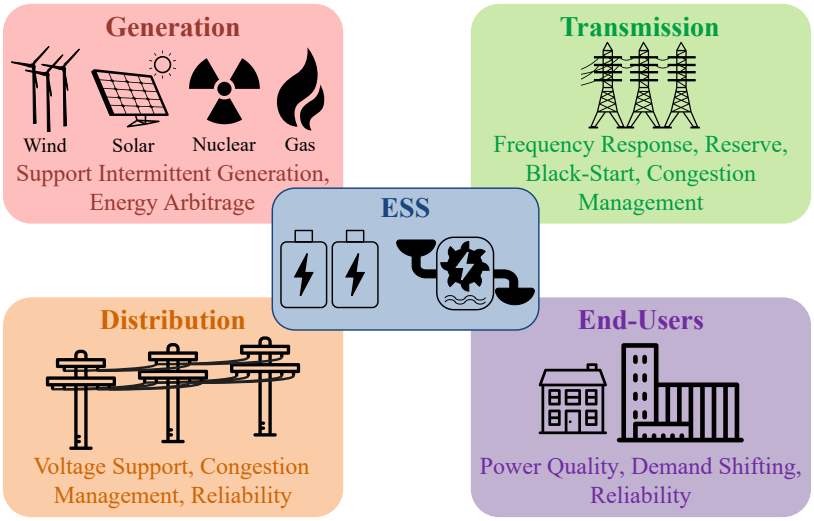


Fig. 2.1: Different services that ESS can provide to the several sectors of the energy system [1].

As such, a simple deterministic ESS business model is considered for this chapter and consists in the coordinated provision of energy arbitrage and AS to support the transmission system operation. Thus, the AS considered for this business model is based of the provision of reserve services to the TSO. This business model seeks to maximize the operational revenue of the ESS by maximizing energy sold and provided AS in the day-ahead energy and AS markets and minimizing costs associated with storing energy in the ESS. The objective of building such a business case is twofold: to analyse the value of providing AS and how ESS scheduling is impacted; to create an initial modelling framework from which more advanced models presented in this Thesis have been built.

2.3 Mathematical Formulation

2.3.1 Key properties and assumptions

The model presented in this section serves to illustrate the independent operation of an ESS and a WF in the day-ahead energy and AS markets. The day-ahead energy market is assumed to clear at every time period (hourly in the market considered in this work) when the market operator matches the aggregated suppliers' and consumers' submitted power bids as a function of the selling/buying price, and a strike price is set which is used to pay all accepted bids. The day-ahead AS markets assumed in this work, much like the SPR markets adopted by PJM in the US (Day-Ahead Scheduling Reserve Market) [59] and the Iberian Electricity Market (MIBEL) in Portugal and Spain [60], are assumed to occur after the clearing of the energy market. The market operator must meet a reliability standard, usually defined a SPR or FR requirement, by accepting upward or downward AS bids from providers. For the purpose of this chapter the balancing service is considered to be SPR.

The model described henceforth is classified as a deterministic MILP model in order to maximize the energy and AS market revenue for both installations. The decision variables to be determined are the optimal day-ahead bidding strategy for both facilities with an hourly time resolution, for which the duration of each time period is omitted from this formulation. As previously mentioned, wind power

generation's nature is stochastic and, in power systems with large-scale penetration of wind generation integration, directly influences market prices. As such, it is assumed that wind power availability $\left(W_{w,h}^{\mathrm{AV}}\right)$ and prices $\left(\pi_{e,h}^{\mathrm{En}}, \pi_{a,h}^{\text{AS-Up}} \text{ and } \pi_{a,h}^{\text{AS-Dw}}\right)$ are uncertain parameters characterized by the expected value of the corresponding day-ahead forecasts. However, the size of the ESS and the WF are assumed to not be sufficiently large in size to influence market prices - price-taker approach.

2.3.2 Objective function

$$\underset{\substack{\Omega^{\mathrm{BV}},\Omega^{\mathrm{CV}},\Omega^{\mathrm{CV}^+},\\ \Omega^{\mathrm{SCV}^+},\Omega^{\mathrm{CV}^{\mathrm{SOS1}}}}}{\text{Maximize}} \left\{ \sum_{h\in H} \left(\hat{\pi}_h^{\mathrm{En}} x_h^{\mathrm{En,ESS}} + \hat{\pi}_h^{\mathrm{AS,Up}} x_h^{\text{AS-Up,ESS}} + \hat{\pi}_h^{\mathrm{AS,Dw}} x_h^{\text{AS-Dw,ESS}} \right) \right. \tag{2.1}$$

$$\left. + \sum_{h\in H} \left(\hat{\pi}_h^{\mathrm{En}} x_h^{\mathrm{En,W}} + \hat{\pi}_h^{\mathrm{AS,Up}} x_h^{\text{AS-Up,W}} + \hat{\pi}_h^{\mathrm{AS,Dw}} x_h^{\text{AS-Dw,W}} \right) \right\}.$$

$$\hat{\pi}_h^{\mathrm{En}} = \sum_{e\in S^{\mathrm{E}}} \rho_e \pi_{e,h}^{\mathrm{En}}, \quad \forall h, \tag{2.2}$$

$$\hat{\pi}_h^{\mathrm{AS,Up}} = \sum_{a\in S^{\mathrm{A}}} \rho_a \pi_{a,h}^{\mathrm{AS,Up}}, \quad \forall h, \tag{2.3}$$

$$\hat{\pi}_h^{\mathrm{AS,Dw}} = \sum_{a\in S^{\mathrm{A}}} \rho_a \pi_{a,h}^{\mathrm{AS,Dw}}, \quad \forall h. \tag{2.4}$$

The objective function (2.1) maximizes the daily energy and AS markets revenue for the ESS (1st line) and for the WF (2nd line) . Equations (2.2) to (2.4) calculate the expected value for the energy and AS prices, based on the respective day-ahead forecasts.

2.3.3 Model Constraints

2.3.3.1 Energy market operation

The participation of the ESS in the day-ahead energy market is modelled with constraints (2.5) to (2.8) which, respectively, enforce maximum power consumption during charging, maximum power generation during discharging, energy balance equation, minimum and maximum energy limits. The initial $(h = 0)$ stored energy level is determined by the model. Constraint (2.9) limits wind power generation to the expected wind power availability.

Traditional ESS models utilize binary auxiliary variables in order to prevent simultaneous charging and discharging actions. In order to avoid the use of binary variables (despite the low-scale of this model) the variables associated with charging power $\left(p_h^{\mathrm{C}}\right)$ and discharging power $\left(p_h^{\mathrm{D}}\right)$ are defined as (SOS1) variables, which achieves the same objective without the increased computational burden.

$$p_h^{\mathrm{C}} \le \overline{\mathrm{P}}, \quad \forall h, \tag{2.5}$$

$$p_h^{\mathrm{D}} \le \overline{\mathrm{P}}, \quad \forall h, \tag{2.6}$$

$$e_h = e_{h-1} + \eta\, p_h^{\mathrm{C}} - p_h^{D}, \quad \forall h, \tag{2.7}$$

$$\mathrm{E}^{\mathrm{Min}} \cdot \overline{\mathrm{E}} \le e_h \le \mathrm{E}^{\mathrm{Max}} \cdot \overline{\mathrm{E}}, \quad \forall h, \tag{2.8}$$

$$p_h^{\mathrm{W}} \le \sum_{w\in S^{\mathrm{W}}} \rho_w \mathrm{P}_{w,h}^{\mathrm{AV}} \mathrm{K}^{\mathrm{W}}, \quad \forall h. \tag{2.9}$$

2.3.3.2 AS market operation

ESS, unlike conventional generation, can provide either upwards or downwards AS in both operating modes. Thus, ESS can, on the one hand, provide downwards AS (AS-Dw) by increasing consumption power - constraints (2.10) - and provide upwards AS (AS-Up) by decreasing consumption power - constraints (2.11) - in charging mode. On the other hand, AS-Up can be provided by increasing generation power - constraints (2.12) - and AS-Dw by decreasing generation power - constraints (2.13) - when the ESS is generating.

$$p_h^{\mathrm{C}} + r_h^{\mathrm{Dw,C}} \leq \overline{\mathrm{P}}, \quad \forall h, \tag{2.10}$$

$$r_h^{\mathrm{Up,C}} \leq p_h^{\mathrm{C}}, \quad \forall h, \tag{2.11}$$

$$p_h^{\mathrm{D}} + r_h^{\mathrm{Up,D}} \leq \overline{\mathrm{P}}, \quad \forall h, \tag{2.12}$$

$$r_h^{\mathrm{Dw,D}} \leq p_h^{\mathrm{D}}, \quad \forall h. \tag{2.13}$$

AS markets consider different technical requirements from providers in order to participate. For example, the day-ahead Iberian Electricity Market (MIBEL) secondary reserve auction enforces a ratio between upwards and downwards reserve [60] while National Grid in the UK requires providers to offer a minimum of 3MW of generation or steady demand reduction to participate in the Short Term Operating Reserve (STOR) [61]. As such, total quantities for AS-Up and AS-Dw are given by equalities (2.14) and (2.15), respectively, while constraints (2.16) and (2.17) model minimum provision of AS for the ESS, making $r_h^{\mathrm{Up,ESS}}$ and $r_h^{\mathrm{Dw,ESS}}$ semi-continuous variables.

$$r_h^{\mathrm{Up,ESS}} = r_h^{\mathrm{Up,C}} + r_h^{\mathrm{Up,D}}, \quad \forall h, \tag{2.14}$$

$$r_h^{\mathrm{Dw,ESS}} = r_h^{\mathrm{Dw,C}} + r_h^{\mathrm{Dw,D}}, \quad \forall h, \tag{2.15}$$

$$r_h^{\mathrm{Up,ESS}} \leq \begin{cases} 2\overline{\mathrm{P}} & , r_h^{\mathrm{Up,C}} + r_h^{\mathrm{Up,D}} \geq \underline{\mathrm{AS}}^{\mathrm{Up}} \\ 0 & , r_h^{\mathrm{Up,C}} + r_h^{\mathrm{Up,D}} < \underline{\mathrm{AS}}^{\mathrm{Up}} \end{cases}, \quad \forall h, \tag{2.16}$$

$$r_h^{\mathrm{Dw,ESS}} \leq \begin{cases} 2\overline{\mathrm{P}} & , r_h^{\mathrm{Dw,C}} + r_h^{\mathrm{Dw,D}} \geq \underline{\mathrm{AS}}^{\mathrm{Dw}} \\ 0 & , r_h^{\mathrm{Dw,C}} + r_h^{\mathrm{Dw,D}} < \underline{\mathrm{AS}}^{\mathrm{Dw}} \end{cases}, \quad \forall h, \tag{2.17}$$

The amount of AS-Up is limited by the available wind power and current generation in constraints (2.18), while AS-Dw is constrained by current wind power generation (2.19). Along the same lines as the previous constraints, (2.20) and (2.21) model minimum provision of AS for the WF.

$$p_h^{\mathrm{W}} + r_h^{\mathrm{Up,W}} \leq \sum_{w \in S^{\mathrm{W}}} \rho_w \mathrm{P}_{w,h}^{\mathrm{AV}} \mathrm{K}^{\mathrm{W}}, \quad \forall h, \tag{2.18}$$

$$r_h^{\mathrm{Dw,W}} \leq p_h^{\mathrm{W}}, \quad \forall h. \tag{2.19}$$

$$r_h^{\mathrm{Up,W}} \leq \begin{cases} \mathrm{K}^{\mathrm{W}} & , r_h^{\mathrm{Up,W}} \geq \underline{\mathrm{AS}}^{\mathrm{Up}} \\ 0 & , r_h^{\mathrm{Up,W}} < \underline{\mathrm{AS}}^{\mathrm{Up}} \end{cases}, \quad \forall h, \tag{2.20}$$

$$r_h^{\mathrm{Dw,W}} \leq \begin{cases} \mathrm{K}^{\mathrm{W}} & , r_h^{\mathrm{Dw,W}} \geq \underline{\mathrm{AS}}^{\mathrm{Dw}} \\ 0 & , r_h^{\mathrm{Dw,W}} < \underline{\mathrm{AS}}^{\mathrm{Dw}} \end{cases}, \quad \forall h. \tag{2.21}$$

Despite the flexible ways for ESS to provide AS, it is worth noting that, unlike conventional gen-

eration, the provision of AS is also constrained by the amount of energy stored. Another consideration that must be taken into account is that even though at this stage ESS is bidding for the availability to provide the AS, sufficient stored energy must be ensured in order to provide the full delivery of the AS for durations longer than one time period [40]. As such, constraints (2.22) to (2.25) ensure that sufficient energy is available to provide the AS for its maximum utilization duration $\left(\tau^{\mathrm{AS}}\right)$. When AS are committed $\left(\text{e.g. } Q_h^{\mathrm{Up,D}} = 1\right)$, these constraints ensure that e_{h-1} is larger or equal than $\eta\, p_h^{\mathrm{C}} - \left(p_h^{\mathrm{D}} + r_h^{\mathrm{Up,D}}\right)\tau^{\mathrm{AS}}$, but within energy limits $\left(0, \overline{E}\right)$. When the AS is not committed $\left(\text{e.g. } Q_h^{\mathrm{Up,D}} = 0\right)$, the relevant constraints are relaxed and constraints (2.7) and (2.8) are enforced instead. These constraints are directly connected to constraints (2.26) to (2.29), which allow for the provision of AS to be positive, if enough energy is allocated, or zero, otherwise.

$$\mathrm{E}^{\mathrm{Min}} \cdot \overline{\mathrm{E}} - \mathrm{M}\left(1 - Q_h^{\mathrm{Up,D}}\right) \leq e_{h-1} + \eta\, p_h^{\mathrm{C}} - \left(p_h^{\mathrm{D}} + r_h^{\mathrm{Up,D}}\right)\tau^{\mathrm{AS}} \leq \mathrm{E}^{\mathrm{Max}} \cdot \overline{\mathrm{E}} + \mathrm{M}\left(1 - Q_h^{\mathrm{Up,D}}\right), \quad \forall h, \tag{2.22}$$

$$\mathrm{E}^{\mathrm{Min}} \cdot \overline{\mathrm{E}} - \mathrm{M}\left(1 - Q_h^{\mathrm{Dw,D}}\right) \leq e_{h-1} + \eta\, p_h^{\mathrm{C}} - \left(p_h^{\mathrm{D}} - r_h^{\mathrm{Dw,D}}\right)\tau^{\mathrm{AS}} \leq \mathrm{E}^{\mathrm{Max}} \cdot \overline{\mathrm{E}} + \mathrm{M}\left(1 - Q_h^{\mathrm{Dw,D}}\right), \quad \forall h, \tag{2.23}$$

$$\mathrm{E}^{\mathrm{Min}} \cdot \overline{\mathrm{E}} - \mathrm{M}\left(1 - Q_h^{\mathrm{Up,C}}\right) \leq e_{h-1} + \eta\, \left(p_h^{\mathrm{C}} - r_h^{\mathrm{Up,C}}\right)\tau^{\mathrm{AS}} - p_h^{\mathrm{D}} \leq \mathrm{E}^{\mathrm{Max}} \cdot \overline{\mathrm{E}} + \mathrm{M}\left(1 - Q_h^{\mathrm{Up,C}}\right), \quad \forall h, \tag{2.24}$$

$$\mathrm{E}^{\mathrm{Min}} \cdot \overline{\mathrm{E}} - \mathrm{M}\left(1 - Q_h^{\mathrm{Dw,C}}\right) \leq e_{h-1} + \eta\, \left(p_h^{\mathrm{C}} + r_h^{\mathrm{Dw,C}}\right)\tau^{\mathrm{AS}} - p_h^{\mathrm{D}} \leq \mathrm{E}^{\mathrm{Max}} \cdot \overline{\mathrm{E}} + \mathrm{M}\left(1 - Q_h^{\mathrm{Dw,C}}\right), \quad \forall h, \tag{2.25}$$

$$r_h^{\mathrm{Up,D}} \leq \mathrm{M}\, Q_h^{\mathrm{Up,D}}, \quad \forall h, \tag{2.26}$$

$$r_h^{\mathrm{Dw,D}} \leq \mathrm{M}\, Q_h^{\mathrm{Dw,D}}, \quad \forall h, \tag{2.27}$$

$$r_h^{\mathrm{Up,C}} \leq \mathrm{M}\, Q_h^{\mathrm{Up,C}}, \quad \forall h, \tag{2.28}$$

$$r_h^{\mathrm{Dw,C}} \leq \mathrm{M}\, Q_h^{\mathrm{Dw,C}}, \quad \forall h. \tag{2.29}$$

As it is assumed that the WF participates in the provision of AS, it must be ensured that wind power availability in the time periods following the requirement of the AS is sufficient to provide committed AS. As such, constraints (2.30) and (2.31) ensure the deliverability of the committed AS.

$$p_t^{\mathrm{W}} + r_h^{\mathrm{Up,W}} \leq \sum_{w \in S^{\mathrm{W}}} \rho_w \mathrm{P}_{w,h}^{\mathrm{AV}} \mathrm{K}^{\mathrm{W}}, \quad \forall h,\, h \leq t < h + \tau^{\mathrm{AS}}, \tag{2.30}$$

$$p_t^{\mathrm{W}} - r_h^{\mathrm{Dw,W}} \geq 0, \quad \forall,\, h \leq t < h + \tau^{\mathrm{AS}}. \tag{2.31}$$

2.3.3.3 Energy and Balancing Services Bids

Day-ahead bids for the ESS are calculated in constraints (2.32) to (2.34). Note that the definition for the WF's energy and AS bids is omitted since it is assumed that these equal the variables p_h^{W}, $r_h^{\mathrm{Up,W}}$ and $r_h^{\mathrm{Dw,W}}$, respectively.

$$x^{\mathrm{En,ESS}} = p_h^{\mathrm{D}} - p_h^{\mathrm{C}}, \quad \forall h, \tag{2.32}$$

$$x^{\mathrm{BS\text{-}Up,ESS}} = r_h^{\mathrm{Up,D}} + r_h^{\mathrm{Up,C}}, \quad \forall h, \tag{2.33}$$

$$x^{\mathrm{BS\text{-}Dw,ESS}} = r_h^{\mathrm{Dw,D}} + r_h^{\mathrm{Dw,C}}, \quad \forall h. \tag{2.34}$$

2.3.3.4 Variables types

Lastly, the sign and type constraints for all decision variables are identified in (2.35) and (2.39).

$$\Omega^{\mathrm{BV}} = \left\{ Q_h^{\mathrm{Up,D}}, Q_h^{\mathrm{Dw,D}}, Q_h^{\mathrm{Up,C}}, Q_h^{\mathrm{Dw,C}} \right\} \in \{0,1\}, \quad \forall h, \tag{2.35}$$

$$\Omega^{\mathrm{CV}} = \left\{ x_h^{\mathrm{En,ESS}} \right\} \in \mathbb{R}, \quad \forall h, \tag{2.36}$$

$$\begin{aligned} \Omega^{\mathrm{SCV^+}} = \Big\{ & r_h^{\mathrm{Up,ESS}}, r_h^{\mathrm{Dw,ESS}}, r_h^{\mathrm{Up,W}}, r_h^{\mathrm{Dw,W}}, x_h^{\mathrm{BS\text{-}Up,ESS}}, \\ & x_h^{\mathrm{BS\text{-}Dw,ESS}}, x_h^{\mathrm{En,W}}, x_h^{\mathrm{BS\text{-}Up,W}}, x_h^{\mathrm{BS\text{-}Dw,W}} \Big\} \in \mathbb{R}_{\geq 0}, \quad \forall h, \end{aligned} \tag{2.37}$$

$$\Omega^{\mathrm{CV^{SOS1}}} = \left\{ p_h^{\mathrm{D}}, p_h^{\mathrm{C}} \right\} \in \mathbb{R}_{\geq 0}, \quad \forall h, \tag{2.38}$$

$$\Omega^{\mathrm{CV^+}} = \left\{ p_h^{\mathrm{W}}, e_h, r_h^{\mathrm{Up,D}}, r_h^{\mathrm{Up,C}}, r_h^{\mathrm{Dw,D}}, r_h^{\mathrm{Dw,C}} \right\} \in \mathbb{R}_{\geq 0}, \quad \forall h. \tag{2.39}$$

2.4 Case Studies

This section presents the input data to use in this and the following chapters' case studies. In the first case study, the value of providing AS, such as SPR, against an energy arbitrage only business model is analysed; while in the second case study, the performance of the deterministically calculated bids against uncertainty is analysed to understand how ESS can respond to uncertain outcomes. For comparison purposes for further cases studies in this Thesis, the operation of a WF in the day-ahead energy and AS markets is studied.

2.4.1 Input Data

This analysis is carried out for three days, with each day featuring three day-ahead energy price forecasts $\left(\pi_{e,h}^{\mathrm{En}}\right)$, three day-ahead AS price (assumed equal for both AS-Up and AS-Dw) forecasts $\left(\pi_{a,h}^{\mathrm{AS,Up/Dw}}\right)$ and fifty day-ahead wind power availability forecasts $\left(\mathrm{W}_{w,h}^{\mathrm{AV}}\right)$. Figs. 2.2 and 2.3 illustrated the price and wind generation forecasts. The wind generation forecasts were created through a Monte Carlo sampling process based on historical data of a 50MW WF available in the Elexon Portal [62], while energy and AS prices were extracted from the MIBEL market results [63]. Regarding the provision of AS, it is assumed that maximum utilization time duration for provided services, i.e. the amount of time that is required of the service provider to maintain power levels in order to provide the committed AS quantity, is 2 hours. It is also assumed a minimum of 3 MW for the provision of both AS-Up and AS-Dw $\left(\underline{\mathrm{AS}}^{\mathrm{Up/Dw}}\right)$.

It is assumed that the WF and ESS considered in this work are characterized by the parameters in Table 2.1. For sake of clarity it is assumed that charging and discharging power capacities are the same, and that stored energy is allowed to vary between 0 MW and the energy capacity $\left(\overline{\mathrm{E}}\right)$, making the minimum $\left(\mathrm{E}^{\mathrm{Min}}\right)$ and maximum $\left(\mathrm{E}^{\mathrm{Max}}\right)$ stored energy levels 0% and 100%, respectively.

The model described in the previous section and other models presented in this Thesis were implemented in FICO$^{\mathrm{TM}}$ Xpress [64] and simulated on a desktop computer with 3.20 GHz Intel(R) Xeon (R) processor and 16 GB of RAM, running 64-bit Windows 10, except where specified. FICO$^{\mathrm{TM}}$ Xpress offers a suite of solution methods to solve MILP models, of which Newton Barrier with Branch-and-Bound was selected.

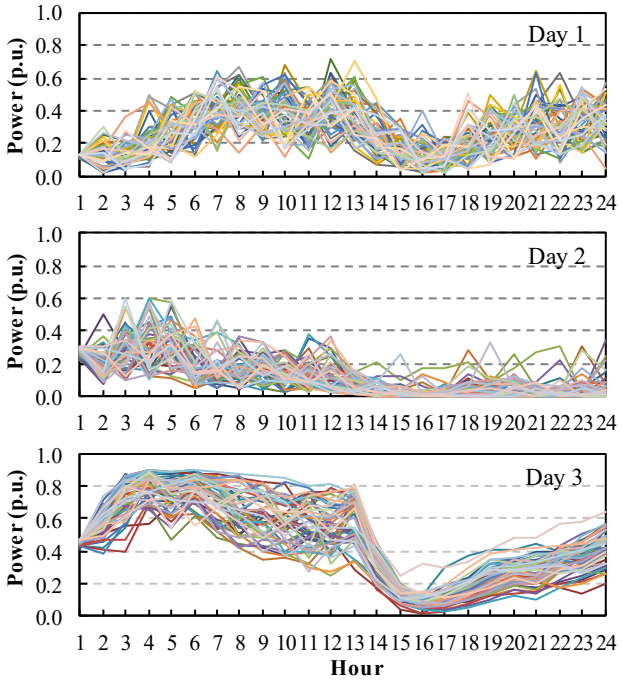


Fig. 2.2: Day-ahead wind power availability forecasts for all days.

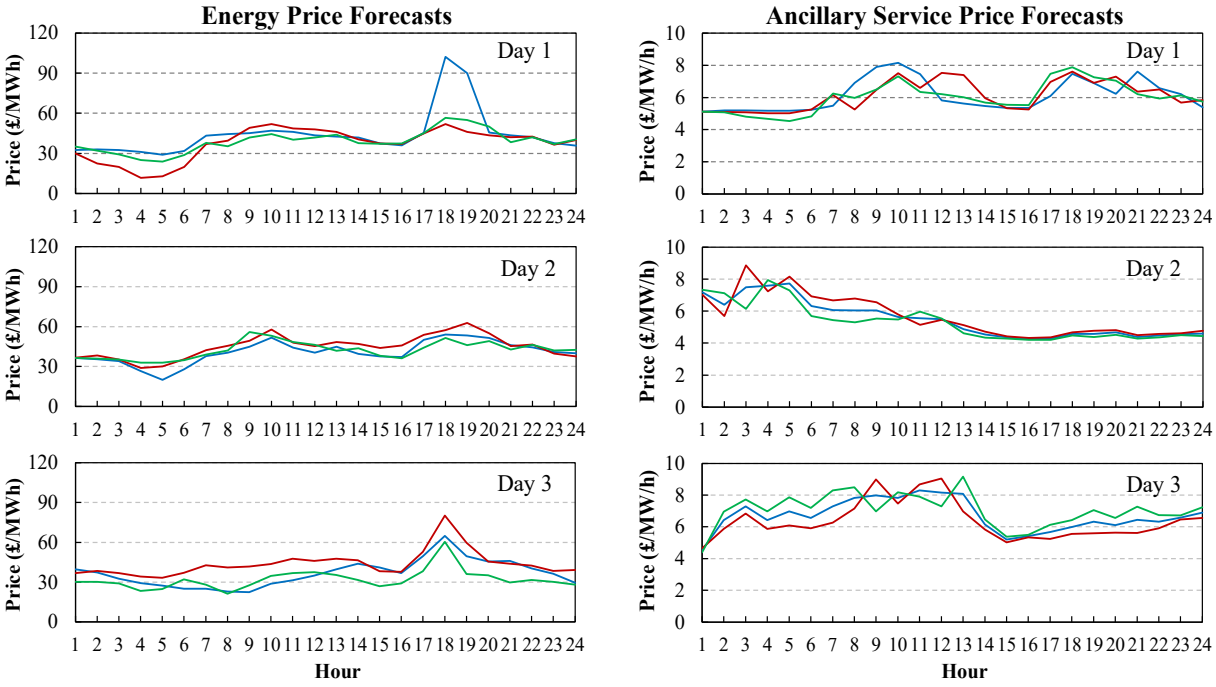


Fig. 2.3: Day-ahead energy and AS market prices.

Table 2.1: WF and ESS parameters

Maximum Charging/Discharging Power $\left(\overline{\mathrm{P}}\right)$	5 MW
Energy Capacity $\left(\overline{\mathrm{E}}\right)$	10 MW
Roundtrip Efficiency (η)	85%
WF Capacity $\left(\mathrm{K}^{\mathrm{W}}\right)$	50 MW

2.4.2 Value of providing ancillary services

The economic benefit of providing AS on top of energy-only market participation for the ESS and for the WF is assessed in this case study. As such, the value is assessed by comparing the profit expectation for two market participations: energy-only (EN) participation and energy and AS (EN-AS). The profit breakdown for each day and installation are illustrated in Figs. 2.4 and 2.5, while Table 2.2 presents the energy and total profits variation between both market participations for all days and installations.

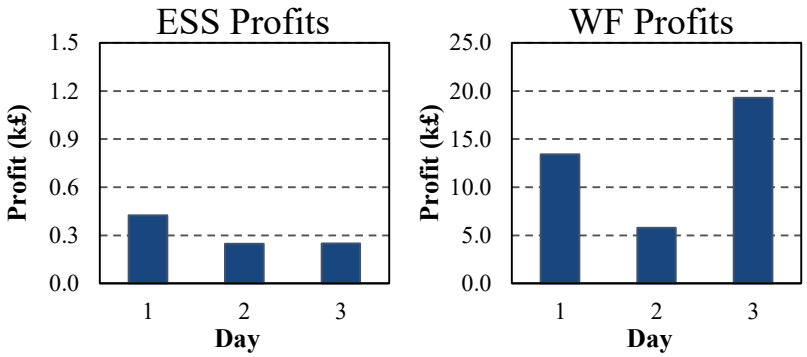


Fig. 2.4: Expected energy profits for the three days for the ESS (left) and the WF (right).

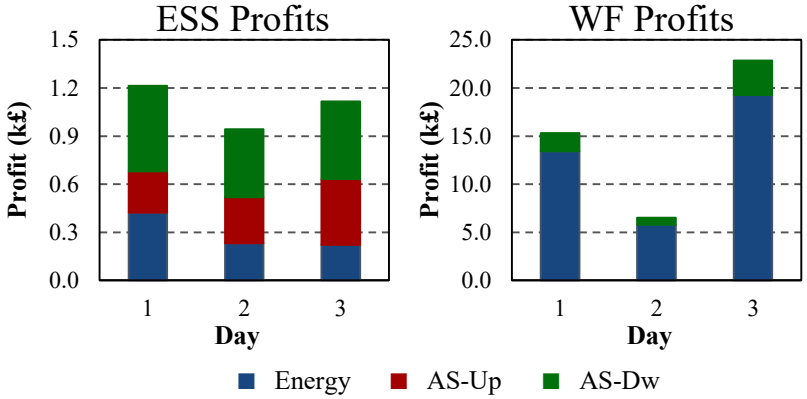


Fig. 2.5: Expected energy and AS profits for the three days for the ESS (left) and the WF (right).

Table 2.2: Profit variation (%) between both market participations for both installations

	ESS		WF	
Day	Energy	Total	Energy	Total
1	-0.60	185.82	0.00	14.17
2	-5.91	282.33	0.00	12.44
3	-11.72	346.01	0.00	18.50

Focusing on the ESS results from the EN market participation, energy profits vary between approximately £247 and £425 and are highly sensitive to prices. As was widely documented, ESS are able to generate profits by seizing arbitrage opportunities when price differentials between off-peak and peak times periods are economically efficient. In other words, when revenue generated from energy sales during discharging time periods is higher than the costs of purchasing energy plus losses (round-trip efficiency inferior to 1) to charge the ESS in off-peak times. Analysing the EN-AS results, it is possible to see that the provision of AS leads to significant profit increases ranging from £697 (Day 2) to £866 (Day

3), despite reducing expected energy market profit by up to £29. It should be noted that, at this stage, there is no information regarding the utilization of committed AS, thus the expected revenue from this market reflects the only payment for the availability for providing this service.

Regarding the WF, profits are mainly generated from selling expected wind generation. It should be noted that at this stage real-time wind generation is not known and that it is to be expected that actual energy delivery will be different. Regarding the provision of AS, as the prices for energy are higher than the availability payments for the AS, the WF operator will prioritize the sale of energy and provide AS by means of being available to reduce its generation output. Nevertheless, the provision of AS-Dw can increase profits ranging between £721 and £3,568.

Fig. 2.6 presents the optimal offering strategy for all days and facilities under the EN-AS market participation. The energy schedule for the ESS shows that the optimal hours for charging and discharging actions align with the expected low and high values for the energy prices, as previously mentioned. It can be observed that the offered AS quantities are higher than the maximum charging and discharging power limits due to the flexible nature of the ESS that allows it to change operation modes within the considered duration of each time period. For instance, in Day 1's hour 16 the committed quantity for AS-DW is 7.875 MW, which consists of reducing charging power by 5 MW and by increasing discharging power by 2.875 MW. Fig. 2.7 presents the resulting variation of the stored energy levels through the considered days. It should be noted that, as it is assumed that AS-Up and AS-Dw prices are the same for each time period, the ESS is fully charged in several time periods to provide AS-Up when it is in standby, i.e. neither charging or discharging. The WF bids show that in the majority of the time periods the quantities for AS-Dw match the energy bids. The exception occurs on Day 2 from hour 13 onwards when expected wind generation is lower than the minimum level of AS provision.

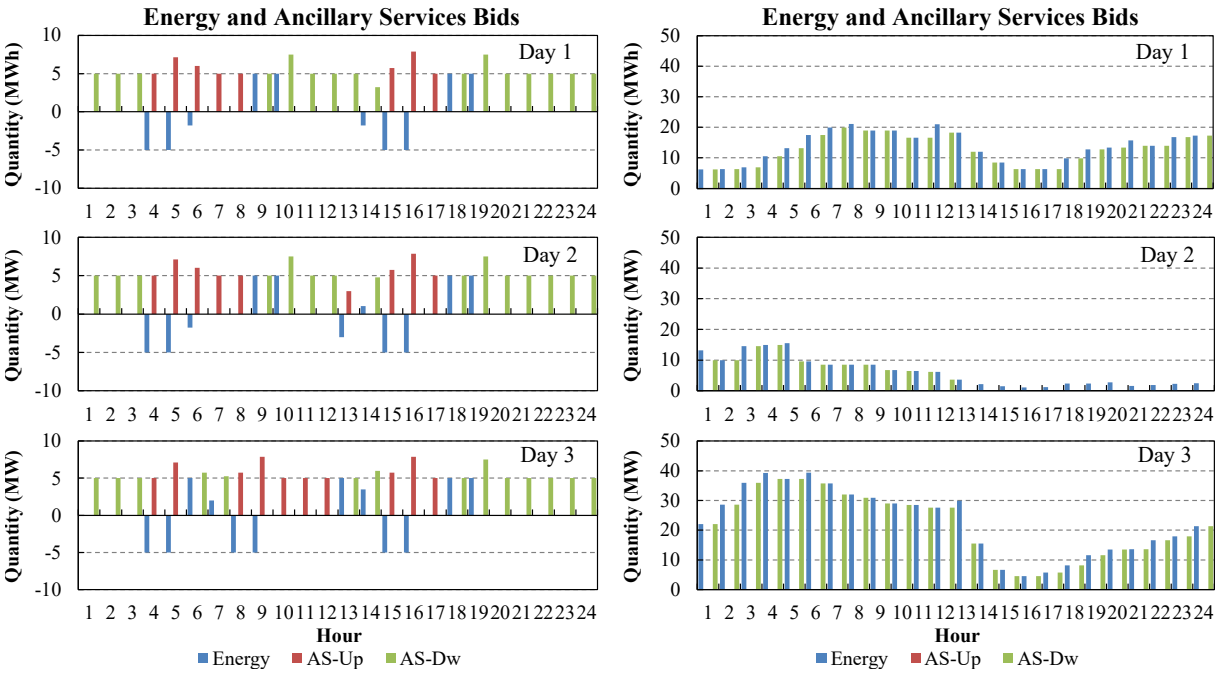


Fig. 2.6: Deterministic day-ahead energy and AS bids for the ESS (left) and the WF (right).

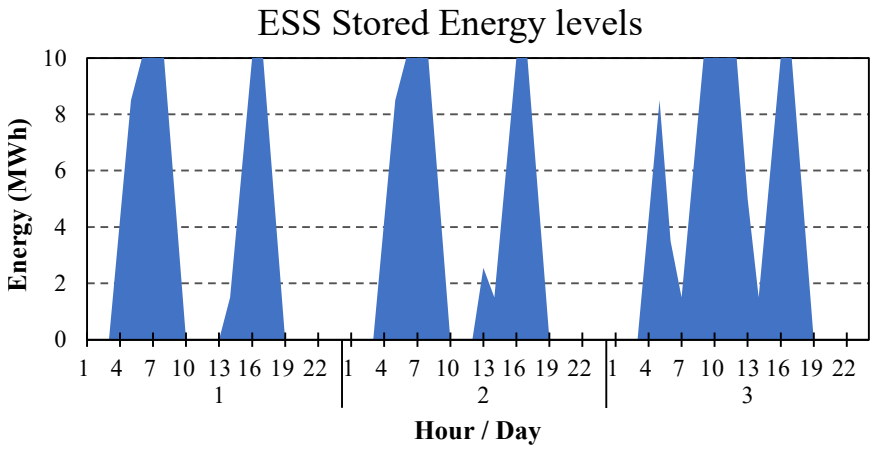


Fig. 2.7: Stored energy levels for the scheduled operation during the 3 days.

2.4.3 Performance against uncertainty

As previously mentioned, the increasing integration of intermittent wind generation leads to increasing uncertainty and volatility energy and AS prices. Coupled with wind generation uncertainty, deterministic models became unsuitable to optimize market operations. As such, this case study aims to analyse the performance of the bids determined in the previous case study against the different forecasts that comprise the uncertainty set in Subsection 2.4.1. For this purpose, a second MILP model was developed and its full formulation can be consulted in Appendix A. This model allows for either the ESS or the WF to settle energy and AS deviations between day-ahead bids and real-time provision, and thus maximizes the expected profit from energy and AS sales related to the bids determined previously minus the costs related to settling deviations.

Considering the stochastic nature of the assessment model, uncertainty is characterized by combining the sets of day-ahead energy and AS prices, and wind power availability forecasts. As such, one scenario is the combination of one forecast from each uncertainty set, which totals 450 scenarios for this model. Regarding the settlement of deviations, it is assumed for this case study that the price penalty factor for positive deviations $\left(\omega^{\mathrm{En/AS^{+}}}\right)$, i.e. surplus, are assumed to be 0.5, while for negative deviations, i.e. shortages, the penalty factor $\left(\omega^{\mathrm{En/AS^{-}}}\right)$ has been set to 1.5.

The performance of the deterministic bids can be assessed using three metrics: deviation of the deterministic profit expectation calculated in Subsection 2.4.2 from the expected value of the total profit distribution when exposed to uncertainty $(\Delta Profit)$; the probability of the deterministic bids resulting in losses $\left(p\left(Profit^{\mathrm{Sto}} < Profit^{\mathrm{Det}}\right)\right)$; standard deviation (STD) stochastic profit distribution $\left(\sigma^{\mathrm{Profit}}\right)$. The results for all days and facilities is summarized in Table 2.3.

Table 2.3: Performance of the deterministic bids against uncertainty

Facility	ESS			WF		
Day	1	2	3	1	2	3
$\Delta Profit$ (£)	0	0	0	-2568	-1558	-2015
$p\left(Profit^{\mathrm{Sto}} < Profit^{\mathrm{Det}}\right)$ (%)	66.7	44.4	44.4	96.4	93.3	74.0
σ^{Profit} (£)	151	39	39	1382	1235	3806

The results for the ESS show that $\Delta Profit$ is zero for all days, and this can be explained due to the fact

that the ESS is only exposed to pricing uncertainty. However, analysing the other two metrics leads to the conclusion that the ESS owner is likely to experience profits lower than initially calculated. In Day 1, the 67% probability of the profit being lower than the deterministic expectation translates in a maximum negative deviation of £179. On the other hand, the maximum positive profit deviation is £206 for this day. Days 2 and 3, feature a lower probability of the profit being below the deterministic expectation (44%) than Day 1 and maximum negative deviation of approximately 7% of the deterministic profit expectation. For the WF owner, as it's exposed to another source of uncertainty, negative deviations vary between 43% (Day 1) and 58% (Day 2) from the deterministic profit expectation and experience very high probabilities of achieving lower profits. It should be noted that wind generation is classified as a non-dispatchable and stochastic resource, therefore, using deterministic tools will result in considerably lower profits which could undermine the large-scale integration of renewable generation technologies, as it has been widely documented.

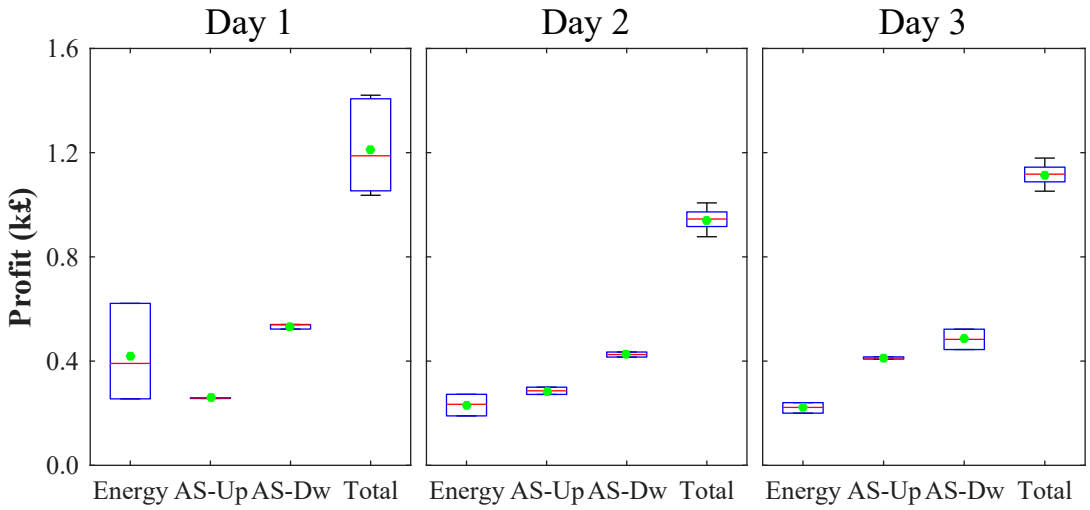


Fig. 2.8: ESS profit distribution when exposed to uncertainty for all days.

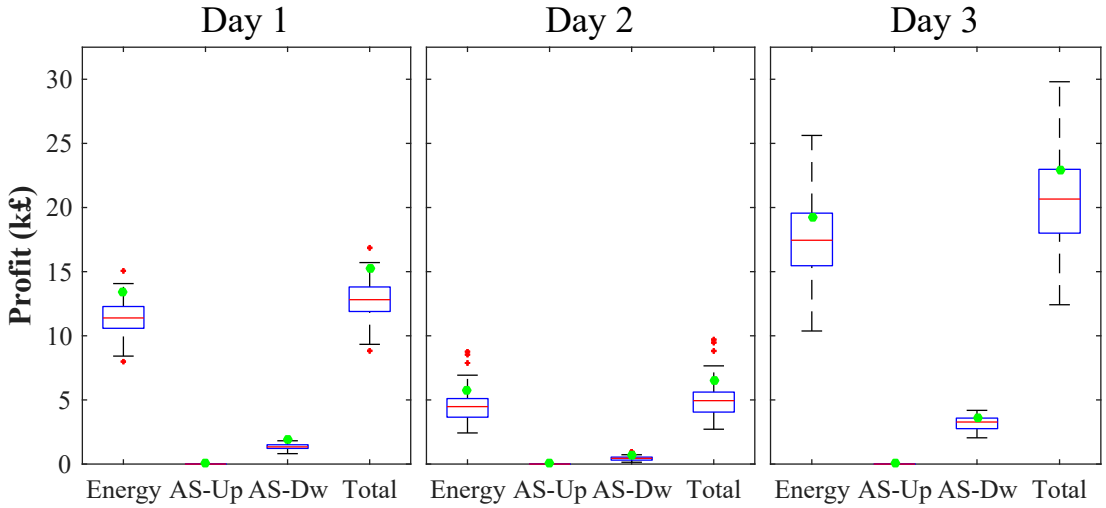


Fig. 2.9: WF profit distribution when exposed to uncertainty for all days.

A more visual representation of the profit distributions for the ESS and WF are presented in Figs. 2.8 and 2.9. Each Fig. illustrates the boxplot for each source of profit (Energy, AS-Up, AS-Dw and

Total) for all days. On each box, the central red line indicates the media, with the 25^{th} and the 75^{th} are respectively represented by the bottom and top edges of the box. Outliers are represented by the red plus signs, while extreme data points not considered outliers are represented by the whiskers. Lastly, the green dots represent the deterministic expectations calculated in Subsection 2.4.2. These plots reinforce the conclusion that deterministic models may lead to unexpected and potentially undesirable outcomes.

2.5 Chapter Conclusions

This chapter presented and analysed a deterministic ESS business model that comprised of provided energy arbitrage and an AS in the form of SPR. It also presented a deterministic bidding model for WF to provide downwards AS besides selling energy in the wholesale market.

The results show that providing an AS such as SPR can increase ESS daily profits by approximately 300% (average of the three days). As ESS can operate on the generation- and demand-side, the provision of AS can be executed in a more flexible manner which maximizes the revenue generated from the provision of this service. As the ESS is only exposed to prices uncertainty, the value of the deterministic profit expectation and the expected value of the profit distribution when exposed to uncertainty were the same, as expected. However, under the analysed circumstances, the risk of profits being lower than initially planned is still considerably high. As recovery of high investments is recognized as a significant barrier to the deployment of ESS, better tools are needed in order to guarantee revenue sufficiency for ESS investors.

Lastly, the modelling of the WF was fulfilled with the intent of establishing a base case to show the value of the models proposed in the following chapters. It also allows quantifying the value for a WF owner to provide AS, however the chosen deterministic approach is unsuitable considering the three assumed sources of uncertainty that the WF is exposed to. As such, the following chapters address this drawback by using two-stage stochastic programming methods to optimize the profit maximization problem.

Chapter 3

Risk-Neutral Wind Generation and Energy Storage Coordination Strategies

ESS have been widely proposed in literature as a facilitator in the integration of intermittent renewable resources. As such, the possibility of coordinated operating strategies for ESS and renewables such as wind generation has been of great interest for stakeholders looking to manage wind uncertainty. Despite the potential economic savings gained by the management of wind generation imbalance costs, these may not be enough to cover high investment costs associated with ESS. Therefore, the business models for WF and ESS coordination strategies must be upgraded in order to maximize its economic potential.

As analysed in Section 2.4 of the previous chapter, the provision of AS by ESS can lead to significant profit increases. Moreover, ESS flexibility and capacity to respond to uncertainty make it an ideal candidate to enhance the provision of SPR by WF. In this chapter a novel two-stage stochastic programming model in order to optimize the participation of WF in day-ahead energy and SPR markets through coordination with an ESS. In other words, this MILP model determines the optimal energy and SPR joint bidding strategy (JBS) in order to maximize profit generated in both markets.

The proposed coordination strategy is applied to two types of ESS: a generic ESS based on a Li-ion battery, and PHSP. The formulation of the second model (wind and PHSP coordination model) allows quantifying the value that a mature ESS technology with potential for large quantities of energy to be stored can bring to a WF. As such, this chapter is structured as follows: the nomenclature for both models in Sections 3.1 and 3.2; an Introduction which covers work related to this topic and detailed explanation of this proposal in 3.3; the mathematical formulation for both models in 3.4 and 3.5; the value of the proposed JBS for both models is analysed by series of case studies in Sections 3.6 and 3.7; Section 3.8 summarizes the conclusions from this chapter and identifies the avenues for improvement taken in the following chapters.

3.1 Wind-ESS Model Nomenclature

3.1.1 Indices, Sets and Sub-Sets

$e \in S^{\mathrm{E}}$ Day-ahead Energy price forecasts.

$r \in S^{\mathrm{R}}$ Day-ahead SPR price forecasts.

$w \in S^{\mathrm{W}}$ Day-ahead available wind power forecasts.

$h \in H$	Time periods.
Ω^{BV}	Set of all binary decision variables.
Ω^{CV}	Set of all continuous decision variables.
$\Omega^{\mathrm{CV^+}}$	Set of all positive continuous decision variables.
$\Omega^{\mathrm{SCV^+}}$	Set of all positive semi-continuous decision variables.
$\Omega^{\mathrm{CV^{SOS1}}}$	Set of all positive SOS1 continuous decision variables.

3.1.2 Parameters

$\mathrm{K^W}$	WF generation capacity [MW].
$\mathrm{P}^{\mathrm{AV}}_{w,h}$	Wind power availability at forecast w and time period h [p.u.].
η	Roundtrip efficiency of the ESS [p.u.].
$\overline{\mathrm{P}}$	Maximum charge/discharge rate of the ESS [MW].
$\overline{\mathrm{E}}$	Energy capacity of the ESS [MWh].
$\mathrm{E^{Min/Max}}$	Minimum/Maximum stored energy level in the ESS [p.u.].
$\pi^{\mathrm{En}}_{e,h}$	Energy market price at forecast e and time period h [£/MWh].
$\omega^{\mathrm{En^{+/-}}}_{e,h}$	Price penalty factor for positive/negative energy imbalances at forecast e and time period h [p.u.].
$\pi^{\mathrm{SPR,Up}}_{r,h}$	Upward SPR market price at forecast r and time period h [£/MW/h].
$\pi^{\mathrm{SPR,Dw}}_{r,h}$	Downward SPR market price at forecast r and time period h [£/MW/h].
$\omega^{\mathrm{SPR^{+/-}}}_{r,h}$	Price Penalty factor for positive/negative SPR imbalances at forecast r and time period h [p.u.].
τ^{SPR}	Maximum duration of the SPR requirement [h].
$\underline{\mathrm{SPR}}^{\mathrm{Up/Dw}}$	Minimum level for upward/downward SPR provision [MW].
ρ_e, ρ_r, ρ_w	Probability of each forecast e, r and w [p.u.].
M	Large number for constraint relaxation.

3.1.3 Binary Variables

$Q^{\mathrm{Up,D/C}}_{e,r,w,h}$	Commitment of upward SPR in discharging/charging mode for scenario e,r,w at time period h.
$Q^{\mathrm{Dw,D/C}}_{e,r,w,h}$	Commitment of downward SPR in discharging/charging mode for scenario e,r,w at time period h.

3.1.4 Continuous Variables

$e_{e,r,w,h}$	Energy stored in the ESS for scenario e,r,w at time period h [MWh].
$p^{\mathrm{C}}_{e,r,w,h}$	Power charged by the ESS for scenario e,r,w at time period h [MW].

$p^{\mathrm{D}}_{e,r,w,h}$ Power generated by the ESS for scenario e,r,w at time period h [MW].

$p^{\mathrm{W}}_{e,r,w,h}$ Power output of the WF for scenario e,r,w at time period h [MW].

$r^{\mathrm{Up,D/C}}_{e,r,w,h}$ Upward SPR contribution by the ESS during discharging/charging mode for scenario e,r,w at time period h [MW].

$r^{\mathrm{Dw,D/C}}_{e,r,w,h}$ Downward SPR contribution by the ESS during discharging/charging mode for scenario e,r,w at time period h [MW].

$r^{\mathrm{Up,W}}_{e,r,w,h}$ Upward SPR contribution of the WF for scenario e,r,w at time period h [MW].

$r^{\mathrm{Dw,W}}_{e,r,w,h}$ Downward SPR contribution of the WF for scenario e,r,w at time period h [MW].

$r^{\mathrm{Up}}_{e,r,w,h}$ Total Upward SPR contribution from both facilities for scenario e,r,w at time period h [MW].

$r^{\mathrm{Dw}}_{e,r,w,h}$ Total Downward SPR contribution from both facilities for scenario e,r,w at time period h [MW].

$i^{\mathrm{En}^{+/-}}_{e,r,w,h}$ Positive/Negative energy deviation from the day-ahead bid at scenario e,r,w, and time period h [MW].

$i^{\mathrm{SPR,Up}^{+/-}}_{e,r,w,h}$ Positive/Negative upward SPR deviation from the day-ahead bid at scenario e,r,w, and time period h [MW].

$i^{\mathrm{SPR,Dw}^{+/-}}_{e,r,w,h}$ Positive/Negative downward SPR deviation from the day-ahead bid at scenario e,r,w, and time period h [MW].

x^{En}_{h} Joint energy bid for time period h [MWh].

$x^{\mathrm{SPR,Up}}_{h}$ Joint upward SPR bid for time period h [MW].

$x^{\mathrm{SPR,Dw}}_{h}$ Joint downward SPR bid for time time period h [MW].

3.2 Wind-PHSP Model Nomenclature

3.2.1 Indices, Sets and Sub-Sets

$e \in S^{\mathrm{E}}$ Day-ahead Energy price forecasts.

$r \in S^{\mathrm{R}}$ Day-ahead SPR price forecasts.

$w \in S^{\mathrm{W}}$ Day-ahead available wind power forecasts.

$h \in H$ Time periods.

Ω^{IV} Set of all integer decision variables.

Ω^{BV} Set of all binary decision variables.

Ω^{CV} Set of all continuous decision variables.

$\Omega^{\mathrm{CV}^{+}}$ Set of all positive continuous decision variables.

$\Omega^{\mathrm{SCV}^{+}}$ Set of all positive semi-continuous decision variables.

$\Omega^{\mathrm{CV}^{\mathrm{SOS1}}}$ Set of all SOS1 decision variables.

3.2.2 Parameters

K^{W} WF generation capacity [MW].

$\mathrm{P}^{\mathrm{AV}}_{w,h}$ Wind power available at forecast w and time period h [p.u.].

$\mathrm{c}^{\mathrm{SU/SD,P}}$ SU and SD costs in pumping mode [£/start] [£/shutdown].

$\mathrm{c}^{\mathrm{SU/SD,T}}$ SU and SD costs in turbine mode [£/start] [£/shutdown].

$\underline{\mathrm{P}}^{\mathrm{P}}, \overline{\mathrm{P}}^{\mathrm{P}}$ Upper and lower power consumption limits for each pump-turbine unit in pumping mode [MW].

$\underline{\mathrm{P}}^{\mathrm{T}}, \overline{\mathrm{P}}^{\mathrm{T}}$ Upper and lower power generation limits for each pump-turbine unit in turbine mode[MW].

$\mathrm{N}^{\mathrm{units}}$ Number of identical pump-turbine units in the PHSP.

$\underline{\mathrm{V}}^{\mathrm{U}}, \overline{\mathrm{V}}^{\mathrm{U}}$ Lower and upper stored energy limits for the upper reservoir [MWh].

$\underline{\mathrm{V}}^{\mathrm{L}}, \overline{\mathrm{V}}^{\mathrm{L}}$ Lower and upper stored energy limits for the lower reservoir [MWh].

η Roundtrip efficiency of PHSP [p.u.].

$\pi^{\mathrm{En}}_{e,h}$ Energy market price at forecast e and time period h [£/MWh].

$\omega^{\mathrm{En}^{+/-}}_{e,h}$ Price penalty factor for positive/negative energy imbalances at forecast e and time period h [p.u.].

$\pi^{\mathrm{SPR,Up}}_{r,h}$ Upward SPR market price at forecast r and time period h [£/MW/h].

$\pi^{\mathrm{SPR,Dw}}_{r,h}$ Downward SPR market price at forecast r and time period h [£/MW/h].

$\omega^{\mathrm{SPR}^{+/-}}_{r,h}$ Price penalty factor for positive/negative SPR imbalances at forecast r and time period h [p.u.].

τ^{SPR} Maximum duration of SPR [h].

$\underline{\mathrm{SPR}}^{\mathrm{Up/Dw}}$ Minimum level for upward/downward SPR provision [MW].

ρ_e, ρ_r, ρ_w Probability of each forecast e, r and w [pu].

M Large number for constraint relaxation.

3.2.3 Binary Variables

$B^{\mathrm{En}}_{e,r,w,h}$ Indicates if the energy imbalance is positive or negative at scenario e, r, w and time period h.

$B^{\mathrm{SPR,Up}}_{e,r,w,h}$ Indicates if the upward SPR imbalance is positive or negative at scenario e, r, w and time period h.

$B^{\mathrm{SPR,Dw}}_{e,r,w,h}$ Indicates if the downward SPR imbalance is positive or negative at scenario e, r, w and time period h.

$Q^{\mathrm{Up,T/P}}_{e,r,w,h}$ Commitment of upward SPR in turbine/pumping mode at scenario e, r, w and time period h.

$Q^{\text{Dw,T/P}}_{e,r,w,h}$ Commitment of downward SPR in turbine/pumping mode at scenario e,r,w and time period h.

$T_{e,r,w,h}$ Indicates wether the PHSP is working or not in turbine mode at scenario e,r,w and time period h.

3.2.4 Integer Variables

$U^{\text{P,On}}_{e,r,w,h}$ Number of online units that are in pumping mode at scenario e,r,w and time period h.

$U^{\text{P,On,SD}}_{e,r,w,h}$ Number of online units that are in pumping mode and need to be SD due to provision of SPR at scenario e,r,w and time period h.

$U^{\text{P,Off}}_{e,r,w,h}$ Number of offline units that are in pumping mode at scenario e,r,w and time period h.

$U^{\text{T,On}}_{e,r,w,h}$ Number of online units that are in turbine mode at scenario e,r,w and time period h.

$U^{\text{T,On,SD}}_{e,r,w,h}$ Number of online units that are in turbine mode and need to be SD due to provision of SPR at scenario e,r,w and time period h.

$U^{\text{T,Off}}_{e,r,w,h}$ Number of offline units that are in turbine mode at scenario e,r,w and time period h.

$Y^{\text{P}}_{e,r,w,h}, Z^{\text{P}}_{e,r,w,h}$ Number of SU and SD events in pumping mode at scenario e,r,w and time period h.

$Y^{\text{T}}_{e,r,w,h}, Z^{\text{T}}_{e,r,w,h}$ Number of SU and SD events in turbine mode at scenario e,r,w and time period h.

3.2.5 Continuous Variables

$v^{\text{U}}_{e,r,w,h}$ Energy stored in the upper reservoir at scenario e,r,w, and time period h [MWh].

$v^{\text{L}}_{e,r,w,h}$ Energy stored in the lower reservoir at scenario e,r,w, and time period h [MWh].

$p^{\text{P}}_{e,r,w,h}$ Power consumed in pumping mode at scenario e,r,w, and time period h [MW].

$p^{\text{T}}_{e,r,w,h}$ Power generated in turbine mode at scenario e,r,w and time period h [MW].

$p^{\text{W}}_{e,r,w,h}$ Power output of the WF at scenario e,r,w and time period h [MW].

$i^{\text{En}^{+/-}}_{e,r,w,h}$ Positive/Negative energy deviation from the day-ahead bid at scenario e,r,w and time period h [MW].

$i^{\text{SPR,Up}^{+/-}}_{e,r,w,h}$ Positive/Negative SPR-Up deviation from the day-ahead bid at scenario e,r,w and time period h [MW].

$i^{\text{SPR-Dw}^{+/-}}_{e,r,w,h}$ Positive/Negative SPR-Dw deviation from the day-ahead bid at scenario e,r,w and time period h [MW].

$r^{\text{Up,T,On}}_{e,r,w,h}$ Upward SPR contribution of online units in turbine mode at scenario e,r,w and time period h [MW].

$r^{\text{Up,T,Off}}_{e,r,w,h}$ Upward SPR contribution of offline units in turbine mode at scenario e,r,w and time period h [MW].

$r^{\text{Dw,T}}_{e,r,w,h}$ Downward SPR contribution in turbine mode at scenario e,r,w and time period h [MW].

$r^{\text{Up,P}}_{e,r,w,h}$ Upward SPR contribution in pumping mode at scenario e,r,w and time period h [MW].

$r^{\text{Dw,P,On}}_{e,r,w,h}$ Downward SPR contribution of online units in pumping mode at scenario e,r,w and time period h [MW].

$r^{\text{Dw,P,Off}}_{e,r,w,h}$ Downward SPR contribution of offline units in pumping mode at scenario e,r,w and time period h [MW]

$r^{\text{Up,W}}_{e,r,w,h}$ Upward SPR contribution of the WF at scenario e,r,w and time period h [MW].

$r^{\text{Dw,W}}_{e,r,w,h}$ Downward SPR contribution of the WF at scenario e,r,w and time period h [MW].

x^{En}_{h} Joint energy bid for time period h [MW].

$x^{\text{SPR-Up}}_{h}$ Joint upward SPR bid for time period h [MW].

$x^{\text{SPR-Dw}}_{h}$ Joint downward SPR bid for time time period h [MW].

3.3 Introduction

3.3.1 Literature Review

As analysed in last chapter's Section 2.2, the value of the provision of AS, such as SPR, from ESS and WF has been widely investigated in current literature [15, 22, 23, 56]. The economic results of [15] show that the provision of reserve from WF can potentially amount to approximately 1% in generation costs savings, while the authors of [65] show that earnings of up to €8,000/MW can be achieved by providing negative tertiary control reserve, despite being heavily influenced by the quality of wind speed forecasts. [22] estimates that the potential revenue from the provision of a single service is but a fraction of the total revenue created by the aggregation of the multiple application such as energy arbitrage, reduction of time of use energy costs for residential customers, reduction of energy costs of residential solar PV systems and deferral of distribution network upgrades. The results in this paper show that the potential benefit for aggregation of these different services can amount to $4,603 during a 5 year period for a small scale ESS. The authors of [23] have found that an ESS's cycle efficiency and discharge duration heavily influence potential profits from energy arbitrage in the face of price fluctuations in the day-ahead electricity markets in the Netherlands. These price fluctuations could, in turn, influence the revenue generated from the aggregated provision of different services by an ESS.

An analysis of the benefits of the different types of ESS can bring to Finland's electricity market is carried out in [66]. The authors note that the implementation of new market regulations will allow ESS to simultaneously provide energy arbitrage and balancing services in order to achieve profitability. Chazarra et al. demonstrated in [56] that the highest source of revenue for a PHSP equipped with variable speed pumps comes from the provision of secondary regulation reserve. [67] determines the bidding strategy for a PHSP that maximizes profit in the face of rising wind generation uncertainty, which shows that the SPR market revenue becomes the most significant component of the PHSP's profit. Contrary to the two previous papers, Lagarto et al. propose in [68] an optimal scheduling strategy for PHSP with VS pumps in the day-ahead energy and secondary reserve markets that achieves higher profitability.

Stochastic programming approaches are used in [69] and [70] to determine the optimal bidding strategies for ESS under pricing uncertainty. The former shows how profits generated from participating in day-ahead energy and reserve markets is affected by the impact of size and location of the ESS,

while the latter shows that profits can be increased up to 7.93% for the analysed day using stochastic programming. A bi-level model to determine the most beneficial trading actions in day-ahead energy and reserve pool-based markets with balancing settlements by ESS is proposed in [71]. The authors take a price-maker approach for the ESS and consider net-demand uncertainty to reach the conclusion that ESS have the potential influence market outcomes through strategic price and quantity offers. [72] analyses the benefit of providing reserve in all operating modes for a PHSP through a stochastic unit commitment model.

The coordination of ESS and renewable generation technologies has garnered considerable attention in the last decade [26, 32, 73]. While [26] presents a stochastic model for the management of wind imbalances with a PHSP in order to reduce penalty costs for day-ahead energy deviations (profit increases of up to 4% per day), the authors of [73] present a more sceptic view on the coordination of co-located CAES and WF with downsized transmission. The latter argues that the value of reducing transmission costs is not as high as the value that CAES can provide while load-site. The authors also note that with increasing wind penetration, the value of co-location may become more attractive. Offering and operating strategies for price-making WF-ESS in day-ahead markets is analysed in [74], in which the potential value of price-making strategies being significantly larger than through price-taking strategies (an average of 15.33% profit increase). The coordinated provision of energy and SPR by combined WF and ESS is analysed by Rodrigues et al. in [75]. Taking into account uncertainty in day-ahead energy prices and wind power availability, the WF-ESS coordination strategy can reach profit increases of up to 13% and reduce expected energy imbalances by up to 50%.

Despite the provision of AS by ESS and WF, and their coordination being widely studied in literature, this chapter addresses a gap in understanding the full range of services that can be provided by combined WF-ESS in the day-ahead markets and their offering strategies are affected by pricing and generation uncertainty. While WF-ESS coordination strategies are approached in [26, 73], the consideration of uncertainty is only applied to energy bidding and disregard the provision of AS by both facilities. Although [15, 76] consider the possibility of WF providing reserve through wind deration, generation uncertainty is disregarded. Generation uncertainty is considered in [72, 75], which investigate the impact of generation uncertainty in the provision of AS, but lack the consideration of uncertainty in the price of these services.

3.3.2 Joint Energy and SPR Bidding Strategies for WF and ESS

This chapter proposes a JBS that allows optimizing the participation of a WF in the day-ahead energy and SPR markets by operating in coordination with an ESS in order to manage exposure to uncertainty and maximizing expected profit. It is assumed that the WF seeks to minimize costs associated with managing deviations between day-ahead bids and real-time generation, i.e. imbalances, and to provide AS such as SPR with more confidence by resorting to the flexibility provided by an ESS, such as Li-ion battery or a PHSP. As the WF is affected by generation and pricing uncertainty, the models presented herein are formulated as two-stage stochastic MILP models that incorporate uncertain parameters such as energy and SPR prices, and wind power availability forecasts. Imbalances are settled on the day of delivery through a balancing mechanism in which the operator is given the opportunity to sell excess resources or by paying for shortages. A computationally efficient tight reformulation using SOS1 variables for calculating the value of energy and SPR imbalances is also proposed.

The WF and ESS are assumed to be either co-operated locally through a single owner or as part of a consortium between owning companies without co-located resources. In both cases, it is assumed that the operator of the WF and the ESS submits one set of energy and SPR (upwards and downwards) bids, instead of submitting two sets of bids. Fig. 3.1 presents a conceptual diagram in order to better illustrate the differences of a JBS against an uncoordinated bidding strategy (UBS).

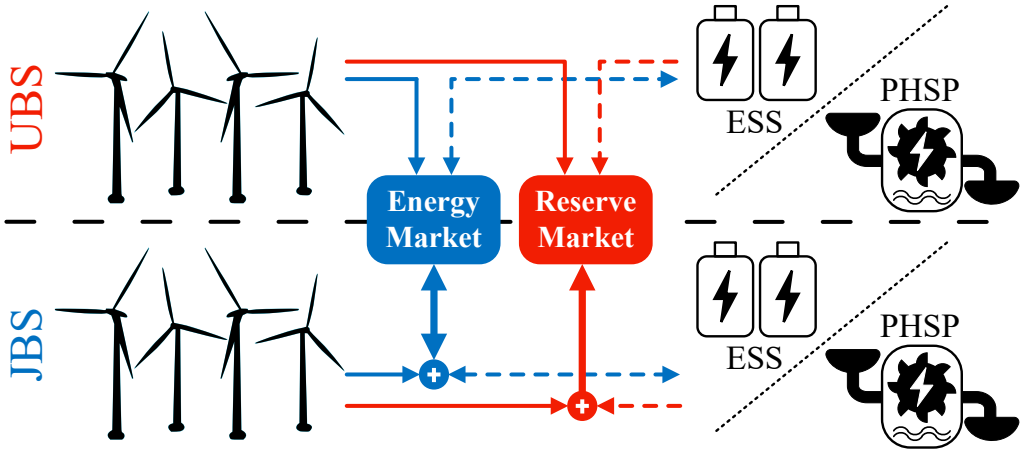


Fig. 3.1: Graphical representation of the difference between the Uncoordinated (red) and the Joint (blue) Bidding Strategies.

The main benefit of the JBS translates into higher profits given the ESS's two modes of operation in order to manage positive and negative wind deviations, thus reducing costs associated with the settlement of negative imbalances or (potential) lower revenue from selling surplus wind generation. In certain time periods, excess wind generation can be used to charge the ESS (or pump water in the case of the PHSP) for later use when wind generation is lower than scheduled in the day-ahead market. This type of coordination also allows for a better utilization of wind energy which improves the efficiency of renewables' investment and lowers dependency on carbon-emitting flexible generation resources. The day-ahead energy and SPR markets described in Section 2.3 are considered for this model as well.

As was pointed out in Chapter 1 of this Thesis, the uncertain and highly variable nature of wind generation requires more sophisticated tools that allow taking more informed decisions and reduce exposure to low-profit scenarios. Dealing with uncertainty has been studied extensively in literature through the application of multi-stage stochastic programming [46, 47] or through robust optimization [77, 78]. Stochastic programming has been applied widely to power systems in [79–81], while robust optimization has been attracting further interest due to the reduced complexity when compared to stochastic programming [82–84]. Despite the computational advantage of robust optimization over stochastic programming, the former may lead to very conservative solutions. In stochastic optimization, it is assumed that uncertainty evolves over time as a discrete process that can be approximated by a finite probability distribution in the problem formulation in the form of a set of scenarios for the random variables. In two-stage stochastic models, the first stage decisions correspond to actions that must be taken before the outcome of the random variables is known (*here-and-now* decisions), while second sage decisions are actions that are taken after the outcome of the random variables is known (*wait-and-see* decisions). As the operation of WF and the ESS is affected by different sources of uncertainty, the work proposed in this chapter considers uncertainty related to day-ahead energy price, SPR price and wind power availability.

3.4 Stochastic Wind and Generic ESS Model

3.4.1 Key Properties and Assumptions

The model proposed in this section is classified as MILP with the objective of solving a two-stage stochastic optimization problem [85] of a WF operator looking to maximize the daily expected profit achieved from the participation in the day-ahead energy and SPR markets with the support of an ESS in order to manage offering uncertainty. In the first-stage of the stochastic problem, the operator must define its day-ahead energy and SPR bidding strategy. While in the second-stage, all variables related to the operation of the WF and the ESS in the provision of energy and SPR are considered recourse actions against the reveal of the uncertain parameters [86]. It is also assumed, as proposed in [15, 76], that the WF can also provide SPR despite wind power availability limitations.

This model considers three types of day-ahead uncertainty: energy prices (e), SPR prices (r) and available wind power (w) forecasts. It is also assumed that the WF and ESS are not large enough in size to directly influence prices and adopt a price-taker approach. As such, this work considers that a scenario is a combination of one energy price forecast, SPR price forecast and wind power availability forecast with a respective probability $(\rho_e \times \rho_r \times \rho_w)$.

Considering that wind generation is affected by uncertainty, imbalances (deviations between submitted day-ahead bids and scenario realizations) are bound to arise. Therefore, an imbalance settlement scheme which penalizes the WF-ESS operator on the absolute value of the deviations at a percentage of the market price is considered here. This imbalance settlement scheme allows the operator to settle real-time deviations through an adjustment auction on the day of delivery, such as the Balancing Mechanism operated by Elexon in the UK [87]. This fundamentally allows for either selling excess energy or paying for energy not delivered through an imbalance settlement scheme using a pair of cash-out prices similar to the System-Buy-Price/System-Sell-Prices. Finally, the model calculates the optimal day-ahead JBS with a time resolution of 1 hour, reason why the time period duration is omitted in the model formulation. The objective function and constraints of this model are presented in Subsections 3.4.2 and 3.4.3, respectively.

3.4.2 Objective Function

3.4.2.1 Non-Linear Objective Function

The objective of the WF and ESS operator is to maximize the expected profit for the scheduled day given in (3.1), which is comprised of the sum of revenues generated from the participation in the day-ahead energy and SPR markets defined in the 1st to 3rd lines in (3.1), minus the sum of the costs of settling energy and SPR imbalances given by lines 4 to 6 in (3.1).

This objective function penalizes imbalances based on the absolute value of the deviation and at a percentage over the market price during each scenario and time period. The presence of absolute value functions in objective function (3.1) make the model a Mixed-Integer Non-Linear Programming (MINLP) problem, which is computationally demanding for large numbers of scenarios and complex to achieve to optimality [88]. Nonetheless, the linearisation of absolute value functions has been widely documented and easily implemented [89]. The following subsection, details the linearisation and objective function reformulation adopted in this work.

$$\underset{\substack{\Omega^{\mathrm{BV}},\Omega^{\mathrm{CV}},\Omega^{\mathrm{CV}^+},\\ \Omega^{\mathrm{SCV}^+},\Omega^{\mathrm{CV}^{\mathrm{SOS1}}}}}{\text{Maximize}} \Bigg\{ \sum_{e\in\mathcal{S}^{\mathrm{E}}}\sum_{r\in\mathcal{S}^{\mathrm{R}}}\sum_{w\in\mathcal{S}^{\mathrm{W}}} \rho_e\rho_r\rho_w \sum_{h\in H} \Big[\pi^{\mathrm{En}}_{e,h}\left(p^{\mathrm{W}}_{e,r,w,h}+p^{\mathrm{D}}_{e,r,w,h}-p^{\mathrm{C}}_{e,r,w,h}\right)$$
$$+\pi^{\mathrm{SPR,Up}}_{r,h}\left(r^{\mathrm{Up,W}}_{e,r,w,h}+r^{\mathrm{Up,D}}_{e,r,w,h}+r^{\mathrm{Up,C}}_{e,r,w,h}\right)$$
$$+\pi^{\mathrm{SPR,Dw}}_{r,h}\left(r^{\mathrm{Dw,W}}_{e,r,w,h}+r^{\mathrm{Dw,D}}_{e,r,w,h}+r^{\mathrm{Dw,C}}_{e,r,w,h}\right) \tag{3.1}$$
$$-\omega^{\mathrm{En}}_{e,h}\pi^{\mathrm{En}}_{e,h}\left|p^{\mathrm{W}}_{e,r,w,h}+p^{\mathrm{D}}_{e,r,w,h}-p^{\mathrm{C}}_{e,r,w,h}-x^{\mathrm{En}}_{h}\right|$$
$$-\omega^{\mathrm{SPR}}_{r,h}\pi^{\mathrm{SPR,Up}}_{r,h}\left|r^{\mathrm{Up,W}}_{e,r,w,h}+r^{\mathrm{Up,D}}_{e,r,w,h}+r^{\mathrm{Up,C}}_{e,r,w,h}-x^{\mathrm{SPR,Up}}_{h}\right|$$
$$-\omega^{\mathrm{SPR}}_{r,h}\pi^{\mathrm{SPR,Dw}}_{r,h}\left|r^{\mathrm{Dw,W}}_{e,r,w,h}+r^{\mathrm{Dw,D}}_{e,r,w,h}+r^{\mathrm{Dw,C}}_{e,r,w,h}-x^{\mathrm{SPR,Dw}}_{h}\right| \Big] \Bigg\}.$$

3.4.2.2 Linearisation of Absolute Value Functions

Traditionally, absolute value functions are linearized by means of using additional auxiliary continuous variables for positive and negative deviations and a binary variable to enforce or relax the bounds of those continuous variables and ensuring that either the positive or the negative auxiliary variable is positive at any given time. However, in order to avoid using binary variables and further computationally taxing the model, this work makes use of SOS1 variables to define each pair of positive and negative imbalance variables $\left(i^{\mathrm{En/SPR}^+}_{e,r,w,h}, i^{\mathrm{En/SPR}^-}_{e,r,w,h}\right)$, which is then interpreted by the model's solver to only allow one variable of each pair to be positive at any scenario and time period. The auxiliary variables for positive (surplus) and negative (shortage) energy and SPR (upward and downward) deviations are defined in equalities (3.2), (3.5) and (3.8) and bounded in constraints (3.3), (3.4), (3.6), (3.7), (3.9) and (3.10).

$$p^{\mathrm{W}}_{e,r,w,h}+p^{\mathrm{D}}_{e,r,w,h}-p^{\mathrm{C}}_{e,r,w,h}-x^{\mathrm{En}}_{h}=i^{\mathrm{En}^+}_{e,r,w,h}-i^{\mathrm{En}^-}_{e,r,w,h},\quad \forall e,r,w,h, \tag{3.2}$$

$$0\le i^{\mathrm{En}^+}_{e,r,w,h}\le \mathrm{P}^{\mathrm{AV}}_{w,h}\mathrm{K}^{\mathrm{W}}+2\overline{\mathrm{P}},\quad \forall e,r,w,h, \tag{3.3}$$

$$0\le i^{\mathrm{En}^-}_{e,r,w,h}\le \mathrm{K}^{\mathrm{W}}+2\overline{\mathrm{P}},\quad \forall e,r,w,h, \tag{3.4}$$

$$r^{\mathrm{Up,W}}_{e,r,w,h}+r^{\mathrm{Up,D}}_{e,r,w,h}+r^{\mathrm{Up,C}}_{e,r,w,h}-x^{\text{SPR-Up}}_{h}=i^{\mathrm{SPR,Up}^+}_{e,r,w,h}-i^{\mathrm{SPR,Up}^-}_{e,r,w,h},\quad \forall e,r,w,h, \tag{3.5}$$

$$0\le i^{\mathrm{SPR,Up}^+}_{e,r,w,h}\le \mathrm{P}^{\mathrm{AV}}_{w,h}\mathrm{K}^{\mathrm{W}}-p^{\mathrm{W}}_{e,r,w,h}+\overline{\mathrm{P}}-p^{\mathrm{D}}_{e,r,w,h}+p^{\mathrm{C}}_{e,r,w,h},\quad \forall e,r,w,h, \tag{3.6}$$

$$0\le i^{\mathrm{SPR,Up}^-}_{e,r,w,h}\le \mathrm{K}^{\mathrm{W}}+2\overline{\mathrm{P}},\quad \forall e,r,w,h, \tag{3.7}$$

$$r^{\mathrm{Dw,W}}_{e,r,w,h}+r^{\mathrm{Dw,D}}_{e,r,w,h}+r^{\mathrm{Dw,C}}_{e,r,w,h}-x^{\text{SPR-Dw}}_{h}=i^{\mathrm{SPR,Dw}^+}_{e,r,w,h}-i^{\mathrm{SPR,Dw}^-}_{e,r,w,h},\quad \forall e,r,w,h, \tag{3.8}$$

$$0\le i^{\mathrm{SPR,Dw}^+}_{e,r,w,h}\le p^{\mathrm{W}}_{e,r,w,h}+p^{\mathrm{D}}_{e,r,w,h}+\overline{\mathrm{P}}-p^{\mathrm{C}}_{e,r,w,h},\quad \forall e,r,w,h, \tag{3.9}$$

$$0\le i^{\mathrm{SPR,Dw}^-}_{e,r,w,h}\le \mathrm{K}^{\mathrm{W}}+2\overline{\mathrm{P}},\quad \forall e,r,w,h. \tag{3.10}$$

As discussed in Subsection 3.4.1, the operator of the WF and the ESS is given the opportunity of settling deviations through an adjustment auction in the day of delivery which utilizes a pair of cash-out prices. For simplicity's sake, these are assumed to be directly related to the day-ahead energy market

prices through positive and negative price penalty factors $\left(\omega_{e,h}^{\mathrm{En}^+} < \omega_{e,h}^{\mathrm{En}^-}\right)$. The same concept is applied to the SPR bids, in which failure to provide the volume in the day-ahead bid is penalized over the market price. Thus the objective function considered for this model is given by (3.11).

$$\begin{aligned}\underset{\substack{\Omega^{\mathrm{BV}},\Omega^{\mathrm{CV}},\Omega^{\mathrm{CV}^+},\\ \Omega^{\mathrm{SCV}^+},\Omega^{\mathrm{CV}^{\mathrm{SOS1}}}}}{\text{Maximize}} \Bigg\{ \sum_{e\in S^{\mathrm{E}}}\sum_{r\in S^{\mathrm{R}}}\sum_{w\in S^{\mathrm{W}}} \rho_e\rho_r\rho_w \Bigg[\sum_{h\in H} \Big(& \pi_{e,h}^{\mathrm{En}} x_h^{\mathrm{En}} + \omega_{r,h}^{\mathrm{En}^+}\pi_{e,h}^{\mathrm{En}} i_{e,r,w,h}^{\mathrm{En}^+} - \omega_{e,h}^{\mathrm{En}^-}\pi_{e,h}^{\mathrm{En}} i_{e,r,w,h}^{\mathrm{En}^-} \\ & + \pi_{r,h}^{\mathrm{SPR,Up}} x_h^{\mathrm{SPR,Up}} + \omega_{r,h}^{\mathrm{SPR}^+}\pi_{r,h}^{\mathrm{SPR,Up}} i_{e,r,w,h}^{\mathrm{SPR,Up}^+} - \omega_{r,h}^{\mathrm{SPR}^-}\pi_{r,h}^{\mathrm{SPR,Up}} i_{e,r,w,h}^{\mathrm{SPR,Up}^-} \\ & + \pi_{r,h}^{\mathrm{SPR,Dw}} x_h^{\mathrm{SPR,Dw}} + \omega_{r,h}^{\mathrm{SPR}^+}\pi_{r,h}^{\mathrm{SPR,Dw}} i_{e,r,w,h}^{\mathrm{SPR,Dw}^+} - \omega_{r,h}^{\mathrm{SPR}^-}\pi_{r,h}^{\mathrm{SPR,Dw}} i_{e,r,w,h}^{\mathrm{SPR,Dw}^-} \Big) \Bigg] \Bigg\}.\end{aligned} \tag{3.11}$$

3.4.3 Model Constraints

3.4.3.1 Generation and Energy Limits

Constraints (3.12) and (3.13) enforce maximum charge and discharge power limits, respectively. It should be noted that this formulation dispenses the use of binary variable in order to ensure that there isn't simultaneous charging and discharging actions, and relies instead in defining $p_{e,r,w,h}^{\mathrm{C}}$ and $p_{e,r,w,h}^{\mathrm{D}}$ as a SOS1 variable pair to achieve the same effect. Stored energy balance and limits are given by equalities (3.14) and constraints (3.15), respectively. Wind power generation is limited to forecasted wind power availability in constraints (3.16).

$$p_{e,r,w,h}^{\mathrm{C}} \le \overline{\mathrm{P}}, \quad \forall e,r,w,h, \tag{3.12}$$

$$p_{e,r,w,h}^{\mathrm{D}} \le \overline{\mathrm{P}}, \quad \forall e,r,w,h, \tag{3.13}$$

$$e_{e,r,w,h} = e_{e,r,w,h-1} + \eta\, p_{e,r,w,h}^{\mathrm{C}} - p_{e,r,w,h}^{D}, \quad \forall e,r,w,h, \tag{3.14}$$

$$\mathrm{E}^{\mathrm{Min}}\cdot\overline{\mathrm{E}} \le e_{e,r,w,h} \le \mathrm{E}^{\mathrm{Max}}\cdot\overline{\mathrm{E}}, \quad \forall e,r,w,h, \tag{3.15}$$

$$p_{e,r,w,h}^{\mathrm{W}} \le \mathrm{P}_{w,h}^{\mathrm{AV}}\mathrm{K}^{\mathrm{W}}, \quad \forall e,r,w,h. \tag{3.16}$$

3.4.3.2 SPR Provision

The provision of SPR by the ESS can be flexibly achieved in both operating modes in each time period. In charging mode, the ESS can provide SPR-Dw by increasing power consumption (constraints (3.17)) and SPR-Up is provided by reducing power consumption (constraints (3.18)). While in discharging mode, the provision of SPR-Up is done by increasing power generation (constraints (3.19)) and SPR-Dw by decreasing power generation (constraints (3.20)). Moreover, the flexibility of an ESS, such as a Li-ion battery, allows it to quickly change operating modes and being able to provide larger quantities of SPR. For example, SPR-Up can be provided by decreasing current power consumption and supplying power to the grid. SPR-Dw can be provided in a symmetrical manner. The contribution of the WF to the provision of SPR is done in constraints (3.21) and (3.22).

$$p_{e,r,w,h}^{\mathrm{C}} + r_{e,r,w,h}^{\mathrm{Dw,C}} \le \overline{\mathrm{P}}, \quad \forall e,r,w,h, \tag{3.17}$$

$$r_{e,r,w,h}^{\mathrm{Up,C}} \le p_{e,r,w,h}^{\mathrm{C}}, \quad \forall e,r,w,h, \tag{3.18}$$

$$p^{\mathrm{D}}_{e,r,w,h} + r^{\mathrm{Up,D}}_{e,r,w,h} \leq \overline{\mathrm{P}}, \quad \forall e,r,w,h, \tag{3.19}$$

$$r^{\mathrm{Dw,D}}_{e,r,w,h} \leq p^{\mathrm{D}}_{e,r,w,h}, \quad \forall e,r,w,h, \tag{3.20}$$

$$p^{\mathrm{W}}_{e,r,w,h} + r^{\mathrm{Up,W}}_{e,r,w,h} \leq \mathrm{P}^{\mathrm{AV}}_{w,h}\mathrm{K}^{\mathrm{W}}, \quad \forall e,r,w,h, \tag{3.21}$$

$$r^{\mathrm{Dw,W}}_{e,r,w,h} \leq p^{\mathrm{W}}_{e,r,w,h}, \quad \forall e,r,w,h. \tag{3.22}$$

3.4.3.3 Service Deliverability Constraints

The coordination of the WF and ESS allows the operator to take advantage of the characteristics of each technology in order to maximize revenue generated from the provision of SPR. As such, total provision of SPR-Up and SPR-Dw from both facilities is defined in equalities (3.23) and (3.24). As in Subsection 2.3.3.2, it is assumed that in order to participate in the SPR market, the operator of these facilities must provide a minimum level of SPR at all time periods $\left(\underline{\mathrm{SPR}}^{\mathrm{Up/Dw}}\right)$. However, through the coordination of the WF and the ESS, the minimum levels for SPR provision applies to both facilities and is given by constraints (3.25) and (3.26). Note that, like in the previous chapter's model, these constraints make $r^{\mathrm{Up}}_{e,r,w,h}$ and $r^{\mathrm{Dw}}_{e,r,w,h}$ semi-continuous variables allowing them to be zero if $\underline{\mathrm{SPR}}^{\mathrm{Up/Dw}}$is not achievable in some time periods.

$$r^{\mathrm{Up}}_{e,r,w,h} = r^{\mathrm{Up,C}}_{e,r,w,h} + r^{\mathrm{Up,D}}_{e,r,w,h} + r^{\mathrm{Up,W}}_{e,r,w,h}, \quad \forall e,r,w,h, \tag{3.23}$$

$$r^{\mathrm{Dw}}_{e,r,w,h} = r^{\mathrm{Dw,C}}_{e,r,w,h} + r^{\mathrm{Dw,D}}_{e,r,w,h} + r^{\mathrm{Dw,W}}_{e,r,w,h}, \quad \forall e,r,w,h, \tag{3.24}$$

$$r^{\mathrm{Up}}_{e,r,w,h} \leq \begin{cases} \mathrm{K}^{\mathrm{W}} + 2\overline{\mathrm{P}} & , r^{\mathrm{Up,C}}_{e,r,w,h} + r^{\mathrm{Up,D}}_{e,r,w,h} + r^{\mathrm{Up,W}}_{e,r,w,h} \geq \underline{\mathrm{SPR}}^{\mathrm{Up}} \\ 0 & , r^{\mathrm{Up,C}}_{e,r,w,h} + r^{\mathrm{Up,D}}_{e,r,w,h} + r^{\mathrm{Up,W}}_{e,r,w,h} < \underline{\mathrm{SPR}}^{\mathrm{Up}} \end{cases}, \quad \forall e,r,w,h, \tag{3.25}$$

$$r^{\mathrm{Dw}}_{e,r,w,h} \leq \begin{cases} \mathrm{K}^{\mathrm{W}} + 2\overline{\mathrm{P}} & , r^{\mathrm{Dw,C}}_{e,r,w,h} + r^{\mathrm{Dw,D}}_{e,r,w,h} + r^{\mathrm{Dw,W}}_{e,r,w,h} \geq \underline{\mathrm{SPR}}^{\mathrm{Dw}} \\ 0 & , r^{\mathrm{Dw,C}}_{e,r,w,h} + r^{\mathrm{Dw,D}}_{e,r,w,h} + r^{\mathrm{Dw,W}}_{e,r,w,h} < \underline{\mathrm{SPR}}^{\mathrm{Dw}} \end{cases}, \quad \forall e,r,w,h. \tag{3.26}$$

It should be noted that, unlike conventional generation, ESS are stored energy-constrained resources. Therefore, sufficient stored energy in the ESS must be ensured in order to provide SPR for the entire maximum commitment time duration required by the TSO $\left(\tau^{\mathrm{SPR}}\right)$, which for this formulation is assumed to be larger or equal than the simulation time-step. In order to achieve this objective, a set of disjunctive constraints ((3.27) to (3.34)) based on the constraints presented in Subsection 2.3.3.2 are added to this formulation for each scenario and time period. Although this model does not consider uncertainty regarding the utilization of committed SPR services, these constraints ensure that the SPR bidding strategy is robust against service utilization uncertainty.

$$\begin{aligned} \mathrm{E}^{\mathrm{Min}} \cdot \overline{\mathrm{E}} - \mathrm{M}\left(1 - Q^{\mathrm{Up,D}}_{e,r,w,h}\right) \leq e_{e,r,w,h-1} + \eta\, p^{\mathrm{C}}_{e,r,w,h} - \left(p^{\mathrm{D}}_{e,r,w,h} + r^{\mathrm{Up,D}}_{e,r,w,h}\right)\tau^{\mathrm{SPR}} \leq \mathrm{E}^{\mathrm{Max}} \cdot \overline{\mathrm{E}} + \\ \mathrm{M}\left(1 - Q^{\mathrm{Up,D}}_{e,r,w,h}\right), \quad \forall e,r,w,h, \end{aligned} \tag{3.27}$$

$$\begin{aligned} \mathrm{E}^{\mathrm{Min}} \cdot \overline{\mathrm{E}} - \mathrm{M}\left(1 - Q^{\mathrm{Dw,D}}_{e,r,w,h}\right) \leq e_{e,r,w,h-1} + \eta\, p^{\mathrm{C}}_{e,r,w,h} - \left(p^{\mathrm{D}}_{e,r,w,h} - r^{\mathrm{Dw,D}}_{e,r,w,h}\right)\tau^{\mathrm{SPR}} \leq \mathrm{E}^{\mathrm{Max}} \cdot \overline{\mathrm{E}} + \\ \mathrm{M}\left(1 - Q^{\mathrm{Dw,D}}_{e,r,w,h}\right), \quad \forall e,r,w,h, \end{aligned} \tag{3.28}$$

$$\begin{aligned} \mathrm{E}^{\mathrm{Min}} \cdot \overline{\mathrm{E}} - \mathrm{M}\left(1 - Q^{\mathrm{Up,C}}_{e,r,w,h}\right) \leq e_{e,r,w,h-1} + \eta \left(p^{\mathrm{C}}_{e,r,w,h} - r^{\mathrm{Up,C}}_{e,r,w,h}\right) \tau^{\mathrm{SPR}} - p^{\mathrm{D}}_{e,r,w,h} \leq \mathrm{E}^{\mathrm{Max}} \cdot \overline{\mathrm{E}} \\ + \mathrm{M}\left(1 - Q^{\mathrm{Up,C}}_{e,r,w,h}\right), \quad \forall e, r, w, h, \end{aligned} \tag{3.29}$$

$$\begin{aligned} \mathrm{E}^{\mathrm{Min}} \cdot \overline{\mathrm{E}} - \mathrm{M}\left(1 - Q^{\mathrm{Dw,C}}_{e,r,w,h}\right) \leq e_{e,r,w,h-1} + \eta \left(p^{\mathrm{C}}_{e,r,w,h} + r^{\mathrm{Dw,C}}_{e,r,w,h}\right) \tau^{\mathrm{SPR}} - p^{\mathrm{D}}_{e,r,w,h} \leq \mathrm{E}^{\mathrm{Max}} \cdot \overline{\mathrm{E}} \\ + \mathrm{M}\left(1 - Q^{\mathrm{Dw,C}}_{e,r,w,h}\right), \quad \forall e, r, w, h, \end{aligned} \tag{3.30}$$

$$r^{\mathrm{Up,D}}_{e,r,w,h} \leq \mathrm{M}\, Q^{\mathrm{Up,D}}_{e,r,w,h}, \quad \forall e, r, w, h, \tag{3.31}$$

$$r^{\mathrm{Dw,D}}_{e,r,w,h} \leq \mathrm{M}\, Q^{\mathrm{Dw,D}}_{e,r,w,h}, \quad \forall e, r, w, h, \tag{3.32}$$

$$r^{\mathrm{Up,C}}_{e,r,w,h} \leq \mathrm{M}\, Q^{\mathrm{Up,C}}_{e,r,w,h}, \quad \forall e, r, w, h, \tag{3.33}$$

$$r^{\mathrm{Dw,C}}_{e,r,w,h} \leq \mathrm{M}\, Q^{\mathrm{Dw,C}}_{e,r,w,h}, \quad \forall e, r, w, h. \tag{3.34}$$

As the WF is assumed provide SPR along with the ESS, its stochastic nature must be taken into account when defining the level of SPR provided by the WF. In other words, wind power availability during the commitment period $\left(\tau^{\mathrm{SPR}}\right)$ must be sufficient to provide SPR for its entire duration. This modelling aspect is accomplished through constraints (3.35) and (3.36). These constraints fundamentally ensure that at any time period h, the total amount of provided SPR is limited by generation availability during all time periods between h and $h + \tau^{\mathrm{SPR}}$. Note that, through the proposed JBS, the provision of SPR by the WF is enhanced by the support of the ESS.

$$\begin{aligned} \left(p^{\mathrm{W}}_{e,r,w,t} + p^{\mathrm{C}}_{e,r,w,t} - p^{D}_{e,r,w,t}\right) + \left(r^{\mathrm{Up,W}}_{e,r,w,h} + r^{\mathrm{Up,D}}_{e,r,w,h} + r^{\mathrm{Up,C}}_{e,r,w,h}\right) \\ \leq \mathrm{P}^{\mathrm{AV}}_{w,t} \mathrm{K}^{\mathrm{W}} + \overline{\mathrm{P}}, \quad \forall e, r, w, h,\ h \leq t < h + \tau^{\mathrm{SPR}}, \end{aligned} \tag{3.35}$$

$$\begin{aligned} \left(p^{\mathrm{W}}_{e,r,w,t} + p^{\mathrm{C}}_{e,r,w,t} - p^{D}_{e,r,w,t}\right) - \left(r^{\mathrm{Dw,W}}_{e,r,w,h} + r^{\mathrm{Dw,D}}_{e,r,w,h} + r^{\mathrm{Dw,C}}_{e,r,w,h}\right) \\ \geq -\overline{\mathrm{P}}, \quad \forall e, r, w, h,\ h \leq t < h + \tau^{\mathrm{SPR}}. \end{aligned} \tag{3.36}$$

3.4.3.4 Bid Limits

The bounds for the joint energy and both SPR bids are established in constraints (3.37) and (3.38). The energy and SPR-Up bids are limited by the ESS and WF generation capacities, while the SPR-Dw bids are limited by current energy bids and the ESS maximum charging capacity.

$$x^{\mathrm{En}}_{h} + x^{\mathrm{SPR,Up}}_{h} \leq \mathrm{K}^{\mathrm{W}} + \overline{\mathrm{P}}, \quad \forall h, \tag{3.37}$$

$$x^{\mathrm{En}}_{h} - x^{\mathrm{SPR,Dw}}_{h} \geq -\overline{\mathrm{P}}, \quad \forall h. \tag{3.38}$$

3.4.3.5 Variable Types

Lastly, the sign and type of all decision variables is given by equalities (3.39) and (3.43).

$$\Omega^{\mathrm{BV}} = \left\{Q^{\mathrm{Up,D}}_{e,r,w,h}, Q^{\mathrm{Dw,D}}_{e,r,w,h}, Q^{\mathrm{Up,C}}_{e,r,w,h}, Q^{\mathrm{Dw,C}}_{e,r,w,h}\right\} \in \{0,1\}, \quad \forall e, r, w, h, \tag{3.39}$$

$$\Omega^{\mathrm{CV}} = \left\{x^{\mathrm{En}}_{h}\right\} \in \mathbb{R}, \quad \forall h, \tag{3.40}$$

$$\Omega^{\mathrm{SCV}^{+}} = \left\{r^{\mathrm{Up}}_{e,r,w,h}, r^{\mathrm{Dw}}_{e,r,w,h}, x^{\mathrm{SPR,Up}}_{h}, x^{\mathrm{SPR,Dw}}_{h}\right\} \in \mathbb{R}_{\geq 0}, \quad \forall e, r, w, h, \tag{3.41}$$

$$\Omega^{\mathrm{CV}^{\mathrm{SOS1}}} = \left\{ \left(p^{\mathrm{D}}_{e,r,w,h}, p^{\mathrm{C}}_{e,r,w,h}\right), \left(i^{\mathrm{En}^{+}}_{e,r,w,h}, i^{\mathrm{En}^{-}}_{e,r,w,h}\right), \left(i^{\mathrm{SPR,Up}^{+}}_{e,r,w,h}, i^{\mathrm{SPR,Up}^{-}}_{e,r,w,h}\right), \left(i^{\mathrm{SPR,Dw}^{+}}_{e,r,w,h}, i^{\mathrm{SPR,Dw}^{-}}_{e,r,w,h}\right) \right\} \in \mathbb{R}_{\geq 0} \quad \forall e, r, w, h, \tag{3.42}$$

$$\Omega^{\mathrm{CV}^{+}} = \left\{ p^{\mathrm{W}}_{e,r,w,h}, e_{e,r,w,h}, r^{\mathrm{Up,D}}_{e,r,w,h}, r^{\mathrm{Up,C}}_{e,r,w,h}, r^{\mathrm{Dw,D}}_{e,r,w,h}, r^{\mathrm{Dw,C}}_{e,r,w,h}, r^{\mathrm{Up,W}}_{e,r,w,h}, r^{\mathrm{Dw,W}}_{e,r,w,h} \right\} \in \mathbb{R}_{\geq 0}, \quad \forall e, r, w, h. \tag{3.43}$$

3.5 Wind and PHSP Model

3.5.1 Key Properties and Assumptions

This model is formulated as a two-stage stochastic MILP problem, in which the operator (single owner or a consortium) determines the day-ahead energy and SPR (upward and downward) bidding strategy that maximizes expected daily profit. The key properties and assumptions identified in Subsection 3.4.1 are valid here except where noted. This model adapts the JBS model proposed in the previous Section in order to consider the characteristics of a PHSP.

It is assumed that the PHSP functions in only one operating mode - turbine mode (generating) or pumping mode (consumption) - within the same time period. The fundamental difference between this model and the previous one lies in the provision of SPR, whereas previously the ESS could provide a higher quantity of SPR by quickly changing operating modes (e.g. SPR-Up could be provided by reducing current power consumption and increasing generating power). The enforcement of this assumption relies on the fact PHSP with reversible pump-turbine units are characterized by non-negligible minimum SU and SD times [90]. However, as these times are much lower than the assumed duration for each time period (1 hour), minimum SU and SD times are disregarded and SU and SD costs for each pump-turbine unit are considered instead.

3.5.2 Objective Function

3.5.2.1 Non-Linear Objective Function

$$\begin{aligned}
\underset{\substack{\Omega^{\mathrm{IV}},\Omega^{\mathrm{BV}},\Omega^{\mathrm{CV}} \\ \Omega^{\mathrm{CV}^{+}},\Omega^{\mathrm{SCV}^{+}}\Omega^{\mathrm{CV}^{\mathrm{SOS1}}}}}{\text{Maximize}} \Bigg\{ & \sum_{e\in S^{\mathrm{E}}} \sum_{r\in S^{\mathrm{R}}} \sum_{w\in S^{\mathrm{W}}} \rho_e \rho_r \rho_w \sum_{h\in H} \Big[\pi^{\mathrm{En}}_{e,h} \left(p^{\mathrm{W}}_{e,r,w,h} + p^{\mathrm{T}}_{e,r,w,h} - p^{\mathrm{P}}_{e,r,w,h} \right) \\
& - \left(\mathrm{c}^{\mathrm{SU,P}} Y^{\mathrm{P}}_{e,r,w,h} + \mathrm{c}^{\mathrm{SU,T}} Y^{\mathrm{T}}_{e,r,w,h} + \mathrm{c}^{\mathrm{SD,P}} Z^{\mathrm{P}}_{e,r,w,h} + \mathrm{c}^{\mathrm{SD,T}} Z^{\mathrm{T}}_{e,r,w,h} \right) \\
& + \pi^{\mathrm{SPR,Up}}_{r,h} \left(r^{\mathrm{Up,W}}_{e,r,w,h} + r^{\mathrm{Up,T,On}}_{e,r,w,h} + r^{\mathrm{Up,T,Off}}_{e,r,w,h} + r^{\mathrm{Up,P}}_{e,r,w,h} \right) \\
& + \pi^{\mathrm{SPR,Dw}}_{r,h} \left(r^{\mathrm{Dw,W}}_{e,r,w,h} + r^{\mathrm{DwT}}_{e,r,w,h} + r^{\mathrm{Dw,P,On}}_{e,r,w,h} + r^{\mathrm{Dw,P,Off}}_{e,r,w,h} \right) \\
& - \left(\mathrm{c}^{\mathrm{SU,P}} U^{\mathrm{P,Off}}_{e,r,w,h} + \mathrm{c}^{\mathrm{SU,T}} U^{\mathrm{T,Off}}_{e,r,w,h} + \mathrm{c}^{\mathrm{SD,P}} U^{\mathrm{P,On,SD}}_{e,r,w,h} + \mathrm{c}^{\mathrm{SD,T}} U^{\mathrm{T,On,SD}}_{e,r,w,h} \right) \\
& - \omega^{\mathrm{En}}_{e,h} \pi^{\mathrm{En}}_{e,h} \left| p^{\mathrm{W}}_{e,r,w,h} + p^{\mathrm{T}}_{e,r,w,h} - p^{\mathrm{P}}_{e,r,w,h} - x^{\mathrm{En}}_{h} \right| \\
& - \omega^{\mathrm{SPR}}_{r,h} \pi^{\mathrm{SPR,Up}}_{r,h} \left| r^{\mathrm{Up,W}}_{e,r,w,h} + r^{\mathrm{Up,T,On}}_{e,r,w,h} + r^{\mathrm{Up,T,Off}}_{e,r,w,h} + r^{\mathrm{Up,P}}_{e,r,w,h} - x^{\mathrm{SPR,Up}}_{h} \right| \\
& - \omega^{\mathrm{SPR}}_{r,h} \pi^{\mathrm{SPR,Dw}}_{r,h} \left| r^{\mathrm{Dw,W}}_{e,r,w,h} + r^{\mathrm{DwT}}_{e,r,w,h} + r^{\mathrm{Dw,P,On}}_{e,r,w,h} + r^{\mathrm{Dw,P,Off}}_{e,r,w,h} - x^{\mathrm{SPR,Dw}}_{h} \right| \Big] \Bigg\}.
\end{aligned} \tag{3.44}$$

The objective function (3.44) maximizes the total expected profit from all scenarios and time periods. The profit for each scenario is comprised by the revenue from the day-ahead energy and SPR markets (1st, 3rd and 4th lines in (3.44)), minus costs associated with SU and SD events of the PHSP (2nd and 5th lines)

and associated with deviations between day-ahead bids and second-stage decisions, i.e. delivered energy and availability for providing SPR (6^{th} to 9^{th} lines). Note that the 5^{th}line of (3.44) represents additional costs that may be incurred by SU (SD) offline (online) pump-turbine units due to the provision of SPR services allowing for more informed decisions to be made.

The above objective function considers penalties for deviating from submitted day-ahead bids (imbalances), which are assumed to be proportional to the absolute value of the imbalance and to the associated price in the same time period. As in the previously presented objective function (3.1), absolute value functions are easily linearised by means of auxiliary variables for positive and negative deviations in order to transform a MINLP into a MILP.

3.5.2.2 Tight Reformulation for absolute value function linearisation

As in Subsection 3.4.2.2, the absolute value functions for the energy and SPR imbalances are separated into continuous positive and negative terms through equalities (3.45), (3.48) and (3.51). Each pair of positive and negative auxiliary imbalance variables $\left(i^{\text{En/SPR}^+}_{e,r,w,h}, i^{\text{En/SPR}^-}_{e,r,w,h}\right)$ are defined as a SOS1 pair of positive continuous variables, and with the modelling of several pump-turbine units in this model, a more computational efficient tight reformulation of the absolute value functions can be achieved. In other words, the combined use of SOS1 and integer variables allows for the positive and negative variables' bounds to be dynamically tightened, decreasing the computational burden of the model when compared to using fixed bounds or binary variables. Fig. 3.2 exemplifies how this tight reformulation allows reducing the solution space for the absolute value of the positive energy imbalances. The leftmost plot represents the solution space for the positive energy imbalance in a given scenario and time period when these are limited with fixed bounds (red and blue regions) and are dependent on the energy bid, wind power generation and the PHSP's power injection. The contribution of the tight reformulation is shown the plots towards the right, in which the solution space is reduced first by bounding it to the operating mode $\left(T_{e,r,w,h}\right)$ and is further reduced depending on the number of online units in each operating mode.

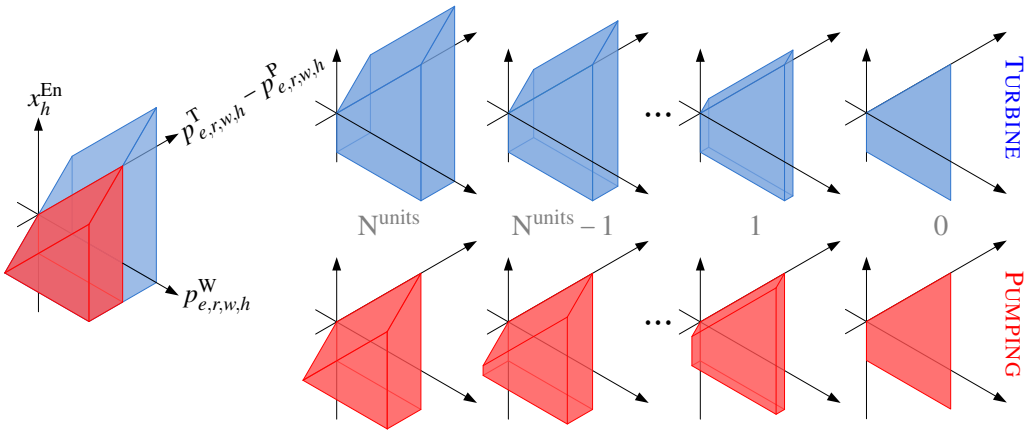


Fig. 3.2: Reduction of the solution space for the positive energy imbalances due to the proposed tight formulation.

Constraints (3.46), (3.47), (3.49), (3.50), (3.52) and (3.53) present the upper and lower bounds for the positive and negative energy and SPR imbalances. Note that these bounds depend not only on the technical limitations of the WF and the pump-turbine units, but also on the online/offline status of each unit, as explained in the previous paragraph.

$$p^{\mathrm{W}}_{e,r,w,h} + p^{\mathrm{T}}_{e,r,w,h} - p^{\mathrm{P}}_{e,r,w,h} - x^{\mathrm{En}}_{h} = i^{\mathrm{En}^+}_{e,r,w,h} - i^{\mathrm{En}^-}_{e,r,w,h}, \quad \forall e,r,w,h, \tag{3.45}$$

$$0 \le i^{\mathrm{En}^+}_{e,r,w,h} \le \mathrm{P}^{\mathrm{AV}}_{w,h}\mathrm{K}^{\mathrm{W}} + U^{\mathrm{T,On}}_{e,r,w,h}\overline{\mathrm{P}}^{\mathrm{T}} - U^{\mathrm{P,On}}_{e,r,w,h}\underline{\mathrm{P}}^{\mathrm{P}} + N^{\mathrm{units}}\overline{\mathrm{P}}^{\mathrm{P}}, \quad \forall e,r,w,h, \tag{3.46}$$

$$0 \le i^{\mathrm{En}^-}_{e,r,w,h} \le -U^{\mathrm{T,On}}_{e,r,w,h}\underline{\mathrm{P}}^{\mathrm{T}} + U^{\mathrm{P,On}}_{e,r,w,h}\overline{\mathrm{P}}^{\mathrm{P}} + \mathrm{K}^{\mathrm{W}} + N^{\mathrm{units}}\overline{\mathrm{P}}^{\mathrm{T}}, \quad \forall e,r,w,h, \tag{3.47}$$

$$r^{\mathrm{Up,W}}_{e,r,w,h} + r^{\mathrm{Up,T,On}}_{e,r,w,h} + r^{\mathrm{Up,T,Off}}_{e,r,w,h} + r^{\mathrm{Up,P}}_{e,r,w,h} - x^{\mathrm{SPR,Up}}_{h} = i^{\mathrm{SPR\text{-}Up}^+}_{e,r,w,h} - i^{\mathrm{SPR\text{-}Up}^-}_{e,r,w,h}, \quad \forall e,r,w,h, \tag{3.48}$$

$$0 \le i^{\mathrm{SPR,Up}^+}_{e,r,w,h} \le \mathrm{P}^{\mathrm{AV}}_{w,h}\mathrm{K}^{\mathrm{W}} - p^{\mathrm{W}}_{e,r,w,h} + U^{\mathrm{T,On}}_{e,r,w,h}\overline{\mathrm{P}}^{\mathrm{T}} - p^{\mathrm{T}}_{e,r,w,h} + U^{\mathrm{T,Off}}_{e,r,w,h}\overline{\mathrm{P}}^{\mathrm{T}} + p^{\mathrm{P}}_{e,r,w,h}, \quad \forall e,r,w,h, \tag{3.49}$$

$$0 \le i^{\mathrm{SPR,Up}^-}_{sh} \le \max\left\{\overline{\mathrm{P}}^{\mathrm{P}}, \overline{\mathrm{P}}^{\mathrm{T}}\right\}\mathrm{N}^{\mathrm{units}} + \mathrm{K}^{\mathrm{W}}, \quad \forall e,r,w,h, \tag{3.50}$$

$$r^{\mathrm{Dw,W}}_{e,r,w,h} + r^{\mathrm{DwT}}_{e,r,w,h} + r^{\mathrm{Dw,P,On}}_{e,r,w,h} + r^{\mathrm{Dw,P,Off}}_{e,r,w,h} - x^{\mathrm{SPR,Dw}}_{h} = i^{\mathrm{SPR,Dw}^+}_{e,r,w,h} - i^{\mathrm{SPR,Dw}^-}_{e,r,w,h}, \quad \forall e,r,w,h, \tag{3.51}$$

$$0 \le i^{\mathrm{SPR,Dw}^+}_{e,r,w,h} \le p^{\mathrm{W}}_{e,r,w,h} + p^{\mathrm{T}}_{e,r,w,h} + U^{\mathrm{P,On}}_{e,r,w,h}\overline{\mathrm{P}}^{\mathrm{P}} - p^{\mathrm{P}}_{e,r,w,h} + U^{\mathrm{P,Off}}_{e,r,w,h}\overline{\mathrm{P}}^{\mathrm{P}}, \quad \forall e,r,w,h, \tag{3.52}$$

$$0 \le i^{\mathrm{SPR,Dw}^-}_{e,r,w,h} \le \max\left\{\overline{\mathrm{P}}^{\mathrm{P}}, \overline{\mathrm{P}}^{\mathrm{T}}\right\}\mathrm{N}^{\mathrm{units}} + \mathrm{K}^{\mathrm{W}}, \quad \forall e,r,w,h. \tag{3.53}$$

Through this reformulation, (3.44) is transformed into the linear objective function (3.54).

$$\begin{aligned}
\underset{\substack{\Omega^{\mathrm{BV}},\Omega^{\mathrm{CV}},\Omega^{\mathrm{CV}^+},\\ \Omega^{\mathrm{SCV}^+},\Omega^{\mathrm{CV^{SOS1}}}}}{\text{Maximize}} \Bigg\{ & \sum_{e\in S^{\mathrm{E}}}\sum_{r\in S^{\mathrm{R}}}\sum_{w\in S^{\mathrm{W}}} \rho_e\rho_r\rho_w \Bigg[\sum_{h\in H} \Big(\pi^{\mathrm{En}}_{e,h} x^{\mathrm{En}}_{h} + \omega^{\mathrm{En}^+}_{e,h}\pi^{\mathrm{En}}_{e,h} i^{\mathrm{En}^+}_{e,r,w,h} - \omega^{\mathrm{En}^-}_{e,h}\pi^{\mathrm{En}}_{e,h} i^{\mathrm{En}^-}_{e,r,w,h} \\
& - \left(\mathrm{c}^{\mathrm{SU,P}}Y^{\mathrm{P}}_{e,r,w,h} + \mathrm{c}^{\mathrm{SU,T}}Y^{\mathrm{T}}_{e,r,w,h} + \mathrm{c}^{\mathrm{SD,P}}Z^{\mathrm{P}}_{e,r,w,h} + \mathrm{c}^{\mathrm{SD,T}}Z^{\mathrm{T}}_{e,r,w,h}\right) \\
& + \pi^{\mathrm{SPR,Up}}_{r,h} x^{\mathrm{SPR,Up}}_{h} + \omega^{\mathrm{SPR}^+}_{r,h}\pi^{\mathrm{SPR,Up}}_{r,h} i^{\mathrm{SPR,Up}^+}_{e,r,w,h} - \omega^{\mathrm{SPR}^-}_{r,h}\pi^{\mathrm{SPR,Up}}_{r,h} i^{\mathrm{SPR,Up}^-}_{e,r,w,h} \\
& + \pi^{\mathrm{SPR,Dw}}_{r,h} x^{\mathrm{SPR,Dw}}_{h} + \omega^{\mathrm{SPR}^+}_{r,h}\pi^{\mathrm{SPR,Dw}}_{r,h} i^{\mathrm{SPR,Dw}^+}_{e,r,w,h} - \omega^{\mathrm{SPR}^-}_{r,h}\pi^{\mathrm{SPR,Dw}}_{r,h} i^{\mathrm{SPR,Dw}^-}_{e,r,w,h} \\
& - \left(\mathrm{c}^{\mathrm{SU,P}}U^{\mathrm{P,Off}}_{e,r,w,h} + \mathrm{c}^{\mathrm{SU,T}}U^{\mathrm{T,Off}}_{e,r,w,h} + \mathrm{c}^{\mathrm{SD,P}}U^{\mathrm{P,On,SD}}_{e,r,w,h} + \mathrm{c}^{\mathrm{SD,T}}U^{\mathrm{T,On,SD}}_{e,r,w,h}\right)\Big) \Bigg] \Bigg\}.
\end{aligned} \tag{3.54}$$

3.5.3 Model Constraints

3.5.3.1 Reservoir Constraints

Traditionally, PHSP modelling represents stored energy in the form of the volume of water in each of the reservoirs. However, for this model the volume of water stored in each reservoir was chosen to be represented in terms of potential energy. As such, equations (3.55) and (3.56) update the amount of stored energy in the upper and lower reservoirs, respectively, while constraints (3.57) and (3.58) enforce reservoir capacity limits. Note that initial (h=0) and final (h=24) stored energy levels are determined by the model in order to maximize revenue.

$$v^{\mathrm{U}}_{e,r,w,h} = v^{\mathrm{L}}_{e,r,w,h-1} + \eta\, p^{\mathrm{P}}_{e,r,w,h} - p^{\mathrm{T}}_{e,r,w,h}, \quad \forall e,r,w,h, \tag{3.55}$$

$$v^{\mathrm{L}}_{e,r,w,h} = v^{\mathrm{L}}_{e,r,w,h-1} - \eta\, p^{\mathrm{P}}_{e,r,w,h} + p^{\mathrm{T}}_{e,r,w,h}, \quad \forall e,r,w,h, \tag{3.56}$$

$$\underline{\mathrm{V}}^{\mathrm{U}} \le v^{\mathrm{U}}_{e,r,w,h} \le \overline{\mathrm{V}}^{\mathrm{U}}, \quad \forall e,r,w,h, \tag{3.57}$$

$$\underline{\mathrm{V}}^{\mathrm{L}} \le v^{\mathrm{L}}_{e,r,w,h} \le \overline{\mathrm{V}}^{\mathrm{L}}, \quad \forall e,r,w,h. \tag{3.58}$$

3.5.3.2 Operating Mode State Equations

It is assumed that the PHSP makes use of several pump-turbine reversible units. As such, the model considers that these units are either in pumping mode (consuming energy) and in turbine mode (generating energy) through the binary variable $T_{e,r,w,h}$. In order to model SU and SD costs for energy operation, this formulation considers that the pump-turbine units can be online $\left(U^{\mathrm{T/P,On}}_{e,r,w,h}\right)$ or offline $\left(U^{\mathrm{T/P,Off}}_{e,r,w,h}\right)$ in each operating mode. Equalities (3.59) represent the unit commitment of online units in turbine mode and associated SU and SD events, while the number of online and offline units is limited by constraints (3.60). Lastly, in order to model the number of online units that need to be shutdown due to the provision of SPR-Dw in turbine mode, constraints (3.61) are enforced.

$$U^{\mathrm{T,On}}_{e,r,w,h+1} = U^{\mathrm{T,On}}_{e,r,w,h} + Y^{\mathrm{T}}_{e,r,w,h} - Z^{\mathrm{T}}_{e,r,w,h}, \quad \forall e,r,w,h, \tag{3.59}$$

$$U^{\mathrm{T,On}}_{e,r,w,h} + U^{\mathrm{T,Off}}_{e,r,w,h} \leq T_{e,r,w,h}\mathrm{N}^{\mathrm{units}}, \quad \forall e,r,w,h, \tag{3.60}$$

$$U^{\mathrm{T,On,SD}}_{e,r,w,h} \leq U^{\mathrm{T,On}}_{e,r,w,h}, \quad \forall e,r,w,h. \tag{3.61}$$

Analogously, equalities (3.62) and constraints (3.63) are applied while in pumping mode. Constraints (3.64) are similar to constraints (3.61), however these reflect the number of online units in pumping mode that need to be shutdown due to the provision of SPR-Up.

$$U^{\mathrm{P,On}}_{e,r,w,h+1} = U^{\mathrm{P,On}}_{e,r,w,h} + Y^{\mathrm{P}}_{e,r,w,h} - Z^{\mathrm{P}}_{e,r,w,h}, \quad \forall e,r,w,h, \tag{3.62}$$

$$U^{\mathrm{P,On}}_{e,r,w,h} + U^{\mathrm{P,Off}}_{e,r,w,h} \leq \left(1 - T_{e,r,w,h}\right)\mathrm{N}^{\mathrm{units}}, \quad \forall e,r,w,h, \tag{3.63}$$

$$U^{\mathrm{P,On,SD}}_{e,r,w,h} \leq U^{\mathrm{P,On}}_{e,r,w,h}, \quad \forall e,r,w,h. \tag{3.64}$$

3.5.3.3 Operational Limits

Power consumption and generation limits are enforced with constraints (3.65) and (3.66), respectively. The provision of SPR in both operating modes by a PHSP with multiple pump-turbine units may result in the SU of offline units (SPR-Up in turbine mode and SPR-Dw in pumping mode). As such, constraints (3.67) and (3.68) model the provision of SPR-Dw in pumping mode through online and offline units, respectively. In this operating mode, SPR-Up can be provided by reducing consuming power in constraints (3.69) and the number of online units that need to be SD is calculated with constraints (3.70).

$$U^{\mathrm{P,On}}_{e,r,w,h}\underline{\mathrm{P}}^{\mathrm{P}} \leq p^{\mathrm{P}}_{e,r,w,h} \leq U^{\mathrm{P,On}}_{e,r,w,h}\overline{\mathrm{P}}^{\mathrm{P}}, \quad \forall e,r,w,h, \tag{3.65}$$

$$U^{\mathrm{T,On}}_{e,r,w,h}\underline{\mathrm{P}}^{\mathrm{T}} \leq p^{\mathrm{T}}_{e,r,w,h} \leq U^{\mathrm{T,On}}_{e,r,w,h}\overline{\mathrm{P}}^{\mathrm{T}}, \quad \forall e,r,w,h, \tag{3.66}$$

$$U^{\mathrm{P,On}}_{e,r,w,h}\underline{\mathrm{P}}^{\mathrm{P}} \leq p^{\mathrm{P}}_{e,r,w,h} + r^{\mathrm{Dw,P,On}}_{e,r,w,h} \leq U^{\mathrm{P,On}}_{e,r,w,h}\overline{\mathrm{P}}^{\mathrm{P}}, \quad \forall e,r,w,h, \tag{3.67}$$

$$U^{\mathrm{P,Off}}_{e,r,w,h}\underline{\mathrm{P}}^{\mathrm{P}} \leq r^{\mathrm{Dw,P,Off}}_{e,r,w,h} \leq U^{\mathrm{P,Off}}_{e,r,w,h}\overline{\mathrm{P}}^{\mathrm{P}}, \quad \forall e,r,w,h, \tag{3.68}$$

$$r^{\mathrm{Up,P}}_{e,r,w,h} \leq p^{\mathrm{P}}_{e,r,w,h}, \quad \forall e,r,w,h, \tag{3.69}$$

$$U^{\mathrm{P,On,SD}}_{e,r,w,h}\underline{\mathrm{P}}^{\mathrm{P}} \leq r^{\mathrm{Up,P}}_{e,r,w,h} \leq U^{\mathrm{P,On,SD}}_{e,r,w,h}\overline{\mathrm{P}}^{\mathrm{P}}, \quad \forall e,r,w,h. \tag{3.70}$$

In turbine mode, the provision of SPR-Up is modelled by constraints (3.71) (increasing power generation from online units) and constraints (3.72) (starting offline units). Reducing current power generation provides SPR-Dw in constraints (3.73), while the number of units that need to be SD is calculated in constraints (3.74).

$$U^{\mathrm{T,On}}_{e,r,w,h}\,\underline{\mathrm{P}}^{\mathrm{T}} \le p^{\mathrm{T}}_{e,r,w,h} + r^{\mathrm{Up,T,On}}_{e,r,w,h} \le U^{\mathrm{T,On}}_{e,r,w,h}\,\overline{\mathrm{P}}^{\mathrm{T}}, \quad \forall e,r,w,h, \tag{3.71}$$

$$U^{\mathrm{T,Off}}_{e,r,w,h}\,\underline{\mathrm{P}}^{\mathrm{T}} \le r^{\mathrm{Up,T,Off}}_{e,r,w,h} \le U^{\mathrm{T,Off}}_{e,r,w,h}\,\overline{\mathrm{P}}^{\mathrm{T}}, \quad \forall e,r,w,h, \tag{3.72}$$

$$r^{\mathrm{Dw,T}}_{e,r,w,h} \le p^{\mathrm{T}}_{e,r,w,h}, \quad \forall e,r,w,h, \tag{3.73}$$

$$U^{\mathrm{T,On,SD}}_{e,r,w,h}\,\underline{\mathrm{P}}^{\mathrm{T}} \le r^{\mathrm{Dw,T}}_{e,r,w,h} \le U^{\mathrm{T,On,SD}}_{e,r,w,h}\,\overline{\mathrm{P}}^{\mathrm{T}}, \quad \forall e,r,w,h. \tag{3.74}$$

3.5.3.4 Wind Power and Reserve Limits

Constraints (3.75) model the provision of SPR-Up by the WF and ensure it's limited by available wind power generation, while constraints (3.76) limit the amount of SPR-Dw provided by the WF.

$$p^{\mathrm{W}}_{e,r,w,h} + r^{\mathrm{Up,W}}_{e,r,w,h} \le \mathrm{P}^{\mathrm{AV}}_{w,h}\mathrm{K}^{\mathrm{W}}, \quad \forall e,r,w,h, \tag{3.75}$$

$$r^{\mathrm{Dw,W}}_{e,r,w,h} \le p^{\mathrm{W}}_{e,r,w,h}, \quad \forall e,r,w,h. \tag{3.76}$$

3.5.3.5 Service Deliverability Constraints

Equalities (3.77) and (3.78) calculate total SPR-Up and SPR-Dw provision from both facilities which are limited by lower and upper bounds in constraints (3.79) and (3.80). Note that, unlike in the previous models for the generic ESS, it is assumed that the PHSP cannot change modes within the same time period and, as such, maximum SPR provision depends on the operating mode in the current scenario and time period.

$$r^{\mathrm{Up}}_{e,r,w,h} = r^{\mathrm{Up,T,On}}_{e,r,w,h} + r^{\mathrm{Up,T,Off}}_{e,r,w,h} + r^{\mathrm{Up,P}}_{e,r,w,h} + r^{\mathrm{Up,W}}_{e,r,w,h}, \quad \forall e,r,w,h, \tag{3.77}$$

$$r^{\mathrm{Dw}}_{e,r,w,h} = r^{\mathrm{Dw,W}}_{e,r,w,h} + r^{\mathrm{DwT}}_{e,r,w,h} + r^{\mathrm{Dw,P,On}}_{e,r,w,h} + r^{\mathrm{Dw,P,Off}}_{e,r,w,h}, \quad \forall e,r,w,h, \tag{3.78}$$

$$r^{\mathrm{Up}}_{e,r,w,h} \le \begin{cases} \mathrm{K}^{\mathrm{W}} + \max\left\{\overline{\mathrm{P}}^{\mathrm{P}}, \overline{\mathrm{P}}^{\mathrm{T}}\right\}\mathrm{N}^{\mathrm{units}} & , r^{\mathrm{Up,T,On}}_{e,r,w,h} + r^{\mathrm{Up,T,Off}}_{e,r,w,h} + r^{\mathrm{Up,P}}_{e,r,w,h} + r^{\mathrm{Up,W}}_{e,r,w,h} \ge \underline{\mathrm{SPR}}^{\mathrm{Up}} \\ 0 & , r^{\mathrm{Up,T,On}}_{e,r,w,h} + r^{\mathrm{Up,T,Off}}_{e,r,w,h} + r^{\mathrm{Up,P}}_{e,r,w,h} + r^{\mathrm{Up,W}}_{e,r,w,h} < \underline{\mathrm{SPR}}^{\mathrm{Up}} \end{cases}, \quad \forall e,r,w,h, \tag{3.79}$$

$$r^{\mathrm{Dw}}_{e,r,w,h} \le \begin{cases} \mathrm{K}^{\mathrm{W}} + \max\left\{\overline{\mathrm{P}}^{\mathrm{P}}, \overline{\mathrm{P}}^{\mathrm{T}}\right\}\mathrm{N}^{\mathrm{units}} & , r^{\mathrm{Dw,W}}_{e,r,w,h} + r^{\mathrm{DwT}}_{e,r,w,h} + r^{\mathrm{Dw,P,On}}_{e,r,w,h} + r^{\mathrm{Dw,P,Off}}_{e,r,w,h} \ge \underline{\mathrm{SPR}}^{\mathrm{Dw}} \\ 0 & , r^{\mathrm{Dw,W}}_{e,r,w,h} + r^{\mathrm{DwT}}_{e,r,w,h} + r^{\mathrm{Dw,P,On}}_{e,r,w,h} + r^{\mathrm{Dw,P,Off}}_{e,r,w,h} < \underline{\mathrm{SPR}}^{\mathrm{Dw}} \end{cases}, \quad \forall e,r,w,h. \tag{3.80}$$

In order to ensure sufficient stored energy in both reservoirs to provide increased (SPR-Up) or reduced (SPR-Dw) power injections, constraints (3.81) through (3.88) adapt the service deliverability constraints presented previously. Note that the presence of two reservoirs necessitates the additional need of ensuring that there is sufficient energy headroom (volume on each reservoir that is not filled with water) to accommodate the increased volume of water moved in each direction when providing SPR - downstream when providing SPR-Up in turbine mode and upstream when providing SPR-Dw in pumping mode.

$$\underline{\mathrm{V}}^{\mathrm{U}} - \mathrm{M}\left(1 - Q^{\mathrm{Up,T}}_{e,r,w,h}\right) \leq v^{\mathrm{U}}_{e,r,w,h-1} + \eta p^{\mathrm{P}}_{e,r,w,h} - \left(p^{\mathrm{T}}_{e,r,w,h} + r^{\mathrm{Up,T,On}}_{e,r,w,h} + r^{\mathrm{Up,T,Off}}_{e,r,w,h}\right)\tau^{\mathrm{SPR}} \leq \overline{\mathrm{V}}^{\mathrm{U}} + \mathrm{M}\left(1 - Q^{\mathrm{Up,T}}_{e,r,w,h}\right), \quad \forall e,r,w,h, \tag{3.81}$$

$$\underline{\mathrm{V}}^{\mathrm{L}} - \mathrm{M}\left(1 - Q^{\mathrm{Up,T}}_{e,r,w,h}\right) \leq v^{\mathrm{L}}_{e,r,w,h-1} - \eta p^{\mathrm{P}}_{e,r,w,h} + \left(p^{\mathrm{T}}_{e,r,w,h} + r^{\mathrm{Up,T,On}}_{e,r,w,h} + r^{\mathrm{Up,T,Off}}_{e,r,w,h}\right)\tau^{\mathrm{SPR}} \leq \overline{\mathrm{V}}^{\mathrm{L}} + \mathrm{M}\left(1 - Q^{\mathrm{Up,T}}_{e,r,w,h}\right), \quad \forall e,r,w,h, \tag{3.82}$$

$$\underline{\mathrm{V}}^{\mathrm{U}} - \mathrm{M}\left(1 - Q^{\mathrm{Dw\text{-}T}}_{e,r,w,h}\right) \leq v^{\mathrm{U}}_{e,r,w,h-1} + \eta p^{\mathrm{P}}_{e,r,w,h} - \left(p^{\mathrm{T}}_{e,r,w,h} - r^{\mathrm{Dw,T}}_{e,r,w,h}\right)\tau^{\mathrm{SPR}} \leq \overline{\mathrm{V}}^{\mathrm{U}} + \mathrm{M}\left(1 - Q^{\mathrm{Dw\text{-}T}}_{sh}\right), \quad \forall e,r,w,h, \tag{3.83}$$

$$\underline{\mathrm{V}}^{\mathrm{L}} - \mathrm{M}\left(1 - Q^{\mathrm{Dw\text{-}T}}_{e,r,w,h}\right) \leq v^{\mathrm{L}}_{e,r,w,h-1} - \eta p^{\mathrm{P}}_{e,r,w,h} + \left(p^{\mathrm{T}}_{e,r,w,h} - r^{\mathrm{Dw,T}}_{e,r,w,h}\right)\tau^{\mathrm{SPR}} \leq \overline{\mathrm{V}}^{\mathrm{L}} + \mathrm{M}\left(1 - Q^{\mathrm{Dw\text{-}T}}_{e,r,w,h}\right), \quad \forall e,r,w,h, \tag{3.84}$$

$$\underline{\mathrm{V}}^{\mathrm{U}} - \mathrm{M}\left(1 - Q^{\mathrm{Up,P}}_{e,r,w,h}\right) \leq v^{\mathrm{U}}_{e,r,w,h-1} + \eta\left(p^{\mathrm{P}}_{e,r,w,h} - r^{\mathrm{Up,P}}_{e,r,w,h}\right)\tau^{\mathrm{SPR}} - p^{\mathrm{T}}_{e,r,w,h} \leq \overline{\mathrm{V}}^{\mathrm{U}} + \mathrm{M}\left(1 - Q^{\mathrm{Up\text{-}P}}_{e,r,w,h}\right), \quad \forall e,r,w,h, \tag{3.85}$$

$$\underline{\mathrm{V}}^{\mathrm{L}} - \mathrm{M}\left(1 - Q^{\mathrm{Up,P}}_{e,r,w,h}\right) \leq v^{\mathrm{L}}_{e,r,w,h-1} - \eta\left(p^{\mathrm{P}}_{e,r,w,h} - r^{\mathrm{Up,P}}_{e,r,w,h}\right)\tau^{\mathrm{SPR}} + p^{\mathrm{T}}_{e,r,w,h} \leq \overline{\mathrm{V}}^{\mathrm{L}} + \mathrm{M}\left(1 - Q^{\mathrm{Up,P}}_{e,r,w,h}\right), \quad \forall e,r,w,h, \tag{3.86}$$

$$\underline{\mathrm{V}}^{\mathrm{U}} - \mathrm{M}\left(1 - Q^{\mathrm{Dw,P}}_{e,r,w,h}\right) \leq v^{\mathrm{L}}_{e,r,w,h-1} + \eta\left(p^{\mathrm{P}}_{e,r,w,h} + r^{\mathrm{Dw,P,On}}_{e,r,w,h} + r^{\mathrm{Dw,P,Off}}_{e,r,w,h}\right)\tau^{\mathrm{SPR}} - p^{\mathrm{T}}_{e,r,w,h} \leq \overline{\mathrm{V}}^{\mathrm{U}} + \mathrm{M}\left(1 - Q^{\mathrm{Dw,P}}_{e,r,w,h}\right), \quad \forall e,r,w,h, \tag{3.87}$$

$$\underline{\mathrm{V}}^{\mathrm{L}} - \mathrm{M}\left(1 - Q^{\mathrm{Dw,P}}_{e,r,w,h}\right) \leq v^{\mathrm{L}}_{sh-1} - \eta\left(p^{\mathrm{P}}_{e,r,w,h} + r^{\mathrm{Dw,P,On}}_{e,r,w,h} + r^{\mathrm{Dw,P,Off}}_{e,r,w,h}\right)\tau^{\mathrm{SPR}} + p^{\mathrm{T}}_{e,r,w,h} \leq \overline{\mathrm{V}}^{\mathrm{L}} + \mathrm{M}\left(1 - Q^{\mathrm{Dw,P}}_{e,r,w,h}\right), \quad \forall e,r,w,h. \tag{3.88}$$

Constraints (3.89) to (3.92) ensure that each type of SPR is only provided if the previous constraints are verified and (3.93) and (3.94) link the type of SPR to each operating mode. The formulation allows for the PHSP to provide SPR-Up and SPR-Dw in each operating mode, however, as it does not allow for intra-period operating mode transition as previously mentioned. The PHSP cannot provide SPR-Up (decrease consumption and increase generation) or SPR-Dw (decrease generation and increase consumption) through both operating modes in the same time period.

$$r^{\mathrm{Up,T,On}}_{e,r,w,h} + r^{\mathrm{Up,T,Off}}_{e,r,w,h} \leq \mathrm{M}\, Q^{\mathrm{Up,T}}_{e,r,w,h}, \quad \forall e,r,w,h, \tag{3.89}$$

$$r^{\mathrm{Dw,T}}_{e,r,w,h} \leq \mathrm{M}\, Q^{\mathrm{Dw,T}}_{e,r,w,h}, \quad \forall e,r,w,h, \tag{3.90}$$

$$r^{\mathrm{Up,P}}_{e,r,w,h} \leq \mathrm{M}\, Q^{\mathrm{Up,P}}_{e,r,w,h}, \quad \forall e,r,w,h, \tag{3.91}$$

$$r^{\mathrm{Dw,P,On}}_{e,r,w,h} + r^{\mathrm{Dw,P,Off}}_{e,r,w,h} \leq \mathrm{M}\, Q^{\mathrm{Dw,P}}_{e,r,w,h}, \quad \forall e,r,w,h. \tag{3.92}$$

$$Q^{\mathrm{Up,T}}_{e,r,w,h} + Q^{\mathrm{Dw,T}}_{e,r,w,h} \leq 2\, T_{e,r,w,h}, \quad \forall e,r,w,h, \tag{3.93}$$

$$Q^{\mathrm{Up,P}}_{e,r,w,h} + Q^{\mathrm{Dw,P}}_{e,r,w,h} \leq 2\left(1 - T_{e,r,w,h}\right), \quad \forall e,r,w,h. \tag{3.94}$$

3.5.3.6 Bid Limits

Joint energy and SPR bids are limited by the WF capacity and the PHSP's maximum power generation in constraints (3.95), while SPR-Dw bids are limited by the energy bid and maximum power consumption of the PHSP in (3.96).

$$x_h^{\mathrm{En}} + x_h^{\mathrm{SPR,Up}} \leq \mathrm{K}^{\mathrm{W}} + \mathrm{N}^{\mathrm{units}}\overline{\mathrm{P}}^{\mathrm{T}}, \quad \forall h, \tag{3.95}$$

$$x_h^{\mathrm{En}} - x_h^{\mathrm{SPR,Dw}} \geq -\mathrm{N}^{\mathrm{units}}\overline{\mathrm{P}}^{\mathrm{P}}, \quad \forall h. \tag{3.96}$$

3.5.3.7 Other Bounds

The number of SU and SD events is limited by the number of identical pump-turbine units in (3.97).

$$\left\{Y^{\mathrm{T}}_{e,r,w,h}, Z^{\mathrm{T}}_{e,r,w,h}, Y^{\mathrm{P}}_{e,r,w,h}, Z^{\mathrm{P}}_{e,r,w,h}\right\} \leq \mathrm{N}^{\mathrm{units}}, \quad \forall e,r,w,h. \tag{3.97}$$

3.5.3.8 Variables Type and Sign Constrains

Finally, equations (3.98) to (3.103) represent the sign and type constraints for all decision variables.

$$\begin{aligned}\Omega^{\mathrm{IV}} = \Big\{ & U^{\mathrm{T,On}}_{e,r,w,h}, U^{\mathrm{T,On,SD}}_{e,r,w,h}, U^{\mathrm{T,Off}}_{e,r,w,h}, Y^{\mathrm{T}}_{e,r,w,h}, Z^{\mathrm{T}}_{e,r,w,h}, \\ & U^{\mathrm{P,On}}_{e,r,w,h}, U^{\mathrm{P,On,SD}}_{e,r,w,h}, U^{\mathrm{P,Off}}_{e,r,w,h}, Y^{\mathrm{P}}_{e,r,w,h}, Z^{\mathrm{P}}_{e,r,w,h} \Big\} \in \mathbb{Z}_{\geq 0}, \quad \forall e,r,w,h,\end{aligned} \tag{3.98}$$

$$\Omega^{\mathrm{BV}} = \left\{T_{e,r,w,h}, Q^{\mathrm{Up,T}}_{e,r,w,h}, Q^{\mathrm{Dw,T}}_{e,r,w,h}, Q^{\mathrm{Up,P}}_{e,r,w,h}, Q^{\mathrm{Dw,P}}_{e,r,w,h}, b^{\mathrm{En}}_{e,r,w,h}, b^{\mathrm{SPR,Up}}_{e,r,w,h}, b^{\mathrm{SPR,Dw}}_{e,r,w,h}\right\} \in \{0,1\}, \quad \forall e,r,w,h, \tag{3.99}$$

$$\Omega^{\mathrm{CV}} = \left\{x_h^{\mathrm{En}}\right\} \in \mathbb{R}, \quad \forall e,r,w,h, \tag{3.100}$$

$$\Omega^{\mathrm{SCV^+}} = \left\{r^{\mathrm{Up}}_{e,r,w,h}, r^{\mathrm{Dw}}_{e,r,w,h}, x_h^{\mathrm{SPR,Up}}, x_h^{\mathrm{SPR,Dw}}\right\} \in \mathbb{R}_{\geq 0}, \quad \forall e,r,w,h, \tag{3.101}$$

$$\begin{aligned}\Omega^{\mathrm{CV^+}} = \Big\{ & v^{\mathrm{U}}_{e,r,w,h}, v^{\mathrm{L}}_{e,r,w,h}, p^{\mathrm{W}}_{e,r,w,h}, r^{\mathrm{Up,T,On}}_{e,r,w,h}, r^{\mathrm{Up,T,Off}}_{e,r,w,h}, r^{\mathrm{Dw,T}}_{e,r,w,h}, r^{\mathrm{Up,P}}_{e,r,w,h}, \\ & r^{\mathrm{Dw,P,On}}_{e,r,w,h}, r^{\mathrm{Dw,P,Off}}_{e,r,w,h}, r^{\mathrm{Up,W}}_{e,r,w,h}, r^{\mathrm{Dw,W,C}}_{e,r,w,h} \Big\} \in \mathbb{R}_{\geq 0}, \quad \forall e,r,w,h,\end{aligned} \tag{3.102}$$

$$\begin{aligned}\Omega^{\mathrm{CV^{SOS1}}} = \Big\{ & \left(i^{\mathrm{En^+}}_{e,r,w,h}, i^{\mathrm{En^-}}_{e,r,w,h}\right), \left(i^{\mathrm{SPR,Up^+}}_{,h}, i^{\mathrm{SPR,Up^-}}_{e,r,w,h}\right), \left(i^{\mathrm{SPR,Dw^+}}_{e,r,w,h}, i^{\mathrm{SPR,Dw^-}}_{e,r,w,h}\right), \left(p^{\mathrm{P}}_{e,r,w,h}, p^{\mathrm{T}}_{e,r,w,h}\right) \Big\} \\ & \in \mathbb{R}_{\geq 0}, \quad \forall e,r,w,h.\end{aligned} \tag{3.103}$$

3.6 The Value of an ESS for a WF

3.6.1 Input data

This case study utilizes the same input data presented in Section 2.4 to assess the value of the proposed JBS in Section 3.4 against the results achieved in Section 2.4. The forecasts for SPR services are assumed to be the same for the previous chapter's AS services. Similarly, the maximum utilization time duration for SPR $\left(\tau^{\mathrm{SPR}}\right)$ is assumed to be 2 hours, and minimum SPR provision levels $\left(\underline{\mathrm{SPR}}^{\mathrm{Up/Dw}}\right)$ is assumed to be 3MW. Price penalty factors for this case study are assumed to be 0.5 for positive deviations $\left(\omega^{\mathrm{En/SPR^+}}_{e/r,h}\right)$ and 1.5 for negative deviations $\left(\omega^{\mathrm{En/SPR^-}}_{e/r,h}\right)$. The JBS model was implemented in FICO$^{\mathrm{TM}}$ Xpress [64] and simulated in the same Windows 10 desktop machine.

The following two case studies analyse the results for three bidding strategies: the JBS proposed in this chapter where the WF and ESS operate as a single entity; the Sto.UBS, in which both facilities operate independently and use a stochastic model to determine the optimal day-ahead energy and SPR bids; and the Det.UBS, in which the day-ahead bids are optimized deterministically (essentially the bids and results from Subsection 2.4.3).

3.6.2 The benefit of WF-ESS coordination

As previously stated, the main benefit of the coordinated operation of WF and ESS is the increased profit due to the management of wind imbalances and the provision of SPR. Two market participations are again considered in this case study: energy market (EN), and energy and SPR markets (EN-SPR). The economic benefit of the JBS is established by comparing the expected profit and imbalance costs for each day against the other strategies. Tables 3.1 and 3.2 summarize the economic results of the EN and EN-SPR market participations for the Sto.UBS and JBS. Fig. 3.3 presents the absolute and relative variations of expected profit and imbalance costs of the JBS over the Sto.UBS and the Det.UBS.

Table 3.1: Economic results for each EN bidding strategy (£).

Day	1		2		3	
Bidding Strategy	Sto.UBS	JBS	Sto.UBS	JBS	Sto.UBS	JBS
Energy Market Revenue	13,656	13,699	5,327	5,743	19,633	19,365
Energy Surplus Revenue	1,043	485	792	394	781	627
Energy Penaties	2,837	1,594	1,278	913	2,492	1,937
Profit	11,862	12,590	4,841	5,224	17,922	18,055

Table 3.2: Economic results for each EN-SPR bidding strategy (£).

Day	1		2		3	
Bidding Strategy	Sto.UBS	JBS	Sto.UBS	JBS	Sto.UBS	JBS
Energy Market Revenue	13,773	13,699	5,370	5,750	19,587	19,410
SPR Market Revenue	2,428	2,585	1,243	1,488	4,406	4,538
Energy Surplus Revenue	1,014	485	777	393	785	616
SPR Surplus Revenue	119	142	78	90	148	156
Energy Penaties	2,926	2,012	1,321	919	2,480	1,973
SPR Penalties	385	418	146	278	480	524
Profit	14,022	14,900	6,001	6,524	21,967	22,222

The JBS allows for expected profit increases ranging from 0.74% (Day 3) to 7.91% (Day 2) for the EN market participation, which is mainly achieved by reducing expected energy imbalance costs of up to 43.81% (Day 1). On the other hand, the JBS allows increase profits up to 8.71% and reducing imbalance costs up to 26.6% for the EN-SPR market participation.

Overall, the JBS allows for increasing the total profits for the 3 days by 4% in the EN-SPR participation and by 3.6% for the EN participation. The increased benefit in the EN-SPR participation can be explained due to the fact that there are certain time periods where available wind power generation is

insufficient to provide minimum SPR levels in the Sto.UBS. Whereas, through the JBS it is possible to increase the amount of SPR the WF and ESS operator can provide. Other variations in the benefit of the JBS can be explained due to differences in the day-ahead price and wind power forecasts, as the ESS's capability to manage imbalances throughout the day will dependent on its impact on expected profit. Consequently, stored energy must be carefully managed in order to ensure that imbalances that occur in time periods where energy prices are higher can be adequately mitigated.

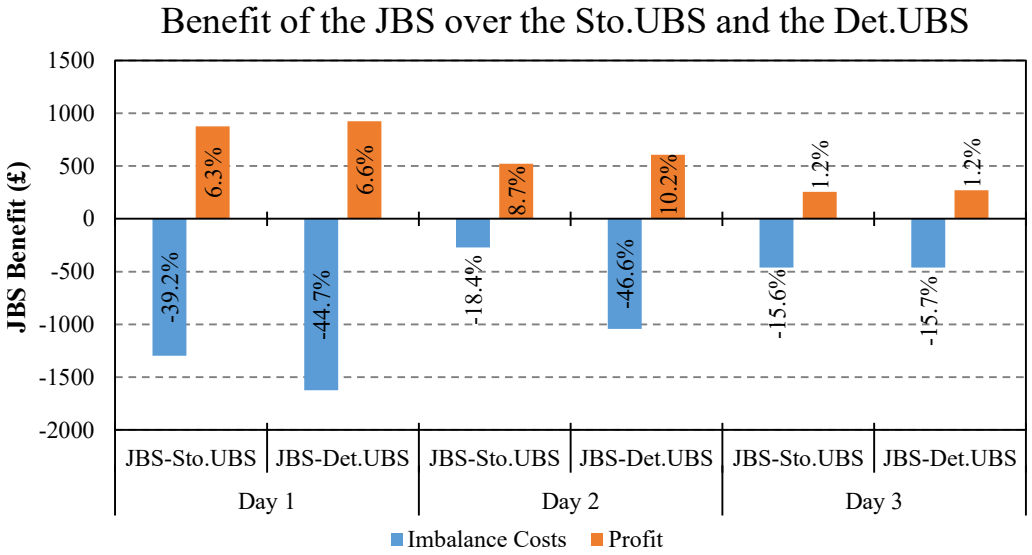


Fig. 3.3: Summary of benefit of the JBS in expected profits and imbalance costs over the stochastic UBS and deterministic UBS.

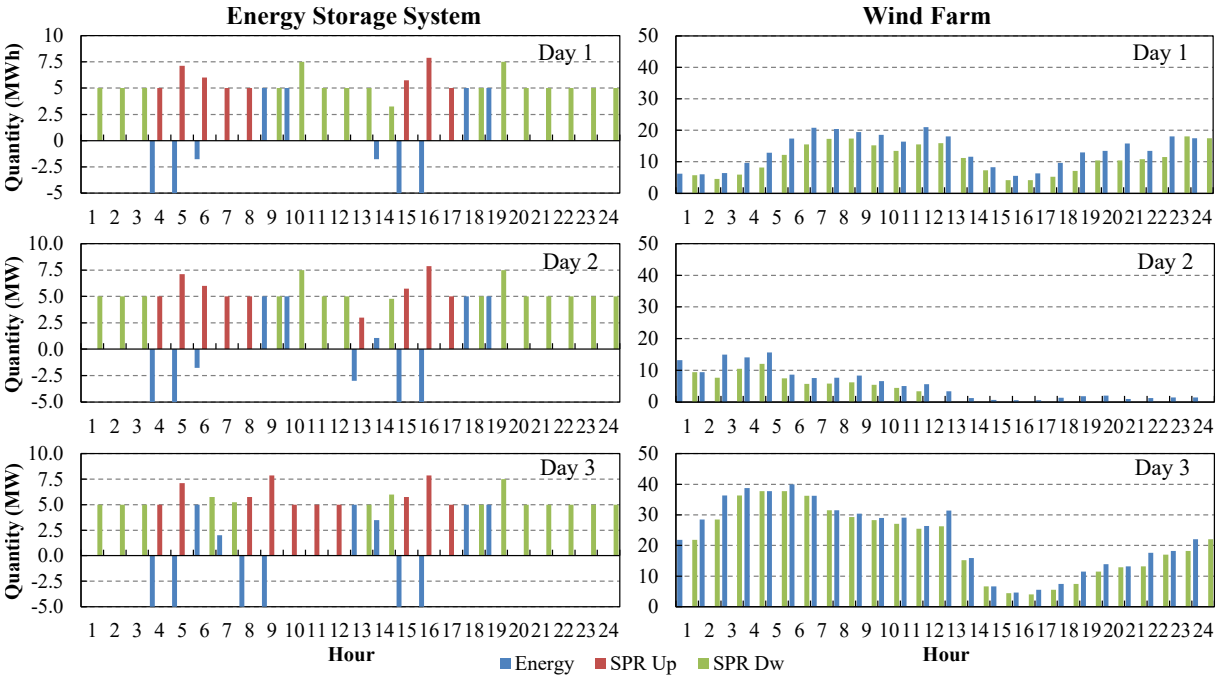


Fig. 3.4: Resulting bids for the EN-SPR Sto.UBS for all days.

Providing SPR leads to profit increases varying between 18.2% (Day 1, UBS) and 24.9% (Day 2, JBS) in regards to the EN market participation. When compared to the Det.UBS EN market participation, the EN-SPR JBS achieves profits increases varying between 24.1% (Day 3) and 36.7% (Day 2), which

averages 26.4% for the three days. Lastly, the optimal bids determined for the Sto.UBS and JBS are presented in Figs. 3.4 and 3.5, respectively. Note that the Sto.UBS bids show in Day 2 after hour 12, the WF does not provide SPR-Dw due to the available wind power generation being lower than the minimum 3MW required to provide SPR.

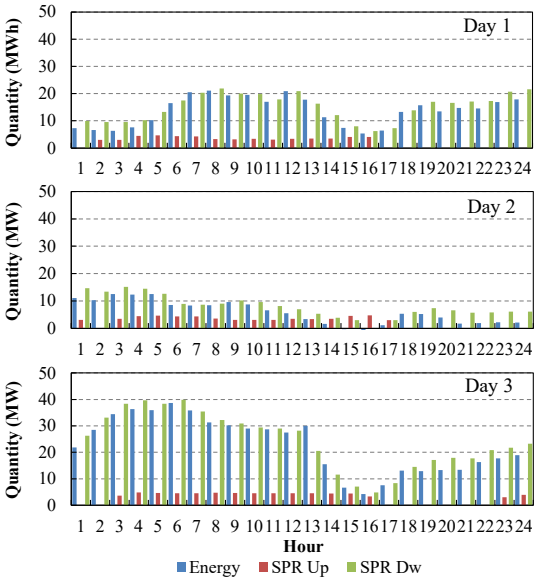


Fig. 3.5: Resulting bids for the EN-SPR JBS for all days.

3.6.3 Impact of WF-ESS coordination on generation uncertainty

The reduction of the WF's offering uncertainty is not only beneficial for its operator due to the increased profits, as evidenced in the previous section, but also for the TSO as less flexible generation needs to be committed in order to handle potential deviations. This case study aims to show how the JBS reduces wind generation uncertainty for all analysed days by comparing the 450 scenario realizations of the injected power and optimal energy bids by the WF and ESS for both bidding strategies (the Sto.UBS, power injections and energy bids of the ESS and the WF are summed) represented in Figs. 3.6 to 3.8. The average value (AVG) and STD for the energy imbalances for all days and both bidding strategies are presented in Table 3.3.

The previous case study showed the benefit of the JBS in reducing expected imbalance costs for the analysed days. However, it should be noted that imbalance costs are related to negative deviations while generation surplus can be sold in the balancing mechanism, albeit at prices lower than the day-ahead market. Consequently, the revenue generated from positive energy deviations is less valuable than the revenue generation in the day-ahead market. Therefore, the JBS manages to reduce both positive and negative deviations from the day-ahead energy bids as evidenced in Figs. 3.6 to 3.8, as the dispersion of the injected power in the JBS is less vertically scattered than that of the Sto.UBS. From Table 3.3 it is possible to understand that the JBS manages to reduce the AVG of the energy imbalances between 21.2% (Day 3) and 48.4% (Day 1), while the STD has been reduced between 16.3% and 16.8% (there was a 2.1% increase in Day 3).

Table 3.3: AVG and STD of the energy imbalances for all days in MW.

Strategy	Sto.UBS		JBS	
	AVG	STD	AVG	STD
Day 1	4.022	2.984	2.076	2.429
Day 2	2.489	2.431	1.721	2.035
Day 3	3.667	2.646	2.890	2.701

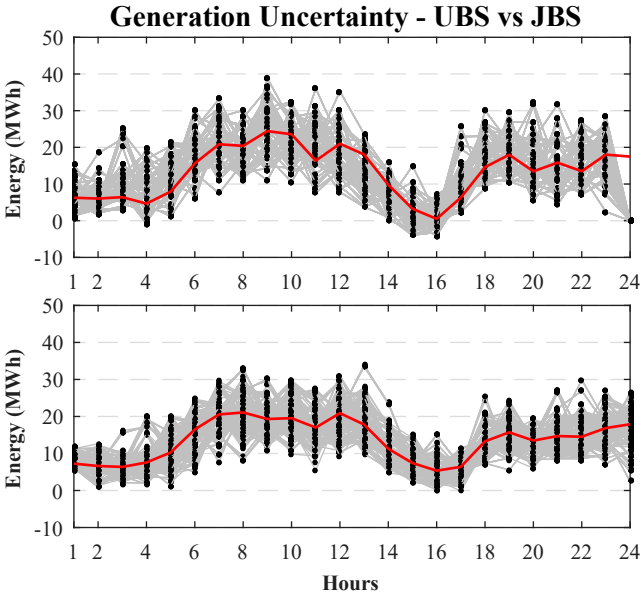


Fig. 3.6: Comparison of the injected power (black dots) and energy bid (red line) for all scenarios of the Sto.UBS (up) and the JBS (down) for day 1.

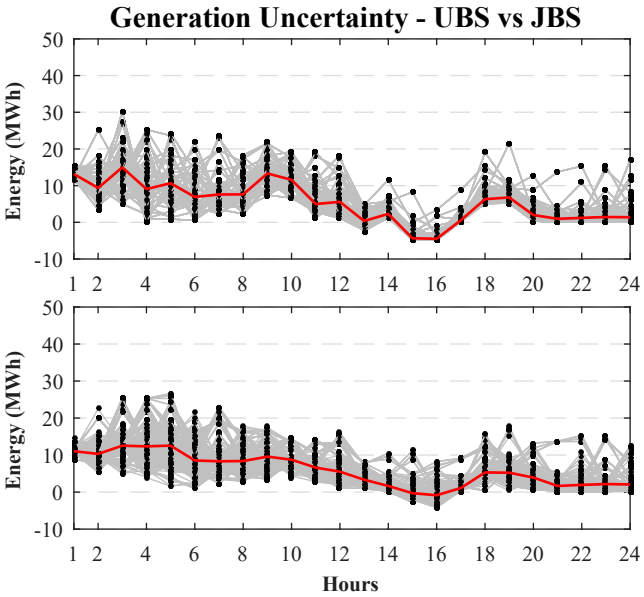


Fig. 3.7: Comparison of the injected power (black dots) and energy bid (red line) for all scenarios of the Sto.UBS (up) and the JBS (down) for day 2.

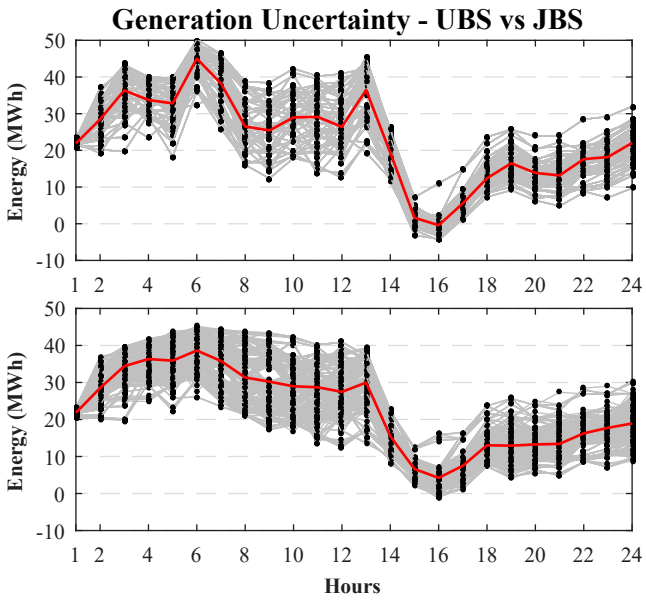


Fig. 3.8: Comparison of the injected power (black dots) and energy bid (red line) for all scenarios of the Sto.UBS (up) and the JBS (down) for day 3.

The previous case study argues that the quality of the forecasts and imbalance penalty factors for each day are factors that impact the ESS's capability for managing imbalance costs. This case study shows that Day 1 features higher uncertainty (measured by the AVG and STD of the Sto.UBS imbalances) and reduction on the energy imbalances. Day 2 features the lowest amount of uncertainty and intermediate imbalance reduction, while Day 3 features an intermediate amount of uncertainty but the lowest reduction in the energy imbalances. Taking into account this behaviour for the analysed days, it can be concluded that the pattern and amount of variability of the available wind power generation forecasts directly influence how the JBS benefits a WF.

3.7 Joint Bidding Strategies for Combined WF and PHSP

The case studies presented in this Section assess the benefit of the proposed JBS for the WF and the PHSP in different situations:

1. analysing the economic benefit for both entities to jointly provide energy and SPR for two days;
2. assessing the impact of the modelling of additional SU and SD costs for SPR provision;
3. mitigating wind energy spillage through coordination with PHSP;
4. determining how the benefit JBS over the UBS varies depending on the size of the WF and technical specifications of the PHSP.

The last case study analyses the computational performance of the proposed model. More concretely, it compares the execution times achieved with the tight reformulation of the absolute value functions against using a traditional formulation using binary variables and a third reformulation without using binary variables and tight bounds.

3.7.1 Input data

3.7.1.1 WF and PHSP Parameters

Similarly to the case studies in Section 3.6, it is assumed that the operator/consortium of a 50MW WF and a PHSP composed of 4 identical pump-turbine units, and upper and lower reservoirs with the technical characteristics specified in Table 3.4. The case study presented in Subsection 3.7.5, however, carries out sensitivity studies on the WF's and the PHSP's capacities. With regards to the SU and SD costs, the SU costs were divided for pumping mode $\left(c^{\mathrm{SU,P}}\right)$ and for turbine mode $\left(c^{\mathrm{SU,T}}\right)$ and based on the estimations presented in [91, 92], while the SD costs are assumed to be 10% of the SU costs.

Table 3.4: Pump-Turbine Unit Specifications

N^{units} (#)	η (p.u.)	$\underline{P}^{P}$ (MW)	$\overline{P}^{P}$ (MW)	$c^{SU,P}$ (£/unit)	$\underline{P}^{T}$ (MW)	$\overline{P}^{T}$ (MW)	$c^{SU,T}$ (£/unit)	$\overline{V}^{U/L}$ (MWh)
4	0.85	2.5	5	6.25	0	6	7.5	100

3.7.1.2 Day-ahead Wind Power Availability and Price Forecasts

Unlike the previous case studies, it is assumed that day-ahead wind power availability and energy prices forecasts are correlated and only two days are analysed. SPR prices are assumed constant across all time periods and forecasts at £6/MW/h for both SPR-Up and SPR-Dw, with the maximum utilisation time of the committed SPR assumed to be 2 hours. As such, a scenario for these case studies is defined as a pair of day-ahead wind power availability and energy price forecasts, each containing 24 time periods for each day, and are illustrated in Fig. 3.9.

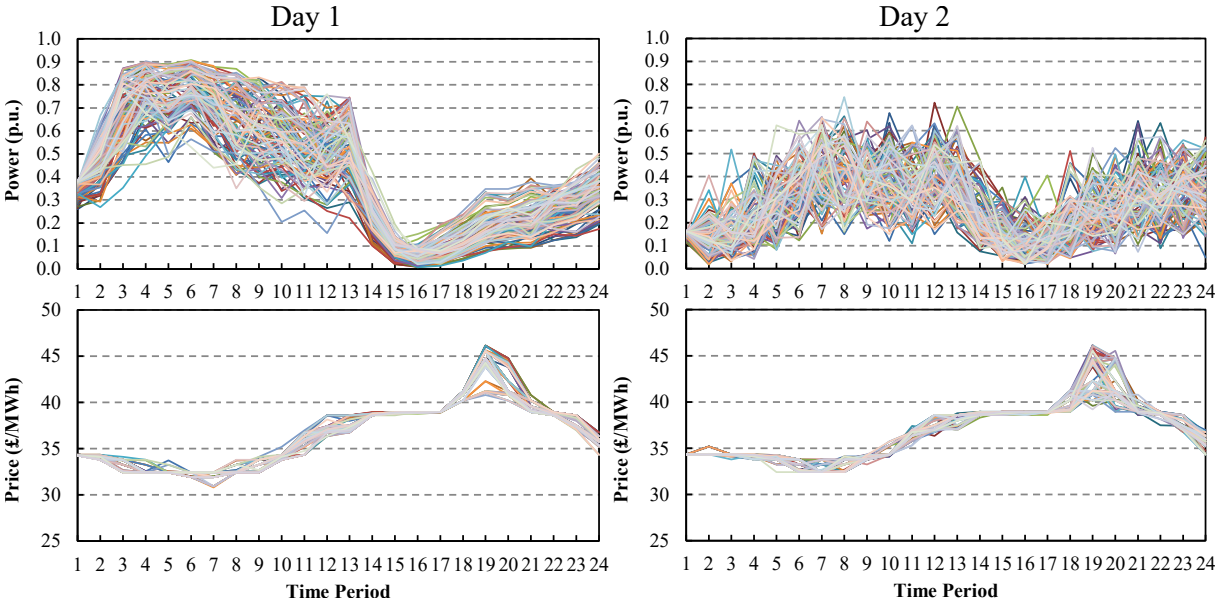


Fig. 3.9: Day-ahead wind generation and energy price scenarios for both days.

The wind power availability forecasts were created through the same process as the ones presented in Fig. 2.2. In order to create correlated energy price forecasts, these wind power forecasts were used as input for simulating the market operation of an approximation of the Great Britain electricity system with AURORAxmp [93] provided by EPIS. Consequently, the energy price results from these simulations

were used as the day-ahead energy price forecasts used in these case studies. Lastly, imbalance price penalty factors are assumed to be 0.5 for positive deviations $\left(\omega_{e/r,h}^{\mathrm{En/SPR}^{+}}\right)$ and 2.5 for negative deviations $\left(\omega_{e/r,h}^{\mathrm{En/SPR}^{-}}\right)$, as in the previous case studies.

3.7.2 The value of PHSP for enhancing the offering of a WF

The economic benefit created for the WF and PHSP by the JBS can be assessed by comparing its performance against the UBS, in which both facilities operate independently and each submits a set of energy and SPR bids. The benefit of the JBS over the UBS is analysed for 2 market participations in the same manner as the previous case studies: EN and EN-SPR. Consequently, the expected profits and costs are compared for each day and for four strategies/participations: EN UBS, EN JBS, EN-SPR UBS, EN-SPR JBS.

3.7.2.1 Day 1

The economic results for Day 1 and each market participation are summarized in Tables 3.5 and 3.6, which detail the components for each source of profit and show that a consistent increase in expected profit can be increased through the JBS by reducing expected imbalance costs. The profits for the WF and the PHSP for the JBS are also increased when compared to the UBS, which leads to the conclusion that the JBS is also beneficial for both entities. The PHSP has access to excess cost-free wind generation for pumping water and avoids purchasing additional energy from the market, increasing market revenue. On the other hand, the WF benefits from coordinating with the PHSP by reducing imbalance costs related to uncertainty and, consequently, the uncertainty in the day-ahead offering. In the EN-SPR participation, the JBS allows reducing the UBS's total imbalance costs by approximately 30%, which translates into reducing the AVG of the daily total imbalances by 13% (219 MW for the UBS).

Fig. 3.10 presents a visual summary of the four bidding strategies expected profits, imbalance costs and impact of the JBS. Comparing the EN-SPR JBS against the EN UBS, expected profits are increased by 41%. Fig 3.11 presents the optimal EN-SPR offering determined in the UBS (top and middle plots) and the JBS (bottom plot) for this day. Note that in some time periods, the operator/consortium seeks to maximize the revenue collected from selling all available wind energy and by providing SPR-Up through the PHSP.

Table 3.5: Expected Day 1 Profit Breakdown for the EN Participation (£)

Bidding Strategy	EN UBS			EN JBS		
Facility	PHSP	WF	Total	PHSP	WF	Total
Market Revenue	318	17,169	17,487	971	16,439	17,411
SU Costs	49	-	49	50	-	50
SD Costs	3	-	3	3	-	3
Imbalance Costs	0	2,266	2,266	-	-	1,256
Total Profit	266	14,902	15,169	918	16,439	16,101

Table 3.6: Expected Day 1 Profit Breakdown for the EN-SPR Participation (£)

Bidding Strategy	EN-SPR UBS			EN-SPR JBS		
Facility	PHSP	WF	Total	PHSP	WF	Total
Energy Market Revenue	318	17,169	17,487	212	17,169	17,381
SU Costs	60	-	60	70	-	70
SD Costs	5	-	5	6	-	6
Energy Imbalance Costs	0	2,266	2,266	-	-	1,351
SPR Up Revenue	2,075	0	2,075	1,914	0	1,914
SPR Down Revenue	876	2,963	3,840	1,183	2,964	4,146
SPR SU Costs	33	-	33	17	-	17
SPR SD Costs	21	-	21	23	-	23
SPR Up Imbalance Costs	17	0	17	-	-	288
SPR Down Imbalance Costs	33	383	416	-	-	240
Total Imbalance Costs	50	2,649	2,699	-	-	1,879
Total Profit	3,100	17,483	20,583	3,193	20,132	21,446

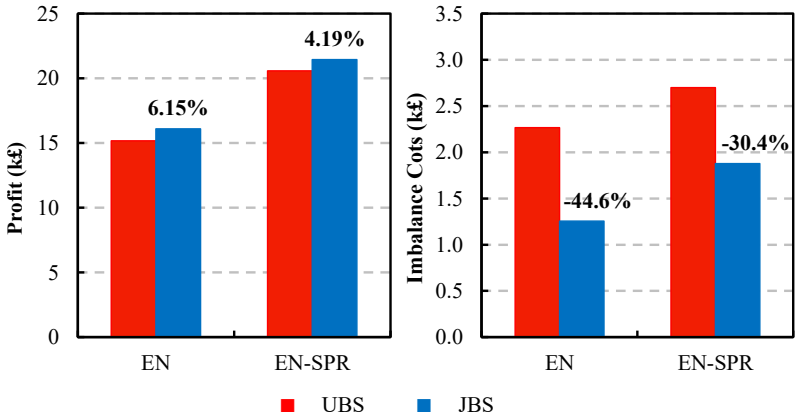


Fig. 3.10: Benefits of the JBS in expected profit and imbalance costs for Day 1.

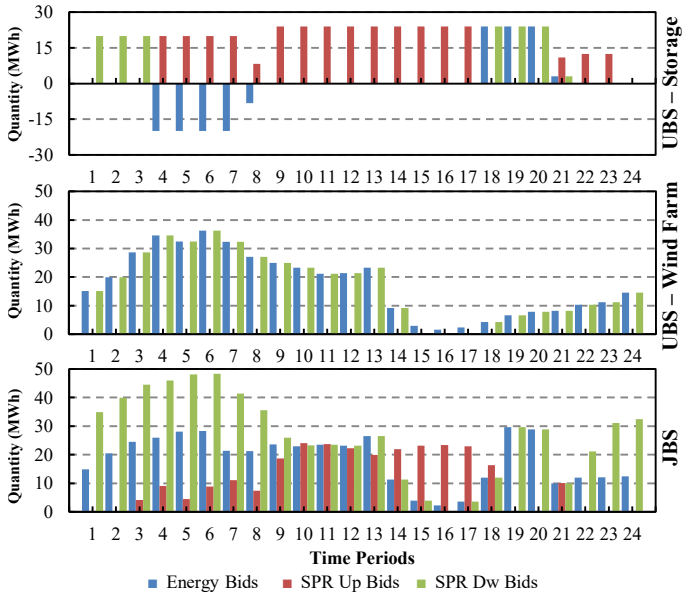


Fig. 3.11: Resulting bids for the EN-SPR bidding strategies for Day 1.

3.7.2.2 Day 2

The results for this day are presented in Tables 3.7 and 3.8 for en EN and EN-SPR market participations, respectively. Fig. 3.12 and 3.13 present the summary of the expected profits, imbalance costs and JBS variation for all bidding strategies, and a comparison of the optimal day-ahead EN-SPR hourly bids for the UBS and JBS cases, respectively.

Table 3.7: Expected Day 2 Profit Breakdown for EN Participation (£)

Bidding Strategy	UBS			JBS		
Facility	PHSP	WF	Total	PHSP	WF	Total
Market Revenue	168	12,005	12,173	915	11,162	12,077
SU Costs	43	-	43	52	-	52
SD Costs	3	-	3	4	-	4
Imbalance Costs	0	2,682	2,682	-	-	579
Total Profit	123	9,323	9,446	858	11,162	11,442

Table 3.8: Expected Day 2 Profit Breakdown for the EN-SPR Participation (£)

Bidding Strategy	UBS			JBS		
Facility	PHSP	WF	Total	PHSP	WF	Total
Energy Market Revenue	168	12,005	12,173	56	12,005	12,061
SU Costs	68	-	68	73	-	73
SD Costs	6	-	6	6	-	6
Energy Imbalance Costs	0	2,682	2,682	-	-	646
SPR Up Revenue	1,660	0	1,660	1,767	0	1,767
SPR Down Revenue	1,392	1,984	3,376	1,220	1,984	3,204
SPR SU Costs	13	-	13	23	-	23
SPR SD Costs	20	-	20	25	-	25
SPR Up Imbalance Costs	0	0	0	-	-	383
SPR Down Imbalance Costs	0	439	439	-	-	185
Total Imbalance Costs	0	3,121	3,121	-	-	1,214
Total Profit	3,116	10,868	13,983	2,917	13,989	15,691

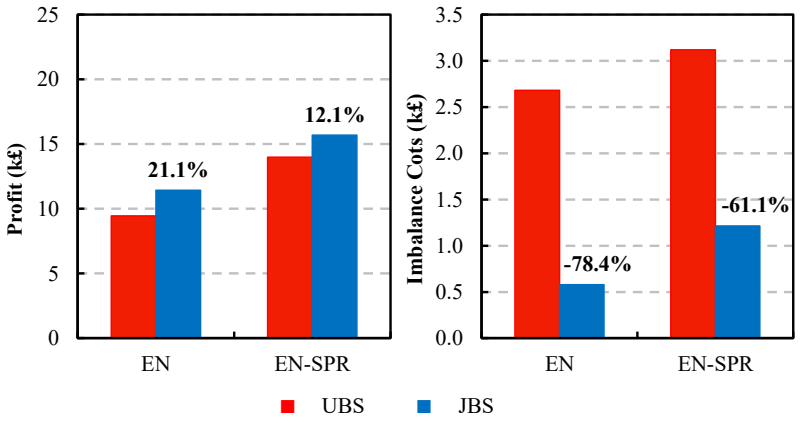


Fig. 3.12: Benefits of the JBS in expected profit and imbalance costs for Day 2.

As in Day 1, a larger expected profit increase can be achieved through the JBS for Day 2 than that of Day 1 percentage-wise. This can be explained, in part, by the fact the lower levels of wind generation for

this day lead to lower expected market revenues. However, this day features higher average imbalance values (236 MW in the UBS) which the JBS manages to reduce by 26% leading to a reduction of 61% in expected imbalance costs in the EN-SPR bidding strategy. Overall, the EN-SPR JBS leads to 66% profit increases with respect to the EN UBS.

Another particularity of this day is the sharp decrease (much larger than Day 1) in the benefit of the JBS in the EN-SPR participation with regards to the EN participation. This can be explained by the fact that it is more profitable in some time periods to ensure that there is sufficient stored energy to provide SPR than to utilize stored energy to manage wind imbalances. However, the 37% profit increase caused by the provision of SPR compensates the slightly higher payment of imbalance costs.

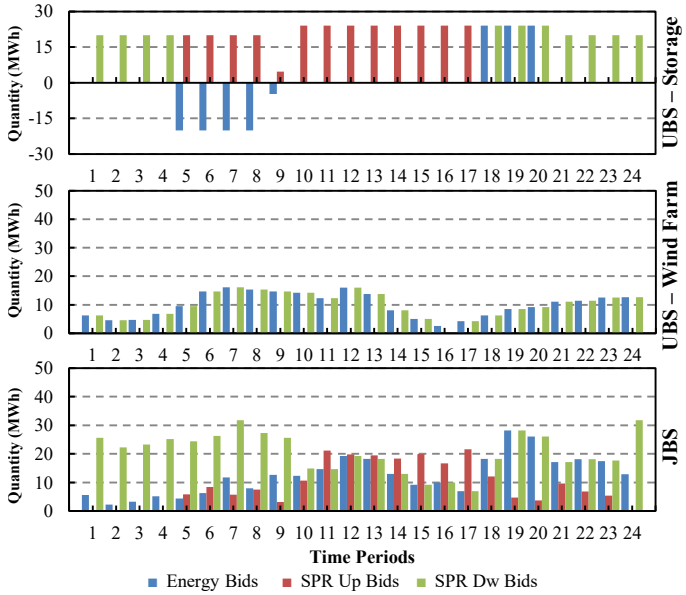


Fig. 3.13: Resulting bids for the EN-SPR bidding strategies for Day 2.

3.7.3 Impact of SU and SD Costs on Energy and SPR Provision

In order to assess the value of the proposed modelling of the SU and SD costs due to the provision of SPR and caused by the SU/SD actions of pump-turbine units that were otherwise offline/online, this case study is divided into two parts: 3.7.3.1 demonstrates that an incorrect representation of the expected operating costs and, consequently, the commitment of pump-turbine units may happen if the SU and SD costs are omitted when searching for an optimal bidding strategy; and the value of VS over FS pumps for the proposed JBS is quantified in 3.7.3.2.

3.7.3.1 Omission of the SU and SD Costs for SPR Provision

Here, it is assumed that the cost associated with the SD (SU) actions of online (offline) units due to the provision of SPR are neglected in objective function (3.54) in the same conditions specified in Section 3.7.1 and the EN-SPR JBS results obtained in Subsection 3.7.2.1 serve as a Base Case. The economic results of this analysis are presented in Table 3.9, while the AVG of SU and SD actions and their STD are presented in Table 3.10 .

Despite the expected profit difference between both simulations being very small (0.28% of the expected profit), it should be noted that the Base Case solution is more robust against uncertain SPR com-

mitment than the solution in this case study. This is due to the fact the PHSP may incur additional costs for SU or SD units if it is called to provide SPR. The omission of these costs leads to a bidding strategy with the potential for profit losses given the need for coordinating the management of wind imbalances and provision of SPR.

A decrease in the AVG and STD of SU and SD events can be observed in Table 3.10. Note that this case study only considers SU and SD events related to the management of wind imbalances and that these are lower than in the Base Case as well. Consequently, it is also possible to argue that the optimal schedule for this case study is not as robust as the Base Case's, as the real number of SU and SD is not properly assessed. Furthermore, with increased wind generation variability and the need for quick changes in the operation mode of the PHSP, an incorrect SU and SD event schedule may negatively impact the operational lifespan and costs of the pump-turbine units.

Table 3.9: Expected Profits for both cases (£)

	Base Case	No SPR SU SD Costs
Energy Market Revenue	17,381	17,377
SU Costs	70	49
SD Costs	6	6
Energy Imbalance Costs	1,351	1,374
SPR Up Revenue	1,914	1,919
SPR Down Revenue	4,146	4,151
SPR SU Costs	17	0
SPR SD Costs	23	0
SPR Up Imbalance Costs	288	280
SPR Down Imbalance Costs	240	231
Total Imbalance Costs	1,879	1,885
Total Profit	21,446	21,507

Table 3.10: AVG and STD of SU and SD Events

	Base Case		No SPR SU SD Costs	
	AVG	STD	AVG	STD
Pumping SU	5.8	1.9	3.0	1.4
Pumping SD	4.4	1.1	4.1	1.0
Turbine SU	4.4	1.1	4.1	0.5
Turbine SD	4.2	1.5	4.1	0.6

3.7.3.2 Fixed-speed vs Variable-speed Pump-turbine units

Current literature has shown the added value that VS pumping technology can bring when compared to FS PHSP plants. As such, a new simulation for Day 1 will be conducted in which the maximum and minimum power consumption limits of the pump-turbine units of the PHSP will be the same, i.e. 5 MW. As previously, the results obtained in Subsection 3.7.2.1 will be used as a Base Case in order to establish how VS technology impacts the benefit of the JBS over the UBS when compared to FS pump-turbine units in the EN-SPR market participation. The economic results for both bidding strategies and the AVG

and STD of the SU and SD events are compared in Tables 3.11 and 3.12 respectively.

The expected profits from FS PHSP are lower in both the UBS and JBS as the energy stored in the lower reservoir can't be fully pumped into the upper reservoir. Moreover, excess wind generation is not as efficiently managed by the PHSP as it is by VS pumps. The application of VS technology allows for an expected profit increase by up to 3.3% and 2.8% in the UBS and JBS, respectively. Note that the PHSP is assumed to operate with 4 identical pump-turbine units, which provides more flexibility than a single equivalent FS 20 MW pump-turbine unit. In other words, the considered FS PHSP allows for power consumption levels to change discretely between 0, 5, 10, 15 and 20 MW, while with a single pump-turbine unit power consumption levels can only be 0 or 20 MW. As the VS's power consumption levels can vary between 2.5 to 20 MW, through efficient SU actions, the benefit of a VS pump-turbine units over a single large VS pump-turbine unit can be considered to be higher than the value determined in this case study. It can also be concluded that the costs associated with the SU and SD actions due to the provision of SPR increase with the use of FS technology.

Table 3.11: Expected Total Profit Breakdown for both cases (£)

Strategy	UBS		JBS	
Technology	VS	FS	VS	FS
Energy Market Revenue	17,487	17,483	17,381	17,346
SU Costs	59	55	69	66
SD Costs	5	6	6	6
Energy Imbalance Costs	2,266	2,278	1,351	1,413
SPR Up Revenue	2,075	1,818	1,914	2,256
SPR Dw Revenue	3,840	4,188	4,146	3,715
SPR SU Costs	31	167	17	89
SPR SD Costs	21	20	23	21
SPR Up Imbalance Costs	17	22	288	286
SPR Dw Imbalance Costs	416	419	239	233
Total Imbalance Costs	2,699	2,719	1,879	1,933
Total Profit	20,583	20,523	21,446	21,202

Table 3.12: AVG of SU and SD Events for both cases

Strategy	UBS				JBS			
Technology	VS		FS		VS		FS	
	AVG	STD	AVG	STD	AVG	STD	AVG	STD
Pumping SU	4.2	2.0	4.0	0.0	5.8	1.9	4.3	1.2
Pumping SD	4.0	0.0	4.0	0.0	4.4	1.1	4.2	1.2
Turbine SU	4.4	0.5	4.0	0.0	4.4	1.1	5.3	1.2
Turbine SD	3.4	1.3	4.0	0.0	4.2	1.5	4.8	2.4

Analysing the results in Table 3.12, the use of VS technology also requires a higher number of SU and SD actions in both bidding strategies, being the highest for the JBS in order to better manage wind generation uncertainty. Consequently, the operational lifespan of VS pump-turbine units will be negatively impacted when compared to an independent FS PSHP. Through the proposed modelling of the SU and SD events and their costs, more informed decisions can be made when managing larger wind generation variability through the JBS.

3.7.4 Constrained Wind Energy Use

The JBS allows for excess wind energy to be stored for later use instead of being curtailed in the UBS. In order to illustrate how wind curtailment can be mitigated through JBS, instead of just managing potential positive deviations, this case study analyses the behaviour of the JBS when the system cannot absorb all wind generation. As such, this study is divided into two cases: Case A assumes that the WF and the PHSP are co-located and connected to the transmission system through the same line with limited capacity; Case B is designed to simulate a scenario where the TSO instructs the WF to reduce wind generation due to aggregate generation being higher than demand. and assumes that both facilities don't need to be co-located. These case studies expose the optimal energy and SPR bids determined for Day 1 in Subsection 3.7.2 to a new second-stage for the stochastic problem with limited capacity for absorbing wind energy.

Constraining the absorption of wind energy is achieved by limiting the amount of energy and SPR that the WF and the PHSP can provide through constraints (3.104) and (3.105) for the JBS and UBS models respectively in Case A. In order to ensure that considerable wind generation couldn't be absorbed for Day 1, the transmission line is assumed to be rated at 60% of the WF's capacity. Only constraints (3.105) are used for Case B as it is assumed that both facilities are not co-located.

$$p^{\mathrm{W}}_{e,r,w,h} + p^{\mathrm{T}}_{e,r,w,h} - p^{\mathrm{P}}_{e,r,w,h} + r^{\mathrm{Up,T,On}}_{e,r,w,h} + r^{\mathrm{Up,T,Off}}_{e,r,w,h} + r^{\mathrm{Up,P}}_{e,r,w,h} + r^{\mathrm{Up,W}}_{e,r,w,h} \leq 0.6\,\mathrm{K}^{\mathrm{W}}, \quad \forall e,r,w,h, \tag{3.104}$$

$$p^{\mathrm{W}}_{e,r,w,h} + r^{\mathrm{Up,W}}_{e,r,w,h} \leq 0.6\,\mathrm{K}^{\mathrm{W}}, \quad \forall e,r,w,h, \tag{3.105}$$

3.7.4.1 Case A

The results for Case A are summarized in Table 3.13 which show that the JBS manages to almost fully utilize all available wind power leading to profit increases by up to 18.8% with respect to the UBS in the EN participation. While for the EN-SPR market participation, the reduced benefit of the JBS over the UBS (6.6% profit increase) is due to the fact that the minimization of the energy imbalance costs contributes more to profit maximization than the provision of SPR-Up. Therefore, the model determines the optimal operation schedule that minimizes energy imbalances by using stored energy ahead of providing SPR. Consequently, the imbalance costs related to the failure to deliver the day-ahead SPR-Up bids increase.

Table 3.13: Economic Results for Case A

Bidding Strategy	EN		EN-SPR	
	UBS	JBS	UBS	JBS
Expected Profit (£)	13,523	16,066	18,619	19,840
Expected Imbalance Costs (£)	2,384	1,261	2,848	2,646
Expected Wind Curtailment (MWh)	47.05	0.16	47.05	0.22
Wind Utilization (%)	90.84	99.97	90.84	99.96

3.7.4.2 Case B

Table 3.14 presents the results for case B, which show that the JBS manages to fully utilize the wind generation that otherwise would need to be curtailed in the UBS for both the EN and EN-SPR bidding strategies and achieving expected profit increases, similarly to Case A. In this case, however, wind generation that cannot be used to store energy is instead used to provide SPR-Up. Nevertheless, the JBS allows for expected profit increases of 18.9% for the EN participation and up to 12.3% for the EN-SPR.

Table 3.14: Economic Results for Case B

Bidding Strategy	EN		EN-SPR	
	UBS	JBS	UBS	JBS
Expected Profit (£)	13,523	16,071	18,623	20,910
Expected Imbalance Costs (£)	2,384	1,272	2,845	1,956
Expected Wind Curtailment (MWh)	47.05	0.11	47.05	0
Wind Utilization (%)	90.84	99.98	90.84	100

As important as the economic benefit of the JBS presented in both cases is, the ability to avoid the curtailment of cheap and carbon-free wind energy achieved through the coordination between the WF and PHSP is more relevant for future low-carbon power systems. Even when these facilities are not co-located, as in Case B, the PHSP can increase power consumption in order to match demand to excess renewable generation. A transmission system-wide analysis, however, is needed in order to better assess the value of WF and PHSP coordination.

3.7.5 Influence of WF and PHSP Capacities on the JBS Benefit

This case study analyses the impact in the JBS's profit increase over the UBS for different capacity values for the WF and the PHSP's pump-turbine units and reservoirs. A comparison between the relative economic benefit of the JBS over the UBS is established for a set of possible WF and PHSP configurations with the parameters described in Table 3.15. The results of these simulations are summarized in Fig. 3.14 which shows how the relative profit difference between the JBS and UBS changes for the EN and EN-SPR market participations.

Table 3.15: Sensitivity Analysis Parameters

WF	K^W	PHSP	N^{units}	$\overline{P}^P$	$\overline{P}^T$	$\overline{V}^{U/L}$
WF1	25	PS1	2	5	6	50
WF2	50	PS2	4	5	6	100
WF3	75	PS3	6	5	6	150
WF4	100	PS4	8	5	6	200
WF5	125	PS5	10	5	6	250

The results show that larger WFs benefit less from smaller PHSPs, as the maximum charging and discharging power levels of the PHSP are smaller than the level of the wind imbalances. Moreover, the quantity of energy that can be stored is also insufficient for an effective imbalance costs reduction. Inversely, smaller WFs benefit less from bigger PHSPs which can be explained by the fact that, when compared to the UBS, the management of wind imbalances achieved by the JBS lowers the expected

revenue from the provision of SPR, which is the main source of revenue for the PHSP in the UBS. Larger PHSPs benefit from more energy and capacity headroom for the provision of SPR beyond managing wind imbalances, which in turn, reduces the difference in expected revenue from SPR provision and, consequently, the relative profit variation between the UBS and JBS.

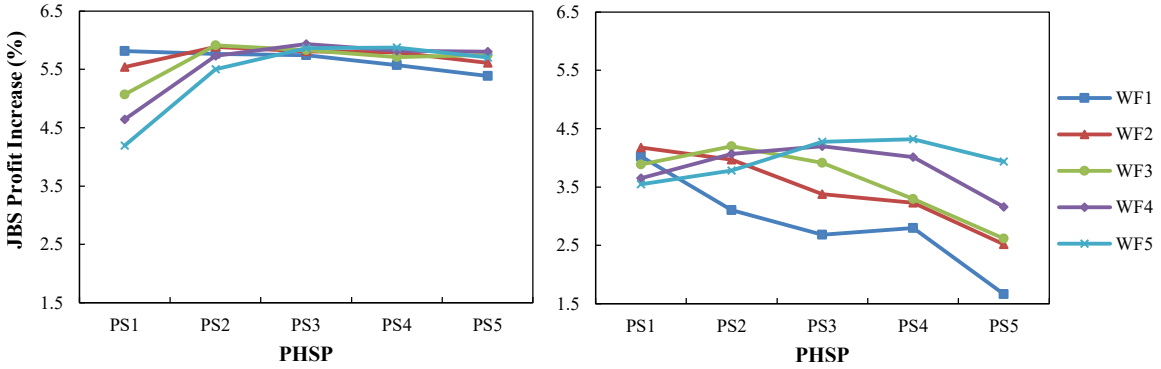


Fig. 3.14: Relative profit increase achieved with the JBS for EN (left) and for the EN-SPR (right) bidding strategies.

3.7.6 Assessment of the Computational Performance

In order to present the value of the proposed tight reformulation using SOS1 variables for positive and negative imbalances - SOS1-T formulation - proposed in Subsection 3.5.2.2 in terms of computational performance, two benchmark formulations are presented: a traditional reformulation of the non-linear absolute value functions using binary variables - BIN formulation - to force only one set of auxiliary variables for positive and negative deviations to be larger than zero at any given time period; a simpler reformulation of the absolute value function without using binary or SOS1 variables to ensure only a set of positive or negative auxiliary variables is positive but with fixed bounds - SIM formulation. In regards to the second benchmark formulation, as it is assumed that the objective function to be maximized features negative costs and prices of the form $\omega^{\text{En/SPR}^+}_{e/r,h}\pi^{\text{En/SPR,Up/Dw}}_{e/r,h} \leq \pi^{\text{En/SPR,Up/Dw}}_{e/r,h} \leq \omega^{\text{En/SPR}^-}_{e/r,h}\pi^{\text{En/SPR,Up/Dw}}_{e/r,h}$, the optimal solution to this problem will always ensure that either $i^{\text{En/SPR,Up/Dw}^+}_{e,r,w,h}$ or $i^{\text{En/SPR,Up/Dw}^-}_{e,r,w,h}$ are positive at any given time. For the traditional BIN and SIM formulations, constraints (3.46), (3.47), (3.49), (3.50), (3.52) and (3.53) in the original formulation are replaced by constraints (3.106) to (3.111), albeit for the SIM the additional binary variables $B^{\text{En}}_{e,r,w,h}$, $B^{\text{SPR,Up}}_{e,r,w,h}$, and $B^{\text{SPR,Dw}}_{e,r,w,h}$ are dropped from these constraints.

$$0 \leq i^{\text{En}^+}_{e,r,w,h} \leq \left(\text{W}^{\text{AV}}_{w,h}\text{K}^{\text{W}} + \text{N}^{\text{units}}\overline{\text{P}}^{\text{T}} + \text{N}^{\text{units}}\overline{\text{P}}^{\text{P}}\right)B^{\text{En}}_{e,r,w,h}, \quad \forall e,r,w,h, \tag{3.106}$$

$$0 \leq i^{\text{En}^-}_{e,r,w,h} \leq \left|-\text{N}^{\text{units}}\overline{\text{P}}^{\text{P}} - \left(\text{W}^{\text{AV}}_{w,h}\text{K}^{\text{W}} + \text{N}^{\text{units}}\overline{\text{P}}^{\text{T}}\right)\right|\left(1 - B^{\text{En}}_{e,r,w,h}\right), \quad \forall e,r,w,h, \tag{3.107}$$

$$0 \leq i^{\text{SPR,Up}^+}_{e,r,w,h} \leq \left(\text{K}^{\text{W}} + \text{N}^{\text{units}}\overline{\text{P}}^{\text{T}} + \text{N}^{\text{units}}\overline{\text{P}}^{\text{P}}\right)B^{\text{SPR,Up}}_{e,r,w,h}, \quad \forall e,r,w,h, \tag{3.108}$$

$$0 \leq i^{\text{SPR,Up}^-}_{sh} \leq \left|\max\left\{\overline{\text{P}}^{\text{P}},\overline{\text{P}}^{\text{T}}\right\}\text{N}^{\text{units}} + \text{K}^{\text{W}}\right|\left(1 - B^{\text{SPR,Up}}_{e,r,w,h}\right), \quad \forall e,r,w,h, \tag{3.109}$$

$$0 \leq i^{\text{SPR,Dw}^+}_{e,r,w,h} \leq \left(\text{K}^{\text{W}} + \text{N}^{\text{units}}\overline{\text{P}}^{\text{T}} + \text{N}^{\text{units}}\overline{\text{P}}^{\text{P}}\right)B^{\text{SPR,Dw}}_{e,r,w,h}, \quad \forall e,r,w,h, \tag{3.110}$$

$$0 \leq i_{e,r,w,h}^{\mathrm{SPR,Dw^-}} \leq \left|\max\left\{\overline{\mathrm{P}}^{\mathrm{P}}, \overline{\mathrm{P}}^{\mathrm{T}}\right\} \mathrm{N}^{\mathrm{units}} + \mathrm{K}^{\mathrm{W}}\right| \left(1 - B_{e,r,w,h}^{\mathrm{SPR,Dw}}\right), \quad \forall e, r, w, h. \tag{3.111}$$

In the same line of the previous case studies, the scenarios from Day 1 were chosen and expanded to a total of 150 scenarios for this performance analysis. The three formulations under analysis were tested with different numbers of scenarios ranging from 1 and up to 150 scenarios, a duality gap set at 0.5% and a maximum run time of 100,000 sec. For each test, the set of scenarios was selected to impact the least the value of the objective function. In other words, the scenario closest to the average profile of the wind power availability forecast was chosen for the test with 1 scenario. For the test with 15 scenarios, the set contains the forecast in the previous test, 7 forescasts closest to maximum values and 7 forecasts closest to the mininum value. The sets for the following tests follow this rule. The results of the performance study are plotted in Fig. 3.15.

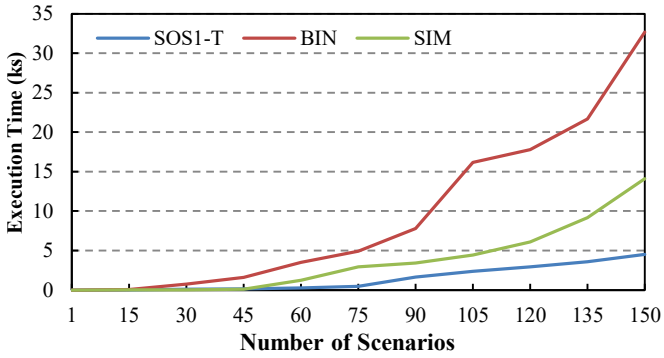


Fig. 3.15: Execution time comparison for different number of scenarios and formulations.

The results clearly show that the proposed SOS1-T formulation solves the problem faster than the other two formulations. When compared to the BIN, execution times can be reduced up to 85% for 150 scenarios. The SIM benchmark formulation also allows for a significant, albeit smaller than the SOS1-T formulation, execution time reduction when compared to the BIN formulation due to the lack of binary variables. The SOS1-T formulation outperforms both benchmark formulations in most simulationsThe SIM is slightly faster (between 30 and 87% faster) than the SOS1-T when the number of scenarios is lower than 60, albeit the maximum absolute execution time difference is approximately 52s. This can be explained due to the reduced size of the problem and the resulting gap of the optimal solutions. The SOS1-T achieved solutions with lower resulting gaps than the SIM formulation, albeit it took longer to find them.

3.8 Chapter Conclusions

This chapter proposes a novel two-stage stochastic programming model that improves the participation of a WF in the day-ahead energy and SPR markets through a coordinated operating strategy with an ESS. Concretely, the model determines the optimal energy and SPR bids for the WF and the recourse actions by the ESS in order to maximize profit generated in both markets and minimize costs associated with settling deviations between real-time delivery of energy and SPR and the day-ahead bids. This coordination strategy is applied to a generic ESS (Li-ion battery based) model and to a PHSP model in order to understand the value of the proposed JBS is impacted by the different characteristics of an emerging

technology and a mature, albeit capital intensive, ESS technology (PHSP). Modelling-wise, the first proposed ESS model ensures that sufficient energy is stored in order to provide committed SPR services for the maximum utilization time, while the second model PHSP model features additional pump-turbine units' SU and SD events to consider costs associated with providing SPR and a tight re-formulation for the calculation of the absolute value of imbalances that improves computational performance over alternative methods.

The results clearly show the economic benefit of the JBS through increased daily profits in both market participations and the added revenue by providing SPR. The results of the case studies in Section 3.6 show that the EN-SPR JBS achieves profit increases averaging £3,038/day when compared to a deterministic UBS, and the benefit of the JBS in the EN-SPR market participation is actually greater than in the EN participation. On the other hand, higher profit increases of up to 21.1% are achieved by the PHSP in Section 3.7, albeit the provision of SPR negatively impacts the benefit of the JBS due to the fact that in the respective case study, the management of energy imbalances is economically more advantageous than providing SPR.

Other benefits of the JBS are translated into reduced offering uncertainty, as the ESS is able to reduce positive and negative deviations to great extent, and the ability to utilize cheap wind energy to store excess generation that would otherwise be curtailed. This makes the JBS particularly interesting for low-carbon power systems with large shares of intermittent renewable generation, as fewer resources need to be deployed in order to balance variable net-demand and improve the integration of renewables.

Another contribution of this chapter is the aforementioned tight reformulation of the absolute value functions to calculate energy and SPR imbalances, using SOS1 auxiliary variables and integer variables to dynamically bound these imbalances. The proposed technique significantly reduces the computational time of the models when compared to traditional linearisation without losing solution accuracy. As such, larger case studies with longer assessment time horizons or with an increased number of scenarios in order to better represent pricing and generation uncertainty can be conducted.

Continuing with the investigation into how uncertainty and profit distributions can be improved through the proposed JBS, the next chapter will address strategies to mitigate exposure to low-profit scenarios for risk-averse wind producers.

Chapter 4

Risk-Averse Coordination Strategies

The previous models assumed that the objective of the WF and ESS operator was to maximize day-ahead profit. However, as daily profit becomes a stochastic variable characterized by a probability distribution, the maximization of the expected profit neglects the representation of relevant information in the tail-ends of the distribution curve which may feature a non-negligible probability of undesirable outcomes. As such, some agents may find it more important to hedge against the risk of experiencing low profits or even losses by adopting risk-averse strategies.

In this chapter, a novel two-stage stochastic programming model which allows a WF with on-site ESS to consider several degrees of risk aversion for optimization the combined participation in the day-ahead energy and SPR markets. In other words, this formulation expands on the model presented in Section 3.4 of the previous chapter by modelling the Conditional Value-at-Risk (CVaR) metric to minimize the risk of experiencing low day-ahead profits.

This chapter is structured as follows: the nomenclature for the model proposed here in Section 4.1; the Introduction in 4.2 approaches the need to consider risk measures for stochastic generation technologies, related work to this topic in current literature and a detailed explanation of this proposal; the mathematical formulation is presented in Section 4.3; the value of the proposed risk-averse JBS is analysed in the case studies in Section 4.4; Section 4.5 concludes this chapter and discusses how the propose risk-averse JBS can be improved and expanded in the following chapter.

4.1 Nomenclature

4.1.1 Indices, Sets and Sub-Sets

$e \in S^{E}$	Day-ahead energy price forecasts.
$r \in S^{R}$	Day-ahead SPR price forecasts.
$w \in S^{W}$	Day-ahead available wind power forecasts.
$h \in H$	Time periods.
Ω^{BV}	Set of all binary decision variables.
Ω^{CV}	Set of all continuous decision variables.
$\Omega^{CV^{+}}$	Set of all positive continuous decision variables.
$\Omega^{SCV^{+}}$	Set of all positive semi-continuous decision variables.

$\Omega^{\text{CV}^{\text{SOS1}}}$ Set of all positive SOS1 continuous decision variables.

4.1.2 Parameters

$\pi^{\text{En}}_{e,h}$ Energy market price at forecast e and time period h [£/MWh].

$\pi^{\text{SPR,Up}}_{r,h}$ SPR-Up market price at forecast r and time period h [£/MW/h].

$\pi^{\text{SPR,Dw}}_{r,h}$ SPR-Dw market price at forecast r and time period h [£/MW/h].

$\omega^{\text{En}^{+/-}}_{e,h}$ Price penalty factor for positive/negative energy imbalances at forecast e and time period h [p.u.].

$\omega^{\text{SPR}^{+/-}}_{r,h}$ Price penalty factor for positive/negative SPR imbalances at forecast r and time period h [p.u.].

ρ_e, ρ_r, ρ_w Probability of each forecast e, r and w [p.u.].

β Risk aversion level [p.u.].

α CVaR Confidence level [p.u.].

M Large number for constraint relaxation.

4.1.3 Continuous Variables

x^{En}_{h} Joint Energy bid for time period h [MWh].

$x^{\text{SPR,Up}}_{h}$ Joint SPR-Up bid for time period h [MW].

$x^{\text{SPR,Dw}}_{h}$ Joint SPR-Dw bid for time time period h [MW].

$i^{\text{En}^{+/-}}_{e,r,w,h}$ Positive/Negative energy deviation from the day-ahead bid at scenario e, r, w, and time period h [MW].

$i^{\text{SPR-Up}^{+/-}}_{e,r,w,h}$ Positive/Negative SPR-Up deviation from the day-ahead bid at scenario e, r, w, and time period h [MW].

$i^{\text{SPR-Dw}^{+/-}}_{e,r,w,h}$ Positive/Negative SPR-Dw deviation from the day-ahead bid at scenario e, r, w, and time period h [MW].

ζ^{En} Value-at-Risk for energy profit [£].

$\zeta^{\text{SPR,Up}}$ Value-at-Risk for SPR-Up profit [£].

$\zeta^{\text{SPR,Dw}}$ Value-at-Risk for SPR-Dw profit [£].

$\mu^{\text{En}}_{e,r,w}$ Auxiliary variable in order to compute the CVaR for energy profit for scenario e, r, w [£].

$\mu^{\text{SPR,Up}}_{e,r,w}$ Auxiliary variable in order to compute the CVaR for SPR-Up profit for scenario e, r, w [£].

$\mu^{\text{SPR,Dw}}_{e,r,w}$ Auxiliary variable in order to compute the CVaR for SPR-Dw profit for scenario e, r, w [£].

4.2 Introduction

4.2.1 Literature Review

The works analysed in the previous chapters' literature reviews assume a risk-neutral approach for modelling profit maximization or cost minimization, in which the decision maker focuses solely on optimizing the expected outcome and disregarding other information in the profit or cost distribution function.

In literature, accounting for the profit or cost values in the worst scenarios make the decision maker a risk-averse agent [86]. As such, a risk-averse optimization can be considered as a set of decisions to minimize the exposure to undesirable outcomes, i.e. risk.

Operation strategies considering risk aversion have been widely studied and adopted in current power systems literature. The authors of [94] present a risk-averse wind energy trading strategy considering prices and generation uncertainty and show that profit deviations can be reduced at the expanse of a small decrease in the expected profit. On the other hand, [95] considers an expanded uncertainty set concerning wind power generation, market prices, demand bids and rivals' offers to determine the optimal strategy for wind producers to maximize expected profit and minimize volatility. A game-theoretic approach to investigate the role of risk-averse renewable portfolio owners (ESS, hydro plants and wind generators) in exercising market power in systems with high amounts of flexible power sources is proposed in [96]. Zhang et al. investigated in [97] the value of CVaR in reducing the expected risk of loss-of-load in stochastic unit commitment problems considering wind power generation uncertainty. The inclusion of the CVaR lead to a reduction in the loss-of-load costs in the extreme scenarios. The authors of [98] analyse the impact of risk aversion in joint day-ahead energy and reserve scheduling in the context of Crete's insular power system. The modelling of CVaR for the behaviour of the ISO allows for reducing total systems, however at the expense of utilizing less wind energy.

Risk-averse operating strategies for ESS have also been studied in literature. [99] determines the optimal marginal cost curves for a risk-averse hydro-generating company participating in the energy and AS markets considering price uncertainty and the opportunity cost of water. Moazeni et al. present risk-averse operation strategies for ESS in [100, 101]. The former proposes the utilization of CVaR to determine an optimal conversion and transmission strategy between the grid, renewable producers and ESS considering transaction costs, while the latter presents an ESS management strategy to maximize profit using CVaR (described as the mean shortfall in the paper). The risk-averse operation of VS PHSPs in the joint energy and secondary regulation reserve markets is studied in [102]. The deployment of VS pumping technology allows for significant profit increases when compared to FS technology, and the adoption of the risk-averse formulation allows moderately increasing the Value-at-Risk and CVaR with small impact to the expected profit.

Although [26, 73] do not explicitly model risk-averse strategies, the coordination of wind generation resources with ESS has the added benefit of reducing low-profit exposure. The authors of [103], however, show that minimizing risk exposure leads to a reduction in expected profit of up to 2.03% for combined WF-cascade hydro systems. Despite this, the impact of risk aversion on the combined operation WF and ESS has not been studied in depth. Furthermore, risk-averse formulations are usually applied to energy and reserve provision to ESS or other flexible generation technologies only. As such, the impact of risk aversion on the provision of AS by combined WF-ESS has not been fully addressed, neither studied in depth. The consideration of profit risks is fundamental for WF and ESS coordination strategies, as risk-neutral approaches do not reflect the behaviour of conservative investors given the involved high capital costs.

4.2.2 Risk-averse Joint Bidding Strategies for WF and ESS

This chapter proposes a two-stage stochastic mathematical programming model which optimizes the bidding strategy for combined WF-ESS that participate in the day-ahead energy and SPR markets for

different degrees of risk aversion [104]. In other words, the proposed model is useful for understanding how a risk-averse wind producer can maximize expected profit and minimize risk exposure with the help of an ESS without adopting very conservative strategies. It also allows understanding how the provision of SPR is conditioned when minimizing exposure to uncertainty, unlike the methodologies proposed in [26, 32, 72–75]. Consequently, the value of coordination strategies for WF and ESS is increased if compared to the original risk-neutral bidding strategy proposed in the previous chapter and in [75].

Section 3.4 presents an objective function which maximizes the expected profit subject to the realization of the random variables. This risk-neutral approach disregards the impact that low probability, albeit with a large impact, extreme scenarios that lead to low profits or even losses have in the operation of a wind producer looking to improve their position in the energy and SPR markets. The risk-averse bidding strategy considered in this work can be defined as a strategy that seeks to minimize the exposure (i.e. risk of experiencing) to low-profit scenarios. Thus, by coupling stochastic programming models with risk control measures, it is possible to mitigate the impact of undesirable profit values with non-negligible probabilities. The modelling of risk-averse behaviour is often achieved by including a risk measure term associated with the profit distribution in the model's formulation [86]. Common risk measures used in literature include profit variance, shortfall probability, VaR and CVaR.

During the development of this work, CVaR was chosen for the following reasons: 1) CVaR possesses superior mathematical properties compared to VaR, which is non-convex and discontinuous [105]; 2) VaR is relatively difficult to optimize in the context of convex MILP problems, while CVaR can be easily linearised in the context of convex linear problems which also provides the VaR; 3) the optimization of the CVaR leads to the optimization of the lowest profit scenarios, which in turn provides more information about the tail-end of the profit distribution; and 4) CVaR is also a coherent measure of risk by satisfying the properties enumerated in [106] (translation invariance, subadditivity, positive homogeneity, and monotonicity). CVaR is one of the most common risk measures in literature for modelling risk-averse behaviour by wind energy producers [94, 95, 99, 100]. Despite this, a risk-averse formulation for the energy and SPR JBS for WF and ESS [104] is uncommon in current literature.

4.3 Risk-averse JBS Model

As previously stated, the model proposed in this chapter is built upon the mathematical formulation of the risk-neutral JBS for WF and ESS presented in Section 3.4. As such, the nomenclature and mathematical formulation presented herein only reflect the new enhancements to the previous model. Further insight into the model's constraints is provided in Section 3.4.

4.3.1 Key Properties and Assumptions

As before, the model proposed in this chapter is formulated as a two-stage stochastic MILP problem in order to maximize the profit from the participation in the day-ahead energy and SPR markets by joint WF and ESS and to minimize exposure to profit uncertainty. The consideration of different levels of risk aversion is achieved by modelling a trade-off objective function which allows considering several degrees of risk aversion. Objective function (3.11) is henceforth regarded as risk-neutral and reference for further comparisons. Other assumptions identified earlier are still valid here.

4.3.2 CVaR measure

The CVaR is defined as the expected value of the $(1-\alpha)\times 100\%$ worst scenarios for a profit distribution [86], in which $\alpha \in (0,1)$ is the desired confidence level. The VaR for such a profit distribution can be defined as the value ζ equal to the maximum profit outcome which ensures that the probability of a profit outcome being less than ζ is lower or equal than $1-\alpha$. The discrete profit distribution $(\boldsymbol{x}, \sigma_{\boldsymbol{x}})$ for a WF participating the in the day-ahead energy and SPR markets obtained from the Sto.UBS results from Subsection 3.6.2 is plotted in Fig. 4.1 to illustrate the relationship between VaR, CVaR and the expected profit.

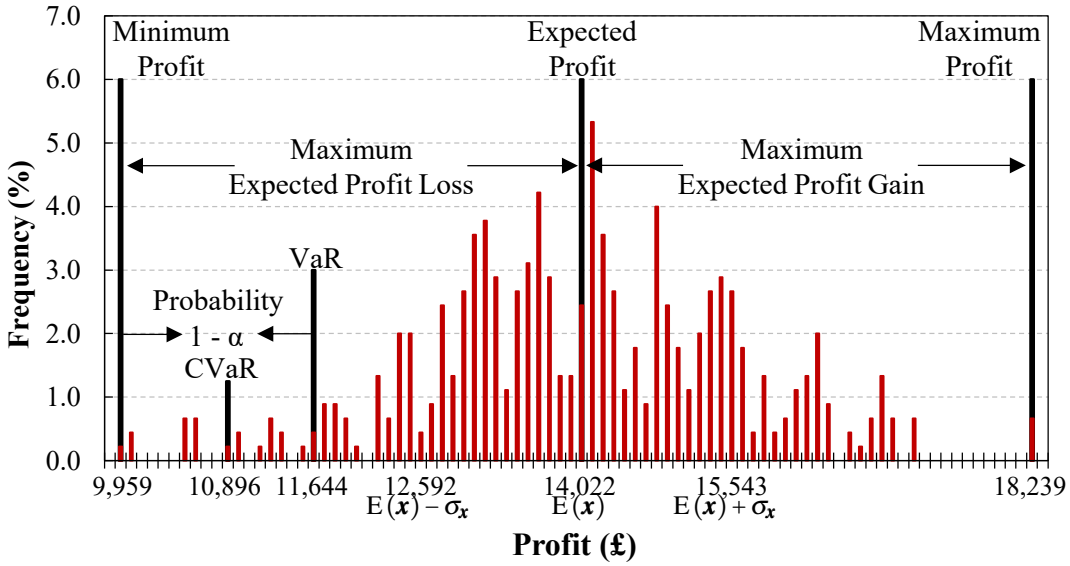


Fig. 4.1: VaR and CVaR for a day-ahead WF profit distribution.

In order to represent the VaR and CVaR in mathematical terms for the discrete profit distribution $\boldsymbol{x}$ represented above, let us first denote $\boldsymbol{x}_\omega$ as the value of the profit distribution for scenario $\omega \in \Omega$ with associated probability ρ_ω. The $\text{VaR}(\alpha,\boldsymbol{x})$ is given by (4.1) to calculate the maximum value ζ which ensures that the probability of the profit outcome being less than ζ is lower or equal than $1-\alpha$. The CVaR $\text{CVaR}(\alpha,\boldsymbol{x})$ is given in equation (4.2) as the expected value of the profit outcomes lower or equal the VaR. The CVaR can be calculated in the context of an optimization problem with equation (4.3), which is adapted from [107], as the difference between a maximum value ζ (which essentially is equal to $\text{VaR}(\alpha,\boldsymbol{x})$) and the expected value of the sum of positive differences between ζ and the profit value for each scenario divided by $1-\alpha$.

$$\text{VaR}(\alpha,\boldsymbol{x}) = \max\{\zeta \in \mathbb{R} : \Pr(\boldsymbol{x} < \zeta) \leq 1-\alpha\}, \quad \forall \alpha \in (0,1), \tag{4.1}$$

$$\text{CVaR}(\alpha,\boldsymbol{x}) = \text{E}[\boldsymbol{x} \,|\, \boldsymbol{x} \leq \text{VaR}(\alpha,\boldsymbol{x})], \quad \forall \alpha \in (0,1), \tag{4.2}$$

$$\text{CVaR}(\alpha,\boldsymbol{x}) = \max\left\{\zeta \in \mathbb{R} : \zeta - \frac{1}{1-\alpha}\sum_{\omega\in\Omega}\rho_\omega[\max\{\zeta - \boldsymbol{x}_\omega, 0\}]\right\}, \quad \forall \alpha \in (0,1). \tag{4.3}$$

Equation (4.4) only serves to minimize risk exposure by maximizing the CVaR. However, this may lead to overly conservative results. A trade-off function should be implemented instead in order control the level of risk aversion against the maximization of the expected profit by the operator. As such, a two-stage stochastic formulation for solving the trade-off between profit maximization and minimizing risk is achieved with a trade-off risk aversion control parameter β:

$$\text{Maximize}_{\boldsymbol{x}} \Big\{ (1-\beta)\, \mathrm{E}_{\omega}\left[f(\boldsymbol{x}, \omega) \right] + \beta\, \mathrm{CVaR}\left(\alpha, \boldsymbol{x}\right) \Big\}. \tag{4.4}$$

4.3.3 Objective Function and Additional Constraints

An objective function that allows considering different degrees of risk aversion for the WF and ESS operator can be created by using the risk-neutral objective function (3.11), equation (4.4) and a risk aversion level β. The resulting objective function (4.5) allows determining the optimal bidding strategy that solves the multi-objective problem for a certain level of risk aversion, or, in other words, the trade-off between maximizing expected profit and maximizing CVaR. A CVaR measure corresponding to each source of profit, i.e. Energy, SPR-Up and SPR-Dw, was used in this formulation for two main reasons as opposed to a single CVaR measure for the total profit: in order to reflect the impact of the different sources of uncertainties on the operation of the ESS and WF; and, given the different price levels for energy and SPR, to ensure that the energy market-related actions do not negatively impact the participation in the SPR market, and vice-versa.

$$\begin{aligned}
\underset{\substack{\Omega^{\mathrm{BV}}, \Omega^{\mathrm{CV}}, \Omega^{\mathrm{CV}^+}, \\ \Omega^{\mathrm{SCV}^+}, \Omega^{\mathrm{CV}^{\mathrm{SOS1}}}}}{\text{Maximize}} \Bigg\{ & (1-\beta) \sum_{e \in S^{\mathrm{E}}} \sum_{r \in S^{\mathrm{R}}} \sum_{w \in S^{\mathrm{W}}} \rho_e \rho_r \rho_w \Bigg[\sum_{h \in H} \Big(\pi^{\mathrm{En}}_{e,h} x^{\mathrm{En}}_h + \omega^{\mathrm{En}^+}_{e,h} \pi^{\mathrm{En}}_{e,h} i^{\mathrm{En}^+}_{e,r,w,h} - \omega^{\mathrm{En}^-}_{e,h} \pi^{\mathrm{En}}_{e,h} i^{\mathrm{En}^-}_{e,r,w,h} \\
& + \pi^{\mathrm{SPR,Up}}_{r,h} x^{\mathrm{SPR,Up}}_h + \omega^{\mathrm{SPR}^+}_{r,h} \pi^{\mathrm{SPR,Up}}_{r,h} i^{\mathrm{SPR,Up}^+}_{e,r,w,h} - \omega^{\mathrm{SPR}^-}_{r,h} \pi^{\mathrm{SPR,Up}}_{r,h} i^{\mathrm{SPR,Up}^-}_{e,r,w,h} \\
& + \pi^{\mathrm{SPR,Dw}}_{r,h} x^{\mathrm{SPR,Dw}}_h + \omega^{\mathrm{SPR}^+}_{r,h} \pi^{\mathrm{SPR,Dw}}_{r,h} i^{\mathrm{SPR,Dw}^+}_{e,r,w,h} - \omega^{\mathrm{SPR}^-}_{r,h} \pi^{\mathrm{SPR,Dw}}_{r,h} i^{\mathrm{SPR,Dw}^-}_{e,r,w,h} \Big) \Bigg] \\
& + \beta \Bigg[\left(\zeta^{\mathrm{En}} - \frac{1}{1-\alpha} \sum_{e \in S^E} \sum_{r \in S^R} \sum_{w \in S^W} \rho_e \rho_r \rho_w \mu^{\mathrm{En}}_{e,r,w} \right) \\
& + \left(\zeta^{\mathrm{SPR,Up}} - \frac{1}{1-\alpha} \sum_{e \in S^E} \sum_{r \in S^R} \sum_{w \in S^W} \rho_e \rho_r \rho_w \mu^{\mathrm{SPR,Up}}_{e,r,w} \right) \\
& + \left(\zeta^{\mathrm{SPR,Dw}} - \frac{1}{1-\alpha} \sum_{e \in S^E} \sum_{r \in S^R} \sum_{w \in S^W} \rho_e \rho_r \rho_w \mu^{\mathrm{SPR,Dw}}_{e,r,w} \right) \Bigg] \Bigg\}.
\end{aligned} \tag{4.5}$$

The method for calculating the CVaR in (4.3) is non-linear by nature. However, as previously mentioned, CVaR can be easily linearised with a set of auxiliary variables and constraints. When compared to the previous objective function, the new terms in objective function (4.5) reflect the calculation of the Energy (4$^{\text{th}}$ line), SPR-Up (5$^{\text{th}}$ line) and SPR-Dw (6$^{\text{th}}$ line) CVaRs respectively, and, in order to linearize the CVaR measure, new constraints (4.6) to (4.8) are added to the formulation. Equations (4.9) and (4.10) define the type for the introduced variables to calculate the CVaR for all sources of profit.

$$\zeta^{\mathrm{En}} - \sum_{h \in H} \left(\pi^{\mathrm{En}}_{e,h} x^{\mathrm{En}}_h + \omega^{\mathrm{En}^+}_{r,h} \pi^{\mathrm{En}}_{e,h} i^{\mathrm{En}^+}_{e,r,w,h} - \omega^{\mathrm{En}^-}_{e,h} \pi^{\mathrm{En}}_{e,h} i^{\mathrm{En}^-}_{e,r,w,h} \right) \leq \mu^{\mathrm{En}}_{e,r,w}, \quad \forall e, r, w, \tag{4.6}$$

$$\zeta^{\mathrm{SPR,Up}} - \sum_{h \in H} \left(\pi^{\mathrm{SPR,Up}}_{r,h} x^{\mathrm{SPR,Up}}_h + \omega^{\mathrm{SPR}^+}_{r,h} \pi^{\mathrm{SPR,Up}}_{r,h} i^{\mathrm{SPR,Up}^+}_{e,r,w,h} - \omega^{\mathrm{SPR}^-}_{r,h} \pi^{\mathrm{SPR,Up}}_{r,h} i^{\mathrm{SPR,Up}^-}_{e,r,w,h} \right) \leq \mu^{\mathrm{SPR,Up}}_{e,r,w}, \quad \forall e, r, w, \tag{4.7}$$

$$\zeta^{\mathrm{SPR,Dw}} - \sum_{h \in H} \left(\pi^{\mathrm{SPR,Up}}_{r,h} x^{\mathrm{SPR,Up}}_h + \omega^{\mathrm{SPR}^+}_{r,h} \pi^{\mathrm{SPR,Up}}_{r,h} i^{\mathrm{SPR,Up}^+}_{e,r,w,h} - \omega^{\mathrm{SPR}^-}_{r,h} \pi^{\mathrm{SPR,Up}}_{r,h} i^{\mathrm{SPR,Up}^-}_{e,r,w,h} \right) \leq \mu^{\mathrm{SPR,Dw}}_{e,r,w}, \quad \forall e, r, w, \tag{4.8}$$

$$\Omega^{\mathrm{CV}} = \left\{ \zeta^{\mathrm{En}}, \zeta^{\mathrm{SPR,Up}}, \zeta^{\mathrm{SPR,Dw}} \right\} \in \mathbb{R}, \tag{4.9}$$

$$\Omega^{\mathrm{CV^+}} = \left\{ \mu^{\mathrm{En}}_{e,r,w}, \mu^{\mathrm{SPR,Up}}_{e,r,w}, \mu^{\mathrm{SPR,Dw}}_{e,r,w} \right\} \in \mathbb{R}_{\geq 0}, \quad \forall e, r, w. \tag{4.10}$$

4.4 Case Studies

The case studies presented in this Section follow the same parameters presented in Subsections 2.4.1 and 3.6.1. Slight variations in the results are mainly caused by the solution gap of the optimal solutions, which was set at 1.0% and adjusted for all tests.

4.4.1 Expected Profit Risk Management

As previously stated, the proposed formulation allows the consideration of different degrees of risk aversion when optimizing the optimal day-ahead energy and SPR bidding for WF with the support of an ESS. In order to assess how these bidding strategies are affected by risk aversion, several simulations with varying degrees of risk aversion (different values for β) are carried out for the UBS (stochastic) and the JBS under a confidence level (α) set at 95% for the three days. The impact of risk aversion is first analysed on the total profit for both bidding strategies by comparing the risk-neutral and risk-averse profit distributions and how the CVaR, expected profit and STD vary for different values of β. The profit distributions are bounded by the minimum profit of the UBS and the maximum profit of the JBS for the risk-neutral results for each day.

4.4.1.1 Day 1

Fig. 4.2, which presents the risk-neutral and risk-averse profit distributions for the UBS and JBS, show that the risk aversion results distributions that are less dispersed. A full risk-averse behaviour $(\beta = 1)$ results in a reduction of the expected profit of approximately 17% for the UBS and 14.2% for the JBS, while the CVaR was increased by 5.9% and 6.5 % respectively when compared to the risk-neutral results. Moreover, when comparing the profit distributions for the risk-neutral and risk-averse behaviours, it is possible to conclude that the distributions become more concentrated. The most probable profit outcome for the UBS lies between £11,396 and £11,496 with 44.9% probability, while for the JBS the profit is more likely to fall between £12,496 and £12,596 at approximately 78% probability (coinciding with the JBS VaR). The plots in Fig. 4.2 also show that minimum profit in the JBS is 1.5% larger than the expected profit in the UBS.

From the efficient frontier in Fig. 4.3 (a), the benefit of the JBS over the UBS in terms of expected profit varies between 4.6% $(\beta = 0.9)$ and 10.2% $(\beta = 1)$, while the CVaR fluctuates between 8.5% $(\beta = 0.1)$ and 10.0% $(\beta = 1)$. Note that, on one hand, when β increases from 0.9 to 1, the CVaR suffers a small increase (JBS) or remains unchanged (UBS) despite a large decrease in expected profit (15.8% for the UBS and 11.3% for the JBS). On the other hand, Fig. 4.3 (b) shows that the STD has been greatly reduced in this interval (72.3% for the UBS and 61% for the JBS). Taking these results into account, it can be argued that the full risk-averse solutions are less economically efficient than those achieved when $\beta = 0.9$ due to the sharp decrease of the expected profit and CVaR remaining unchanged.

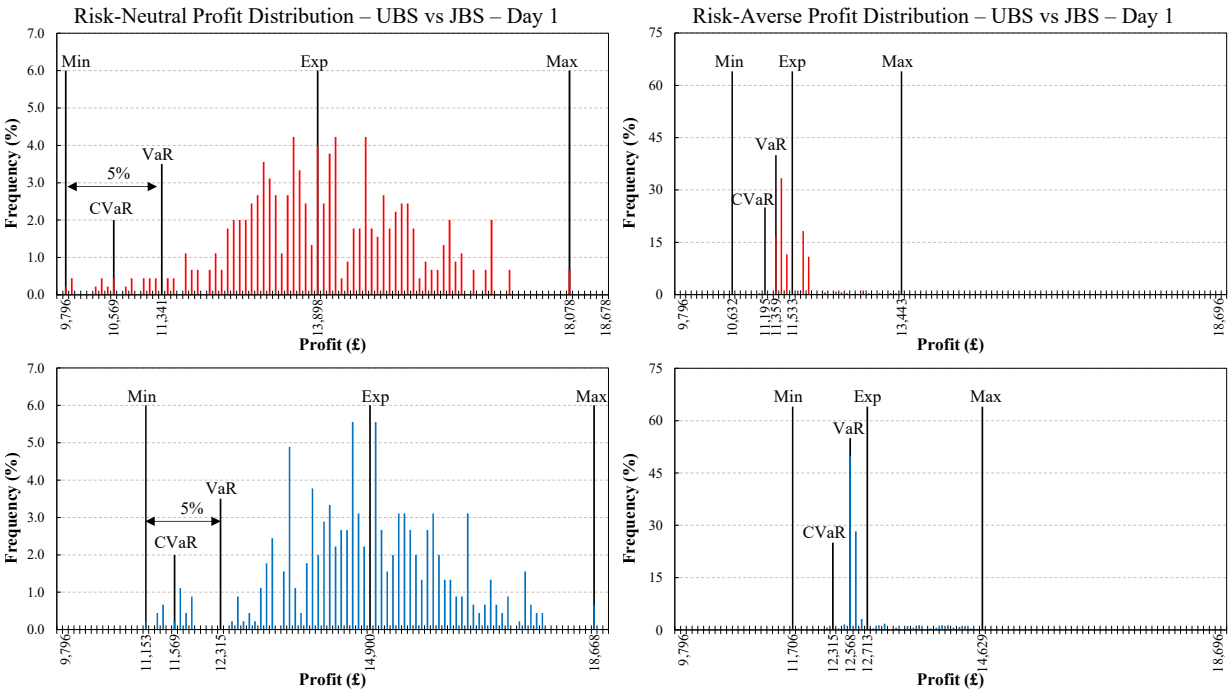


Fig. 4.2: Risk-neutral (left) and risk-averse (right) total profit distributions for the UBS (top) and the JBS (bottom) for day 1.

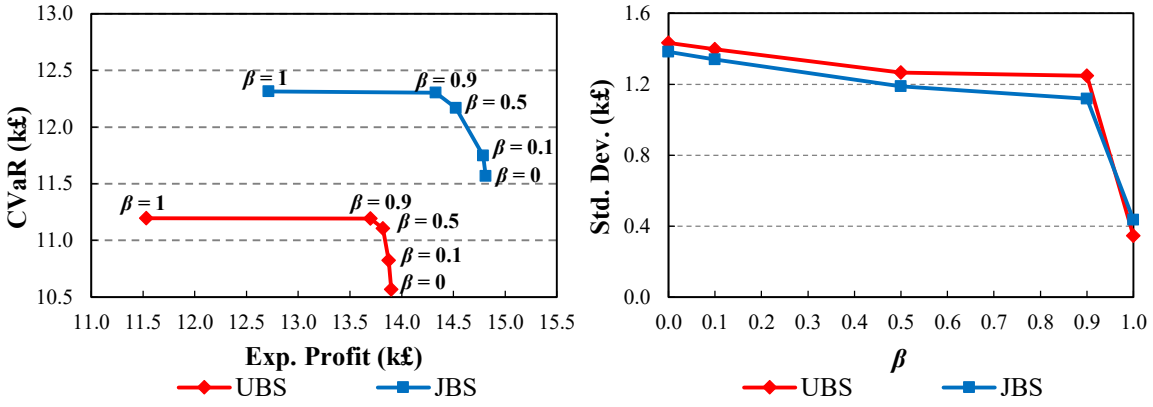


Fig. 4.3: Comparison of CVaR, expected profit and STD for the UBS (red) and the JBS (blue) for day 1 (a) Efficient frontier, (b) Profit STD.

4.4.1.2 Day 2

Similarly to day 1, Fig. 4.4 presents the profit distributions for both strategies and levels of risk aversion for day 2. Despite the showing similar results, the variations due to the full risk-averse behaviour are more pronounced. Expected profits were reduced by 24.4% for the UBS and by 21.2% for the JBS, while the CVaR increased by 14.2% for the UBS and 13.6% for the JBS. In the full risk-averse behaviour, the JBS achieves values for the minimum profit higher than the expected profit value of the UBS (5.3% higher) and the expected profit value of the JBS is also 3% higher than the maximum profit that can be achieved with the UBS. For the UBS, the most probable interval for the total profit is between £4,426 and £4,501 at 86% probability. For the JBS, profit varies between £5,026 and £5,101 with 91.6% probability. Note that for the JBS, the VaR is actually higher than the expected profit which is mainly due to the low value for the profit variation.

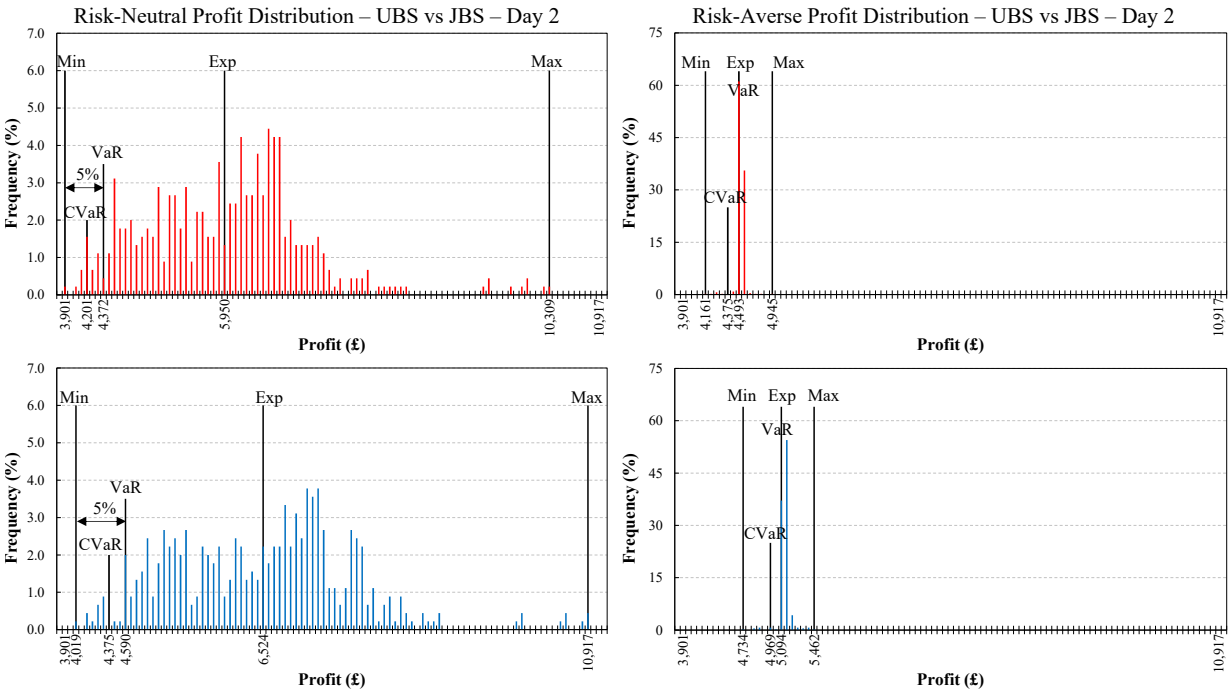


Fig. 4.4: Risk-neutral (left) and risk-averse (right) total profit distributions for the UBS (top) and the JBS (bottom) for day 2.

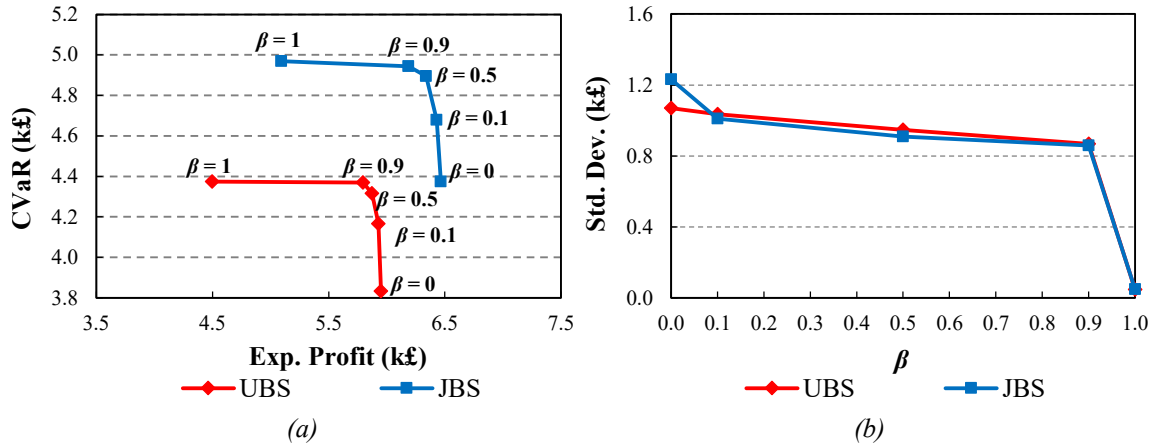


Fig. 4.5: Comparison of CVaR, expected profit and STD for the UBS (red) and the JBS (blue) for day 2 (a) Efficient frontier, (b) Profit STD.

Fig. 4.5 (a) shows a similar trend for the impact of different levels of risk aversion on the UBS, the JBS and the benefit of the latter over the former. The CVaR is increased between 12.3% ($\beta = 0.1$) and 13.6% ($\beta = 1$) by the JBS in regards to the UBS, while in terms of expected profit, the lowest benefit sits at 6.8% ($\beta = 0.9$) and the highest benefit at 13.3% ($\beta = 1$). In the same way as day 1, the CVaR remains relatively unchanged despite the decrease in expected profit for both bidding strategies, when β increases from 0.9 to 1. Expected profit decreases 22.4% for the UBS and 17.7% for the JBS when β increases from 0.9 to 1, which is much higher than the expected profit decrease when β increases from 0 to 0.9 (2.6% for the UBS and 4.3% for the JBS). Profit STD is reduced by 94% for both bidding strategies when $\beta = 1$ as evidenced in Fig. 4.5 (b) . Similarly to day 1, $\beta = 1$ leads to solutions that can be considered to be economically worse given the significant decrease in expected profit.

4.4.1.3 Day 3

Figs 4.6 and 4.7 present the third day's profit distributions, efficient frontier and STD variation. Again, similar conclusions can be made for this day regarding the effect of risk aversion on the expected profits, CVaR and the benefit of the JBS over the UBS. Expected profits decrease by 23.2% for the UBS and 18.2% for the JBS when compared to the risk-neutral results, while CVaR increases by 8.14% and 7.9% for the UBS and JBS respectively. However and unlike previous days, in the full risk-averse simulation the minimum profit of the JBS is not higher than the expected profit the UBS. In fact, the risk-averse profit distributions show that the probability of the UBS achieving a total profit between £16,459 and £16,659 is 75.6%, while the likeliest interval for the JBS profit is between £16,859 and £17,059 at 50.2% probability. Note that the JBS's risk-averse profit distribution is wider than the UBS's and that the likeliest profit value for the JBS is approximately only 2.4% higher than the UBS's (the lowest of the 3 days).

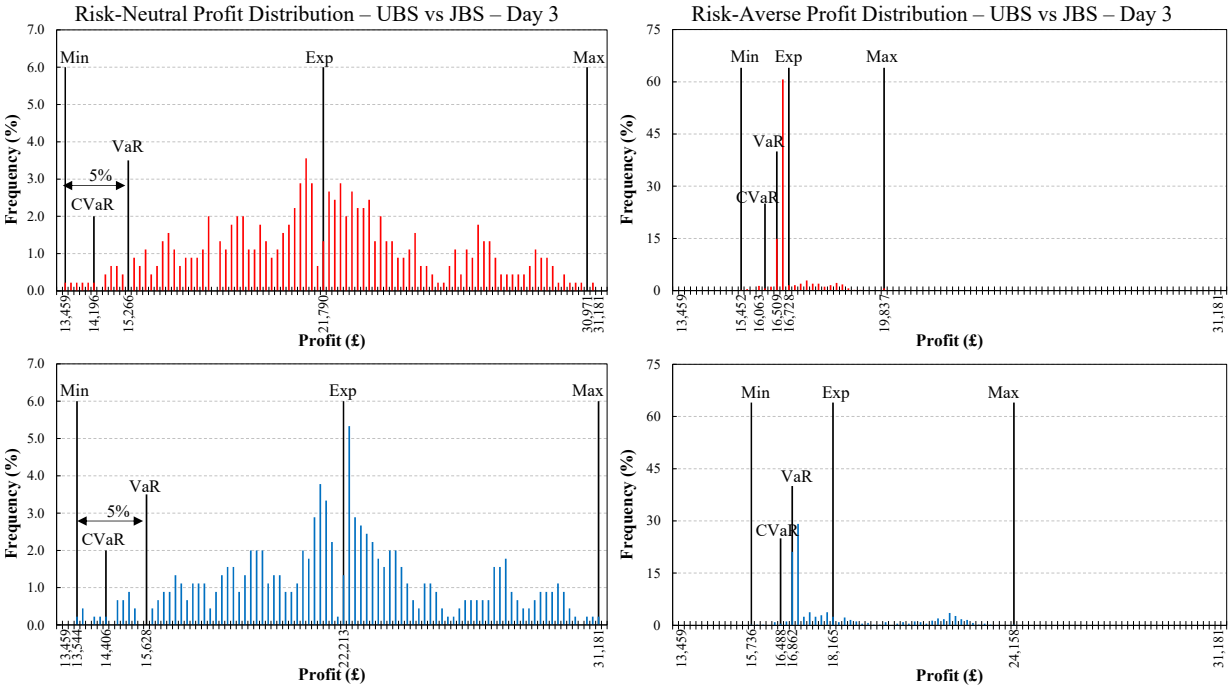


Fig. 4.6: Risk-neutral (left) and risk-averse (right) total profit distributions for the UBS (top) and the JBS (bottom) for day 3.

The efficient frontier in Fig. 4.7 (a) also shows a similar behaviour to the previous days. The benefit of the JBS over the UBS varies from 0.9% ($\beta = 0.9$) to 8.6% ($\beta = 1$) in terms of expected profit, and from 1.1% ($\beta = 0.1$) to 4.4% ($\beta = 0$) for the CVaR. In this day, for $\beta = 1$ the JBS's CVaR is 2.7% higher than the UBS's CVaR. From the (b) side, it is possible to observe that the STD was reduced by 80.2% in the UBS and by 31.9% in the JBS. Analysing the results for the two highest levels of risk aversion, expected profits are reduced by 20.3% and 14.2% for the UBS and JBS, respectively, and the CVaR for both strategies barely increases (<0.5% increase).

To a greater extent than in the previous days, these results reinforce the notion that full risk-averse behaviour leads to overly conservative solutions, i.e. greatly reducing profit variability leads to losing the opportunity of achieving higher profits, greatly reducing its expected value without a significant effect on the CVaR. Taking into consideration the results for all days, it is possible to conclude that $\beta = 0.9$

presents a more economically efficient solution as, for the JBS, the expected profit decreases by £1,805 (4.2%) and the CVaR increases by £3,373 (11.1%) in total for the 3 days.

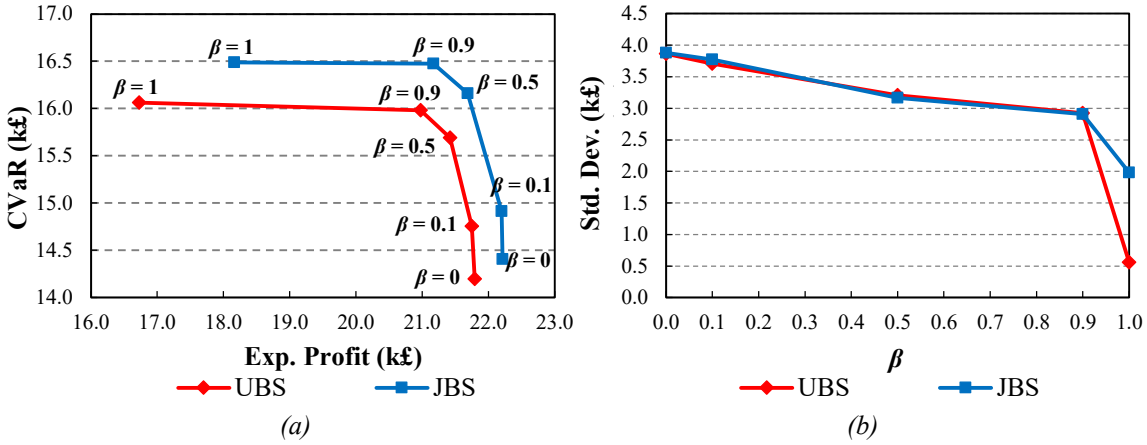


Fig. 4.7: Comparison of CVaR, expected profit and STD for the UBS (red) and the JBS (blue) for day 3 (a) Efficient frontier, (b) Profit STD.

4.4.2 The impact of risk aversion on the management of imbalances

The impact of the JBS on wind generation imbalances has been investigated and discussed in Subsection 3.6.3. The objective of this case study is to understand how adopting risk-averse bidding strategies affects the resulting generation imbalances for both bidding strategies. Table 4.1 presents the AVG and STD of the absolute value of the energy imbalances for all days, both bidding strategies and both risk aversion behaviours. Figs. 4.8 to 4.10, compare the scenario realizations and energy bids for all bidding strategies and days for the full risk-averse behaviour. The relevant plots for the risk-neutral strategies are not plotted here and Figs. 3.6 to 3.8 can be used for comparison purposes instead.

Table 4.1 shows that risk aversion decreases the AVG of the energy imbalances by up to 28.9% for the UBS and up to 60% for the JBS. Regarding the STD, the impact of risk aversion is not as straightforward, as in some cases the STD increases or decreases in some days for both bidding strategies. This behaviour can be explained due to the objective of maximizing CVaR in the full risk-averse simulations leading to recourse actions for each scenario that increase the lowest profit scenarios by reducing negative imbalances (energy shortage) during time periods before energy prices are expected to be higher. Consequently, the profit of scenarios with more favourable forecasts is reduced due to the increase in positive imbalances (energy surplus) and reducing day-ahead market revenue. This behaviour is corroborated by Figs. 4.8 and 4.10, as energy bids are closer to the top of injected power dispersion in the initial time periods and closer to the bottom of the dispersion during the afternoon time periods, which for the UBS also aligns with charging and discharging periods for the ESS. Comparing this behaviour with Figs. 3.6 to 3.8 where the energy bids fall near the middle of the injected power dispersion, which is a consequence of chosen price penalty factors for the imbalances (0.5 for positive and 1.5 for negative imbalances). The energy bids are also, in general, closer to the lower values for the injected power dispersion in order minimize the overall value of negative imbalances and, consequently, imbalances costs.

Table 4.1: AVG and STD of the energy imbalances for all days in MW.

Behaviour	Risk Neutral				Full Risk-averse			
Strategy	UBS		JBS		UBS		JBS	
Metric	AVG	STD	AVG	STD	AVG	STD	AVG	STD
Day 1	4.022	3.008	2.072	2.448	3.241	3.462	1.172	2.307
Day 2	2.489	2.446	1.518	2.067	1.769	2.382	0.847	2.025
Day 3	3.741	2.718	2.939	2.877	3.511	3.835	1.523	3.047

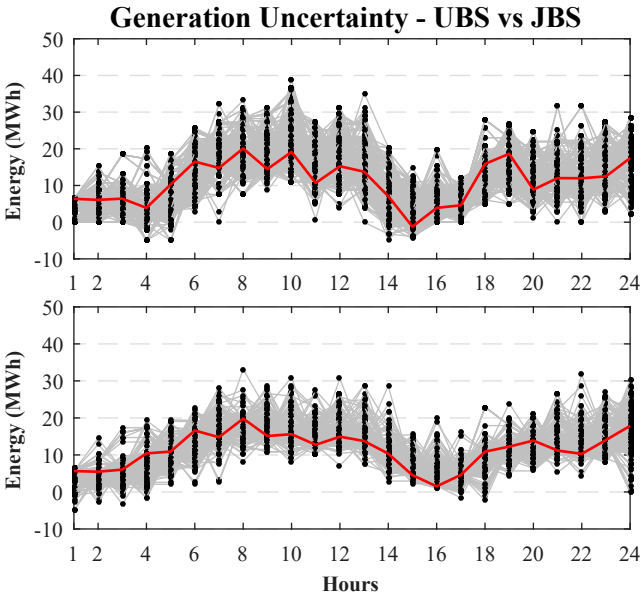


Fig. 4.8: Comparison of the injected power (black dots) and energy bid (red line) for all scenarios of the risk-averse UBS (up) and the JBS (down) for day 1.

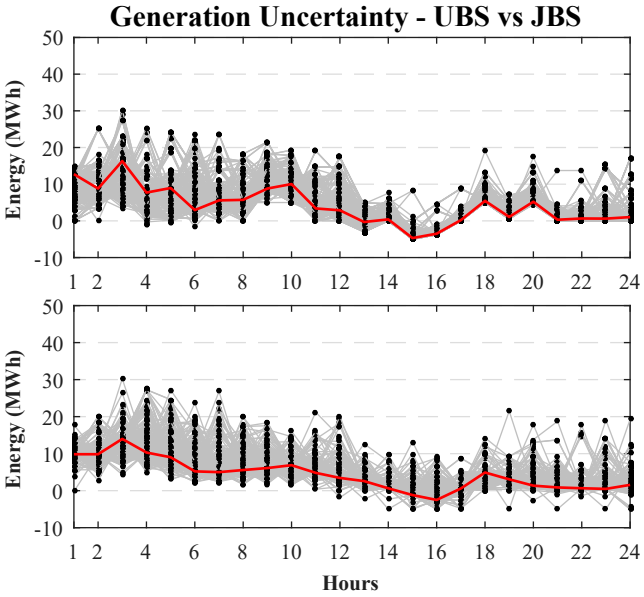


Fig. 4.9: Comparison of the injected power (black dots) and energy bid (red line) for all scenarios of the risk-averse UBS (up) and the JBS (down) for day 2.

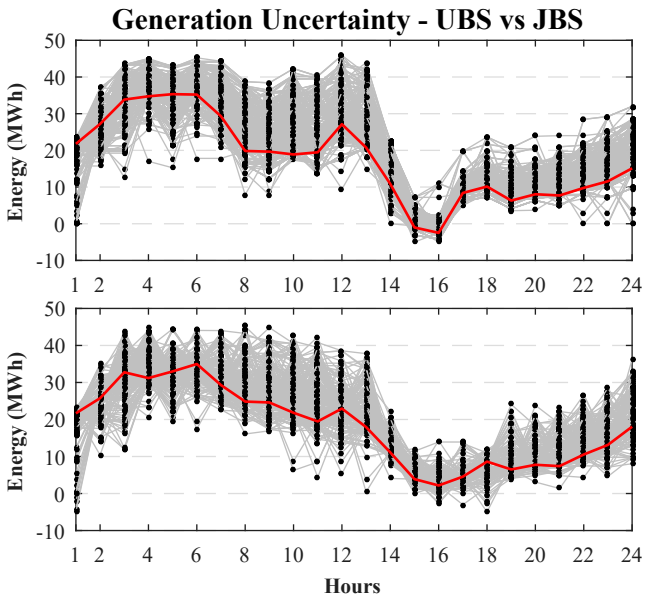


Fig. 4.10: Comparison of the injected power (black dots) and energy bid (red line) for all scenarios of the risk-averse UBS (up) and the JBS (down) for day 3.

The benefit of the JBS over the UBS on the AVG and STD of the absolute value of energy imbalances also increases. Whereas the reduction in AVG varies between 21.4% and 48.5% for the risk-neutral behaviour, this reduction now varies between 52.1% and 63.8% for the risk-averse behaviour. A similar behaviour can be observed for the STD of the energy imbalances.

4.5 Chapter Conclusions

This chapter proposes a novel two-stage stochastic programming framework in order to investigate the effects of several levels of risk aversion for the joint participation of WF and ESS in the day-ahead energy and SPR markets. A trade-off between maximizing expected profit and CVaR is modelled for the objective function in order to find the level of risk aversion that leads to economically efficient bidding strategies.

The case studies analysed here show how the proposed modelling of risk allows further supporting the proposed business case for the coordinated operation of WF and ESS. As analysed in the previous chapter, the JBS for WF and ESS achieves significant expected profit increases and, by adopting a risk-averse approach, the uncertainty relating the day-ahead profit for both facilities is greatly reduced. Consequently, the risk-averse JBS ensures that profit volatility and the probability of experiencing low profits are reduced. By analysing the profit distributions, risk-averse biding strategies lead to more concentrated distributions increasing probabilities for certain profit outcomes. Concretely, the probability of the most likely profit scenarios in the risk-neutral approaches ranged between 3% and 5%, while the risk-averse approaches lead to the probability of the most likely profit outcomes being as high as 60%. The value of the JBS is also increased for a risk-averse WF operator, as the ESS provides a better management of imbalances in order to achieve larger values for the CVaR and, in turn, further reducing the risk of experiencing undesirable profit outcomes.

The efficient frontiers, presented in Figs. 4.3, 4.5 and 4.7, conclude that maximizing the CVaR in a full risk-averse strategy greatly reduces the STD of the day-ahead profit. This is achieved, however, at

the expense of greatly reducing expected profit with little improvements to the CVaR. Thus, pursuing full risk-averse bidding strategies lead to overly conservative solutions, while risk aversion levels between 50% and 90% provide higher expected profits for slightly lower values for CVaR, albeit with higher values for the STD.

Despite this chapter optimizing the value of an ESS for a risk-averse WF operator considering the provision of SPR, it does not consider the provision of other services to increase revenue streams. Also, the power and energy capacities of the ESS considered in the case studies presented thus far have not been optimally determined. The next chapter in this Thesis expands this work by: increasing the types of services that the combined WF and ESS operator can provide to the system operator; expanding the time horizon under analysis from one day to several weeks and a year; developing an investment model for a risk-averse WF operator to determine the optimal values for the power and energy capacities of the ESS.

Chapter 5

Energy Storage Investment for Risk-averse Wind Farm Operators

The previous chapters presented the advantages of coordinating renewable generation technologies with ESS of a pre-determined size in both risk-neutral and risk-averse settings. Although in Subsection 3.7.5 the variation of the benefit of the JBS over the UBS is analysed for different sizes of the PHSP, the discretization of this sensitivity analysis may lead to the optimal value for the size of the ESS to be undetermined. Furthermore, as the previous case studies analyse only a few days, the results and conclusions drawn contain insufficient information to accurately assess the profitability of ESS investments by risk-averse WF operators.

This chapter concludes the evolution of the JBS for WF and ESS presented in the previous chapters by proposing a novel two-stage stochastic programming model in order to determine the optimal sizes for the power and energy capacities of an ESS to manage wind generation imbalances and provide AS for a risk-averse WF operator. In this context, the risk-averse JBS model presented in Chapters 3 and 4 is first expanded to consider multiple consecutive days and analyses a full year of operation. Secondly, the range of services that the WF-ESS operator can provide to the system operator is increased by providing FR besides SPR. However, the resulting problem becomes too large to solve to optimality for a considerable number of scenarios. As such, computational tractability is achieved by representing the year under analyses through representative weeks and through a problem decomposition technique such as the PHA.

This chapter includes: a nomenclature for all sets, parameters, variables for the complete model, as well as additional parameters for the PHA decomposition technique in 5.1; a literature review concerning the long-term modelling of ESS, investment models and application of decomposition techniques in this context, and a description of the proposed model is carried out in 5.2; the complete mathematical formulation of the investment model is described in 5.3; an explanation of the techniques adopted in order to achieve computational tractability are detailed in 5.4; case studies in order to assess the value of the proposed investment model and decomposition technique are carried out in 5.5; and, lastly, 5.7 concludes this chapter.

5.1 Nomenclature

5.1.1 Indices, Sets and Sub-Sets

$e \in S^{\mathrm{E}}$	Day-ahead energy price forecasts $(e = e_1, ..., e_{\mathrm{N^E}})$.
$r \in S^{\mathrm{R}}$	Day-ahead SPR price forecasts $(r = r_1, ..., r_{\mathrm{N^R}})$.
$f \in S^{\mathrm{F}}$	Day-ahead FR price forecasts $(f = f_1, ..., f_{\mathrm{N^F}})$.
$w \in S^{\mathrm{W}}$	Day-ahead available wind power forecasts $(w = w_1, ..., w_{\mathrm{N^W}})$.
$j \in J$	Representative Weeks $\left(j = 1, ..., \mathrm{N^J}\right)$.
$d \in D$	Days $\left(d = 1, ..., \mathrm{N^D}\right)$.
$h \in H$	Hourly Time periods $\left(h = 1, ..., \mathrm{N^H}\right)$.
Ω^{BV}	Set of all binary decision variables.
Ω^{CV}	Set of all continuous decision variables.
$\Omega^{\mathrm{CV^+}}$	Set of all positive continuous decision variables.
$\Omega^{\mathrm{SCV^+}}$	Set of all positive semi-continuous decision variables.
$\Omega^{\mathrm{CV^{SOS1}}}$	Set of all positive SOS1 continuous decision variables.

5.1.2 Parameters

W_j	Weight of the representative week j [p.u.].
$\mathrm{K^L}$	Transmission line capacity [MW].
$\mathrm{K^W}$	WF generation capacity [MW].
$\mathrm{L}^{\mathrm{AV}}_{d,h}$	Transmission line availability for day d and time period h [p.u.]
$\mathrm{P}^{\mathrm{AV}}_{d,w,h}$	Wind power available for day d, forecast w and time period h [p.u.].
η	Roundtrip efficiency of the conversion unit [p.u.].
$\overline{\mathrm{P}}$	Maximum power capacity of the ESS to be sized [MW].
$\overline{\mathrm{E}}$	Maximum energy capacity of the ESS to be sized [MWh].
$\mathrm{E^{Min/Max}}$	Minimum/Maximum stored energy level in the ESS [p.u.].
δ	Annual discount rate for the ESS investment [p.u.].
γ	Equipment lifetime for the ESS [years]
$\mathrm{C^P}$	Current value for the capital cost of the ESS's power-related component [£/MW].
$\mathrm{C^E}$	Current value for the capital cost of the ESS's energy-related component [£/MWh].
$\pi^{\mathrm{En}}_{d,e,h}$	Energy market price for day d, forecast e and time period h [£/MWh].
$\omega^{\mathrm{En^{+/-}}}_{d,e,h}$	Price penalty factor for positive/negative energy imbalances for day d, forecast e and time period h [p.u.].
$\pi^{\mathrm{SPR,Up/Dw}}_{d,r,h}$	SPR-Up/SPR-Dw market price for day d, forecast r and time period h [£/MW/h].

$\omega^{\text{SPR}^{+/-}}_{d,r,h}$ Price penalty factor for positive/negative SPR imbalances for day d, forecast r and time period h [p.u.].

τ^{SPR} Maximum duration of SPR requirement [h].

$\underline{\text{SPR}}^{\text{Up/Dw}}$ Minimum level for SPR-Up/SPR-Dw provision [MW].

$\pi^{\text{FR,Up/Dw}}_{d,f,h}$ FR-Up/FR-Dw market price for day d, forecast f and time period h [£/MW/h].

$\omega^{\text{FR}^{+/-}}_{d,f,h}$ Price penalty factor for positive/negative FR imbalances for day d, forecast f and time period h [p.u.].

τ^{FR} Maximum duration of FR requirement [h].

$\underline{\text{FR}}^{\text{Up/Dw}}$ Minimum level for FR-Up/FR-Dw provision [MW].

$\rho_e, \rho_r, \rho_f, \rho_w$ Probability of each forecast e, f, r and w [p.u.].

β Risk aversion level [p.u.].

α CVaR Confidence level [p.u.].

M Large number for constraint relaxation.

5.1.3 Binary Variables

$Q^{\text{SPR,Up,D/C}}_{d,e,r,f,w,h}$ Commitment of SPR-Up in discharging/charging mode for day d, scenario e,r,f,w and time period h.

$Q^{\text{SPR,Dw,D/C}}_{d,e,r,f,w,h}$ Commitment of SPR-Dw in discharging/charging mode for day d, scenario e,r,f,w and time period h.

5.1.4 Continuous Variables

5.1.4.1 First-Stage Variables

K^{P} Power capacity of the ESS [MW].

K^{E} Energy capacity of the ESS [MWh].

$x^{(.)}_{d,h}$ Joint Energy/SPR-Up/SPR-Dw/FR-Up/FR-Dw bid for day d and time period h [MWh].

$\xi^{(.)}$ Energy/SPR-Up/SPR-Dw/FR-Up/FR-Dw CVaR [£].

$\zeta^{(.)}$ Energy/SPR-Up/SPR-Dw/FR-Up/FR-Dw VaR [£].

5.1.4.2 Second-Stage Variables

$e^{0}_{e,r,f,w}$ Initial stored energy level in the ESS for scenario e,r,f,w [MWh].

$e_{d,e,r,f,w,h}$ Energy stored in the ESS for day d, scenario e,r,f,w and time period h [MWh].

$p^{\text{C}}_{d,e,r,f,w,h}$ Power consumed by the ESS for day d, scenario e,r,f,w and time period h [MW].

$p^{\text{D}}_{d,e,r,f,w,h}$ Power generated by the ESS for day d, scenario e,r,f,w and time period h [MW].

$p^{\text{W}}_{d,e,r,f,w,h}$ Power output of the WF for day d, scenario e,r,f,w and time period h [MW].

$r^{\text{SPR,Up,D/C}}_{d,e,r,f,w,h}$ SPR-Up contribution by the ESS during discharging/charging for day d, scenario e,r,f,w and time period h [MW].

$r^{\text{SPR,Dw,D/C}}_{d,e,r,f,w,h}$ SPR-Dw contribution by the ESS during discharging/charging for day d, scenario e,r,f,w and time period h [MW].

$r^{\text{SPR,Up,W}}_{d,e,r,f,w,h}$ SPR-Up contribution of the WF for day d, scenario e,r,f,w and time period h [MW].

$r^{\text{SPR,Dw,W}}_{d,e,r,f,w,h}$ SPR-Dw contribution of the WF for day d, scenario e,r,f,w and time period h [MW].

$r^{\text{SPR,Up/Dw}}_{d,e,r,f,w,h}$ Total SPR-Up/SPR-Dw contribution from both facilities for day d, scenario e,r,f,w and time period h [MW].

$r^{\text{FR,Up,D/C}}_{d,e,r,f,w,h}$ FR-Up contribution by the ESS during discharging/charging for day d, scenario e,r,f,w and time period h [MW].

$r^{\text{FR,Dw,D/C}}_{d,e,r,f,w,h}$ FR-Dw contribution by the ESS during discharging/charging for day d, scenario e,r,f,w and time period h [MW].

$r^{\text{FR,Up,W}}_{d,e,r,f,w,h}$ FR-Up contribution of the WF for day d, scenario e,r,f,w and time period h [MW].

$r^{\text{FR,Dw,W}}_{d,e,r,f,w,h}$ FR-Dw contribution of the WF for day d, scenario e,r,f,w and time period h [MW].

$r^{\text{FR,Up/Dw}}_{d,e,r,f,w,h}$ Total FR-Up/FR-Dw contribution from both facilities for day d, scenario e,r,f,w and time period h [MW].

$i^{(.)+/-}_{d,e,r,f,w,h}$ Positive/Negative Energy/SPR-Up/SPR-Dw/FR-Up/FR-Dw deviation from the day-ahead bid for day d, scenario e,r,f,w and and time period h [MW].

$\mu^{(.)}_{e,r,f,w}$ Auxiliary variable in order to compute the CVaR for Energy/SPR-Up/SPR-Dw/FR-Up/FR-Dw profit for scenario e,r,f,w [£].

5.1.5 Parameters and Auxiliary Variables for the Progressive Hedging Algorithm

$\text{i} \in \text{I}$ Iteration counter $\left(i = 0,1,...,\text{N}^{\text{I}}\right)$.

ε Error tolerance.

N^{PP} Number of parallel implementations of the decomposed sub-problems.

N^{S} Total number of scenarios.

$K^{\text{P/E (i)}}_{e,r,f,w}$ Decomposed solution for the power/energy capacity of the ESS in scenario e,r,f,w and iteration i [MW].

$\hat{K}^{\text{P/E (i)}}$ Probability-weighted average value for the power/energy capacity of the ESS in iteration i [MW].

$m^{\text{P/E (i)}}_{e,r,f,w}$ Lagrange multiplier for the power/energy capacity of the ESS in scenario e,r,f,w and iteration i.

$\lambda^{\text{P/E (i)}}$ Penalty factor for the power/energy capacity of the ESS in iteration i.

$g^{\text{K,P/E (i)}}$ Average per-scenario deviation from the probability-weighted average value of the power/energy capacity of the ESS in iteration i.

$x^{(.)\,\text{(i)}}_{d,e,r,f,w,h}$ Decomposed solution for the joint Energy/SPR-Up/SPR-Dw/FR-Up/FR-Dw bid for day d, scenario e,r,f,w, time period h and iteration i [MWh].

$\hat{x}^{(.)\,\text{(i)}}_{d,h}$ Probability-weighted average value for the joint Energy/SPR-Up/SPR-Dw/FR-Up/FR-Dw bid for day d, time period h and iteration i [MWh].

$m^{\mathrm{x},(.)\,(\mathrm{i})}_{d,e,r,f,w,h}$ Lagrange multiplier for the joint Energy/SPR-Up/SPR-Dw/FR-Up/FR-Dw bid for day d, scenario e,r,f,w, time period h and iteration i.

$\lambda^{\mathrm{x},(.)\,(\mathrm{i})}_{d,h}$ Penalty factor for the joint Energy/SPR-Up/SPR-Dw/FR-Up/FR-Dw bid for day d, time period h and iteration i.

$g^{(.)\,(\mathrm{i})}$ Average per-scenario and time period deviation from the probability-weighted average value of the joint Energy/SPR-Up/SPR-Dw/FR-Up/FR-Dw bid in iteration i.

$\zeta^{(.)\,(\mathrm{i})}_{e,r,f,w}$ Decomposed solution for the Energy/SPR-Up/SPR-Dw/FR-Up/FR-Dw VaR in scenario e,r,f,w and iteration i [£].

$\hat{\zeta}^{(.)\,(\mathrm{i})}$ Probability-weighted average value for the Energy/SPR-Up/SPR-Dw/FR-Up/FR-Dw VaR in scenario e,r,f,w and iteration i [£].

$m^{\zeta,(.)\,(\mathrm{i})}_{e,r,f,w}$ Lagrange multiplier for the Energy/SPR-Up/SPR-Dw/FR-Up/FR-Dw profit VaR for scenario e,r,f,w and iteration i.

$\lambda^{\zeta,(.)\,(\mathrm{i})}$ Penalty factor for the Energy/SPR-Up/SPR-Dw/FR-Up/FR-Dw profit VaR for iteration i.

$g^{\zeta,(.)\,(\mathrm{i})}$ Average per-scenario and time period deviation from the probability-weighted average value of the energy/SPR-Up/SPR-Dw/FR-Up/FR-Dw profit VaR in iteration i.

$\xi^{(.)\,(\mathrm{i})}_{e,r,f,w}$ Decomposed solution for the Energy/SPR-Up/SPR-Dw/FR-Up/FR-Dw profit CVaR in scenario e,r,f,w in iteration i [£].

$\hat{\xi}^{(.)\,(\mathrm{i})}$ Probability-weighted average value for the Energy/SPR-Up/SPR-Dw/FR-Up/FR-Dw profit CVaR in iteration i [£].

$g^{(\mathrm{i})}$ Total average per-scenario deviation from the probability-weighted average value for all decision variables in iteration i.

5.2 Introduction

5.2.1 Literature Review

The deployment of ESS in order to support system operations is becoming a technically feasible option, considering the several benefits that ESS can provide to the different sectors of the energy system and falling investment costs. By 2030, it is expected that the total installed costs of battery-type ESS could fall between 50% and 66% due to recent improvements to manufacturing facilities and materials science [108]. Furthermore, these improvements also translate into increased performance and battery lifetimes. Despite the technological advancements and falling costs, ensuring that payback periods for ESS investments are adequate for the expected ESS technology and lifetime is of special interest for investors. [20] provides an estimation for the variation of the payback period of a 25MW ESS co-located with a 100 MW WF depending on the business case for the installations' operator. The provision of FR and curtailment avoidance on top of wind balancing, energy arbitrage and balancing market services allows for the reduction of the payback period from 14 years to 5 years. [109] argues that ESS provide the highest in systems with large shares of renewable energy generation and under strict emissions limits, and ESS is not a requisite for systems with a diverse mix of flexible, low-carbon power sources.

Achieving short payback periods is of fundamental importance also considering that ESS such as Li-ion batteries are also characterized by capacity degradation profiles which heavily impact the lifetime

and range of operation for ESS. Battery degradation models have been widely investigated and published in literature [110–114]. One the one hand, [110, 111] analyse battery cell degradation and wear costs for EV in vehicle-to-grid (V2G) applications and conclude that ambient temperature, depth-of-discharge (DoD) and processed energy significantly impact battery cycle life. These papers also find that DoD by itself isn't a reliable single metric for battery degradation from V2G operation due to rapid discharge and charge events and that capacity loss per unit energy processed from V2G utilization is approximately half of that associated with rapid cycling encountered while driving. On the other hand, [112–114] study the impact of grid application for ESS on capacity degradation and find that the limiting DoD or state-of-charge (SoC) to a reduced range of operation (i.e. 0-25% SoC) can reach higher values for total gross revenues (present value at a 5% discount rate) due to the increased lifespan of the ESS and the provision of reserve services.

Despite falling capital costs and increased knowledge regarding capacity degradation, failure to recover investment costs is still regarded as the biggest hurdle for the widespread integration of ESS. Consequently, the development of ESS investment models that ensure that sufficient revenue is collected to achieve profitability have been widely proposed in current literature [115–118]. While [115, 116] propose methodologies to determine the size of ESS in order to provide frequency control and, thus, reduce generation costs, [117, 118] argue that profitable ESS investments can be achieved through strategic siting and sizing in order maximize the benefits of spatiotemporal arbitrage. While the first set of papers model a full year of operation, the second set of papers approaches the investment problem for a set number of representative days. All papers though, do not consider wind generation uncertainty or consider the risk of failing to recover investment costs. It is recognized that transmission expansion can negatively impact ESS investments as it reduces the value that ESS provide in congestion management and, as previously mentioned, ESS can be deployed in order to defer investment in transmission assets. In this context, [119, 120] investigate the co-optimization of transmission expansion planning and merchant ESS investments under a realistically sized system. Both papers conclude that buses in proximity to renewable generation facilities, congested lines and inflexible generation present more profitable opportunities for ESS deployment and that transmission expansion significantly reduces the penetration of ESS.

ESS investment models considering intermittent wind generation and the provision of AS by the ESS have been proposed in [121–124]. Firstly, these papers acknowledge that ESS provide an economic solution to the problem of integrating large shares of renewable generation as ESS are able to mitigate the impacts of uncertain wind generation. Secondly, it is recognized that the value of ESS investments is tied to the amount of uncertainty in the wind generation forecasts [124] and/or the need for specialized FR and SPR services [122]. Thirdly, the resulting large-scale of problems under study lead to the application of alternative solution methods such as Benders decomposition algorithm [121], Monte-Carlo simulation embedded differential evolution algorithm [122] or chance constraints in order to achieve computational tractability [124]. Decomposition techniques have been successfully applied to investment problems in power systems in [125–129]. Despite the proposal of decomposition techniques in order to solve investment problems under uncertainty, only a few consider risk measures in their formulation [128, 129].

Despite the widespread research into the problem of optimal ESS investment, there are a few topics that haven't been fully addressed in current literature and that this chapter seeks to address. The economic and non-economic benefits of ESS and WF coordination have been well established and researched,

however, a full investment model in order to determine the optimal values for the ESS's parameters for a WF operator hasn't been fully realized. Furthermore, the consideration of the risk of experiencing low profit outcomes in investment problems under uncertainty, as such is the case of a risk-averse WF operator, has not been proposed in literature to the best knowledge of this Thesis's author. Lastly, given the popularity of the utilization of decomposition techniques to solve large-scale investment problems under uncertainty in reasonable execution times, the consideration of risk measures such as CVaR in the problem's formulation to be decomposed has not been fully realized in the context of ESS and WF coordination.

5.2.2 Risk-averse Investment in ESS

In order to address the research gap described in the previous Subsection, this chapter proposes a novel, computationally efficient framework for solving the ESS investment problem for a risk-averse WF operator. The problem is first formulated as a two-stage stochastic mathematical problem which takes into account energy and services pricing, and wind generation uncertainty and allows the consideration of several degrees of risk aversion in the optimization of the bidding strategy for the combined WF-ESS operator participation in day-ahead energy market and the provision of AS such as SPR and FR. In other words, the business model for the WF and the ESS presented in Chapters 3 and 4 is expanded to allow the provision of FR on top of SPR and wind imbalance management in order to maximize expected profit and CVaR for a certain level of risk aversion for a year of operation. The model determines the power and energy capacities of ESS to minimize the annuitized value of the total investment costs.

Solving the two-stage stochastic investment model for a full year of operation for an adequate (in terms of uncertainty representation) number of scenarios gives rise to a large-scale MILP with millions of continuous, semi-continuous and binary variables which can exponentially rise due to the number of scenarios used. As such, the original investment problem is made computationally tractable by means of using the PHA decomposition technique and representing the assessment horizon through typical weeks. This technique allows the original stochastic problem to be decomposed by scenario, which translates into relaxing the non-anticipativity conditions and first-stage decision variables (investment decisions and day-ahead bids) are transformed into scenario-dependent decisions. Thus the original problem is transformed into small-scale scenario-specific sub-problems. Non-anticipativity is reintroduced iteratively by penalizing the objective function for deviations between the scenario-specific solutions for the decision variables (ESS power and energy capacities and day-ahead bids) and their probability-weighted average value. Another aspect of this technique that further improves computational efficiency is the possibility of parallelizing the execution of the scenario-specific sub-problems due to their independent nature.

One aspect of the minimization of the risk of experiencing low profit outcomes using measures such as CVaR is that the lack of separability of risk measures can present difficulties in the context of decomposing large-scale stochastic problems. The PHA was mainly chosen to decompose the two-stage stochastic investment problem proposed in this chapter due to the possibility of solving risk-averse problems by introducing additional variables which can be decomposed and updated through aggregation of the scenario-dependent solutions [130]. Thus, one of the significant contributions of this chapter is the successful application of the PHA to decompose an investment problem to determine the optimal value of the ESS's power and energy capacities to maximize the profit achieved by coordinating with a WF

and the CVaR under several degrees of risk aversion.

This work differentiates from [121–124] as it directly couples the operation of the WF and the ESS in a stochastic framework in order to increase the value of the ESS investments. Unlike [128, 129], this work directly considers CVaR in the problems' objective function as it is considered to be fundamental for a WF operator to consider the risk of failing to recover capital costs when deciding to invest in an ESS to improve its position in the day-ahead markets.

5.3 Risk-averse ESS Investment Problem

5.3.1 Key Properties and Assumptions

As stated in the previous section, the proposed risk-averse ESS investment model is formulated as a two-stage stochastic MILP problem in order to: 1) maximize the yearly expected profit of the WF and ESS participating in day-ahead energy, FR and SPR markets; 2) maximize the profit CVaR considering different levels of risk aversion; 3) minimize investment costs related to the sizing of the power and energy capacities of the ESS. In the first-stage of the optimization problem, the value of the power and energy capacities of the ESS and day-ahead energy, SPR and FR bids are determined (*here-and-now* decisions). Note that the assessment horizon starts after the construction of the ESS, which creates a dependency between the bids and the size of the ESS. As in the previous models, the secondstage decisions (*wait-and-see*) are taken after the full revelation of the uncertain parameters (prices and wind power availability) in order to reduce deviations from the day-ahead bids and maximize profit.

The consideration of FR price uncertainty (FR price forecasts - f) in the problem's formulation increases the total number of sources of uncertainty to four (Energy, SPR and FR prices, and wind power availability). It is assumed that the combined size of the WF and ESS are not big enough to directly influence prices and adopt a price-taker approach. A scenario for this model is a combination of one energy price, SPR price, FR price and wind power availability forecasts and the respective probability is calculated as $\rho_e \times \rho_r \times \rho_f \times \rho_w$. The time periods in this model have been separated in days (d) and hours (h) in order to represent day-ahead uncertainty, however time continuity between consecutive days is ensured.

The previous models have assumed that all energy generated by the WF was absorbable by the transmission system. The case study presented in Subsection 3.7.4 demonstrated how the ESS can be used to better utilize wind energy that otherwise would need to be curtailed in the face of grid unavailability. In order to consider the possibility for the grid not being able to absorb all the energy generated by the WF-ESS, it is now assumed that these are connected to a transmission line with varying availability throughout the day which can correlate with periods of grid congestion.

5.3.2 Objective Function

The objective function (5.1) consists in maximizing the expected yearly profit from participating in the day-ahead Energy, SPR and FR markets (2^{nd} through 6^{th} line) and CVaR for each source of profit - Energy, SPR-Up, SPR-Dw, upwards FR (FR-Up) and downwards FR (FR-Dw) - depending on the level of risk aversion β (7^{th} line), minus the investment costs of power and energy capacity of the ESS. As it is assumed that the ESS is built before the start of the assessment horizon, the investment cost for each component is calculated by multiplying the present value of the investment cost per MW (MWh) and

the maximum discharge power (maximum stored energy), i.e. the power (energy) capacity of the ESS, for γ years of equipment lifetime and annual discount rate δ. The CVaR for each source of profit is calculated and linearized with equations and constraints (5.2) to (5.11). Positive and negative deviations from the day-ahead bids are calculated with equations and constraints (5.12) to (5.26). These constraints follow the same structure and objective of similar constraints presented in previous chapters and are expanded to calculate the CVaR and imbalances related to FR provision. Note that the variables for positive $\left(i^{(.)^+}_{d,e,r,f,w,h}\right)$ and negative $\left(i^{(.)^-}_{d,e,r,f,w,h}\right)$ deviations constitute a SOS1 variable pair.

$$
\begin{aligned}
\underset{\substack{\Omega^{\mathrm{BV}},\Omega^{\mathrm{CV}},\Omega^{\mathrm{CV}^+},\\ \Omega^{\mathrm{SCV}^+},\Omega^{\mathrm{CV^{SOS1}}}}}{\text{Maximize}} \Bigg\{ & (1-\beta) \sum_{e\in S^{\mathrm{E}}} \sum_{r\in S^{\mathrm{R}}} \sum_{r\in S^{\mathrm{F}}} \sum_{w\in S^{\mathrm{W}}} \rho_e \rho_r \rho_f \rho_w \Bigg[\sum_{d\in D} \sum_{h\in H} \\
& \Big(\pi^{\mathrm{En}}_{d,e,h} x^{\mathrm{En}}_{d,h} + \omega^{\mathrm{En}^+}_{d,e,h} \pi^{\mathrm{En}}_{d,e,h} i^{\mathrm{En}^+}_{d,e,r,f,w,h} - \omega^{\mathrm{En}^-}_{d,e,h} \pi^{\mathrm{En}}_{d,e,h} i^{\mathrm{En}^-}_{d,e,r,f,w,h} \\
& + \pi^{\mathrm{SPR,Up}}_{d,r,h} x^{\mathrm{SPR,Up}}_{d,h} + \omega^{\mathrm{SPR}^+}_{d,r,h} \pi^{\mathrm{SPR,Up}}_{d,r,h} i^{\mathrm{SPR,Up}^+}_{d,e,r,f,w,h} - \omega^{\mathrm{SPR}^-}_{d,r,h} \pi^{\mathrm{SPR,Up}}_{d,r,h} i^{\mathrm{SPR,Up}^-}_{d,e,r,f,w,h} \\
& + \pi^{\mathrm{SPR,Dw}}_{d,r,h} x^{\mathrm{SPR,Dw}}_{d,h} + \omega^{\mathrm{SPR}^+}_{d,r,h} \pi^{\mathrm{SPR,Dw}}_{d,r,h} i^{\mathrm{SPR,Dw}^+}_{d,e,r,f,w,h} - \omega^{\mathrm{SPR}^-}_{d,r,h} \pi^{\mathrm{SPR,Dw}}_{d,r,h} i^{\mathrm{SPR,Dw}^-}_{d,e,r,f,w,h} \\
& + \pi^{\mathrm{FR,Up}}_{d,f,h} x^{\mathrm{FR,Up}}_{d,h} + \omega^{\mathrm{FR}^+}_{d,f,h} \pi^{\mathrm{SPR,Up}}_{d,r,h} i^{\mathrm{FR,Up}^+}_{d,e,r,f,w,h} - \omega^{\mathrm{FR}^-}_{d,f,h} \pi^{\mathrm{F,Up}}_{d,f,h} i^{\mathrm{FR,Up}^-}_{d,e,r,f,w,h} \\
& + \pi^{\mathrm{FR,Dw}}_{d,f,h} x^{\mathrm{FR,Dw}}_{d,h} + \omega^{\mathrm{FR}^+}_{d,f,h} \pi^{\mathrm{FR,Dw}}_{d,f,h} i^{\mathrm{FR,Dw}^+}_{d,e,r,f,w,h} - \omega^{\mathrm{FR}^-}_{d,f,h} \pi^{\mathrm{FR,Dw}}_{d,f,h} i^{\mathrm{FR,Dw}^-}_{d,e,r,f,w,h} \Big) \Bigg] \\
& + \beta \left(\xi^{\mathrm{En}} + \xi^{\mathrm{SPR,Up}} + \xi^{\mathrm{SPR,Dw}} + \xi^{\mathrm{FR,Up}} + \xi^{\mathrm{FR,Dw}} \right) \\
& - \mathrm{C}^{\mathrm{P}} \frac{\delta(1+\delta)^{\gamma}}{(1+\delta)^{\gamma}-1} K^{\mathrm{P}} - \mathrm{C}^{\mathrm{E}} \frac{\delta(1+\delta)^{\gamma}}{(1+\delta)^{\gamma}-1} K^{\mathrm{E}} \Bigg\}.
\end{aligned}
\tag{5.1}
$$

$$
\xi^{\mathrm{En}} = \zeta^{\mathrm{En}} - \frac{1}{1-\alpha} \sum_{e\in S^{\mathrm{E}}} \sum_{r\in S^{\mathrm{R}}} \sum_{f\in S^{\mathrm{F}}} \sum_{w\in S^{\mathrm{W}}} \rho_e \rho_r \rho_f \rho_w \mu^{\mathrm{En}}_{e,r,f,w}, \tag{5.2}
$$

$$
\mu^{\mathrm{En}}_{e,r,f,w} \geq \zeta^{\mathrm{En}} - \sum_{d\in D} \sum_{h\in H} \left(\pi^{\mathrm{En}}_{d,e,h} x^{\mathrm{En}}_{d,h} + \omega^{\mathrm{En}^+}_{d,e,h} \pi^{\mathrm{En}}_{d,e,h} i^{\mathrm{En}^+}_{d,e,r,f,w,h} - \omega^{\mathrm{En}^-}_{d,e,h} \pi^{\mathrm{En}}_{d,e,h} i^{\mathrm{En}^-}_{d,e,r,f,w,h} \right), \quad \forall e,r,f,w, \tag{5.3}
$$

$$
\xi^{\mathrm{SPR,Up}} = \zeta^{\mathrm{SPR,Up}} - \frac{1}{1-\alpha} \sum_{e\in S^{\mathrm{E}}} \sum_{r\in S^{\mathrm{R}}} \sum_{f\in S^{\mathrm{F}}} \sum_{w\in S^{\mathrm{W}}} \rho_e \rho_r \rho_f \rho_w \mu^{\mathrm{SPR,Up}}_{e,r,f,w}, \tag{5.4}
$$

$$
\zeta^{\mathrm{SPR,Up}} - \sum_{d\in D} \sum_{h\in H} \left(\pi^{\mathrm{SPR,Up}}_{d,r,h} x^{\mathrm{SPR,Up}}_{d,h} + \omega^{\mathrm{SPR}^+}_{d,r,h} \pi^{\mathrm{SPR,Up}}_{d,r,h} i^{\mathrm{SPR,Up}^+}_{d,e,r,f,w,h} - \omega^{\mathrm{SPR}^-}_{d,r,h} \pi^{\mathrm{SPR,Up}}_{d,r,h} i^{\mathrm{SPR,Up}^-}_{d,e,r,f,w,h} \right) \leq \mu^{\mathrm{SPR,Up}}_{e,r,f,w}, \quad \forall e,r,f,w, \tag{5.5}
$$

$$
\xi^{\mathrm{SPR,Dw}} = \zeta^{\mathrm{SPR,Dw}} - \frac{1}{1-\alpha} \sum_{e\in S^{\mathrm{E}}} \sum_{r\in S^{\mathrm{R}}} \sum_{f\in S^{\mathrm{F}}} \sum_{w\in S^{\mathrm{W}}} \rho_e \rho_r \rho_f \rho_w \mu^{\mathrm{SPR,Dw}}_{e,r,f,w}, \tag{5.6}
$$

$$
\zeta^{\mathrm{SPR,Dw}} - \sum_{d\in D} \sum_{h\in H} \left(\pi^{\mathrm{SPR,Dw}}_{d,r,h} x^{\mathrm{SPR,Dw}}_{d,h} + \omega^{\mathrm{SPR}^+}_{d,r,h} \pi^{\mathrm{SPR,Dw}}_{d,r,h} i^{\mathrm{SPR,Dw}^+}_{d,e,r,f,w,h} - \omega^{\mathrm{SPR}^-}_{d,r,h} \pi^{\mathrm{SPR,Dw}}_{d,r,h} i^{\mathrm{SPR,Dw}^-}_{d,e,r,f,w,h} \right) \leq \mu^{\mathrm{SPR,Dw}}_{e,r,f,w}, \quad \forall e,r,f,w, \tag{5.7}
$$

$$
\xi^{\mathrm{FR,Up}} = \zeta^{\mathrm{FR,Up}} - \frac{1}{1-\alpha} \sum_{e\in S^{\mathrm{E}}} \sum_{r\in S^{\mathrm{R}}} \sum_{f\in S^{\mathrm{F}}} \sum_{w\in S^{\mathrm{W}}} \rho_e \rho_r \rho_f \rho_w \mu^{\mathrm{FR,Up}}_{e,r,f,w}, \tag{5.8}
$$

$$\zeta^{\mathrm{FR,Up}} - \sum_{d\in D}\sum_{h\in H}\left(\pi^{\mathrm{FR,Up}}_{d,r,h}x^{\mathrm{FR,Up}}_{d,h} + \omega^{\mathrm{FR}^+}_{d,r,h}\pi^{\mathrm{FR,Up}}_{d,r,h}i^{\mathrm{FR,Up}^+}_{d,e,r,f,w,h} - \omega^{\mathrm{FR}^-}_{d,r,h}\pi^{\mathrm{FR,Up}}_{d,r,h}i^{\mathrm{FR,Up}^-}_{d,e,r,f,w,h}\right) \le \mu^{\mathrm{FR,Up}}_{e,r,f,w}, \quad \forall e,r,f,w, \tag{5.9}$$

$$\xi^{\mathrm{FR,Dw}} = \zeta^{\mathrm{FR,Dw}} - \frac{1}{1-\alpha}\sum_{e\in S^{\mathrm{E}}}\sum_{r\in S^{\mathrm{R}}}\sum_{f\in S^{\mathrm{F}}}\sum_{w\in S^{\mathrm{W}}}\rho_e\rho_r\rho_f\rho_w\mu^{\mathrm{FR,Dw}}_{e,r,f,w}, \tag{5.10}$$

$$\zeta^{\mathrm{FR,Dw}} - \sum_{d\in D}\sum_{h\in H}\left(\pi^{\mathrm{FR,Dw}}_{d,r,h}x^{\mathrm{FR,Dw}}_{d,h} + \omega^{\mathrm{FR}^+}_{d,r,h}\pi^{\mathrm{FR,Dw}}_{d,r,h}i^{\mathrm{FR,Dw}^+}_{d,e,r,f,w,h} - \omega^{\mathrm{FR}^-}_{d,r,h}\pi^{\mathrm{FR,Dw}}_{d,r,h}i^{\mathrm{FR,Dw}^-}_{d,e,r,f,w,h}\right) \le \mu^{\mathrm{FR,Dw}}_{e,r,f,w}, \quad \forall e,r,f,w, \tag{5.11}$$

$$p^{\mathrm{W}}_{d,e,r,f,w,h} + p^{\mathrm{D}}_{d,e,r,f,w,h} - p^{\mathrm{C}}_{d,e,r,f,w,h} - x^{\mathrm{En}}_{d,h} = i^{\mathrm{En}^+}_{d,e,r,f,w,h} - i^{\mathrm{En}^-}_{d,e,r,f,w,h}, \quad \forall d,e,r,f,w,h, \tag{5.12}$$

$$0 \le i^{\mathrm{En}^+}_{d,e,r,f,w,h} \le \mathrm{W}^{\mathrm{AV}}_{d,w,h}\mathrm{K}^{\mathrm{W}} + 2K^{\mathrm{P}}, \quad \forall d,e,r,f,w,h, \tag{5.13}$$

$$0 \le i^{\mathrm{En}^-}_{d,e,r,f,w,h} \le \mathrm{K}^{\mathrm{W}} + 2K^{\mathrm{P}}, \quad \forall d,e,r,f,w,h, \tag{5.14}$$

$$r^{\mathrm{SPR,Up,W}}_{d,e,r,f,w,h} + r^{\mathrm{SPR,Up,D}}_{d,e,r,f,w,h} + r^{\mathrm{SPR,Up,C}}_{d,e,r,f,w,h} - x^{\mathrm{SPR,Up}}_{d,h} = i^{\mathrm{SPR,Up}^+}_{d,e,r,f,w,h} - i^{\mathrm{SPR,Up}^-}_{d,e,r,f,w,h}, \quad \forall d,e,r,f,w,h, \tag{5.15}$$

$$0 \le i^{\mathrm{SPR,Up}^+}_{d,e,r,f,w,h} \le \mathrm{W}^{\mathrm{AV}}_{d,w,h}\mathrm{K}^{\mathrm{W}} - p^{\mathrm{W}}_{d,e,r,f,w,h} + K^{\mathrm{P}} - p^{\mathrm{D}}_{d,e,r,f,w,h} + p^{\mathrm{C}}_{d,e,r,f,w,h}, \quad \forall d,e,r,f,w,h, \tag{5.16}$$

$$0 \le i^{\mathrm{SPR,Up}^-}_{d,e,r,f,w,h} \le \mathrm{K}^{\mathrm{W}} + 2K^{\mathrm{P}}, \quad \forall d,e,r,f,w,h, \tag{5.17}$$

$$r^{\mathrm{SPR,Dw,W}}_{d,e,r,f,w,h} + r^{\mathrm{SPR,Dw,D}}_{d,e,r,f,w,h} + r^{\mathrm{SPR,Dw,C}}_{d,e,r,f,w,h} - x^{\mathrm{SPR,Dw}}_{d,h} = i^{\mathrm{SPR,Dw}^+}_{d,e,r,f,w,h} - i^{\mathrm{SPR,Dw}^-}_{d,e,r,f,w,h}, \quad \forall d,e,r,f,w,h. \tag{5.18}$$

$$0 \le i^{\mathrm{SPR,Dw}^+}_{d,e,r,f,w,h} \le p^{\mathrm{W}}_{d,e,r,f,w,h} + p^{\mathrm{D}}_{d,e,r,f,w,h} + K^{\mathrm{P}} - p^{\mathrm{C}}_{d,e,r,f,w,h}, \quad \forall d,e,r,f,w,h, \tag{5.19}$$

$$0 \le i^{\mathrm{SPR,Dw}^-}_{d,e,r,f,w,h} \le \mathrm{K}^{\mathrm{W}} + 2K^{\mathrm{P}}, \quad \forall d,e,r,f,w,h, \tag{5.20}$$

$$r^{\mathrm{FR,Up,W}}_{d,e,r,f,w,h} + r^{\mathrm{FR,Up,D}}_{d,e,r,f,w,h} + r^{\mathrm{FR,Up,C}}_{d,e,r,f,w,h} - x^{\mathrm{FR,Up}}_{d,h} = i^{\mathrm{FR,Up}^+}_{d,e,r,f,w,h} - i^{\mathrm{FR,Up}^-}_{d,e,r,f,w,h}, \quad \forall d,e,r,f,w,h, \tag{5.21}$$

$$0 \le i^{\mathrm{FR,Up}^+}_{d,e,r,f,w,h} \le \mathrm{W}^{\mathrm{AV}}_{d,w,h}\mathrm{K}^{\mathrm{W}} - p^{\mathrm{W}}_{d,e,r,f,w,h} + K^{\mathrm{P}} - p^{\mathrm{D}}_{d,e,r,f,w,h} + p^{\mathrm{C}}_{d,e,r,f,w,h}, \quad \forall d,e,r,f,w,h, \tag{5.22}$$

$$0 \le i^{\mathrm{FR,Up}^-}_{d,e,r,f,w,h} \le \mathrm{K}^{\mathrm{W}} + 2K^{\mathrm{P}}, \quad \forall d,e,r,f,w,h, \tag{5.23}$$

$$r^{\mathrm{FR,Dw,W}}_{d,e,r,f,w,h} + r^{\mathrm{FR,Dw,D}}_{d,e,r,f,w,h} + r^{\mathrm{FR,Dw,C}}_{d,e,r,f,w,h} - x^{\mathrm{FR,Dw}}_{d,h} = i^{\mathrm{FR,Dw}^+}_{d,e,r,f,w,h} - i^{\mathrm{FR,Dw}^-}_{d,e,r,f,w,h}, \quad \forall d,e,r,f,w,h. \tag{5.24}$$

$$0 \le i^{\mathrm{FR,Dw}^+}_{d,e,r,f,w,h} \le p^{\mathrm{W}}_{d,e,r,f,w,h} + p^{\mathrm{D}}_{d,e,r,f,w,h} + K^{\mathrm{P}} - p^{\mathrm{C}}_{d,e,r,f,w,h}, \quad \forall d,e,r,f,w,h, \tag{5.25}$$

$$0 \le i^{\mathrm{FR,Dw}^-}_{d,e,r,f,w,h} \le \mathrm{K}^{\mathrm{W}} + 2K^{\mathrm{P}}, \quad \forall d,e,r,f,w,h, \tag{5.26}$$

5.3.3 Model Constraints

5.3.3.1 Generation and Energy Limits

The ESS's maximum charging and discharging power are limited by the sized power capacity in constraints (5.27) and (5.28), respectively. Note that these are assumed to be the same, however, the model allows for different values to imposed on the maximum and minimum charging and discharging power to constrain the DoD of the ESS. To prevent simultaneous charging and discharging actions, $p^{\mathrm{C}}_{d,e,r,f,w,h}$ and $p^{\mathrm{D}}_{d,e,r,f,w,h}$ are made into a SOS1 variable pair.

$$p^{\mathrm{C}}_{d,e,r,f,w,h} \leq K^{\mathrm{P}}, \quad \forall d,e,r,f,w,h, \tag{5.27}$$

$$p^{\mathrm{D}}_{d,e,r,f,w,h} \leq K^{\mathrm{P}}, \quad \forall d,e,r,f,w,h. \tag{5.28}$$

Equations (5.29) to (5.31) enforce initial, inter-day and final stored energy levels in the ESS. Note that the initial and final stored energy levels are assumed to be the same and determined by the model $\left(e^{0}_{e,r,f,w}\right)$. Stored energy levels are updated for each time period by equations (5.32) and are limited by minimum and maximum stored energy levels as a function of the sized energy capacity in constraints (5.33). This methodology allows for a constrained range of operation in order to minimize degradation as discussed in papers [112–114].

$$e_{d,e,r,f,w,h} = e^{0}_{e,r,f,w}, \quad \forall e,r,f,w,\ d=1, h=0, \tag{5.29}$$

$$e_{d,e,r,f,w,h} = e_{d-1,e,r,f,w,\mathrm{N^H}}, \quad \forall d,e,r,f,w,\ d\geq 2, h=0 \tag{5.30}$$

$$e_{d,e,r,f,w,h} = e^{0}_{e,r,f,w}, \quad \forall e,r,f,w,\ d=\mathrm{N^D}, h=\mathrm{N^H}, \tag{5.31}$$

$$e_{d,e,r,f,w,h} = e_{d,e,r,f,w,h-1} + \eta\, p^{\mathrm{C}}_{d,e,r,f,w,h} - p^{D}_{d,e,r,f,w,h}, \quad \forall d,e,r,f,w,h, \tag{5.32}$$

$$\mathrm{E^{Min}} \cdot K^{\mathrm{E}} \leq e_{d,e,r,f,w,h} \leq \mathrm{E^{Max}} \cdot K^{\mathrm{E}}, \quad \forall d,e,r,f,w,h. \tag{5.33}$$

Power generated by the WF is limited by available wind power in constraints (5.34). Constraints (5.35) limit the injected power from both facilities in both directions to grid availability due to the WF-ESS being connected to a transmission line with capacity $\mathrm{K^L}$.

$$p^{\mathrm{W}}_{d,e,r,f,w,h} \leq \mathrm{P}^{\mathrm{AV}}_{d,w,h}\mathrm{K^W}, \quad \forall d,e,r,f,w,h, \tag{5.34}$$

$$-\mathrm{K^L L}^{\mathrm{AV}}_{d,h} \leq p^{\mathrm{W}}_{d,e,r,f,w,h} + p^{\mathrm{D}}_{d,e,r,f,w,h} - p^{\mathrm{C}}_{d,e,r,f,w,h} \leq \mathrm{K^L L}^{\mathrm{AV}}_{d,h}, \quad \forall d,e,r,f,w,h. \tag{5.35}$$

5.3.3.2 Provision of SPR and FR Services

In the same manner of the SPR in the previous chapters, FR can also be provided in different ways depending on the operating status of the ESS. During charging, downwards FR and SPR can be provided by increasing consumption in constraints (5.36), while decreasing consumption leads to the provision of upwards FR and SPR in constraints (5.37). Inversely and while discharging, upwards services are provided by increasing generation and downwards services are provided by decreasing consumption in constraints (5.38) and (5.39), respectively. The contribution of the WF to the provision of these services

is modelled with constraints (5.40) and (5.41). The provision of services by both facilities is constrained by grid availability in constraints (5.42) and (5.43), as these entail changes to the current power injections by WF-ESS.

$$p^{\mathrm{C}}_{d,e,r,f,w,h} + r^{\mathrm{SPR,Dw,C}}_{d,e,r,f,w,h} + r^{\mathrm{FR,Dw,C}}_{d,e,r,f,w,h} \leq K^{\mathrm{P}}, \quad \forall d,e,r,f,w,h, \tag{5.36}$$

$$r^{\mathrm{SPR,Up,C}}_{d,e,r,f,w,h} + r^{\mathrm{FR,Up,C}}_{d,e,r,f,w,h} \leq p^{\mathrm{C}}_{d,e,r,f,w,h}, \quad \forall d,e,r,f,w,h, \tag{5.37}$$

$$p^{\mathrm{D}}_{d,e,r,f,w,h} + r^{\mathrm{SPR,Up,D}}_{d,e,r,f,w,h} + r^{\mathrm{FR,Up,D}}_{d,e,r,f,w,h} \leq K^{\mathrm{P}}, \quad \forall d,e,r,f,w,h, \tag{5.38}$$

$$r^{\mathrm{SPR,Dw,D}}_{d,e,r,f,w,h} + r^{\mathrm{FR,Dw,D}}_{d,e,r,f,w,h} \leq p^{\mathrm{D}}_{d,e,r,f,w,h}, \quad \forall d,e,r,f,w,h, \tag{5.39}$$

$$p^{\mathrm{W}}_{d,e,r,f,w,h} + r^{\mathrm{SPR,Up,W}}_{d,e,r,f,w,h} + r^{\mathrm{FR,Up,W}}_{d,e,r,f,w,h} \leq \mathrm{P}^{\mathrm{AV}}_{d,w,h}\mathrm{K}^{\mathrm{W}}, \quad \forall d,e,r,f,w,h, \tag{5.40}$$

$$r^{\mathrm{SPR,Dw,W}}_{d,e,r,f,w,h} + r^{\mathrm{FR,Dw,W}}_{d,e,r,f,w,h} \leq p^{\mathrm{W}}_{d,e,r,f,w,h}, \quad \forall d,e,r,f,w,h, \tag{5.41}$$

$$\begin{aligned}&\left(p^{\mathrm{W}}_{d,e,r,f,w,h} + p^{\mathrm{C}}_{d,e,r,f,w,h} - p^{D}_{e,r,w,h}\right) + \left(r^{\mathrm{FR,Up,W}}_{d,e,r,f,w,h} + r^{\mathrm{FR,Up,D}}_{d,e,r,f,w,h} + r^{\mathrm{FR,Up,C}}_{d,e,r,f,w,h}\right) + \\ &\left(r^{\mathrm{SPR,Up,W}}_{d,e,r,f,w,h} + r^{\mathrm{SPR,Up,D}}_{d,e,r,f,w,h} + r^{\mathrm{SPR,Up,C}}_{d,e,r,f,w,h}\right) \leq \mathrm{K}^{\mathrm{L}}\mathrm{L}^{\mathrm{AV}}_{d,w,h}, \quad \forall d,e,r,f,w,h\end{aligned} \tag{5.42}$$

$$\begin{aligned}&\left(p^{\mathrm{W}}_{d,e,r,f,w,h} + p^{\mathrm{C}}_{d,e,r,fw,h} - p^{D}_{d,e,r,f,w,h}\right) - \left(r^{\mathrm{FR,Dw,W}}_{d,e,r,f,w,h} + r^{\mathrm{FR,Dw,D}}_{d,e,r,f,w,h} + r^{\mathrm{FR,Dw,C}}_{d,e,r,f,w,h}\right) - \\ &\left(r^{\mathrm{SPR,Dw,W}}_{d,e,r,f,w,h} + r^{\mathrm{SPR,Dw,D}}_{d,e,r,f,w,h} + r^{\mathrm{SPR,Dw,C}}_{d,e,r,f,w,h}\right) \geq -\mathrm{K}^{\mathrm{L}}\mathrm{L}^{\mathrm{AV}}_{d,w,h}, \quad \forall d,e,r,f,w,h.\end{aligned} \tag{5.43}$$

5.3.3.3 SPR Service Deliverability Constraints

The provision of SPR is affected by minimum provision levels, and sufficient stored energy or resource availability must be ensured to provide the full commited SPR during the maximum utilization time requested by the TSO. The coordinated operation of the WF and the ESS enhances the provision of this service as stored excess wind energy provides decreases costs associated with charging the ESS to provide SPR-Up during discharging. Therefore, total provided levels for SPR-Up and SPR-Dw are calculated with equations (5.44) and (5.45), while minimum provision levels are established in constraints (5.46) and (5.47).

$$r^{\mathrm{SPR,Up}}_{d,e,r,f,w,h} = r^{\mathrm{SPR,Up,C}}_{d,e,r,f,w,h} + r^{\mathrm{SPR,Up,D}}_{d,e,r,f,w,h} + r^{\mathrm{SPR,Up,W}}_{d,e,r,f,,w,h}, \quad \forall d,e,r,f,w,h, \tag{5.44}$$

$$r^{\mathrm{SPR,Dw}}_{d,e,r,f,w,h} = r^{\mathrm{SPR,Dw,C}}_{d,e,r,f,w,h} + r^{\mathrm{SPR,Dw,D}}_{d,e,r,f,w,h} + r^{\mathrm{SPR,Dw,W}}_{d,e,r,f,w,h}, \quad \forall d,e,r,f,w,h, \tag{5.45}$$

$$r^{\mathrm{SPR,Up}}_{d,e,r,f,w,h} \leq \begin{cases} \mathrm{K}^{\mathrm{W}} + 2K^{\mathrm{P}} & , r^{\mathrm{SPR,Up,C}}_{d,e,r,f,w,h} + r^{\mathrm{SPR,Up,D}}_{d,e,r,f,w,h} + r^{\mathrm{SPR,Up,W}}_{d,e,r,f,w,h} \geq \underline{\mathrm{SPR}}^{\mathrm{Up}} \\ 0 & , r^{\mathrm{SPR,Up,C}}_{d,e,r,f,w,h} + r^{\mathrm{SPR,Up,D}}_{d,e,r,f,w,h} + r^{\mathrm{SPR,Up,W}}_{d,e,r,f,w,h} < \underline{\mathrm{SPR}}^{\mathrm{Up}} \end{cases}, \quad \forall d,e,r,f,w,h, \tag{5.46}$$

$$r^{\mathrm{SPR,Dw}}_{d,e,r,f,w,h} \leq \begin{cases} \mathrm{K}^{\mathrm{W}} + 2K^{\mathrm{P}} & , r^{\mathrm{SPR,Dw,C}}_{d,e,r,f,w,h} + r^{\mathrm{SPR,Dw,D}}_{d,e,r,f,w,h} + r^{\mathrm{SPR,Dw,W}}_{d,e,r,f,w,h} \geq \underline{\mathrm{SPR}}^{\mathrm{Dw}} \\ 0 & , r^{\mathrm{SPR,Dw,C}}_{d,e,r,f,w,h} + r^{\mathrm{SPR,Dw,D}}_{d,e,r,f,w,h} + r^{\mathrm{SPR,Dw,W}}_{d,e,r,f,w,h} < \underline{\mathrm{SPR}}^{\mathrm{Dw}} \end{cases}, \quad \forall d,e,r,f,w,h. \tag{5.47}$$

The set of disjunctive constraints (5.48) to (5.55) ensure sufficient stored energy in order to provide the committed SPR quantity, as it is assumed that the maximum commitment time duration for the provision of SPR $\left(\tau^{\mathrm{SPR}}\right)$ services is larger than the time-step of the model (1 hour).

$$\begin{aligned}\mathrm{E}^{\mathrm{Min}}\cdot K^{\mathrm{E}}-\mathrm{M}\left(1-Q^{\mathrm{SPR,Up,D}}_{d,e,r,f,w,h}\right)\leq e_{d,e,r,f,w,h-1}+\eta\, p^{\mathrm{C}}_{d,e,r,f,w,h}-\left(p^{\mathrm{D}}_{e,r,w,h}+r^{\mathrm{SPR,Up,D}}_{d,e,r,f,w,h}\right)\tau^{\mathrm{SPR}}\leq\\ \mathrm{E}^{\mathrm{Max}}\cdot K^{\mathrm{E}}+\mathrm{M}\left(1-Q^{\mathrm{SPR,Up,D}}_{d,e,r,f,w,h}\right),\quad\forall d,e,r,f,w,h,\end{aligned}\tag{5.48}$$

$$\begin{aligned}\mathrm{E}^{\mathrm{Min}}\cdot K^{\mathrm{E}}-\mathrm{M}\left(1-Q^{\mathrm{SPR,Dw,D}}_{d,e,r,f,w,h}\right)\leq e_{d,e,r,f,w,h-1}+\eta\, p^{\mathrm{C}}_{d,e,r,f,w,h}-\left(p^{\mathrm{D}}_{e,r,w,h}-r^{\mathrm{SPR,Dw,D}}_{d,e,r,f,w,h}\right)\tau^{\mathrm{SPR}}\leq\\ \mathrm{E}^{\mathrm{Max}}\cdot K^{\mathrm{E}}+\mathrm{M}\left(1-Q^{\mathrm{SPR,Dw,D}}_{d,e,r,f,w,h}\right),\quad\forall d,e,r,f,w,h,\end{aligned}\tag{5.49}$$

$$\begin{aligned}\mathrm{E}^{\mathrm{Min}}\cdot K^{\mathrm{E}}-\mathrm{M}\left(1-Q^{\mathrm{SPR,Up,C}}_{d,e,r,f,w,h}\right)\leq e_{d,e,r,f,w,h-1}+\eta\left(p^{\mathrm{C}}_{d,e,r,f,w,h}-r^{\mathrm{SPR,Up,C}}_{d,e,r,f,w,h}\right)\tau^{\mathrm{SPR}}-p^{\mathrm{D}}_{d,e,r,f,w,h}\leq\\ \mathrm{E}^{\mathrm{Max}}\cdot K^{\mathrm{E}}+\mathrm{M}\left(1-Q^{\mathrm{SPR,Up,C}}_{d,e,r,f,w,h}\right),\quad\forall d,e,r,f,w,h,\end{aligned}\tag{5.50}$$

$$\begin{aligned}\mathrm{E}^{\mathrm{Min}}\cdot K^{\mathrm{E}}-\mathrm{M}\left(1-Q^{\mathrm{SPR,Dw,C}}_{d,e,r,f,w,h}\right)\leq e_{d,e,r,f,w,h-1}+\eta\left(p^{\mathrm{C}}_{d,e,r,f,w,h}+r^{\mathrm{SPR,Dw,C}}_{d,e,r,f,w,h}\right)\tau^{\mathrm{SPR}}-p^{\mathrm{D}}_{d,e,r,f,w,h}\leq\\ \mathrm{E}^{\mathrm{Max}}\cdot K^{\mathrm{E}}+\mathrm{M}\left(1-Q^{\mathrm{SPR,Dw,C}}_{d,e,r,f,w,h}\right),\quad\forall d,e,r,f,w,h,\end{aligned}\tag{5.51}$$

$$r^{\mathrm{SPR,Up,D}}_{d,e,r,f,w,h}\leq\mathrm{M}\,Q^{\mathrm{SPR,Up,D}}_{d,e,r,f,w,h},\quad\forall d,e,r,f,w,h,\tag{5.52}$$

$$r^{\mathrm{SPR,Dw,D}}_{d,e,r,f,w,h}\leq\mathrm{M}\,Q^{\mathrm{SPR,Dw,D}}_{d,e,r,f,w,h},\quad\forall d,e,r,f,w,h,\tag{5.53}$$

$$r^{\mathrm{SPR,Up,C}}_{d,e,r,f,w,h}\leq\mathrm{M}\,Q^{\mathrm{SPR,Up,C}}_{d,e,r,f,w,h},\quad\forall d,e,r,f,w,h,\tag{5.54}$$

$$r^{\mathrm{SPR,Dw,C}}_{d,e,r,f,w,h}\leq\mathrm{M}\,Q^{\mathrm{SPR,Dw,C}}_{d,e,r,f,w,h},\quad\forall d,e,r,f,w,h.\tag{5.55}$$

Constraints (5.56) and (5.57) are adapted from constraints (3.35) and (3.36) in order to take into account wind power availability uncertainty and the provision of FR services during the commitment period of SPR.

$$\begin{aligned}&\left(p^{\mathrm{W}}_{d,e,r,f,w,t}+p^{\mathrm{C}}_{d,e,r,f,w,t}-p^{D}_{d,e,r,f,w,t}\right)+\left(r^{\mathrm{FR,Up,W}}_{d,e,r,f,w,t}+r^{\mathrm{FR,Up,D}}_{d,e,r,f,w,t}+r^{\mathrm{FR,Up,C}}_{d,e,r,f,w,t}\right)+\\&\left(r^{\mathrm{SPR,Up,W}}_{d,e,r,f,w,h}+r^{\mathrm{SPR,Up,D}}_{d,e,r,f,w,h}+r^{\mathrm{SPR,Up,C}}_{d,e,r,f,w,h}\right)\leq\mathrm{P}^{\mathrm{AV}}_{d,w,t}\mathrm{K}^{\mathrm{W}}+K^{\mathrm{P}},\quad\forall d,e,r,f,w,h,\,h\leq t<h+\tau^{\mathrm{SPR}},\end{aligned}\tag{5.56}$$

$$\begin{aligned}&\left(p^{\mathrm{W}}_{d,e,r,f,w,t}+p^{\mathrm{C}}_{d,e,r,fw,t}-p^{D}_{d,e,r,f,w,t}\right)-\left(r^{\mathrm{FR,Dw,W}}_{d,e,r,f,w,t}+r^{\mathrm{FR,Dw,D}}_{d,e,r,f,w,t}+r^{\mathrm{FR,Dw,C}}_{d,e,r,f,w,t}\right)-\\&\left(r^{\mathrm{SPR,Dw,W}}_{d,e,r,f,w,h}+r^{\mathrm{SPR,Dw,D}}_{d,e,r,f,w,h}+r^{\mathrm{SPR,Dw,C}}_{d,e,r,f,w,h}\right)\geq-K^{\mathrm{P}},\quad\forall d,e,r,f,w,h,\,h\leq t<h+\tau^{\mathrm{SPR}}.\end{aligned}\tag{5.57}$$

5.3.3.4 FR Service Deliverability Constraints

The provision of FR follows similar rules to the provision of SPR and, consequently, it is also affected by minimum provision levels and stored energy sufficiency to provide the service for the maximum commitment time duration $\left(\tau^{\mathrm{FR}}\right)$. As a result, the model employs equations and constraints (5.58) through (5.61) to calculate the total provision of FR-Up and FR-Dw and their respective minimum levels.

$$r^{\mathrm{FR,Up}}_{d,e,r,f,w,h}=r^{\mathrm{FR,Up,C}}_{d,e,r,f,w,h}+r^{\mathrm{FR,Up,D}}_{d,e,r,f,w,h}+r^{\mathrm{FR,Up,W}}_{d,e,r,f,,w,h},\quad\forall d,e,r,f,w,h,\tag{5.58}$$

$$r^{\text{FR,Dw}}_{d,e,r,f,w,h} = r^{\text{FR,Dw,C}}_{d,e,r,f,w,h} + r^{\text{FR,Dw,D}}_{d,e,r,f,w,h} + r^{\text{FR,Dw,W}}_{d,e,r,f,w,h}, \quad \forall d,e,r,f,w,h, \tag{5.59}$$

$$r^{\text{FR,Up}}_{d,e,r,f,w,h} \leq \begin{cases} \text{K}^{\text{W}} + 2K^{\text{P}} & , r^{\text{FR,Up,C}}_{d,e,r,f,w,h} + r^{\text{FR,Up,D}}_{d,e,r,f,w,h} + r^{\text{FR,Up,W}}_{d,e,r,f,w,h} \geq \underline{\text{FR}}^{\text{Up}} \\ 0 & , r^{\text{FR,Up,C}}_{d,e,r,f,w,h} + r^{\text{FR,Up,D}}_{d,e,r,f,w,h} + r^{\text{FR,Up,W}}_{d,e,r,f,w,h} < \underline{\text{FR}}^{\text{Up}} \end{cases}, \quad \forall d,e,r,f,w,h, \tag{5.60}$$

$$r^{\text{FR,Dw}}_{d,e,r,f,w,h} \leq \begin{cases} \text{K}^{\text{W}} + 2K^{\text{P}} & , r^{\text{FR,Dw,C}}_{d,e,r,f,w,h} + r^{\text{FR,Dw,D}}_{d,e,r,f,w,h} + r^{\text{FR,Dw,W}}_{d,e,r,f,w,h} \geq \underline{\text{FR}}^{\text{Dw}} \\ 0 & , r^{\text{FR,Dw,C}}_{d,e,r,f,w,h} + r^{\text{FR,Dw,D}}_{d,e,r,f,w,h} + r^{\text{FR,Dw,W}}_{d,e,r,f,w,h} < \underline{\text{FR}}^{\text{Dw}} \end{cases}, \quad \forall d,e,r,f,w,h. \tag{5.61}$$

It is assumed that the main differentiating factor between providing SPR and FR besides price, is the time frame required for the provision of the service, i.e. the maximum commitment time duration. Consequently, it is also assumed that the time duration required for providing FR is shorter than both the time-step of the model and duration of SPR services. Modelling-wise, the implications of this assumption for the provision of FR are seen in constraints (5.62) through (5.65). Note that the presence of binary variables is no longer required as it is assumed that τ^{FR} is smaller than 1 hour and that these constraints ensure that sufficient energy is always stored in each time period to provide the service.

$$\text{E}^{\text{Min}} \cdot K^{\text{E}} \leq e_{d,e,r,f,w,h-1} + \eta\, p^{\text{C}}_{d,e,r,f,w,h} - \left(p^{\text{D}}_{e,r,w,h} + r^{\text{FR,Up,D}}_{d,e,r,f,w,h}\right)\tau^{\text{FR}} \leq \text{E}^{\text{Max}} \cdot K^{\text{E}}, \quad \forall d,e,r,f,w,h, \tag{5.62}$$

$$\text{E}^{\text{Min}} \cdot K^{\text{E}} \leq e_{d,e,r,f,w,h-1} + \eta\, p^{\text{C}}_{d,e,r,f,w,h} - \left(p^{\text{D}}_{e,r,w,h} - r^{\text{FR,Dw,D}}_{d,e,r,f,w,h}\right)\tau^{\text{FR}} \leq \text{E}^{\text{Max}} \cdot K^{\text{E}}, \quad \forall d,e,r,f,w,h, \tag{5.63}$$

$$\text{E}^{\text{Min}} \cdot K^{\text{E}} \leq e_{d,e,r,f,w,h-1} + \eta\, \left(p^{\text{C}}_{d,e,r,f,w,h} - r^{\text{FR,Up,C}}_{d,e,r,f,w,h}\right)\tau^{\text{FR}} - p^{\text{D}}_{d,e,r,f,w,h} \leq \text{E}^{\text{Max}} \cdot K^{\text{E}}, \quad \forall d,e,r,f,w,h, \tag{5.64}$$

$$\text{E}^{\text{Min}} \cdot K^{\text{E}} \leq e_{d,e,r,f,w,h-1} + \eta\, \left(p^{\text{C}}_{d,e,r,f,w,h} + r^{\text{FR,Dw,C}}_{d,e,r,f,w,h}\right)\tau^{\text{FR}} - p^{\text{D}}_{d,e,r,f,w,h} \leq \text{E}^{\text{Max}} \cdot K^{\text{E}}, \quad \forall d,e,r,f,w,h. \tag{5.65}$$

5.3.3.5 Bid Limits

The bounds for joint bids submitted by the WF-ESS operator and the relationship between them are modelled with constraints (5.66) and (5.67). Note that, besides the joint bids being upper-bounded by the WF's and the ESS's power capacities and lower-bounded by the ESS's maximum charging capacity, these are also bounded by the capacity of the transmission line. The latter set of bounds are omitted in this formulation for brevity's sake. Constraints (5.68) and(5.69) define the joint SPR and FR bids' domain to be zero, minimum provision level and maximum value, respectively.

$$x^{\text{En}}_{d,h} + x^{\text{SPR,Up}}_{d,h} + x^{\text{FR,Up}}_{d,h} \leq \text{K}^{\text{W}} + K^{\text{P}}, \quad \forall d,h, \tag{5.66}$$

$$x^{\text{En}}_{d,h} - x^{\text{SPR,Dw}}_{d,h} - x^{\text{FR,Dw}}_{d,h} \geq -K^{\text{P}}, \quad \forall d,h, \tag{5.67}$$

$$x^{\text{SPR,Up/Dw}}_{d,h} \in 0 \cup \left[\underline{\text{SPR}}^{\text{Up/Dw}}, \text{K}^{\text{W}} + 2K^{\text{P}}\right], \quad \forall d,h, \tag{5.68}$$

$$x^{\text{FR,Up/Dw}}_{d,h} \in 0 \cup \left[\underline{\text{FR}}^{\text{Up/Dw}}, \text{K}^{\text{W}} + 2K^{\text{P}}\right], \quad \forall d,h. \tag{5.69}$$

5.3.3.6 Sized ESS Parameters' Limits

The sized power and energy capacities of the ESS are limited by the maximum charge/discharge power and energy capacity in constraints (5.70) and (5.71), respectively.

$$K^{\mathrm{P}} \leq \overline{\mathrm{P}}, \tag{5.70}$$

$$K^{\mathrm{E}} \leq \overline{\mathrm{E}}. \tag{5.71}$$

5.3.3.7 Variable Types

Lastly, the sign and type of all decision variables is given by equalities (5.72) to (5.76). SOS1 pairs of variables are identified in parentheses in equation (5.75).

$$\Omega^{\mathrm{BV}} = \left\{ Q^{\mathrm{Up,D}}_{d,e,r,f,w,h}, Q^{\mathrm{Dw,D}}_{d,e,r,f,w,h}, Q^{\mathrm{Up,C}}_{d,e,r,f,w,h}, Q^{\mathrm{Dw,C}}_{d,e,r,f,w,h} \right\} \in \{0,1\}, \quad \forall d,e,r,f,w,h, \tag{5.72}$$

$$\Omega^{\mathrm{CV}} = \left\{ \xi^{\mathrm{En}}, \xi^{\mathrm{SPR,Up}}, \xi^{\mathrm{SPR,Dw}}, \xi^{\mathrm{FR,Up}}, \xi^{\mathrm{FR,Dw}}, \zeta^{\mathrm{En}}, \zeta^{\mathrm{SPR,Up}}, \zeta^{\mathrm{SPR,Dw}}, \zeta^{\mathrm{FR,Up}}, \zeta^{\mathrm{FR,Dw}}, x^{\mathrm{En}}_{d,h} \right\} \in \mathbb{R}, \quad \forall d,h, \tag{5.73}$$

$$\Omega^{\mathrm{SCV}^+} = \left\{ r^{\mathrm{SPR,Up}}_{d,e,r,f,w,h}, r^{\mathrm{SPR,Dw}}_{d,e,r,f,w,h}, x^{\mathrm{SPR,Up}}_{d,h}, x^{\mathrm{SPR,Dw}}_{d,h}, r^{\mathrm{FR,Up}}_{d,e,r,f,w,h}, r^{\mathrm{FR,Dw}}_{d,e,r,f,w,h}, x^{\mathrm{FR,Up}}_{d,h}, x^{\mathrm{FR,Dw}}_{d,h} \right\} \in \mathbb{R}_{\geq 0}, \quad \forall d,e,r,f,w,h, \tag{5.74}$$

$$\begin{aligned} \Omega^{\mathrm{CV}^{\mathrm{SOS1}}} = \Big\{ & \left(p^{\mathrm{D}}_{d,e,r,f,w,h}, p^{\mathrm{C}}_{d,e,r,f,w,h} \right), \left(i^{\mathrm{En}^+}_{d,e,r,f,w,h}, i^{\mathrm{En}^-}_{d,e,r,f,w,h} \right), \left(i^{\mathrm{SPR,Up}^+}_{d,e,r,f,w,h}, i^{\mathrm{SPR,Up}^-}_{d,e,r,f,w,h} \right), \\ & \left(i^{\mathrm{SPR,Dw}^+}_{d,e,r,f,w,h}, i^{\mathrm{SPR,Dw}^-}_{d,e,r,f,w,h} \right), \left(i^{\mathrm{FR,Up}^+}_{d,e,r,f,w,h}, i^{\mathrm{FR,Up}^-}_{d,e,r,f,w,h} \right), \left(i^{\mathrm{FR,Dw}^+}_{d,e,r,f,w,h}, i^{\mathrm{FR,Dw}^-}_{d,e,r,f,w,h} \right) \Big\} \in \mathbb{R}_{\geq 0}, \quad \forall d,e,r,f,w,h, \end{aligned} \tag{5.75}$$

$$\begin{aligned} \Omega^{\mathrm{CV}^+} = \Big\{ & K^{\mathrm{P}}, K^{\mathrm{E}}, p^{\mathrm{W}}_{d,e,r,f,w,h}, e^{0}_{e,r,f,w}, e_{d,e,r,f,w,h}, r^{\mathrm{SPR,Up,D}}_{d,e,r,f,w,h}, r^{\mathrm{SPR,Up,C}}_{d,e,r,f,w,h}, r^{\mathrm{SPR,Dw,D}}_{d,e,r,f,w,h}, r^{\mathrm{SPR,Dw,C}}_{d,e,r,f,w,h}, \\ & r^{\mathrm{SPR,Up,W}}_{d,e,r,f,w,h}, r^{\mathrm{SPR,Dw,W}}_{d,e,r,f,w,h}, r^{\mathrm{FR,Up,D}}_{d,e,r,f,w,h}, r^{\mathrm{FR,Up,C}}_{d,e,r,f,w,h}, r^{\mathrm{FR,Dw,D}}_{d,e,r,f,w,h}, r^{\mathrm{FR,Dw,C}}_{d,e,r,f,w,h}, r^{\mathrm{FR,Up,W}}_{d,e,r,f,w,h}, \\ & r^{\mathrm{FR,Dw,W}}_{d,e,r,f,w,h}, \mu^{\mathrm{En}}_{e,r,f,w}, \mu^{\mathrm{SPR,Up}}_{e,r,f,w}, \mu^{\mathrm{SPR,Dw}}_{e,r,f,w}, \mu^{\mathrm{FR,Up}}_{e,r,f,w}, \mu^{\mathrm{FR,Dw}}_{e,r,f,w} \Big\} \in \mathbb{R}_{\geq 0}, \quad \forall d,e,r,f,w,h. \end{aligned} \tag{5.76}$$

5.4 Achieving Computational Tractability

5.4.1 Representative weeks

One of the most common strategies to improve computational efficiency in long-term planning MILP models is to divide the assessment horizon into a set of representative periods [10, 117–119]. Representative periods can be defined in order to characterize a year by typical weeks or months focusing on seasonal patterns for the parameters considered in the problem's formulation, i.e. wind speed profiles during the spring weeks or price patterns for winter weeks. As such, this technique allows reducing the number of time-dependent variables.

Modelling-wise, this approach requires the introduction of a new set of indices $j \in J$ for all time-dependent decision variables and parameters. It is assumed in this formulation that the the year in the assessment horizon is outlined by N^J weeks. Furthermore, each time period is now affected by weighting factor W_j in the objective function and reflects the weight that each typical week is meant to represent in relation to the full year.

As previously mentioned, the concept of representative weeks can be used to characterize typical seasonal profiles in order to capture the most common patterns for the time-dependent parameters (prices and wind power availability). One approach to determine representative weeks is to apply a scenario reduction technique to each parameter in order to find the reduced set of weeks or days that minimize the difference from the full year. While representative weeks can be found using techniques as proposed in [131, 132], other scenario reduction techniques also allow identifying extreme scenarios in the reduction process [133].

5.4.1.1 Objective Function with Representative Weeks

The objective function that determines the power and energy capacities of ESS and maximizes the expected yearly profit and the CVaR under different levels of risk aversion for the WF and ESS must be adapted to reflect the representative weeks approach. As such, objective function (5.77) is updated to maximize the expected profit for all time periods, days and weeks subject to the weight of each week, W_j.

$$
\begin{aligned}
\underset{\substack{\Omega^{\mathrm{BV}},\Omega^{\mathrm{CV}},\Omega^{\mathrm{CV}^+},\\ \Omega^{\mathrm{SCV}^+},\Omega^{\mathrm{CV}^{\mathrm{SOS1}}},}}{\text{Maximize}} \Bigg\{ & (1-\beta) \sum_{e\in S^{\mathrm{E}}} \sum_{r\in S^{\mathrm{R}}} \sum_{r\in S^{\mathrm{F}}} \sum_{w\in S^{\mathrm{W}}} \rho_e \rho_r \rho_f \rho_w \Bigg[\sum_{j\in J} \mathrm{W}_j \sum_{d\in D} \sum_{h\in H} \\
& \Big(\pi^{\mathrm{En}}_{j,d,e,h} x^{\mathrm{En}}_{j,d,h} + \omega^{\mathrm{En}^+}_{j,d,e,h} \pi^{\mathrm{En}}_{j,d,e,h} i^{\mathrm{En}^+}_{j,d,e,r,f,w,h} - \omega^{\mathrm{En}^-}_{j,d,e,h} \pi^{\mathrm{En}}_{j,d,e,h} i^{\mathrm{En}^-}_{j,d,e,r,f,w,h} \\
& + \pi^{\mathrm{SPR,Up}}_{j,d,r,h} x^{\mathrm{SPR,Up}}_{j,d,h} + \omega^{\mathrm{SPR}^+}_{j,d,r,h} \pi^{\mathrm{SPR,Up}}_{j,d,r,h} i^{\mathrm{SPR,Up}^+}_{j,d,e,r,f,w,h} - \omega^{\mathrm{SPR}^-}_{j,d,r,h} \pi^{\mathrm{SPR,Up}}_{j,d,r,h} i^{\mathrm{SPR,Up}^-}_{j,d,e,r,f,w,h} \\
& + \pi^{\mathrm{SPR,Dw}}_{j,d,r,h} x^{\mathrm{SPR,Dw}}_{j,d,h} + \omega^{\mathrm{SPR}^+}_{j,d,r,h} \pi^{\mathrm{SPR,Dw}}_{j,d,r,h} i^{\mathrm{SPR,Dw}^+}_{j,d,e,r,f,w,h} - \omega^{\mathrm{SPR}^-}_{j,d,r,h} \pi^{\mathrm{SPR,Dw}}_{j,d,r,h} i^{\mathrm{SPR,Dw}^-}_{j,d,e,r,f,w,h} \\
& + \pi^{\mathrm{FR,Up}}_{j,d,f,h} x^{\mathrm{FR,Up}}_{j,d,h} + \omega^{\mathrm{FR}^+}_{j,d,f,h} \pi^{\mathrm{SPR,Up}}_{j,d,r,h} i^{\mathrm{FR,Up}^+}_{j,d,e,r,f,w,h} - \omega^{\mathrm{FR}^-}_{j,d,f,h} \pi^{\mathrm{F,Up}}_{j,d,f,h} i^{\mathrm{FR,Up}^-}_{j,d,e,r,f,w,h} \\
& + \pi^{\mathrm{FR,Dw}}_{j,d,f,h} x^{\mathrm{FR,Dw}}_{j,d,h} + \omega^{\mathrm{FR}^+}_{j,d,f,h} \pi^{\mathrm{FR,Dw}}_{j,d,f,h} i^{\mathrm{FR,Dw}^+}_{j,d,e,r,f,w,h} - \omega^{\mathrm{FR}^-}_{j,d,f,h} \pi^{\mathrm{FR,Dw}}_{j,d,f,h} i^{\mathrm{FR,Dw}^-}_{j,d,e,r,f,w,h} \Big) \Bigg] \\
& + \beta \left(\xi^{\mathrm{En}} + \xi^{\mathrm{SPR,Up}} + \xi^{\mathrm{SPR,Dw}} + \xi^{\mathrm{FR,Up}} + \xi^{\mathrm{FR,Dw}} \right) \\
& - \mathrm{C}^{\mathrm{P}} \frac{\delta(1+\delta)^{\gamma}}{(1+\delta)^{\gamma}-1} K^{\mathrm{P}} - \mathrm{C}^{\mathrm{E}} \frac{\delta(1+\delta)^{\gamma}}{(1+\delta)^{\gamma}-1} K^{\mathrm{E}} \Bigg\}.
\end{aligned}
\tag{5.77}
$$

5.4.1.2 Model Constraints with Representative Weeks

The operation of the ESS must be adapted to account for the stored energy at the beginning and ending of each representative horizon, and a linkage between the final and initial values must be ensured for the wind power availability in every week to avoid unrealistic variations in wind generation. As such, constraints (5.78) to (5.80), update the previous constraints for each representative week, while constraints (5.81) link each representative week in terms of initial stored energy level in the ESS.

$$
e_{j,d,e,r,f,w,h} = e^{0}_{j,e,r,f,w}, \quad \forall j,e,r,f,w,\ d=1,h=0, \tag{5.78}
$$

$$
e_{j,d,e,r,f,w,h} = e_{j,d-1,e,r,f,w,\mathrm{N^H}}, \quad \forall j,d,e,r,f,w,\ d\geq 2,h=0 \tag{5.79}
$$

$$
e_{j,d,e,r,f,w,h} = e^{0}_{j,e,r,f,w}, \quad \forall j,e,r,f,w,\ d=\mathrm{N^D},h=\mathrm{N^H}, \tag{5.80}
$$

$$
e_{j-1,d,e,r,f,w,h} = e^{0}_{j,e,r,f,w}, \quad \forall j,e,r,f,w,\ d=\mathrm{N^D},h=\mathrm{N^H}. \tag{5.81}
$$

The indexing for the representative weeks presented here should extend to the rest of the model's formulation, which was omitted for brevity's sake. Despite using representative periods leading to increased computational efficiency, the resulting representative set might still produce undesirable execution times. While further reduction addresses this issue, the reduced accuracy of the results might lead to incorrect conclusions.

5.4.2 Decomposition Techniques – Progressive Hedging Algorithm

Another approach to achieve computational tractability without sacrificing the representativity of the parameter set is to adopt decomposition techniques to divide the original problem into small-scale sub-problems which are easier to solve. One of the most popular decomposition techniques used to solve large-scale MILP problems is Benders decomposition [134], which separates the original problem into Master- and sub-problems in which both feature a relaxed set of constraints. However, the mathematical formulation of the model proposed in this chapter features binary variables in order to ensure the commitment of SPR in the second-stage of the stochastic problem which complicates the application of the Benders decomposition. This can be explained by the fact that this decomposition technique only allows the presence of binary variables in the Master-problem to ensure the application of duality theory and strong duality theorem.

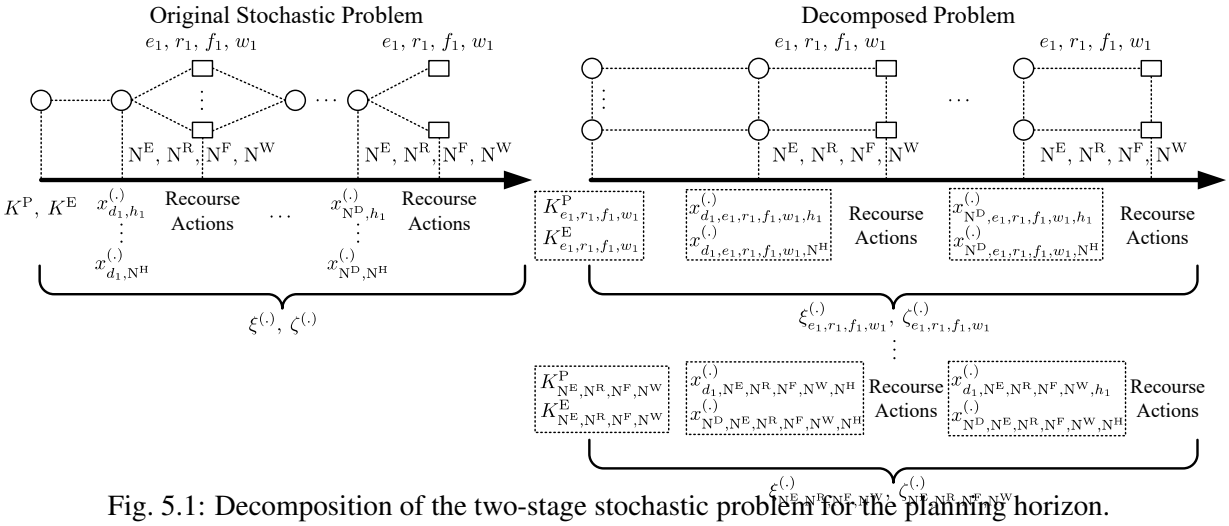


Fig. 5.1: Decomposition of the two-stage stochastic problem for the planning horizon.

Another decomposition technique that is more suitable for the problem in question is the PHA introduced by Rockafellar et al. in [48]. This method, which belongs to a class of augmented Lagrangian relaxation techniques, decomposes the original stochastic problem into scenario-dependent sub-problems in the presence of convexity. In other words, the decomposition allows the non-anticipativity conditions to be relaxed and the first-stage decisions become scenario-dependent (hedged) variables as exemplified in Fig. 5.1. The deterministic nature of these sub-problems allows it to be easily parallelizable in order to further reduce computational burden. The scenario-dependent solutions for the hedged variables are then aggregated by calculating the probability-weighted average of all solutions. Non-anticipativity is restored iteratively in the objective function of each sub-problem by incorporating an additional cost term (in some works it's defined as "price of information") and by penalizing the deviation between the decision variables and the probability-weighted average of the corresponding decision variable in the previous iteration. The PHA has been successfully implemented in power systems literature in [126, 135–137]

and further improved in [49, 130, 138]. Although the PHA has been shown to successfully converge in convex stochastic problems, convergence is not guaranteed for stochastic MILP problems. Despite this, several techniques can be adopted in order to improve the performance of the algorithm. The interested reader should refer to [136, 138] for possible improvements to the PHA for solving stochastic MILP models.

As previously mentioned, the objective of minimizing risk associated with ESS investment (by means of maximizing the profit CVaR) in the model proposed in this chapter complicates the application of scenario decomposition techniques, such as the PHA, due to the lack of scenario-wise separability of the CVaR which can be easily applied to the expected profit value. Nevertheless, as proposed in [130], the PHA can be reformulated through the introduction of extra parameters and reformulation of the profit VaR as a scenario-dependent first-stage variable that through aggregation over the course of several iterations must converge to a single value due to non-anticipativity.

5.4.2.1 Implementation of the PHA

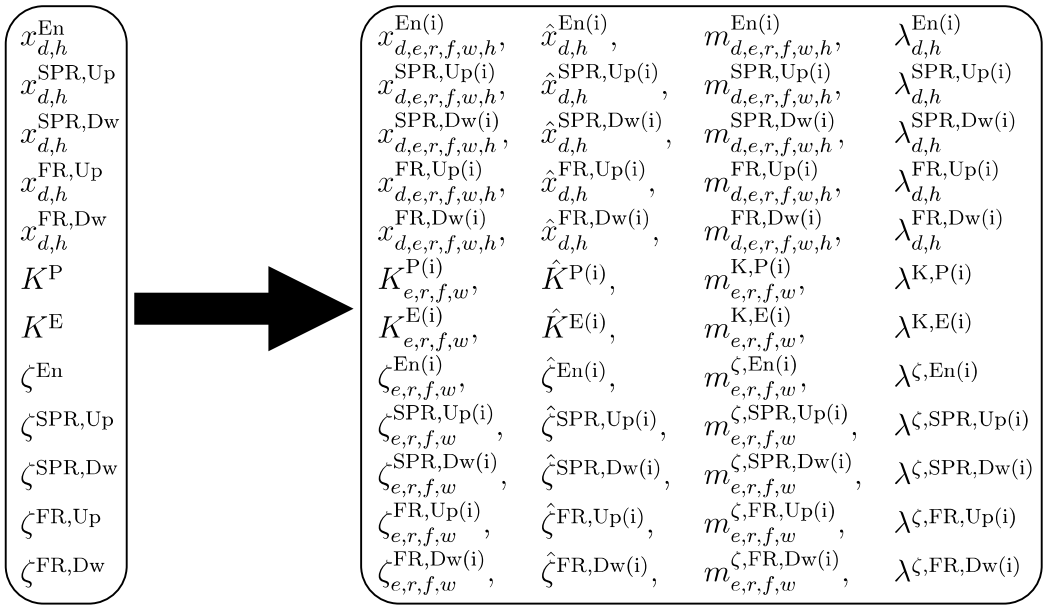


Fig. 5.2: Decomposition of the first-stage decision variables.

In order to implement the PHA to the risk-averse ESS investment model, the first-stage decision variables must be decomposed into scenario-dependent variables $x^{(.)(i)}_{d,e,r,f,w,h}$, $K^{\mathrm{P/E(i)}}_{e,r,f,w}$, $\zeta^{(.)(i)}_{e,r,f,w}$ according to Fig. 5.2 and each sub-problem solved independently. In the next step, a set of candidate first-stage solutions is defined by calculating the probability-weighted average for each day-ahead bids $\hat{x}^{(.)(i)}_{d,h}$, investment decisions $\hat{K}^{\mathrm{P/E(i)}}$ and source of profit VaR $\hat{\zeta}^{(.)(i)}$ with equations (5.83) through (5.85), respectively in each iteration i. In order to reintroduce the non-anticipativity conditions for iterations $i > 0$, a set of Lagrange multipliers $\left(m^{(.)(i)}_{d,e,r,f,w,h}, m^{\mathrm{K,P/E(i)}}_{e,r,f,w}, m^{\zeta,(.)(i)}_{e,r,f,w}\right)$ and penalization factors $\left(\lambda^{(.)(i)}_{d,h}, \lambda^{\mathrm{K,P/E(i)}}, \lambda^{\zeta,(.)(i)} > 0\right)$ are introduced for each hedged variable. Each Lagrange multiplier is calculated with equations (5.86) through (5.88) for each scenario based on the distance between the scenario solutions and their expected value. Note that the Lagrange multipliers are initialized as zero $\left(m^{(.)(-1)}_{d,e,r,f,w,h}, m^{\mathrm{K,P/E(-1)}}_{e,r,f,w}, m^{\zeta,(.)(-1)}_{e,r,f,w} = 0\right)$. The penalization factors control the rate of convergence and degree of suboptimality. The objective function to be maximized for each sub-problem is presented in (5.82), where the terms in line 8 and onwards are

introduced in order to penalize the lack of implementability and move the decision variables towards a single, implementable solution (first term - the aforementioned "price of information"), and to reach the convergence criterion (second term - the square proximal term). Note that for the first iteration of the algorithm ($i = 0$), these terms are not included in the sub-problems' objective function.[1]

$$
\begin{aligned}
\underset{\substack{\Omega^{\mathrm{BV}},\Omega^{\mathrm{CV}},\Omega^{\mathrm{CV}^{+}},\\ \Omega^{\mathrm{SCV}^{+}},\Omega^{\mathrm{CV}^{\mathrm{SOS1}}}}}{\text{Maximize}} \Bigg\{ & (1-\beta) \sum_{d\in D}\sum_{h\in H} \Big(\pi^{\mathrm{En}}_{d,e,h} x^{\mathrm{En(i)}}_{d,e,r,f,w,h} + \omega^{\mathrm{En}^{+}}_{d,e,h} \pi^{\mathrm{En}}_{d,e,h} i^{\mathrm{En}^{+}\mathrm{(i)}}_{d,e,r,f,w,h} - \omega^{\mathrm{En}^{-}}_{d,e,h} \pi^{\mathrm{En}}_{d,e,h} i^{\mathrm{En}^{-}\mathrm{(i)}}_{d,e,r,f,w,h} \\
& + \pi^{\mathrm{SPR,Up}}_{d,r,h} x^{\mathrm{SPR,Up(i)}}_{d,e,r,f,w,h} + \omega^{\mathrm{SPR}^{+}}_{d,r,h} \pi^{\mathrm{SPR,Up}}_{d,r,h} i^{\mathrm{SPR,Up}^{+}\mathrm{(i)}}_{d,e,r,f,w,h} - \omega^{\mathrm{SPR}^{-}}_{d,r,h} \pi^{\mathrm{SPR,Up}}_{d,r,h} i^{\mathrm{SPR,Up}^{-}\mathrm{(i)}}_{d,e,r,f,w,h} \\
& + \pi^{\mathrm{SPR,Dw}}_{d,r,h} x^{\mathrm{SPR,Dw(i)}}_{d,e,r,f,w,h} + \omega^{\mathrm{SPR}^{+}}_{d,r,h} \pi^{\mathrm{SPR,Dw}}_{d,r,h} i^{\mathrm{SPR,Dw}^{+}\mathrm{(i)}}_{d,e,r,f,w,h} - \omega^{\mathrm{SPR}^{-}}_{d,r,h} \pi^{\mathrm{SPR,Dw}}_{d,r,h} i^{\mathrm{SPR,Dw}^{-}\mathrm{(i)}}_{d,e,r,f,w,h} \\
& + \pi^{\mathrm{FR,Up}}_{d,f,h} x^{\mathrm{FR,Up(i)}}_{d,e,r,f,w,h} + \omega^{\mathrm{FR}^{+}}_{d,f,h} \pi^{\mathrm{SPR,Up}}_{d,r,h} i^{\mathrm{FR,Up}^{+}\mathrm{(i)}}_{d,e,r,f,w,h} - \omega^{\mathrm{FR}^{-}}_{d,f,h} \pi^{\mathrm{F,Up}}_{d,f,h} i^{\mathrm{FR,Up}^{-}\mathrm{(i)}}_{d,e,r,f,w,h} \\
& + \pi^{\mathrm{FR,Dw}}_{d,f,h} x^{\mathrm{FR,Dw(i)}}_{d,e,r,f,w,h} + \omega^{\mathrm{FR}^{+}}_{d,f,h} \pi^{\mathrm{FR,Dw}}_{d,f,h} i^{\mathrm{FR,Dw}^{+}\mathrm{(i)}}_{d,e,r,f,w,h} - \omega^{\mathrm{FR}^{-}}_{d,f,h} \pi^{\mathrm{FR,Dw}}_{d,f,h} i^{\mathrm{FR,Dw}^{-}\mathrm{(i)}}_{d,e,r,f,w,h} \Big) \\
& + \beta \left(\xi^{\mathrm{En(i)}}_{e,r,f,w} + \xi^{\mathrm{SPR,Up(i)}}_{e,r,f,w} + \xi^{\mathrm{SPR,Dw(i)}}_{e,r,f,w} + \xi^{\mathrm{FR,Up(i)}}_{e,r,f,w} + \xi^{\mathrm{FR,Dw(i)}}_{e,r,f,w} \right) \\
& - \mathrm{C}^{\mathrm{P}} \frac{\delta(1+\delta)^{\gamma}}{(1+\delta)^{\gamma}-1} K^{\mathrm{P(i)}}_{e,r,f,w} - \mathrm{C}^{\mathrm{E}} \frac{\delta(1+\delta)^{\gamma}}{(1+\delta)^{\gamma}-1} K^{\mathrm{E(i)}}_{e,r,f,w} \\
& - \Bigg[\sum_{d\in D}\sum_{h\in H} \Bigg(m^{\mathrm{En(i\text{-}1)}}_{d,e,r,f,w,h} x^{\mathrm{En}(i)}_{d,e,r,f,w,h} + \frac{\lambda^{\mathrm{En(i)}}_{d,h}}{2} \left(x^{\mathrm{En(i)}}_{d,e,r,f,w,h} - \hat{x}^{\mathrm{En(i)}}_{d,h} \right)^2 \\
& \qquad + m^{\mathrm{SPR,Up(i\text{-}1)}}_{d,e,r,f,w,h} x^{\mathrm{SPR,Up(i)}}_{d,e,r,f,w,h} + \frac{\lambda^{\mathrm{SPR,Up(i)}}_{d,h}}{2} \left(x^{\mathrm{SPR,Up(i)}}_{d,e,r,f,w,h} - \hat{x}^{\mathrm{SPR,Up(i\text{-}1)}}_{d,h} \right)^2 \\
& \qquad + m^{\mathrm{SPR,Dw(i\text{-}1)}}_{d,e,r,f,w,h} x^{\mathrm{SPR,Dw(i)}}_{d,e,r,f,w,h} + \frac{\lambda^{\mathrm{SPR,Dw(i)}}_{d,h}}{2} \left(x^{\mathrm{SPR,Dw(i)}}_{d,e,r,f,w,h} - \hat{x}^{\mathrm{SPR,Dw(i\text{-}1)}}_{d,h} \right)^2 \\
& \qquad + m^{\mathrm{FR,Up(i\text{-}1)}}_{d,e,r,f,w,h} x^{\mathrm{FR,Up(i)}}_{d,e,r,f,w,h} + \frac{\lambda^{\mathrm{FR,Up(i)}}_{d,h}}{2} \left(x^{\mathrm{FR,Up(i)}}_{d,e,r,f,w,h} - \hat{x}^{\mathrm{FR,Up(i\text{-}1)}}_{d,h} \right)^2 \\
& \qquad + m^{\mathrm{FR,Dw(i\text{-}1)}}_{d,e,r,f,w,h} x^{\mathrm{FR,Dw(i)}}_{d,e,r,f,w,h} + \frac{\lambda^{\mathrm{FR,Dw(i)}}_{d,h}}{2} \left(x^{\mathrm{FR,Dw(i)}}_{d,e,r,f,w,h} - \hat{x}^{\mathrm{FR,Dw(i\text{-}1)}}_{d,h} \right)^2 \Bigg) \\
& + m^{\mathrm{K,P(i\text{-}1)}}_{e,r,f,w} K^{\mathrm{P(i)}}_{e,r,f,w} + \frac{\lambda^{\mathrm{K,P(i)}}}{2} \left(K^{\mathrm{P(i)}}_{e,r,f,w} - \hat{K}^{\mathrm{P(i\text{-}1)}}_{e,r,f,w} \right)^2 \\
& + m^{\mathrm{K,E(i\text{-}1)}}_{e,r,f,w} K^{\mathrm{E(i)}}_{e,r,f,w} + \frac{\lambda^{\mathrm{K,E(i)}}}{2} \left(K^{\mathrm{E(i)}}_{e,r,f,w} - \hat{K}^{\mathrm{E(i\text{-}1)}}_{e,r,f,w} \right)^2 \\
& + m^{\zeta,\mathrm{En(i\text{-}1)}}_{e,r,f,w} \zeta^{\mathrm{En(i)}}_{e,r,f,w} + \frac{\lambda^{\zeta,\mathrm{En(i)}}}{2} \left(\zeta^{\mathrm{En(i)}}_{e,r,f,w} - \hat{\zeta}^{\mathrm{En(i\text{-}1)}} \right)^2 \\
& + m^{\zeta,\mathrm{SPR,Up(i\text{-}1)}}_{e,r,f,w} \zeta^{\mathrm{SPR,Up(i)}}_{e,r,f,w} + \frac{\lambda^{\zeta,\mathrm{SPR,Up(i)}}}{2} \left(\zeta^{\mathrm{SPR,Up(i)}}_{e,r,f,w} - \hat{\zeta}^{\mathrm{SPR,Up(i\text{-}1)}} \right)^2 \\
& + m^{\zeta,\mathrm{SPR,Dw(i\text{-}1)}}_{e,r,f,w} \zeta^{\mathrm{SPR,Dw(i)}}_{e,r,f,w} + \frac{\lambda^{\zeta,\mathrm{SPR,Dw(i)}}}{2} \left(\zeta^{\mathrm{SPR,Dw(i)}}_{e,r,f,w} - \hat{\zeta}^{\mathrm{SPR,Dw(i\text{-}1)}} \right)^2 \\
& + m^{\zeta,\mathrm{FR,Up(i\text{-}1)}}_{e,r,f,w} \zeta^{\mathrm{FR,Up(i)}}_{e,r,f,w} + \frac{\lambda^{\zeta,\mathrm{FR,Up(i)}}}{2} \left(\zeta^{\mathrm{FR,Up(i)}}_{e,r,f,w} - \hat{\zeta}^{\mathrm{FR,Up(i\text{-}1)}} \right)^2 \\
& + m^{\zeta,\mathrm{FR,Dw(i\text{-}1)}}_{e,r,f,w} \zeta^{\mathrm{FR,Dw(i)}}_{e,r,f,w} + \frac{\lambda^{\zeta,\mathrm{FR,Dw(i)}}}{2} \left(\zeta^{\mathrm{FR,Dw(i)}}_{e,r,f,w} - \hat{\zeta}^{\mathrm{FR,Dw(i\text{-}1)}} \right)^2 \Bigg] \Bigg\}, \quad \forall e,r,f,w,
\end{aligned}
\tag{5.82}
$$

[1] The mathematical formulation of the parameters for the PHA are presented in its generalized form for each type of decision variable: day-ahead bids; investment decisions; each type of profit VaR. For a full list of expressions used to calculate the expected values, multipliers, penalty factors and gaps associated with each hedged variable, please refer to Appendix B.

$$\hat{x}_{d,h}^{(.)(\mathrm{i})} = \sum_{e\in S^{\mathrm{E}}}\sum_{r\in S^{\mathrm{R}}}\sum_{f\in S^{\mathrm{F}}}\sum_{w\in S^{\mathrm{W}}} \rho_e \rho_r \rho_f \rho_w x_{d,e,r,f,w,h}^{(.)(\mathrm{i})}, \quad \forall i,d,h, \tag{5.83}$$

$$\hat{K}^{\mathrm{P/E(i)}} = \sum_{e\in S^{\mathrm{E}}}\sum_{r\in S^{\mathrm{R}}}\sum_{f\in S^{\mathrm{F}}}\sum_{w\in S^{\mathrm{W}}} \rho_e \rho_r \rho_f \rho_w K_{e,r,f,w}^{\mathrm{P/E(i)}}, \quad \forall i, \tag{5.84}$$

$$\hat{\zeta}^{(.)(\mathrm{i})} = \sum_{e\in S^{\mathrm{E}}}\sum_{r\in S^{\mathrm{R}}}\sum_{f\in S^{\mathrm{F}}}\sum_{w\in S^{\mathrm{W}}} \rho_e \rho_r \rho_f \rho_w \zeta_{e,r,f,w}^{(.)(\mathrm{i})}, \quad \forall i, \tag{5.85}$$

$$m_{d,e,r,f,w,h}^{(.)(\mathrm{i})} = m_{d,e,r,f,w,h}^{(.)(\mathrm{i\text{-}1})} + \lambda_{d,h}^{(.)(\mathrm{i})}\left(x_{d,e,r,f,w,h}^{(.)(\mathrm{i})} - \hat{x}_{d,h}^{(.)(\mathrm{i})}\right), \quad \forall d,e,r,f,w,h,i>0, \tag{5.86}$$

$$m_{e,r,f,w}^{\mathrm{K,P/E(i)}} = m_{e,r,f,w}^{\mathrm{K,P/E(i\text{-}1)}} + \lambda^{\mathrm{K,P(i)}}\left(K_{e,r,f,w}^{\mathrm{P/E(i)}} - \hat{K}^{\mathrm{P/E(i)}}\right), \quad \forall e,r,f,w,i>0, \tag{5.87}$$

$$m_{e,r,f,w}^{\zeta,(.)(\mathrm{i})} = m_{e,r,f,w}^{\zeta,(.)(\mathrm{i\text{-}1})} + \lambda^{\zeta,(.)(\mathrm{i})}\left(\zeta_{e,r,f,w}^{(.)(\mathrm{i})} - \hat{\zeta}^{(.)(\mathrm{i})}\right), \quad \forall e,r,f,w,i>0. \tag{5.88}$$

5.4.2.2 Choice of Penalty factors $\lambda_{d,h}^{(.)(\mathrm{i})}$, $\lambda^{\mathrm{K,P/E(i)}}$ and $\lambda^{\zeta,(.)(\mathrm{i})}$

As pointed out in the previous sub-subsection, the penalty factors $\lambda_{d,h}^{(.)(\mathrm{i})}$, $\lambda^{\mathrm{K,P/E(i)}}$ and $\lambda^{\zeta,(.)(\mathrm{i})}$ control the degree of suboptimality of the results produced with the PHA and rate of convergence. If the penalty factor is too small, many iterations are required for convergence despite the quality of the solution being ensured. Otherwise, the PHA will require fewer iterations for convergence at the expense of the quality of the solution (the PHA may settle in sub-optimal solutions). Coupled with the fact that the PHA does not guarantee a global optimal solution for stochastic MILP problems, fine-tuning these penalty factors is an important step for achieving a successful implementation of the algorithm. Computing effective penalty factor values has been studied in [136, 138], and it is found in the former that a per-iteration penalty factor may lead to better results in terms of quality of the solution and convergence time for a given problem, while the latter identifies power systems-specific methods to determine these factors.

Considering that each first-stage decision variable of the original stochastic problem is easily associated with a price/cost parameter, it is possible to establish a penalty factor for each decision variable that results in a similar impact in the objective function for the risk-averse ESS investment, "price of information" and square proximal terms. This, in turn, helps the sub-model deciding between optimizing the risk-averse ESS investment problem and minimizing the deviation from the expected value for each decision variable in the previous iteration. Equations (5.89) and (5.90) calculate problem-independent and parameter-free values for the penalty factors relating to the hedged day-ahead bids and investment decisions, respectively. These equations are adapted from the selection heuristic SEP method proposed in [138].

$$\lambda_{d,h}^{(.)(\mathrm{i})} = \frac{\sum_{e/r/f\in S^{\mathrm{E/R/F}}} \rho_{e/r/f}\, \pi_{d,e/r/f,h}^{(.)}}{\max\left[\sum_{e\in S^{\mathrm{E}}}\sum_{r\in S^{\mathrm{R}}}\sum_{r\in S^{\mathrm{F}}}\sum_{w\in S^{\mathrm{W}}} \rho_e \rho_r \rho_f \rho_w \left|x_{d,e,r,f,w,h}^{(.)(\mathrm{i})} - \hat{x}_{d,h}^{(.)(\mathrm{i})}\right|, 1\right]}, \quad \forall d,h,i, \tag{5.89}$$

$$\lambda^{\mathrm{K,P/E(i)}} = \frac{\mathrm{C}^{\mathrm{P/E}}\, \frac{\delta(1+\delta)^{\gamma}}{(1+\delta)^{\gamma}-1}}{\max\left[\sum_{e\in S^{\mathrm{E}}}\sum_{r\in S^{\mathrm{R}}}\sum_{r\in S^{\mathrm{F}}}\sum_{w\in S^{\mathrm{W}}} \rho_e \rho_r \rho_f \rho_w \left|K_{e,r,f,w}^{\mathrm{P/E(i)}} - \hat{K}^{\mathrm{P/E(i)}}\right|, 1\right]}, \quad \forall i. \tag{5.90}$$

The lack of a cost/price parameter associated with each type of profit VaR makes the direct implementation of this concept unsuitable for the respective hedged variables. As such, a new policy is needed

for calculating the per-iteration values for the penalty factors that also reflects the size of these variables. In other words, while the day-ahead bids and investment decisions take values in the range of dozens of MW (depending on the size of the ESS and the WF), the VaR can take values in the realm of millions of pounds. Consequently, even for small values for the penalty factors $\left(\lambda^{\zeta,(.)(\mathrm{i})} \approx 1\right)$, the PHA may produce solutions that move instantly towards the expected value of the hedged variables in the first iteration resulting in sub-optimal solutions. If the penalty factors take extremely small values $\left(\lambda^{\zeta,(.)(\mathrm{i})} \approx 10^{-6}\right)$, the PHA will take an unreasonable number of iterations to converge or even fail to converge. In this regard, the desired behaviour for the penalty factors relating to the hedged variables for each VaR should be inversely proportional to the range of values for each scenarios' solutions for the VaR, such that is sufficiently small in the first iterations of the PHA and progressively increases as the model starts to converge. This ensures that each sub-problem correctly balances the optimization of the investment problem and the convergence towards the optimal value of the decision variables. Based on the previous concept, equations (5.91) were derived to calculate optimal values for these penalty factors. An extra parameter k is introduced to control the speed of the convergence and should increase with the level of risk aversion β.

$$\lambda^{\zeta,(.)(\mathrm{i})} = \frac{\mathrm{k}}{\max\left[\left(\zeta_{max}^{(.)(\mathrm{i})} - \zeta_{min}^{(.)(\mathrm{i})}\right), 1\right]}, \quad \forall i. \tag{5.91}$$

5.4.2.3 Convergence Criteria

The PHA provides an optimal solution when the value of the first-stage decision variables in each scenario converge to the same value that maximizes each of the sub-problems' objective function. As such, the PHA should be stopped when a calculated gap reaches a value smaller than a predefined threshold (ε) or a maximum number of iterations is reached. This gap reflects the proximity between the values for each scenarios' solution for the hedged variables and their expected value in each iteration. As such, the gap for each hedged variable is calculated in (5.92), (5.93) and (5.94) for the day-ahead bids, investment decisions and each VaR, respectively. (5.93) calculates the overall gap in each iteration.

$$g^{(.)(\mathrm{i})} = \sum_{e\in S^{\mathrm{E}}}\sum_{r\in S^{\mathrm{R}}}\sum_{r\in S^{\mathrm{F}}}\sum_{w\in S^{\mathrm{W}}} \rho_e\rho_r\rho_f\rho_w \frac{\sum_{d\in D}\sum_{h\in H}\left|x_{d,e,r,f,w,h}^{(.)(\mathrm{i})} - \hat{x}_{d,h}^{(.)(\mathrm{i})}\right|}{\mathrm{N^D N^H}}, \quad \forall i, \tag{5.92}$$

$$g^{\mathrm{K,P/E(i)}} = \sum_{e\in S^{\mathrm{E}}}\sum_{r\in S^{\mathrm{R}}}\sum_{r\in S^{\mathrm{F}}}\sum_{w\in S^{\mathrm{W}}} \rho_e\rho_r\rho_f\rho_w \left|K_{e,r,f,w}^{\mathrm{P/E(i)}} - \hat{K}^{\mathrm{P/E(i)}}\right|, \quad \forall i, \tag{5.93}$$

$$g^{\zeta,(.)(\mathrm{i})} = \sum_{e\in S^{\mathrm{E}}}\sum_{r\in S^{\mathrm{R}}}\sum_{r\in S^{\mathrm{F}}}\sum_{w\in S^{\mathrm{W}}} \rho_e\rho_r\rho_f\rho_w \left|\zeta_{e,r,f,w}^{(.)(\mathrm{i})} - \hat{\zeta}^{(.)(\mathrm{i})}\right|, \quad \forall i, \tag{5.94}$$

$$\begin{aligned} g^{(\mathrm{i})} = \Big[&\left(g^{\mathrm{En(i)}}\right)^2 + \left(g^{\mathrm{SPR,Up(i)}}\right)^2 + \left(g^{\mathrm{SPR,Dw(i)}}\right)^2 + \left(g^{\mathrm{FR,Up(i)}}\right)^2 + \left(g^{\mathrm{FR,Dw(i)}}\right)^2 + \left(g^{\mathrm{K,P(i)}}\right)^2 + \left(g^{\mathrm{K,E(i)}}\right)^2 \\ &+ \left(g^{\zeta,\mathrm{En(i)}}\right)^2 + \left(g^{\zeta,\mathrm{SPR,Up(i)}}\right)^2 + \left(g^{\zeta,\mathrm{SPR,Dw(i)}}\right)^2 + \left(g^{\zeta,\mathrm{FR,Up(i)}}\right)^2 + \left(g^{\zeta,\mathrm{FR,Dw(i)}}\right)^2 \Big]^{1/2}, \quad \forall i. \end{aligned} \tag{5.95}$$

5.4.2.4 Other Approximations

The square proximal terms included in each sub-problem's objective function (5.82) with the objective of reaching the convergence criterion make each sub-problem a mixed-integer quadratic programming problem. Given the quadratic nature of each sub-problem, significant more computational resources and

execution times are needed to find each sub-problems global optimum, defeating the purpose of applying the PHA to achieve computational tractability.

In order to overcome this problem, it is recommended to rewrite the square proximal terms in linear form. As the hedged variables are continuous, a piecewise linear approximation for the square proximal term was chosen with the intent to achieve an approximate behaviour to the square proximal term. Piecewise linearisation of a square function can also be considered an optimization problem in order to determine the optimal number of intervals and slopes to reduce the overall approximation error. Nevertheless, this work uses three segments for each hedged variable. For a full formulation of the piecewise linear approximation of the square proximal term, please refer to Section B.5.

5.4.2.5 Algorithm and Parallel Computing Implementation

The PHA consists of several steps presentedin Algorithm 5.1. The first step initializes the iteration counter and is followed by solving the original problem for each scenario in order to determine the initial solutions for the hedged variables for all time periods and scenarios (step 2). Thirdly, the probability-weighted average value for all scenario-specific solutions of the hedged variables is calculated, followed by the Lagrange Multipliers in step 4. For subsequent iterations, the penalty factors are calculated in step 6 and each sub-problem is optimized with the aim of solving the risk-averse ESS investment problem with restored non-anticipativity conditions and moving the solutions towards their expected value in the previous iteration to reach convergence (step 7). The following steps recalculate the new values for the probability-weighted average of the decision variables and associated Lagrange multipliers for each scenario. Steps 5 through 9 are repeated until the algorithm satisfies the convergence criteria in step 10.

Algorithm 5.1 PHA for scenario decomposition.

1. **Initialization**: i := 0
2. **Iteration 0**: $\forall\, e \in S^{\mathrm{E}},\ r \in S^{\mathrm{R}},\ f \in S^{\mathrm{F}},\ w \in S^{\mathrm{W}},\ \forall\, d \in D,\ h \in H,\ \lambda_{d,h}^{(.)(0)} = 0,\ \lambda^{\mathrm{K,P/E(0)}} = 0,\ \lambda^{\zeta,(.)(0)} = 0$: $x_{d,e,r,f,w,h}^{(.)(0)}, K_{e,r,f,w}^{\mathrm{P/E(0)}}, \zeta_{e,r,f,w}^{(.)(0)} \leftarrow argmax\{(5.82)\}$
3. **Aggregation**: $\forall d \in D, h \in H:\ \hat{x}_{d,h}^{(.)(0)}, \hat{K}^{\mathrm{P/E(0)}}, \hat{\zeta}^{(.)(0)} \leftarrow$ Equations (5.83) to (5.85)
4. **Lagrange Multiplier**: $\forall e \in S^{\mathrm{E}}, r \in S^{\mathrm{R}}, f \in S^{\mathrm{F}}, w \in S^{\mathrm{W}}:\ m_{d,e,r,f,w,h}^{(.)(0)}, m_{e,r,f,w}^{\mathrm{K,P/E(0)}}, m_{e,r,f,w}^{\zeta,(.)(0)} \leftarrow$ Equations (5.86) to (5.88)
5. **Iteration Update**: i := i+1
6. **Penalty factors**: $\forall d \in D, h \in H:\ \lambda_{d,h}^{(.)(\mathrm{i})}, \lambda^{\mathrm{K,P/E(i)}}, \lambda^{\zeta,(.)(\mathrm{i})} \leftarrow$ Equations (5.89) to (5.91)
7. **Iteration i**: $\forall\, e \in S^{\mathrm{E}},\ r \in S^{\mathrm{R}},\ f \in S^{\mathrm{F}},\ w \in S^{\mathrm{W}}:\ x_{d,e,r,f,w,h}^{(.)(\mathrm{i})}, K_{e,r,f,w}^{\mathrm{P/E(i)}}, \zeta_{e,r,f,w}^{(.)(\mathrm{i})} \leftarrow argmax\{(5.82)\}$
8. **Aggregation**: $\forall d \in D, h \in H:\ \hat{x}_{d,h}^{(.)(\mathrm{i})}, \hat{K}^{\mathrm{P/E(i)}}, \hat{\zeta}^{(.)(\mathrm{i})} \leftarrow$ Equations (5.83) to (5.85)
9. **Lagrange Multiplier**: $\forall e \in S^{\mathrm{E}}, r \in S^{\mathrm{R}}, f \in S^{\mathrm{F}}, w \in S^{\mathrm{W}}:\ m_{d,e,r,f,w,h}^{(.)(\mathrm{i})}, m_{e,r,f,w}^{\mathrm{K,P/E(i)}}, m_{e,r,f,w}^{\zeta,(.)(\mathrm{i})} \leftarrow$ Equations (5.86) to (5.88)
10. **Convergence**: If $g^{(i)} < \varepsilon \vee i > \mathrm{N^I}$ - exit, otherwise go to Step 5.

As previously stated, the deterministic nature and isolated manner in which each sub-problem is

solved open the possibility for this stage to be parallelizable. Considering that modern CPUs feature multiple logical processors, it is possible to better manage computational resources by solving several sub-problems is parallel instead of waiting for each sub-problem to finish to start the one. Fig. 5.3 illustrates the structure of Algorithm 5.1 implemented through a sequential approach and through a parallel computing approach under a given number of parallel processors $\left(\mathrm{N}^{\mathrm{PP}}\right)$.

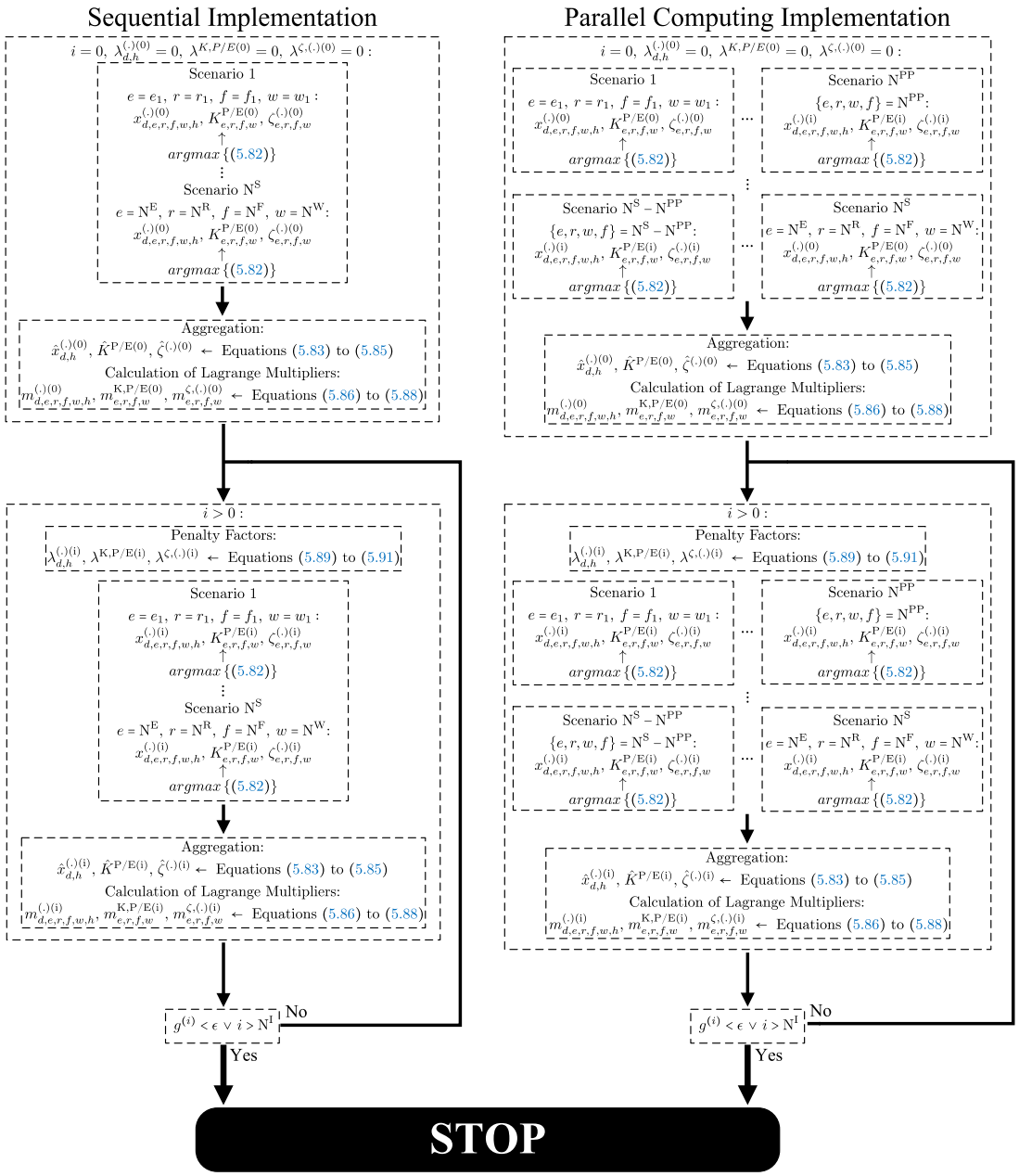


Fig. 5.3: Sequential vs Parallel Implementation of the PHA.

Note that this algorithm is implemented in FICO$^{\mathrm{TM}}$ Xpress , which takes advantage of modern CPUs' multi-core features for computational efficiency. In other words, Xpress automatically determines the appropriate amount of resources to solve each model. In the context of sequential or parallel implementations of the PHA, this means that each sub-problem in the sequential approach will make use of all available resources, while resources will be split to solve each sub-problem in the parallel computing implementation. Thus, in order to achieve better computational efficiency, and consequently minimiz-

ing the computational time needed for each iteration, the selection of N^{PP} becomes a trade-off between maximizing the number of parallel processes and devoting more resources for each sub-problem.

The objective of the PHA is to determine the values of the first-stage decision variables that maximize the objective function 5.1. It does not provide however the exact optimal value for the second-stage variables, except when the convergence gap reaches zero. In order to avoid an unreasonable number of iterations todetermine the optimal solution for the second-stage variables, an additional run of the stochastic model with fixed first-stage decision variables (determined with the PHA) is carried out. Fig. 5.4 presents a flowchart that describes the complete structure of the PHA implemented with Xpress. The model starts by reading the simulation parameters stored in an Excel file and proceeds to solve the risk-averse ESS investment problem using the PHA. When the algorithm converges, the solutions for the first-stage decision variables are treated in order to be used as additional input data for solving the stochastic problem to determine the optimal value for the second-stage decision variables, i.e. the optimal value for the recourse actions.

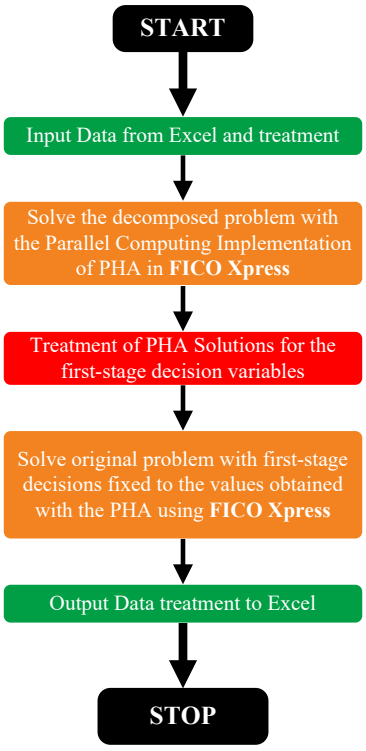


Fig. 5.4: Structure of the solution algorithm for the risk-averse investment problem.

5.5 Performance assessment of the PHA against Stochastic Models

5.5.1 Input Data

The objective of this case study is to assess the performance of the proposed PHA decomposition technique against a full Stochastic formulation. As such, the Stochastic and PHA models are used to solve the risk-averse ESS investment problem a 3 sets of scenarios: 15 scenarios (3 energy price and 5 wind power availability forecasts); 30 scenarios (3 energy price and 10 wind power availability forecasts); 270 scenarios (3 energy, 3 SPR and 3 FR price, and 10 wind power availability forecasts). In order to ensure that the stochastic problems are tractable for comparison purposes, the year under analysis is assumed to

be represented by 5 typical weeks. Table 5.1 presents the number of variables in the investment problem as a function of the total number of scenarios, N^S $\left(N^S = N^E \cdot N^R \cdot N^F \cdot N^W\right)$, for a full year $\left(N^D = 365\right)$ and for 5 representative weeks $\left(N^D = 7 \text{ per week } j\right)$. It is assumed that each day is comprised of 24 hourly time periods. The definition and relative weight of each representative week are presented in Table 5.3. The technical and economic specifications of the ESS that a 100 MW WF operator is assumed to invest in are presented in Table 5.4[2].

Table 5.1: Number of decision variables for each problem as a function of the number of scenarios

	Variable Category	General Formulation	Full Year	5 Typical Weeks
1st-Stage	Investment Decisions		2	
	CVaR and VaR		10	
	Day-ahead Bids	$5 \cdot N^D \cdot N^H$	43,800	4,200
2nd-Stage	Binary Variables	$4 \cdot N^D \cdot N^E \cdot N^R \cdot N^F \cdot N^W \cdot N^H$	$35,040 \cdot N^S$	$3,360 \cdot N^S$
	Continuous Variables	$30 \cdot N^D \cdot N^E \cdot N^R \cdot N^F \cdot N^W \cdot N^H$ $+6 \cdot N^E \cdot N^R \cdot N^F \cdot N^W$	$262,806 \cdot N^S$	$25,206 \cdot N^S$

Table 5.2: Number of constraints for each problem as a function of the number of scenarios

Constraint Dependency	General Formulation	Full Year	5 Typical Weeks
Non-scenario, Non-time period		7	
Scenario Only	$8 \cdot N^E \cdot N^R \cdot N^F \cdot N^W$	$8 \cdot N^S$	
Time Period Only	$4 \cdot N^D \cdot N^H$	35,040	3,360
Scenario & Time Period	$52 \cdot N^D \cdot N^E \cdot N^R \cdot N^F \cdot N^W \cdot N^H$	$455,250 \cdot N^S$	$43,680 \cdot N^S$

Table 5.3: Representative Weeks definition and Weight factors in weeks/year

Week j	Season	Value
1	Winter	16.75
2	Extreme winter	0.25
3	Spring	9.00
4	Summer	13.00
5	Autumn	13.00

Note that the maximum power capacity of the ESS is constrained to 10% of the size of the WF in order to reduce the size of the problem's solution space to make it more tractable. Several studies in current literature consider a 20 years lifetime for a Li-ion battery ESS. For these case studies, however, it is assumed that the coordination between the ESS and the WF have a non-negligible impact on the degradation profile of this ESS, and in order to prevent the untimely retirement of the ESS due to excessive capacity loss, the equipment lifetime is assumed at 10 years. It is also assumed that stored energy levels are allowed to vary between 0% and 100% of the sized energy capacity.

[2]The capital costs for the energy and power capacities were provided courtesy of DNV GL.

Table 5.4: Technical and Economic Specifications of the ESS

Parameter	Unit	Value
Roundtrip Efficiency η	[p.u.]	0.85
Maximum power capacity $\overline{P}$	[MW]	10
Maximum energy capacity $\overline{E}$	[MWh]	50
Power capacity capital cost C^P	[£/kW]	109.15
Energy capacity capital cost C^E	[£/kWh]	395.25
Annual discount rate δ	[%]	5
Equipment Lifetime γ	[years]	10

It is assumed for these case studies that the penalty factors are 50% for positive imbalances and 150% for negative imbalances. Grid unavailability is not considered for these case studies, hence all wind power generation is assumed to be absorbable by the transmission system. These assumptions are taken in order to ensure that variations in the execution times are solely due to the number of scenarios. The forecasts used for each test can be found in Appendix C. For the tests with 15 and 30 scenarios, it is assumed a constant value of £6/MW and £8/MW for the provision of SPR and FR services, respectively. The maximum duration of the utilization time is assumed to be 2 hours for SPR $\left(\tau^{SPR}\right)$ and 0.5 hours for FR $\left(\tau^{FR}\right)$, while minimum provision levels are assumed to be 3MW for SPR $\left(\underline{SPR}^{Up/Dw}\right)$ and 2 MW for FR $\left(\underline{FR}^{Up/Dw}\right)$ following National Grid regulations. The confidence level (α) for the risk-averse tests was set at 95%.

The PHA and Stochastic models were implemented in and solved with FICO^{TM} Xpress on a server with two 2.60 GHz Intel(R) Xeon (R) processors (14 cores each) and 512 GB of RAM, running Windows Server 2012. For the testing of the Stochastic model, the optimality gap was set at 1.0% and the maximum runtime at 10^6s. In order to test the PHA, the optimality gap was set at 0.15% and a maximum runtime of 1600s for each sub-problem, while for the convergence of the algorithm a gap $\varepsilon = 10^{-3}$ and a maximum of 500 iterations.

5.5.2 15 Scenarios

The first round of testing of the Stochastic and PHA models is done with 15 scenarios making use of the forecasts presented in Figs. C.1 and C.4 in Appendix C to build the scenario set. Testing is also conducted for 3 levels of risk aversion: $\beta = 0.0$; $\beta = 0.5$; $\beta = 1.0$. Table 5.5 compares each models' performance in terms of execution time, solution gap, number of iterations (applicable to the PHA only), objective function and power and energy capacities of the ESS. Note that due to the different nature of the solution gap in both models, the solution gap for the Stochastic model is relative (percentage-wise), while the one for the PHA is absolute. The PHA was solved using 15 parallel processes. The convergence of the PHA is presented in Fig. 5.5 which shows how the solution gap evolves as a function of the number of iterations.

Although the Stochastic model manages to find an optimal solution for the risk-neutral investment problem in approximately 3.5 hours, the execution times for the two levels of risk aversion under consideration are not as favourable and took longer than a day to solve. On the other hand, the PHA clearly outperforms the Stochastic model by reducing execution times up to 95%.

Table 5.5: Performance of the PHA and Stochastic Models with 15 Scenarios

β	Model	Time [s]	Iterations [#]	Obj. Function [£]	K^{P} [MW]	K^{E} [MWh]
0.0	Stochastic	12,904	-	12,290,238	10	12.000
	PHA	1,519	36	12,353,999	10	10.061
0.5	Stochastic	95,349	-	11,619,481	10	12.000
	PHA	4,428	40	11,687,943	10	10.115
1.0	Stochastic	203,389	-	10,249,861	10	12.000
	PHA	9,845	77	11,029,565	10	10.000

Besides outperforming the Stochastic model in terms of execution time, the PHA also achieves slightly higher values for the objective function (0.5% for $\beta = 0.0$ and $\beta = 0.5$) which is in part due to the fact that the Stochastic model sized a larger energy capacity for the ESS (12 MWh as opposed to 10MWh in the PHA). Despite higher operating profits being achieved with a higher capacity to store energy, these solutions prove to be economically inefficient as the PHA produces solutions with higher overall profits due to the smaller energy capacity of the ESS. For the full risk-averse behaviour, in which the value of the objective function reflects only the sum of each profit's CVaR minus the investment costs, the PHA achieves a significantly higher value for the CVaR (7.61% higher) than the Stochastic model. Note that this is not only explained by the reduced investment costs in the PHA solution but also on a better day-ahead bidding strategy and more precise decisions on the second-stage. In other words, the PHA provides a better solution in terms of profit volatility with the total profit STD being approximately £2,211, whereas in the Stochastic model's solution, the total profit STD is approximately £933,618.

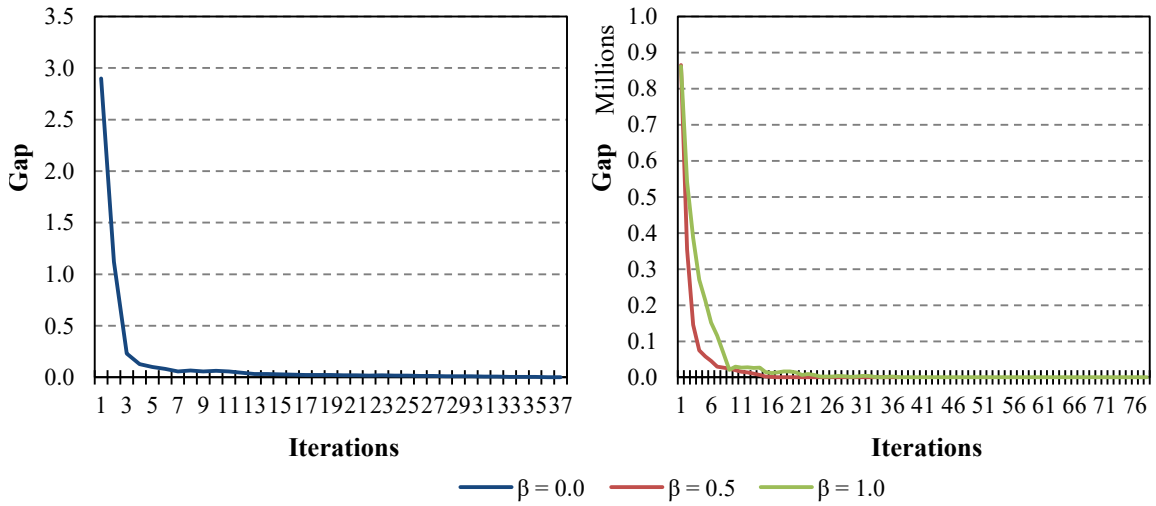


Fig. 5.5: Variation of the convergence gap for the PHA, risk-neutral simulation (left) and risk-averse simulations (right).

Analysing Fig. 5.5, it is to possible observe that the convergence gap is significantly reduced in the first 10 iterations of the algorithm and that subsequent iterations serve to fine-tune the solution. Note that the initial value for the convergence gap in the risk-averse simulations is significantly higher than the gap in the risk-neutral simulations due to the dispersion in the initial scenario-dependent solutions for the profit VaR. Despite the significant increase in the number iterations needed to solve the risk-averse investment problems, the relative increase in execution time in the PHA due to the complexity of these

simulations is noticeably smaller than in the Stochastic model. The execution time was increased by 548% in the PHA and by 1476% in the Stochastic model between the risk-neutral and full risk-averse simulations.

5.5.3 30 Scenarios

With 30 scenarios, the objective is to analyse how both models perform under increased wind power availability uncertainty. As such, the wind forecasts used in the previous test are replaced by the forecasts presented in Fig. C.5. Besides analysing how both models' performance changes with doubling the number of scenarios, this test also aims to find how the sizing of the ESS is impacted by increased uncertainty regarding wind power availability. Table 5.6 compares both models' performance. The number of parallel processes was set at 27 for these tests. Despite the Stochastic model being able to solve the investment problem for the $\beta = 0.0$ and $\beta = 0.5$ simulations, this model did not find a solution under the chosen optimality gap and maximum execution time for $\beta = 1.0$. Note that, not only the PHA reduces execution times by an average of 95%, but is also able to solve the full risk-averse investment problem in less time than the Stochastic model needed to solve risk-neutral investment problem. Fig. 5.6 presents the evolution of the convergence gap in the PHA.

Table 5.6: Performance of the PHA and Stochastic Models with 30 Scenarios

β	Model	Time [s]	Iterations [#]	Obj. Function [£]	K^{P} [MW]	K^{E} [MWh]
0.0	Stochastic	49,326	-	11,943,956	10	9.496
	PHA	1,205	28	11,938,362	10	10.000
0.5	Stochastic	386,381	-	10,608,744	10	10.000
	PHA	25,288	76	10,610,329	10	9.999
1.0	Stochastic	-	-	-	-	-
	PHA	29,975	91	9,821,306	10	10.019

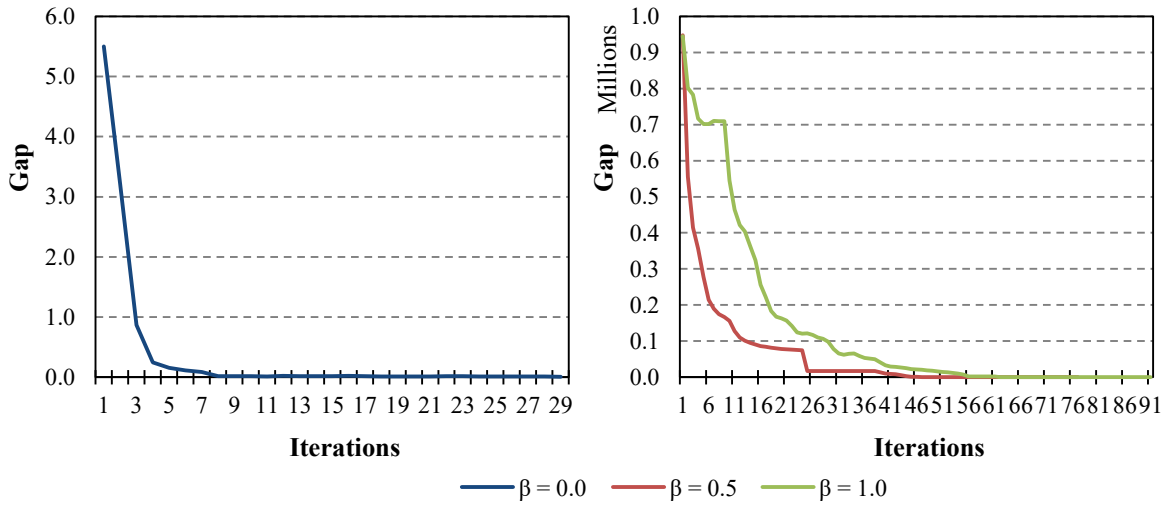


Fig. 5.6: Variation of the convergence gap for the PHA, risk-neutral simulation (left) and risk-averse simulations (right).

Contrasting with the previous simulations, the PHA and Stochastic models converge to similar solutions in terms of objective function and the power and energy capacities of ESS (0.05% error in terms of

objective function), validating the solutions produced by the PHA. The power and energy capacities of the ESS in both models were closer in value unlike in the previous tests. This can be explained, by the fact that the resulting optimality gap of the solutions determined with the Stochastic model was lower in these simulations as opposed to the simulations with 15 scenarios. On the other hand, it can also be concluded from the PHA, that even with increased wind power uncertainty, the energy capacity of the ESS is mainly dependent on the value of the power capacity of the ESS which in this case is constrained to 10 MW.

Fig. 5.6 shows that despite the increased number of scenarios the PHA easily converges towards the solution in the risk-neutral simulation. It is worth noting that the execution time and the number of iterations for this simulation are smaller than in the previous case. The same cannot be said of the risk-averse simulations, as the complexity of the problem is further increased by the number of scenarios and for each profit VaR to converge to a single value. Besides needing more iterations (49 for $\beta = 0.5$ and 63 for $\beta = 1.0$), the convergence isn't as smooth as in Fig. 5.5 due to the gap oscillating during some iterations (namely between iterations 11 and 16 for $\beta = 1.0$). This can be explained due to the different impact that each VaR has on the objective function. In other words, as each scenario's solution for the energy profit VaR converges to closer values, the solutions for the other profits VaR $\left(\zeta^{\text{SPR,Up}}_{e,r,w,f}, \zeta^{\text{SPR,Dw}}_{e,r,w,f}, \zeta^{\text{FR,Up}}_{e,r,w,f}\right.$ and $\left.\zeta^{\text{FR,Dw}}_{e,r,w,f}\right)$ slightly diverge in order to maximize the profit or CVaR, before converging to optimal values.

5.5.4 270 Scenarios

Lastly, the 270 scenario set now includes SPR and FR pricing uncertainty by including the forecasts presented in Figs. C.2 and C.3, respectively. Given the large-scale of the problem under these conditions (7,717,032 variables and 11,799,127 constraints for 5 representative weeks), the Stochastic model didn't find an optimal solution in any of the tests under 10^6s. The PHA, however, successfully converged for all risk aversion levels under an acceptable execution time. Table 5.7 summarizes the performance of the PHA for all risk aversion levels. Considering that the server's CPU used for testing these models is composed of 28 cores, the number of parallel processes was set at 27. Besides being an integer divisor of 270, further testing showed that performance decreased for higher or lower number of parallel processes.

Table 5.7: Performance of the PHA with 270 Scenarios

β	Time [s]	Iterations [#]	Obj. Function [£]	K^{P} [MW]	K^{E} [MWh]
0.0	10,125	29	11,574,802	10	10.000
0.5	63,885	95	10,201,911	10	9.834
1.0	103,633	122	9,507,326	10	9.966

Comparing the execution time of the PHA with 270 scenarios against the previous tests, only the risk-neutral simulation increases approximately at the same rate of the number of scenarios (the execution time increases approximately 8.4x when compared to the performance with 30 scenarios). For $\beta = 0.5$ and $\beta = 1.0$, despite the execution time increase being smaller (2.5x for $\beta = 0.5$ and 3.5x $\beta = 1.0$), these problems were significantly harder to solve and needed more iterations to converge. Note that despite the full risk-averse simulation taking longer than a day to converge, the execution time can be decreased by increasing the value of k in equations (5.91), albeit decreasing the accuracy of the solution.

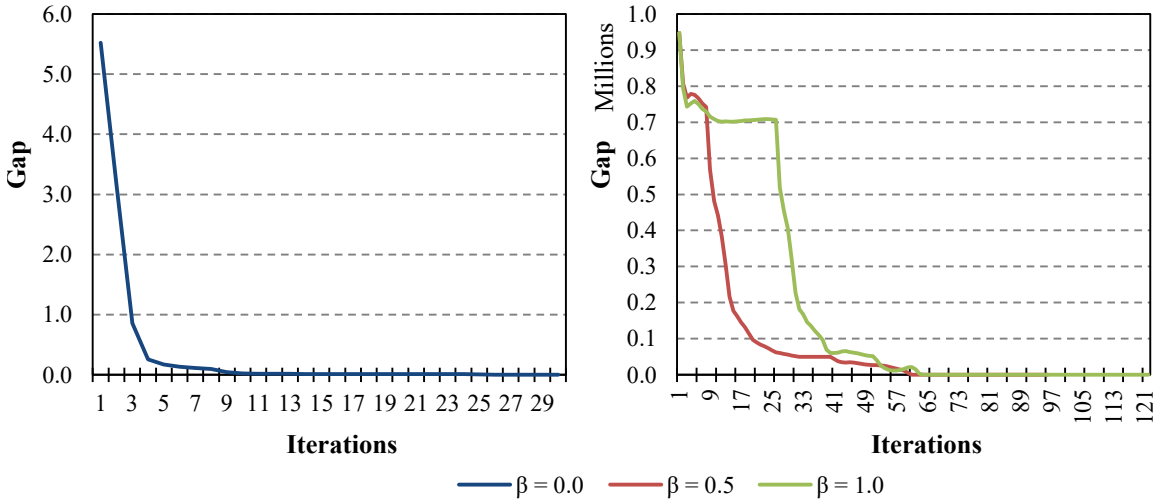


Fig. 5.7: Variation of the convergence gap for the PHA, risk-neutral simulation (left) and risk-averse simulations (right).

Fig. 5.7 shows a similar convergence to the simulations with 30 scenarios, although the convergence gap for β = 1.0 fluctuates between iterations 9 and 25. Although the explanation for this effect in the previous simulation holds true, a higher number of scenarios in this case further hindered the convergence for the values for the VaR for SPR and FR profits before the progression of the VaR for the Energy profit, whose deviation between the probability-weighted average and scenario solutions, at this point, is the main component of the convergence gap.

The results presented in these case studies clearly show the advantages of the PHA when compared to the Stochastic model as, besides achieving significant reductions in execution times, it is able to solve more complex problems such as the investment problem with β = 1 and for larger number of scenarios and, consequently, opening the possibility for more significant (with longer assessment horizon and conditions) studies to be performed. Lastly, in order to better present the benefit of the PHA over the Stochastic model, Fig. 5.8 shows a visual comparison of the execution time and objective function for each test and model for all simulations.

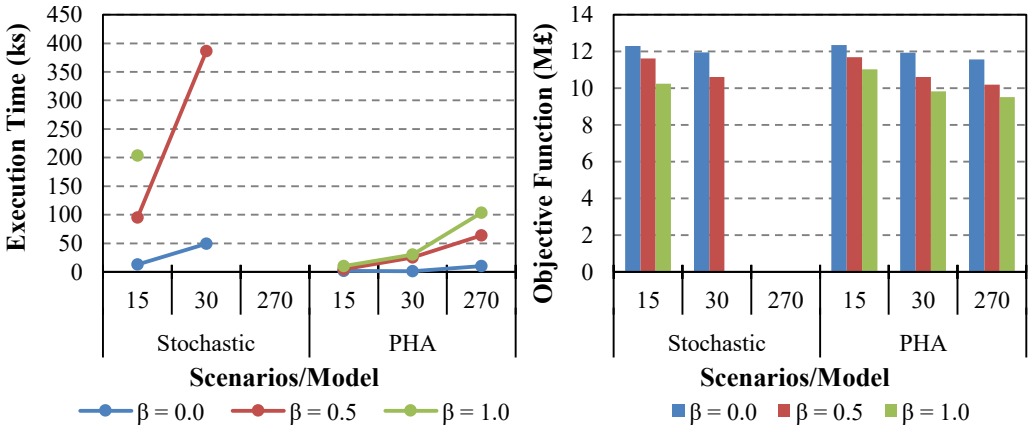


Fig. 5.8: Variation of performance of the PHA and Stochastic models in terms of execution time (left) and objective function (right).

5.6 Profitability of ESS investments

5.6.1 270 Scenarios Performance Test

Despite the limited scope of the tests conducted in Section 5.5, it is still possible to draw some conclusions from them regarding the value of the ESS investments for risk-averse wind producers. The Stochastic model was used to solve the problem of the 100 MW WF participating in the day-ahead markets without the support of the ESS to analyse of the profitability of the investments determined in the 270 scenarios test. Table 5.8 presents the yearly breakdown of profits, total VaR and CVaR for the WF and WF+ESS configurations under the considered risk aversion levels.

Table 5.8: Economic Results of the WF and WF+ESS operation in £

Risk Aversion		$\beta = 0.0$		$\beta = 0.5$		$\beta = 1.0$	
Facility Type		WF	WF+ESS	WF	WF+ESS	WF	WF+ESS
Revenue	Energy	9,986,707	9,984,740	9,976,989	9,966,271	9,338,677	9,478,967
	SPR	250	26,879	170	27,510	2,332	24,710
	FR	1,958,866	3,152,282	1,903,585	3,041,071	1,796,023	3,021,587
Imbalance Costs	Energy	864,672	741,682	1,025,164	821,021	972,795	916,322
	SPR	0	2,378	0	0	24	2,550
	FR	159,722	192,349	187,573	187,573	133,327	149,277
Investment Costs		0	652,690	0	644,211	0	650,939
Total Profit		10,921,429	11,574,802	10,668,007	11,419,346	10,030,886	10,806,176
VaR		8,598,806	9,898,817	8,748,044	10,274,614	8,870,149	10,480,107
CVaR		8,000,673	9,185,527	8,477,693	9,628,686	8,867,982	10,158,264

The value of investing in a 10 MW ESS is translated into increasing total profits up to 7.7% and the total CVaR by up to 16.2%. Although the combined operation of the WF and the ESS allows decreasing total imbalance costs, these costs increase as the level of risk aversion increases for both configurations (except for the WF configuration when $\beta = 1.0$). This behaviour can be explained by the fact that the recourse actions in the second-stage of the stochastic investment problem were adjusted in order to optimize the expected value of the 5% lowest profit scenarios taking into account the PHA determined day-ahead bids and VaR relating to each source of profit. In other words, the risk-averse WF+ESS operator strategically under delivers on the day-ahead bids in order to adjust the expected profit value in the worst scenarios.

Under the assumed capital costs and maximum values for the power and energy capacities of the ESS and the results of the typical year in assessment, the proposed coordination strategy achieves a ROI ranging between 159% and 184% ($\beta = 0.0$ and $\beta = 1.0$, respectively). Furthermore, the lifetime of 10 years considered for the ESS is significantly higher than the discounted payback period (4.4 years for $\beta = 0$, 4.0 years for $\beta = 0.5$ and $\beta = 1.0$). Note, however, the ESS power capacity is constrained to 10 MW and the assumed capital costs (£109/kW for power capacity and £395/kWh for the energy capacity) can be considered low. On the one hand, this investment becomes unprofitable if the capital costs of the power capacity are 5.62x for $\beta = 0$, 6.32x for $\beta = 0.5$ and 6.49x for $\beta = 1.0$ higher than considered, for the same cost for the energy capacity. On the other hand, for the same cost for the power capacity, this investment becomes unprofitable if the energy capacity costs are 2.28x for $\beta = 0$, 2.5x for $\beta = 0.5$ and 2.52x for $\beta = 1.0$ higher than considered. This suggests that the profitability of the JBS for the WF+ESS

is more sensitive to the power capacity than the energy capacity of the ESS.

The efficient frontier for both configurations is presented in Fig. 5.9 comparing the CVaR and the expected profit (the WF+ESS configuration includes the annuitized investment costs) for the three risk aversion levels. With a risk aversion level of 50%, the CVaR increases 5.96% for the WF configuration and 3.57% for the WF+ESS configuration, while the expected profit is reduced by 2.32% for the former and by 1.34% for the latter when compared to the risk-neutral behaviour. Further increasing the level of risk aversion leads to a 4.60% (WF) and 5.50% (WF+ESS) increase in CVaR, and a reduction of 5.97% (WF) and 5.37% (WF+ESS) for the expected profit. While there is a similar impact on the expected profit compared to Subsection 4.4.1.1 for the WF configuration, the increased impact of the risk aversion level on the value of the CVaR and lower decrease in expected profit in the WF+ESS configuration can be attributed to the additional source of revenue (FR services) and associated uncertainty.

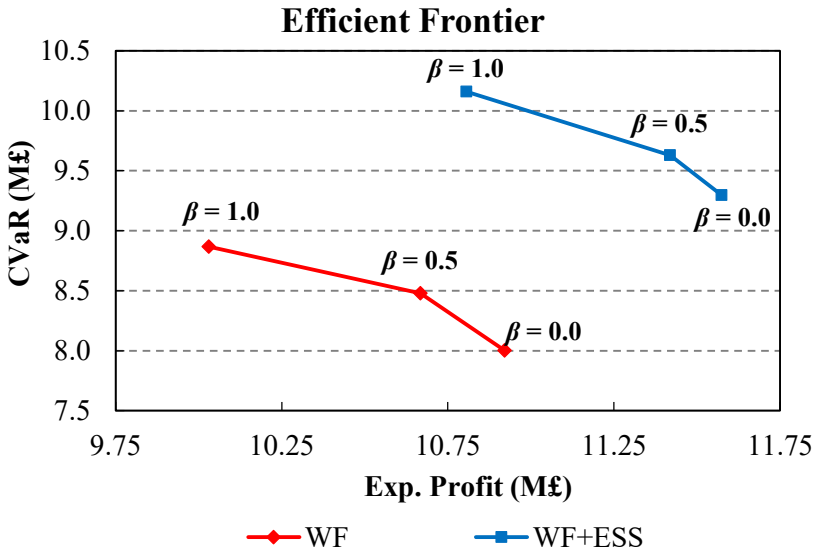


Fig. 5.9: Efficient frontier for the WF only and WF+ESS configurations.

5.6.2 Impact of larger capacities and higher investment costs

In order to assess the benefit of larger capacity ESS for the same 100 MW WF operator, the PHA model was used to solve the risk-neutral investment problem for an ESS with the characteristics of Table 5.9 under the same forecasts as in the previous 270 scenarios case study. Fig. 5.10 compares the expected value for each source of revenue, imbalance costs, investment costs, profit, VaR and CVaR achieved with the WF, WF and 10 MW ESS and 25 MW ESS.

Table 5.9: Technical and Economic Specifications of the larger ESS

Parameter	Unit	Value
Roundtrip Efficiency η	[p.u.]	0.85
Maximum power capacity $\overline{P}$	[MW]	25
Maximum energy capacity $\overline{E}$	[MWh]	125
Power capacity capital cost C^P	[£/kW]	241.93
Energy capacity capital cost C^E	[£/kWh]	568.48

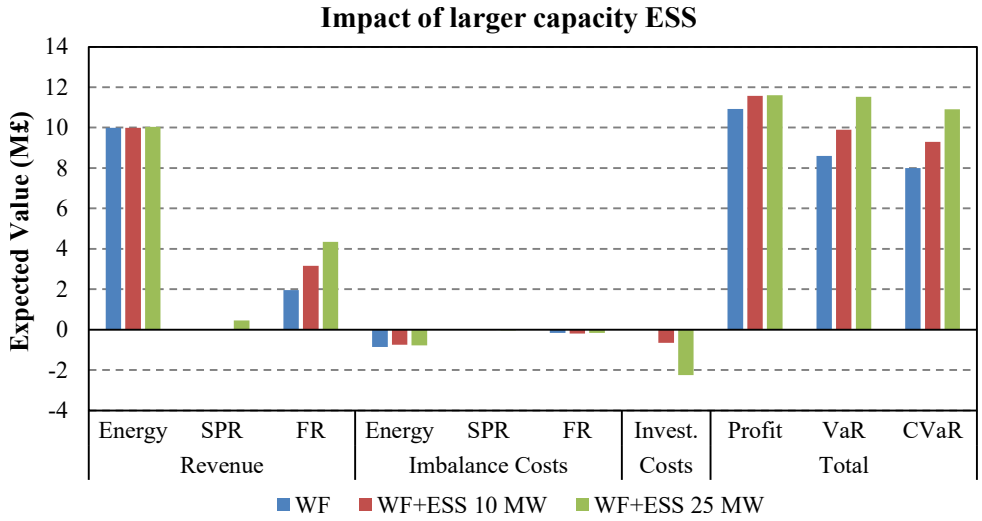


Fig. 5.10: Yearly breakdown of profits, total VaR and CVaR for all three configurations.

The PHA takes 9,898s and 19 iterations to solve the risk-neutral investment problem and determines a 25MW and 20.013MWh ESS. The increased market revenue achieved with the larger ESS is mainly attributed to the increased provision of AS. Despite energy prices being significantly higher than the prices for the provision of SPR and FR services, it is, in fact, more profitable to provide AS than managing wind generation imbalances. Total market revenue is increased by 12.68% and total imbalance costs are increased by 3.84% when comparing the results for both ESS, which shows that, for larger ESS, the provision of AS becomes the main component of its business model and, consequently, reduces the value of the ESS for the WF operator. This conclusion follows similar results presented in Subsection 3.7.5, which showed that the value of the JBS decreases as the capacity of the PHSP increases for lower capacity WF. The main benefit of larger ESS for the risk-averse WF producer is the significant increase in the VaR and CVaR, which are increased by 16.49% and 17.40% respectively, even in the risk-neutral behaviour.

With the higher investment costs, the ROI is reduced to 68.7% and the discounted payback period increases to 7.21 years when compared to the previous case study. In the previous case study, the energy and power capacities of the ESS were fairly close (10MW and 10/~9.9MWh, respectively), the power capacity of the ESS is significantly higher than the energy capacity in this case study. Despite the differences in capital costs between the two case studies, the energy capacity cost is 3.6x higher than power capacity cost for the 10MW ESS, which is higher than the energy-to-power capacity cost ratio for the 25MW ESS (2.4x higher), does not fully explain the observed differences. In fact, this can be explained due to the provision of SPR and (mainly) FR services being a significant part of the business case for the 25MW ESS, the capacity to store large amounts of energy is less valuable than higher charging and discharging power due to the maximum utilization time for FR services (0.5 hours) being lower than model's discretized time step, and due to the reduced role of larger ESS in managing wind generation imbalances.

This case study also finds that the expected market profit difference between the WF+ESS and the WF configurations increases linearly with the sum of the power and energy capacities. The expected market profit difference between both configurations for the 25MW ESS is approximately 2.25x times higher than the expected market profit difference for the 10MW ESS, which correlates with the ratio between the sum of the power and energy capacities for both sized ESS.

5.7 Chapter Conclusions

This chapter proposes a novel two-stage stochastic programming model to solve the ESS investment problem for coordination with a WF under several degrees of risk aversion. The objective function to be maximized considers the trade-off between maximizing yearly profit from the participation of the combined WF-ESS in the day-ahead energy, SPR and FR markets and maximizing the total CVaR (thus minimizing exposure to low profit scenarios), and minimizing the investment costs in order to determine the optimal size of the power and energy capacities of the ESS. While the resulting MILP problem becomes significantly complex to solve under a full year of day-ahead bidding and an acceptable number of scenarios to adequately represent the several sources of uncertainty that the WF-ESS is exposed to, computational tractability is achieved through solving the risk-averse ESS investment and day-ahead bidding model with the PHA decomposition technique.

The performance case studies show that, despite utilizing typical weeks to reduce computational burden, a full stochastic formulation for the risk-averse investment problem is unable to find solutions under adequate execution times. While the Stochastic model solves the risk-neutral investment problem in a few hours for 15 and 30 scenarios, the increased complexity of the risk-averse simulations and considering a higher number of scenarios proves to be too complex to solve under the specified execution time. The PHA, on the other hand, successfully solves the investment problem under all number of scenarios and risk aversion levels considered in the case studies. In fact, when comparing the simulations which both models were able to solve, the PHA reduced the execution times by up to 97.5% when compared to the Stochastic model. The sizeable improvement in computational efficiency achieved by the PHA allows for larger studies with longer time frames (full year representation) and larger numbers of scenarios to be conducted to properly assess the profitability of ESS investments.

The proposed JBS for managing imbalances and providing SPR and FR services is able to achieve profitability under the assumed conditions. Furthermore, the market profits achieved with WF+ESS for the typical year achieve payback periods lower than the assumed (conservative) equipment lifetime. This is a fundamental conclusion considering the incomprehension regarding the impact that managing imbalances and providing AS have on ESS capacity degradation. The inclusion of risk metrics in this investment model presents a fundamental contribution compared to other ESS investment models proposed in literature.

The work presented in this chapter also concluded the evolution of the proposed JBS for WF and ESS to manage generation uncertainty and provide AS in order to maximize the profitability of ESS investments and, thus, provide a solution to the ever-increasing difficult task of integrating renewables. However, the application of coordinated strategies between renewables and ESS is not limited to WF or at the transmission level. The coordination between distributed renewable generation such as rooftop PV and ESS has also been widely proposed in literature. As such, the next chapter provides an operational strategy for coordinating residential energy procurement with distributed flexible resources, such as combined PV and ESS installations, to minimize costs and generate additional revenue from the provision of AS from the ESS.

Chapter 6

Coordinated Residential Energy Trading and Service Provision

The previous chapters have approached the subject of renewables and ESS coordination problem at the transmission level. In recent years, system operators have procured flexibility on the demand side, and pro-active behaviours such as the provision of balancing services are being encouraged.

This chapter looks into the possibility of coordinating distributed residential renewable generation such as PV and household scale battery ESS to minimize energy procurement costs, provide system operators with essential ancillary services and provide peak demand reduction at the distribution network level. The model proposed in this chapter allows households with excess generation to share with other households within the community in a P2P arrangement to minimize supply costs. Furthermore, the provision of FR and reserve services are also considered to be remunerated.

This chapter's structure includes: a nomenclature for the proposed model featured in Section 6.1; a literature review and proposal description is presented in Section 6.2; Section 6.3 featuring the model's mathematical formulation and in-depth explanation; Section 6.4 analyses the benefit of the proposed residential coordinated energy trading and service provision strategy; Section 6.5 concludes this chapter.

6.1 Nomenclature

6.1.1 Indices, Sets and Sub-Sets

$h \in H$	Households
$t \in T$	Time periods.
Ω^{BV}	Set of all binary decision variables.
Ω^{CV}	Set of all continuous decision variables.
$\Omega^{\mathrm{CV}^{+}}$	Set of all positive continuous decision variables.
$\Omega^{\mathrm{CV}^{\mathrm{SOS1}}}$	Set of all positive SOS1 continuous decision variables.

6.1.2 Parameters

π_t^{En}	Household energy tariff for imports from the grid for time period t [£/kWh].

$\pi^{\text{Exp_G}}$ Household energy tariff for exports to the grid [£/kWh].

$\pi^{\text{Imp_H}}$ Household energy tariff for imports from within the community [£/kWh].

$\pi^{\text{Exp_H}}$ Household energy tariff for exports within the community [£/kWh].

π_t^{Rese} Remuneration for the provision of reserve services [£/kW/h].

π_t^{Resp} Remuneration for the provision of FR services [£/kW/h].

π^{Peak} Price for peak power flows at the primary substation [£/kW].

π^{FiT} Feed-in-tariff for PV generation [£/kWh]

$\overline{\text{HD}}_h$ Maximum power capacity for household h [kW].

$\text{HD}_{h,t}$ Power demand for household h and time period t [kW].

$\text{P}_{h,t}^{\text{PV}}$ PV power generation for household h and time period t [p.u.].

$\overline{\text{P}}_h^{\text{PV}}$ PV capacity for household h [kW]

η_h Roundtrip efficiency of the ESS's conversion unit for household h [p.u.].

$\overline{\text{D}}_h^{\text{ESS}}, \overline{\text{C}}_h^{\text{ESS}}$ Maximum discharge and charge power capacities of the ESS in household h [kW].

$\overline{\text{E}}_h^{\text{ESS}}, \underline{\text{E}}_h^{\text{ESS}}$ Maximum and minimum stored energy level of the ESS in household h [kWh].

K^{GRID} Maximum capacity of the primary substation [kW].

τ^{Rese} Maximum duration for delivery of reserve services [h].

τ^{Resp} Maximum duration for delivery of FR services [h].

d Time period duration [h].

M Large number for constraint relaxation.

6.1.3 Binary Variables

$X_{h,t}^{\text{Up}}$ Commitment of upward reserve by the ESS in household h at time period t.

$X_{h,t}^{\text{Dw}}$ Commitment of downward reserve by the ESS in household h at time period t.

6.1.4 Continuous Variables

$Imp_{h,t}^{\text{GRID}}$ Power imports from the supplier for household h and time period t [kW].

$Exp_{h,t}^{\text{GRID}}$ Power exports to the supplier for household h and time period t [kW].

$Imp_{h,t}^{\text{P2P}}$ Power imports from within the community for household h and time period t [kW].

$Exp_{h,t}^{\text{P2P}}$ Power exports to the community for household h and time period t [kW].

$Imp_{h,t}$ Total power imports for household h and time period t [kW].

$Exp_{h,t}$ Total power exports for household h and time period t [kW].

$Imp_{h,t}^{\text{HD}}$ Imported power to supply demand for household h and time period t [kW].

$P_{h,t}^{\text{PV_HD}}$ Power generated from the PV to supply demand for household h and time period t [kW].

$P_{h,t}^{\text{PV_Exp}}$ Power generated from the PV for exports from household h and time period t [kW].

$P_{h,t}^{\text{PV_ESS}}$	Power generated from the PV to charge the ESS for household h and time period t [kW].
$E_{h,t}^{\text{ESS}}$	Stored energy level in the ESS for household h and time period t [kWh]
$P_{h,t}^{\text{ESS}}$	Injected power by the ESS for household h and time period t [kW].
$C_{h,t}^{\text{ESS}}$	Power demand to charge the ESS for household h and time period t [kW].
$D_{h,t}^{\text{ESS}}$	Power generated from discharging the ESS for household h and time period t [kW].
$C_{h,t}^{\text{Imp_ESS}}$	Imported power to charge the ESS for household h and time period t [kW].
$D_{h,t}^{\text{ESS_Exp}}$	Exported power from the discharging of the ESS for household h and time period t [kW].
$D_{h,t}^{\text{ESS_HD}}$	Power generated from discharging the ESS to supply demand for household h and time period t [kW].
$Resp_{h,t}^{\text{Up}}$	Upwards reserve contribution by household h and time period t [kW].
$Resp_{h,t}^{\text{Dw}}$	Downwards reserve contribution by household h and time period t [kW].
$Rese_{h,t}^{\text{Up}}$	Upwards FR contribution by household h and time period t [kW].
$Rese_{h,t}^{\text{Dw}}$	Downwards FR contribution by household h and time period t [kW].
P^{Peak}	Peak power demand at the primary substation [kW].

6.2 Introduction

6.2.1 Literature Review

As previously mentioned, the changing landscape of the electricity industry is also being impacted by the increasing penetration of EV, small-scale rooftop PV and ESS, which are expected to further complicate the already complex and costly balancing of volatile net-demand. However, the increasing penetration of these distributed generation technologies could also be seen as an opportunity to provide flexibility and as a viable option to support system operation.

Recently, network and system operators have been looking into the value of extending the procurement of flexibility to end-users as a viable alternative to capital intensive investments. As such, optimal strategies to manage end-users energy consumption have been proposed in literature [139–143]. Note that [142] analyses the ability of residential ESS to provide flexible consumption strategies by proposing two utility functions: a cost minimization function to achieve a 12% reducing in energy supply costs; and a consumption levelling function that achieves 8% reduction in energy costs and a peak to average ratio close to 1. [143], on the other hand, chooses to model user-comfort demand functions to balance consumer's maximum comfort levels with minimum electricity costs in smart residential buildings.

The coordination of flexible residential resources such as ESS or EV and distributed generation such as rooftop PV is recognized as an opportunity to achieve operational savings, reduce peak demand and minimize grid dependency. Coordinating distributed residential renewable generation with ESS was also studied in [144–146]. Furthermore, coordinating EV charging schedule through a centralized aggregator has also been shown to provide great economic benefits in [147, 148]. Besides the potential of shifting peak demands to off-peak periods, ESS have also been shown to be able to provide balancing services to the system operator in [53, 57, 104, 149]. [57] proposes an alternative operating strategy which, besides

providing a multiple service business model for ESS to maximize stakeholders' revenue by providing energy arbitrage, balancing support and network support, is able to support the local Distribution Network Operator (DNO) by providing corrective support from the ESS instead of allocating sufficient energy to provide preventive support. Similarly [149] devises a coordination strategy with dynamic pricing and provision of network services to the local DNO to minimize supply costs for residential consumers.

Energy trading arrangements for households equipped with PV and ESS have been proposed in [150–152]. The objective of these arrangements is to incentivize low carbon households (households equipped with rooftop PV and ESS) to share with their neighbours with generation capabilities in order to reduce overall grid dependency and electricity consumption bills. [150] makes use of an incentive-based and multi-agent system scheme to reward intra-community energy trading, while [151] proposes a game theoretic approach to determine the optimal intra-community energy trades at prices lower than those practised by their energy supplier so as to minimize transmission costs. Concluding, these papers successfully demonstrate the value of P2P energy trading arrangement in order to supply costs. However, this approach is but a fraction of the flexibility that distributed residential ESS resources can offer to system and network operators and do not consider the provision of balancing and network support services.

6.2.2 Coordinated P2P Energy Trading and Services Provision

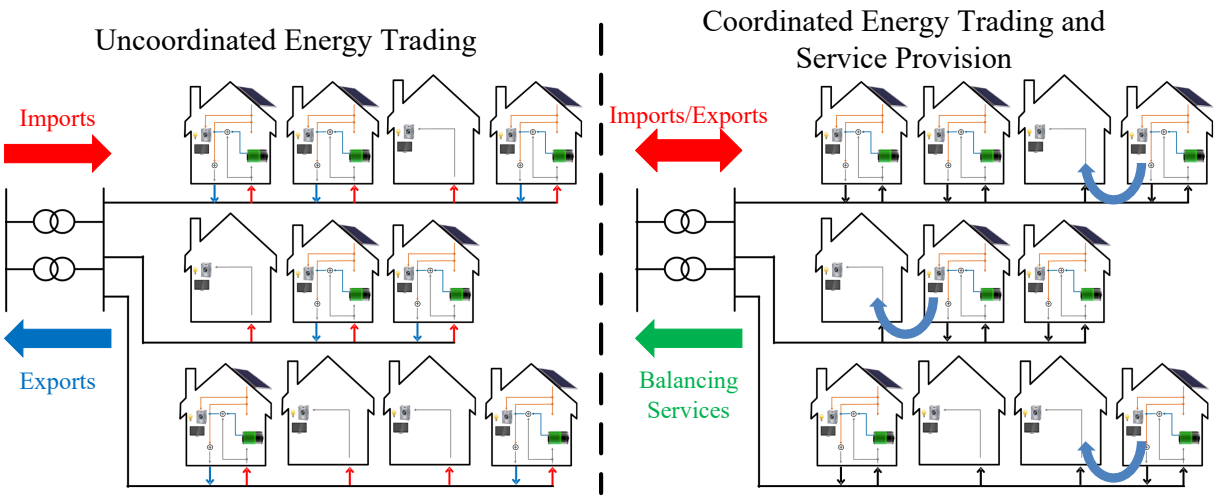


Fig. 6.1: Schematic diagram differentiating the proposed coordinated energy trading and service provision strategy.

Despite the P2P energy trading arrangements that coordinate residential energy consumption and generation in low carbon neighbourhoods having been widely addressed in literature, the provision of ancillary services through coordinated energy trading strategies has not been fully addressed. This chapter proposes a novel coordinated operation strategy for communities with large penetration of low carbon households [153]. The main objective of this strategy is to make use of the flexibility of coordinating renewable generation and ESS to allow the sharing energy resources within the community and to provide services to the DNO and system operator and, consequently, minimize the overall supply costs for the community. A conceptual diagram is presented in Fig. 6.1 in order to demonstrate the differences between the proposed strategy (Coordinated Energy Trading and Service Provision) and a conventional energy trading arrangement (Uncoordinated).

The P2P trading strategy proposed in this chapter allows any given household to procure energy from other households in the same neighbourhood with excess energy resources at prices that are at the same time more advantageous for both parties when compared with the prices practised by energy supplier (energy supply and export prices). Through the effective coordination of PV and ESS resources, it is possible to incentivize self-sufficiency within the community and to provide network and balancing services to the DNO and system operator respectively.

6.3 Coordinated Storage Operation in Low Carbon Communities

6.3.1 Key Properties and Assumptions

The objective of the model proposed in this chapter is to quantify the benefit of a coordinated operation of ESS and low carbon distributed generation at the residential level can bring to the system and network operators. Therefore, it considers a residential community of which a significant proportion of households are equipped with PV and ESS and able to: provide FR and reserve services to the system operator; provide peak demand shaving to the local DNO; minimize electricity supply costs for other households without installed generation technologies.

As with the previous models, FICO^{TM} Xpress [64] was chosen to implement and optimize the resulting MILP problem.

6.3.2 Objective Function

It is assumed that this low-carbon community's objective is to minimize overall energy supply costs and to maximize the revenue from the provision of network and system operators. Objective function (6.1) minimizes the overall energy supply costs of the community from the supplier, which are composed by importing/exporting energy to/from the supplier (1st term of the 1st line), and from the community, resulting from buying/selling energy from/to other households (2nd term of the 1st line). Besides selling excess energy, households with PV and ESS installations are also remunerated on solar generation (2nd term of the 2nd line) and the provision of FR (3rd term of the 2nd line) and reserve services (4th term of the 2nd line) to the system operator. Peak power flows at the primary substation are charged (1st term of the 2nd line) in order to, fundamentally, incentivize the minimization of peak power flows while maximizing the revenues associated with the provision of services to the system operator.

$$\begin{aligned}\underset{\substack{\Omega^{\mathrm{BV}},\Omega^{\mathrm{CV}},\\ \Omega^{\mathrm{CV}^{+}},\Omega^{\mathrm{CV}^{\mathrm{SOS1}}}}}{\text{Minimize}} \Bigg\{ \sum_{h\in H}\sum_{t\in T}\Big[\left(Imp_{h,t}^{\mathrm{GRID}}\pi_{t}^{\mathrm{En}} - Exp_{h,t}^{\mathrm{GRID}}\pi^{\mathrm{Exp_G}}\right) + \left(Imp_{h,t}^{\mathrm{P2P}}\pi^{\mathrm{Imp_H}} - Exp_{h,t}^{\mathrm{P2P}}\pi^{\mathrm{Exp_H}}\right) \\ + P^{\mathrm{Peak}}\pi^{\mathrm{Peak}} - P_{h,t,}^{\mathrm{PV}}\pi^{\mathrm{FiT}} - \left(Resp_{h,t}^{\mathrm{Up}} + Resp_{h,t}^{\mathrm{Dw}}\right)\pi_{t}^{\mathrm{Resp}} - \left(Rese_{h,t}^{\mathrm{Up}} + Rese_{h,t}^{\mathrm{Dw}}\right)\pi_{t}^{\mathrm{Rese}} \Big] d \Bigg\}.\end{aligned} \tag{6.1}$$

6.3.3 Household Constraints

Equalities (6.2) and (6.3) define the total energy imports and exports, respectively, for each household as a combination of energy imports or exports from the supplier and other households. These quantities are limited by each household maximum contracted power capacity in constraints (6.4) and (6.5), which are,

for the sake of simplicity, assumed to be the same for both directions. However, different capacities can be considered in order to limit the level of reverse power flows.

$$Imp_{h,t} = Imp^{\text{GRID}}_{h,t} + Imp^{\text{P2P}}_{h,t}, \quad \forall h,t, \tag{6.2}$$

$$Exp_{h,t} = Exp^{\text{GRID}}_{h,t} + Exp^{\text{P2P}}_{h,t}, \quad \forall h,t, \tag{6.3}$$

$$Imp_{h,t} \leq \overline{\text{HD}}_h, \quad \forall h, \tag{6.4}$$

$$Exp_{h,t} \leq \overline{\text{HD}}_h, \quad \forall h. \tag{6.5}$$

An household's energy imports can be used for supplying domestic demand and for charging the ESS, in the case for households with ESS, as given in equalities (6.6). Similarly, equalities (6.7) define energy exports as a combination of the energy generated by the ESS and the PV which is not used to supply domestic demand.

$$Imp_{h,t} = Imp^{\text{HD}}_{h,t} + C^{\text{Imp_ESS}}_{h,t}, \quad \forall h,t, \tag{6.6}$$

$$Exp_{h,t} = D^{\text{ESS_Exp}}_{h,t} + P^{\text{PV_Exp}}_{h,t}, \quad \forall h,t. \tag{6.7}$$

Households' domestic demand can be supplied by discharging the ESS, PV production and from energy imports as illustrated by equalities (6.8). Note that, the imported energy destined to supply domestic demand can be met by the energy supplier and/or other neighbours. These equalities also show that it is also possible for a given household's domestic demand to be exclusively met by the PV and ESS, allowing it to become self-sufficient in terms of electrical energy needs.

$$\text{HD}_{h,t} = D^{\text{ESS_HD}}_{h,t} + P^{\text{PV_HD}}_{h,t} + Imp^{\text{HD}}_{h,t}, \quad \forall h,t. \tag{6.8}$$

Lastly, energy generated by the PV in each household can be used for charging the ESS, supply domestic demand or exported to the energy supplier or other households in (6.9).

$$\text{P}^{\text{PV}}_{h,t}\,\overline{\text{P}}^{\text{PV}}_{h} = P^{\text{PV_ESS}}_{h,t} + P^{\text{PV_HD}}_{h,t} + P^{\text{PV_Exp}}_{h,t}, \quad \forall h,t. \tag{6.9}$$

6.3.4 ESS Operational Constraints

The charging and discharging actions of the ESS are modelled with equalities (6.10) that define the injected power by the ESS, while charging and discharging power is limited by constraints (6.11) and (6.12). Note that this formulation excludes the use of binary variables to prevent simultaneous charging and discharging actions and assumes a SOS1 variable set for $D^{\text{ESS}}_{h,t}$ and $C^{\text{ESS}}_{h,t}$ in the same line of the previous models.

$$P^{\text{ESS}}_{h,t} = D^{\text{ESS}}_{h,t} - C^{\text{ESS}}_{h,t}, \quad \forall h,t, \tag{6.10}$$

$$C^{\text{ESS}}_{h,t} \leq \overline{\text{C}}^{\text{ESS}}_{h}, \quad \forall h,t. \tag{6.11}$$

$$D^{\text{ESS}}_{h,t} \leq \overline{\text{D}}^{\text{ESS}}_{h}, \quad \forall h,t. \tag{6.12}$$

Stored energy levels in the ESS are updated for each household and time period in equalities (6.13) and are limited by minimum and maximum values in constraints (6.14). Note that these values can

be user-defined to constrain the range of operation of the ESS and, consequently, mitigate capacity degradation.

$$E_{h,t}^{\mathrm{ESS}} = E_{h,t-1}^{\mathrm{ESS}} + \left(C_{h,t}^{\mathrm{ESS}}\eta_h - D_{h,t}^{\mathrm{ESS}}\right)d, \quad \forall h,t, \tag{6.13}$$

$$\underline{\mathrm{E}}_h^{\mathrm{ESS}} \leq E_{h,t}^{\mathrm{ESS}} \leq \overline{\mathrm{E}}_h^{\mathrm{ESS}}, \quad \forall h,t. \tag{6.14}$$

The charging of the ESS can be achieved through a combination of energy imports and PV generation in (6.15). Similarly, (6.16) allows for the energy discharged by the ESS to be used to supply domestic demand and to export to the energy supplier or other households.

$$C_{h,t}^{\mathrm{ESS}} = C_{h,t}^{\mathrm{Imp_ESS}} + P_{h,t}^{\mathrm{PV_ESS}}, \quad \forall h,t, \tag{6.15}$$

$$D_{h,t}^{\mathrm{ESS}} = D_{h,t}^{\mathrm{ESS_HD}} + D_{h,t}^{\mathrm{ESS_Exp}}, \quad \forall h,t. \tag{6.16}$$

6.3.5 Services Constraints

As studied in the previous chapters and literature, ESS are able to provide frequency regulation services to system operators in the form of FR and reserve services. As one of the objectives of this model is to quantify the value that distributed residential ESS can bring by providing these services, constraints (6.17) limit the provision of upwards services (increasing injected power) by the maximum discharge capacity, while constraints (6.18) limit the provision of downwards services (decreasing injected power) to the maximum charging capacity.

$$P_{h,t}^{\mathrm{ESS}} + Resp_{h,t}^{\mathrm{Up}} + Rese_{h,t}^{\mathrm{Up}} \leq \overline{\mathrm{D}}_h^{\mathrm{ESS}}, \quad \forall h,t, \tag{6.17}$$

$$P_{h,t}^{\mathrm{ESS}} - Resp_{h,t}^{\mathrm{Dw}} - Rese_{h,t}^{\mathrm{Dw}} \geq -\overline{\mathrm{C}}_h^{\mathrm{ESS}}, \quad \forall h,t. \tag{6.18}$$

The provision of these services is also limited by the level of stored energy in the ESS. As such, sufficient energy must be stored in order to provide each service for the longest time for service delivery (τ^{Resp} and τ^{Rese}). The model ensures this with constraints (6.19) and (6.20) for the provision of FR services, and with constraints (6.21) and (6.22) for reserve services.

$$\underline{\mathrm{E}}_h^{\mathrm{ESS}} \leq E_{h,t-1}^{\mathrm{ESS}} - \left(P_{h,t}^{\mathrm{ESS}} + Resp_{h,t}^{\mathrm{Up}}\right)\tau^{\mathrm{Resp}} \leq \overline{\mathrm{E}}_h^{\mathrm{ESS}}, \quad \forall h,t, \tag{6.19}$$

$$\underline{\mathrm{E}}_h^{\mathrm{ESS}} \leq E_{h,t-1}^{\mathrm{ESS}} - \left(P_{h,t}^{\mathrm{ESS}} - Resp_{h,t}^{\mathrm{Dw}}\right)\tau^{\mathrm{Resp}} \leq \overline{\mathrm{E}}_h^{\mathrm{ESS}}, \quad \forall h,t, \tag{6.20}$$

$$\underline{\mathrm{E}}_h^{\mathrm{ESS}} - \mathrm{M}\left(1 - X_{h,t}^{\mathrm{Up}}\right) \leq E_{h,t-1}^{\mathrm{ESS}} - \left(P_{h,t}^{\mathrm{ESS}} + Rese_{h,t}^{\mathrm{Up}}\right)\tau^{\mathrm{Rese}} \leq \overline{\mathrm{E}}_h^{\mathrm{ESS}} + \mathrm{M}\left(1 - X_{h,t}^{\mathrm{Up}}\right), \quad \forall h,t, \tag{6.21}$$

$$\underline{\mathrm{E}}_h^{\mathrm{ESS}} - \mathrm{M}\left(1 - X_{h,t}^{\mathrm{Dw}}\right) \leq E_{h,t-1}^{\mathrm{ESS}} - \left(P_{h,t}^{\mathrm{ESS}} - Rese_{h,t}^{\mathrm{Dw}}\right)\tau^{\mathrm{Rese}} \leq \overline{\mathrm{E}}_h^{\mathrm{ESS}} + \mathrm{M}\left(1 - X_{h,t}^{\mathrm{Dw}}\right), \quad \forall h,t. \tag{6.22}$$

It is assumed that τ^{Rese} is larger than both the model's discretized time step (d) and τ^{Resp}. For this reason, ensuring sufficient stored energy for the provision of reserve requires the disjunctive constraints and binary variables (for further explanation, please refer to constraints (2.22) to (2.25) and corresponding description in Subsection 2.3.3.2). The robustness of this model can be further increased by modelling another set of constraints similar to (6.19)-(6.22), in which the ESS energy levels for period

$t-1$ $\left(E^{\text{ESS}}_{h,t-1}\right)$ should be substituted by energy levels for period t $\left(E^{\text{ESS}}_{h,t}\right)$. Essentially, this ensures sufficient energy is stored for cases when the provision of services is activated between the beginning $(t-1)$ and the end (t) of the time period.

6.3.6 Network Constraints

Lastly, another potential benefit of coordinated distributed ESS is to support the deferment of network reinforcement and, consequently, support network operators. In the context of this model, this can be achieved by modelling a set of constraints to provide peak demanding shaving.

Constraints (6.23) and (6.24) are used to determine the maximum power flow in both directions. The former set of constraints captures daily peak demand composed of the sum of the households' demands and the provision of downwards frequency regulation services, as these may contribute to increase of peak demand. On the other hand, the latter set of constraints captures the peak power flow associated the community's energy export to the grid and the provision of upwards frequency regulation services, which may result in increasing power exported to the distribution network. The inclusion of the variable P^{Peak} in objective function (6.1) allows capturing the flexibility offered by coordinating the operation of several ESS and provide peak demand reduction. Power flows and the provision of frequency regulation services in both directions must also be constrained by the primary substation's capacity in (6.25) and (6.26).

$$\sum_{h\in H}\left(Imp^{\text{GRID}}_{h,t}+Resp^{\text{Dw}}_{h,t}+Rese^{\text{Dw}}_{h,t}\right)\leq P^{\text{Peak}},\quad \forall t, \tag{6.23}$$

$$\sum_{h\in H}\left(Exp^{\text{GRID}}_{h,t}+Resp^{\text{Up}}_{h,t}+Rese^{\text{Up}}_{h,t}\right)\leq P^{\text{Peak}},\quad \forall t, \tag{6.24}$$

$$\sum_{h\in H}\left(Imp^{\text{GRID}}_{h,t}+Resp^{\text{Dw}}_{h,t}+Rese^{\text{Dw}}_{h,t}\right)\leq \text{K}^{\text{GRID}},\quad \forall t, \tag{6.25}$$

$$\sum_{h\in H}\left(Exp^{\text{GRID}}_{h,t}+Resp^{\text{Dw}}_{h,t}+Rese^{\text{Dw}}_{h,t}\right)\leq \text{K}^{\text{GRID}},\quad \forall t. \tag{6.26}$$

In order to consider the possibility of households sharing energy amongst each others, constraints (6.27) are included to equalize the total volume of imported and exported energy within the community. It should be noted that network losses are not considered and that these constraints are a model approximation.

$$\sum_{h\in H}Imp^{\text{P2P}}_{h,t}=\sum_{h\in H}Exp^{\text{P2P}}_{h,t},\quad \forall h,t. \tag{6.27}$$

6.4 Case Studies

6.4.1 Input Data for UK studies

A residential community comprising of 100 households, of which 50% are equipped with rooftop PV and ESS with the specifications in Table 6.1, are analysed in order to quantify the value of coordinating P2P energy trading and to provide services to the network and system operators for a week (168 hourly time periods). Energy imports from the energy supplier are tariffed through an Economy-7 scheme for all households. Consequently, energy bought during off-peak hours (1h - 8h) is priced at £0.07/kWh and priced at £0.14/kWh during peak hours (9h - 24h). Exports sold to the energy supplier are priced at

£0.05/kWh, while energy traded within the community (P2P trading) is priced at £0.06/kWh for households exporting and at £0.061/kWh for households importing. PV generation is remunerated by a FiT of £0.04/kWh. The provision of frequency regulation services is incentivized by remunerating reserve at £0.006/kW/h, while FR is remunerated at £0.008/kW/h. The maximum time duration for the utilization of reserve services is assumed to be 2 hours and 0.5 hours for FR services. Peak power flows at the primary substation are priced at £0.30/kW to incentivize the minimization of energy imports/exports and, consequently, reduce peak demand. Each household's contracted power capacity and the primary substations capacity are appropriately sized for the community's energy needs.

Table 6.1: ESS and PV Capacities and level of penetration

Household Type	$\overline{D}_h^{ESS}/\overline{C}_h^{ESS}$ [kW]	$\overline{E}_h^{ESS}$ [kWh]	η_h [p.u.]	$\overline{P}_h^{PV}$ [kW]	Penetration [%]
A	2.0	2.0	0.9	2.0	15
B	3.0	3.0	0.9	3.0	25
C	4.0	4.0	0.9	4.0	10

The households considered for this community follow two demand profiles (economic and comfort) and peak domestic demands range from 0.8 kW and 1.2 kW so as to model different consumer needs of typical UK consumers. The number of households for each domestic demands peak value and profile are presented in Table 6.2 and in Fig. 6.2, respectively. Lastly, it is assumed that solar exposure is evenly spread throughout the community and is presented in Fig. 6.3, which was taken from real data in the UK.

Table 6.2: Distribution of the number households for each demand profile

Peak Demand [kW]	0.7	0.8	0.9	1.0	1.1	1.2
Economy [#]	9	18	9	9	0	0
Confort [#]	0	9	18	9	9	10

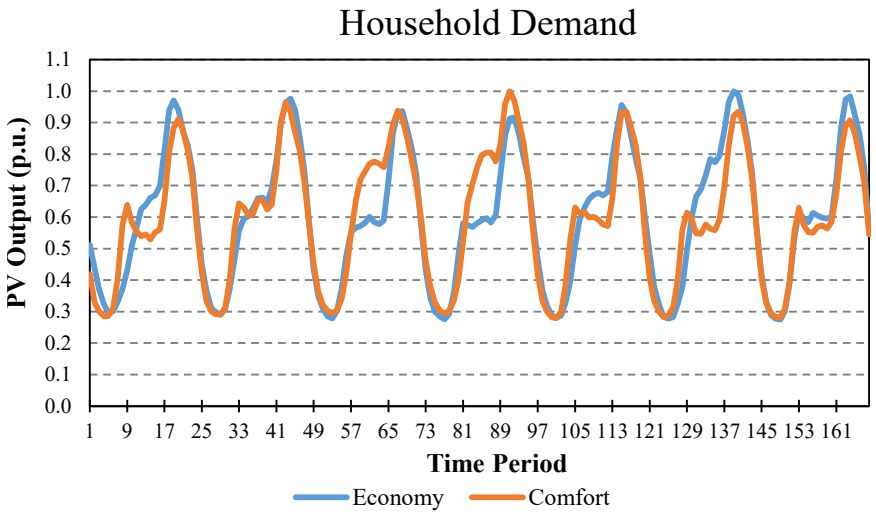


Fig. 6.2: WF profit distribution when exposed to uncertainty for all days.

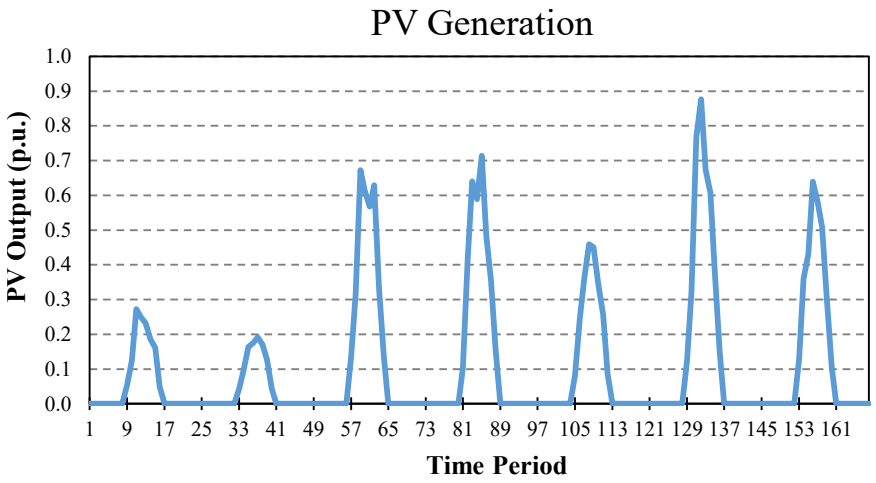


Fig. 6.3: Rooftop PV profile for the considered week.

6.4.2 The Value of Coordinating Residential ESS Operation

The case study aims to quantify the value of a coordinated energy trading and service provision strategy for multiple households in a low carbon community. To achieve this objective, the study analyses three different operating strategies: Uncoordinated, in which all household's trade exclusively with their energy supplier; Coordinated, which allows households to procure energy from their neighbours in a P2P trading arrangement; and Coordinated & Services, which expands the previous strategy by providing frequency regulation and network services. The aggregated revenues and costs for the community under analysis for the three strategies are presented in Fig. 6.4.

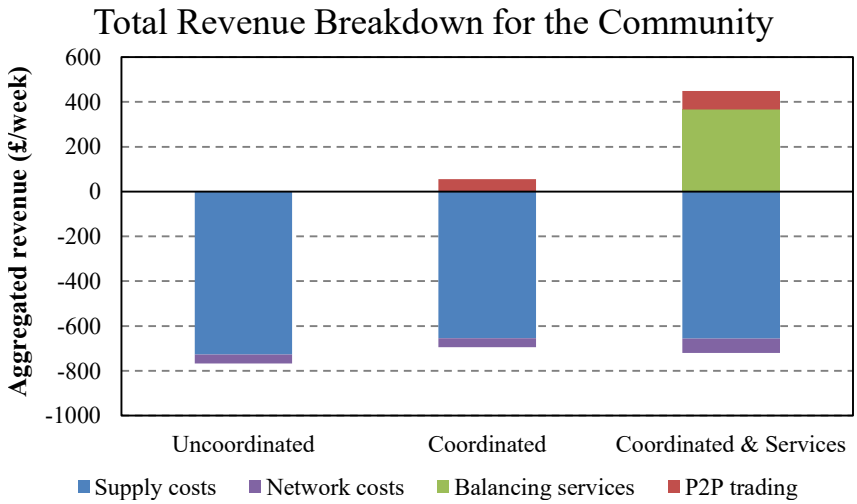


Fig. 6.4: Breakdown of costs and revenues for the community across all operating strategies.

The results conclude that the Coordinated strategy lowers the energy supply costs for the whole community, which can be explained due to the synergies between the ESS and PV generation. In other words, the ESS allow storing excess PV generation for export during peak demand periods to households without generation technologies. Furthermore, the provision balancing services in the third strategy results in the increase of the energy traded between households as ESS resources are optimized for service provision, in contrast to the Coordinated strategy. Another key finding from the presented results is that peak power flows at the primary substation increase (consequently increased network costs) due to the provision of balancing services. This can be explained due to the value of providing these services

being significantly larger than reducing peak demand at the substation. Nonetheless, the volume of energy traded at the primary substation is reduced, despite the increase in peak power flows.

Fig. 6.5 presents the overall value of the Coordinated & Services strategy over the Uncoordinated strategy for a year and each household. It should be noted that the value of this strategy is also dependent on the penetration of low carbon households which is investigated in the following case study.

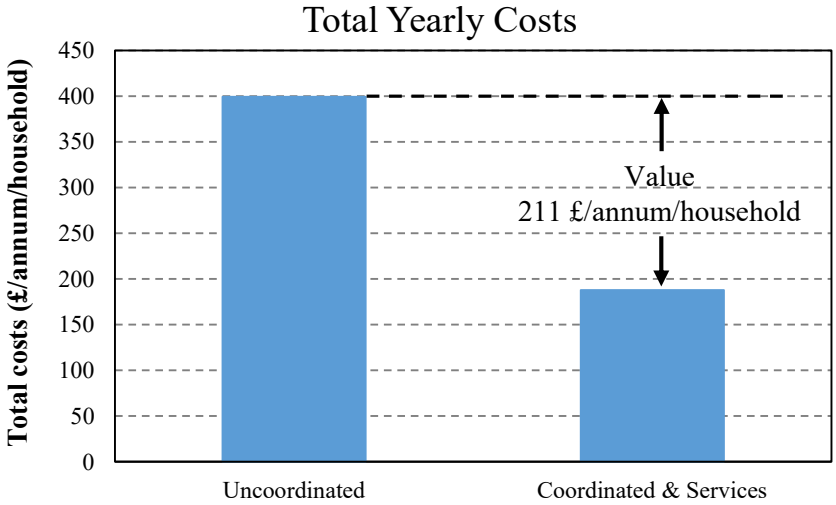


Fig. 6.5: Yearly value of the Coordinated & Services Strategy.

6.4.3 Influence of different PV and ESS Penetration levels

In order to understand how the value of the Coordinated & Services strategies is dependent of the penetration of households with PV and ESS installations, this case study compares the community's total costs in the Coordinated & Services and the Uncoordinated strategy for different penetrations of low carbon households. The results are plotted in Fig. 6.6 which present the value of the Coordinated & Services strategy over the Uncoordinated strategy for different penetrations of ESS and PV.

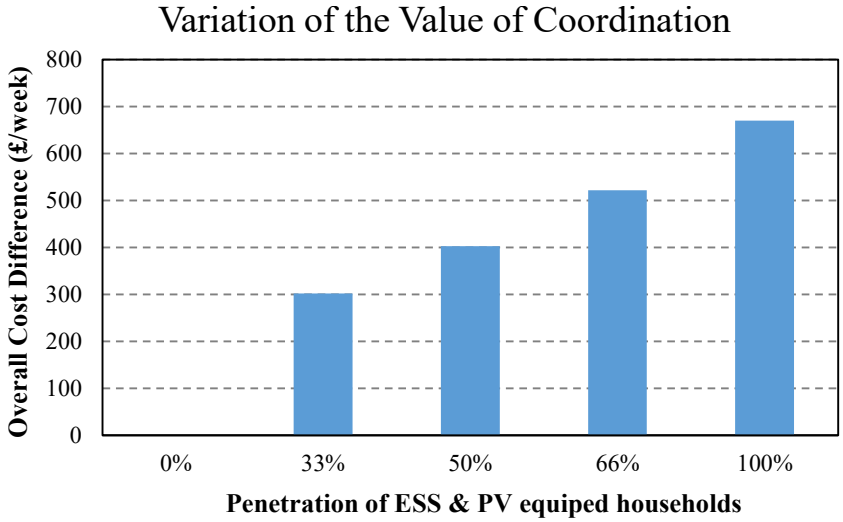


Fig. 6.6: Value of the Coordinated & Services Strategy depending on the ESS and PV penetration.

This case study's results show that significant cost reductions can be achieved even with 33% penetration and can potentially achieve values of up to £700/week with 100% penetration. In the case of a low carbon community in which all households are equipped with PV and ESS, the Coordinated & Services allows for an operational profit of up £303/week to be achieved.

6.5 Chapter Conclusions

This chapter proposes a coordinated P2P energy trading and service provision strategy for low carbon communities by making use of the flexibility provided by PV and ESS equipped households. This research highlights the effective capability of distributed residential generation technologies to reduce grid dependency and share energy among households in order to reduce energy supply costs. Furthermore, the results also show that the provision of flexibility in the form of FR and reserve services can be extremely beneficial for consumers, as the associated revenues can potentially exceed energy supply costs.

On the one hand, when considering only P2P energy trading within the community (in the Coordinated strategy), the ESS are mainly used in order to store excess PV generation for later utilization during evening periods. On the other hand, the provision of balancing services fundamentally changes the operation of the ESS in order to maximize the revenues associated with the provision of FR and reserve services in the Coordinated & Services strategy. Furthermore, excess PV generation is used to export energy to other neighbours.

Lastly, the results can be clearly used to support a self-sufficiency business case for low carbon communities and also to provide flexibility to the system operator.

Chapter 7

Conclusion and Future Work

This Chapter presents the conclusions and future work derived from the work carried out in this PhD, starting by the main conclusions of each chapter considering the research questions in Chapter 1, as well as a summary of this research's proposals and contributions. This is followed by recommendations for future work in Section 7.2 to expand upon the proposed coordination strategies detailed in this Thesis.

7.1 Conclusions

The objective of achieving the significant carbon emissions reduction, which has been agreed upon by many governments worldwide in order to tackle climate change is drastically changing the electricity industry landscape and bringing a set of new and complex challenges at multiple levels. The decommissioning of old and carbon-intensive thermal generation in favour of inflexible carbon-free generation, such as nuclear generation, and intermittent renewables has aggravated balancing demand and supply in a cost-effective manner due to the variable, uncertain and seasonal patterns of renewable generation. In order to ensure security of supply in the face of increased variability and uncertainty, larger volumes of operational reserve and flexibility sources are needed. Although renewable generation can provide some degree of flexibility by curtailing excess generation, this option is seen as undesirable as it translates into the loss of cheap carbon-free generation and in the reduction of the efficiency of renewable investments.

ESS have been shown to reliably provide flexibility to the different sectors of the electricity industry and are considered as a key technology for facilitating the large-scale integration of renewables. The widespread deployment of ESS is, however, hindered by the lack of regulation and long-term signalling and the subsequent risk of recovering capital investment. Thus, system operators and renewable producers are faced with procuring a cost-effective solution to reduce uncertainty and flexibility services.

In order to provide an efficient and profitable business strategy to manage renewables uncertainty, improve the role of ESS in integrating renewables and provide system operators with flexibility solutions, this research proposes a novel two-stage stochastic ESS investment and operational model for coordination with risk-averse wind producers. The investment part of the model focuses on determining the optimal power and energy capacities of the ESS in order to minimize capital costs for the WF operator. The operational part of the model focuses on coordinating the WF and ESS operation in order to determine the optimal day-ahead bidding strategy in the energy and AS markets with the objective of maximizing total profit (revenue from provision of energy and services) and minimize imbalance costs related with generation uncertainty under a certain level of risk aversion.

This Thesis presents the proposed model by first constructing the coordinated bidding strategy for WF and ESS. While Chapter 2 presents a deterministic business model for uncoordinated ESS and WF, this approach is shown to be insufficient to handle wind power availability and pricing uncertainty in terms of profit outcomes due to the lack of optimization against uncertainty. Furthermore, being able to anticipate potential wind imbalances is a fundamental aspect of a combined ESS and WF business model. As such, using two-stage stochastic programming, the JBS presented in Chapter 3, despite only considering the management of wind generation imbalances and the provision of SPR, is able to achieve significant profit increases compared to when both facilities operate independently. Considering the uncertain nature of renewables and prices in markets with a large share of intermittent generation, minimizing the exposure to low profit outcomes is fundamental for renewable producers. With this objective, the JBS proposed in Chapter 3 is reformulated to allow the consideration of several degrees of risk aversion and maximizing the total profit CVaR in order to considerably reduce the risk exposure and increase the benefit of the proposed JBS in Chapter 4.

The final upgrade of the model was the extension of the assessment horizon to a full year and provision of FR services on top of SPR in order to assess the profitability of an ESS investment for a risk-averse WF operator in Chapter 5. Due to the consideration of multiple sources of uncertainty (energy, SPR and FR pricing and wind power availability), the longer assessment horizon and the increased complexity of risk-averse problems, the resulting stochastic MILP model becomes too large to solve to optimality under reasonable execution times.The decomposition technique PHA is used to reformulate the original problem into smaller, easier to solve, scenario-specific sub-problems by relaxing the non-anticipativity conditions. These are, in turn, reintroduced iteratively in order to move the scenario-specific solutions for the decision variables towards a common value for all scenarios. Problems which feature risk measures, however, complicate the application of decomposition techniques such as the PHA due to requiring the separability of the objective function, i.e. the expected profit is easily separable whereas the CVaR requires information of the tail-end of the profit distribution. In order to apply the PHA, additional decision variables that need to converge to single value are introduced and relate directly to the VaR. This work's main contribution and novelty is the successful development of an ESS investment and coordinated operational model for WF operators that is computationally efficient due to the application of the PHA to solve risk-averse large-scale problems.

Finaly, Chapter 6 investigated the value of coordinating distributed renewables and ESS in low-carbon residential communities. The proposed model is able to coordinate the PV and ESS operation to minimize a community's energy procurement costs by sharing excess available generation and to provide flexibility services to the system operator in the form of reserve and FR. This type of coordination strategy has the potential of significantly reducing energy costs and provides evidence for the business case for low-carbon communities with distributed generation technologies.

7.1.1 Response to the research questions

Q1: How to maximize the value of an ESS in facilitating an efficient integration of variable renewable generation and minimize the impacts of intermittent generation uncertainty? How can uncertainty be reduced and revenue maximized?

Chapter 3 proposes a novel two-stage stochastic MILP model that allows a WF to improve energy and SPR market participation with the support of an ESS. In other words, the model determines the op-

timal day-ahead Energy and SPR-Up/SPR-Dw bids for the WF to submit to the respective markets and optimizes the recourse actions with the support of the ESS to minimize costs associated with settling deviations between real-time delivery of energy and SPR and the submitted day-ahead bids. Modelling-wise, the proposed JBS takes into account the unique operational characteristics of ESS (two modes of operation and energy constrained resource) that directly impact this technology's ability to manage wind uncertainty and provide AS. One of the main aspects to consider in providing AS, besides managing imbalances, is to ensure that sufficient energy is stored to fully provide the committed SPR services during the entire commitment period due to these being determined without knowing the level of utilization ahead of real-time. Furthermore, the proposed JBS is applied to a mature technology such as a PHSP, in order to understand the benefits and limitations of this strategy given the characteristics of a different type of ESS. The presence of pump-turbine units affected by SU and SD events in the PHSP complicate, not only, the ability to manage generation uncertainty, but also in the provision of SPR due to the presence of additional costs of SU offline units and SD online units.

The case studies in this chapter draw the following conclusions:

- Section 3.6 provides evidence of the value of coordinating ESS and WF, as the proposed JBS is able to achieve a significant benefit when comparing to both facilities operating independently. Such benefit is translated into higher profits (£3,038/day which translates into an overall profit increase of 4% for the three days) and lower offering uncertainty (the AVG of the energy imbalances was reduced by an average of 34.3% of the three days, resulting in a reduction of 26% in total imbalance costs). The provision of SPR is shown to increase profits by 21.7% over the 3 days when compared to only managing wind generation imbalances. This benefit is increased when compared to the independent operation of both facilities in both markets, as with the JBS it is possible to cover minimum provision levels in time periods where it was not possible in the UBS.

- Testing the proposed JBS for PHSP has yielded similar benefits for the WF operator, albeit at slightly different levels in Section 3.7. With higher penalties for the negative deviations between the day-ahead bids and scenario realizations, the JBS achieves higher profit increases (ranging between 4.2% and 21.1%) and greater reductions in imbalance costs (ranging between 30.4% and 78.4%). Despite the increased benefit, it is worth mentioning that the provision of SPR contributes to a reduction in the benefit of the JBS over the UBS when compared to the energy only market participation. This is due to the fact that under higher penalties for deviations, the provision of SPR is not as attractive as managing uncertainty (Subsection 3.7.2).

- The case studies presented in Subsection 3.7.3.1 help showing the benefit of modelling SU and SD costs for SPR provision in order to make more informed decisions. It is also demonstrated how VS pump-turbine units are better suited for managing uncertainty and providing SPR than FS units in Subsection 3.7.3.2 and the ability of the JBS in storing wind generation that would need to be curtailed due to constraints in the transmission system is studied in Subsection 3.7.4. Finally, Subsection 3.7.5 analyses how the value of the JBS decreases as the power and energy capacities of the PHSP increase for the same WF capacity .

- Lastly, the value of the JBS over the UBS can be impacted by a number of factors. The case studies provide evidence that the benefit of the JBS is not only impacted by the quality of the prices and

wind power availability forecasts and the value of the imbalance penalty factors, but also by the pattern and variability of the wind power forecasts.

Q2: How can the exposure to risk of experiencing low profits be mitigated through the operation of combined WF-ESS facilities in the day-ahead markets? Does the mitigation of the probability of experiencing low profits interfere with ESS's ability to manage wind generation uncertainty?

A new formulation of the proposed coordinated energy and SPR provision strategy for WF and ESS is presented in Chapter 4 to consider different levels of risk aversion when maximizing the expected daily profit and minimizing risk exposure. In order to minimize exposure to low profit outcomes of the combined WF-ESS, the CVaR risk measure was introduced in the model proposed in Chapter 3. The objective function of the model becomes a trade-off between maximizing expected profit and minimizing risk under a considered risk aversion level, which fundamentally allows quantifying the advantages and disadvantages (in terms of expected profit and total profit CVaR) of minimizing risk. Fundamentally, this allows a risk-averse WF operator to optimize bidding strategies with the support of ESS and determine a risk aversion level that optimizes the scenarios where profit is lower without adopting excessively conservative strategies.

Analysing the impact of optimizing risk-averse bidding strategies in Section 4.4 lead the following conclusions:

- Subsection 4.4.1 shows that considering a confidence level of 95%, a full risk-averse behaviour (only the profit CVaR is maximized) manages to significantly decrease the dispersion of the daily profit distributions. For the UBS, this translates into increasing the minimum profit by 10%, the CVaR by 7.7% and reducing the profit STD deviation by 85.6%, at the expense of reducing expected profit by 21.8% and the maximum profit by 37.9% averaging the three days. In this regard, the value of the JBS over the UBS is clearly increased, as the minimum profit and CVaR are increased by 13% and 11.5%, respectively, the profit STD is reduced by 71.1% at the expense of reducing the expected and maximum profit by 17.9% and 31.4%, respectively. The likeliest profit intervals are also shown to be approximately 6.5% higher in the JBS than in the UBS and with higher probabilities (average of 73.3% for the JBS and 68.8% for the UBS).

- Through the efficient frontiers shown in Figs. 4.3, 4.5 and 4.7, it is possible to understand that full risk-averse bidding strategies lead to overly conservative results. When the level of risk aversion β increases from 0.9 to 1, for all days and considered strategies, the small increase in CVaR is met with a substantial reduction in expected profit (although the STD is greatly reduced as well). Averaging the results in the 3 days for $\beta = 0.9$, the CVaR increases by 10.3% for the UBS and by 11.1% for the JBS, while the expected profit is reduced by 2.8% for the UBS and 4.1% for the JBS when compared to the risk-neutral results. For $\beta = 1$, the CVaR increases by 0.3% for the UBS and by 0.1% for the JBS, while the expected profit is reduced by 19.1% for the UBS and 13.7% for the JBS when compared to the results when $\beta = 0.9$. Thus it is possible to conclude that, despite the increased profit STD, a risk aversion level of 90% yields better economic results than full risk-averse bidding behaviour.

- Subsection 4.4.2 analyses the impact of risk aversion on the JBS' ability to manage wind power uncertainty. This case study shows that by maximizing CVaR in the full risk-averse bidding behaviours leads to optimizing the recourse actions for each scenario in order to increase the value

of 5% lowest profit scenarios. In other words, the JBS determines day-ahead bids and recourse actions that lead to negative imbalances (energy shortages) being reduced at the expense of causing positive imbalances (energy surplus) which leads to a reduction of the value of the highest profit scenarios. Note that this also translates into reduced day-ahead market revenue. Risk-averse bidding also leads to an overall better management of the imbalances, as the reduction in its AVG by the JBS varies between 52.1% and 63.8%, whereas for the risk-neutral behaviour, the AVG was reduced between 21.4% and 48.5%.

Q3: Is it economically feasible for a risk-averse wind producer to invest in an ESS in order minimize the impact of uncertainty and to provide ancillary services? How can the benefits of wind-ESS coordination be efficiently modelled for long-term horizons and maximized for recovery of investment costs?

The topic of investigating the profitability of ESS business models has been widely addressed in literature. While some works approach this problem from an ESS-centric perspective and seek to maximize profit by combining optimal operation and siting, Chapter 5 approaches the ESS investment problem from the perspective of a risk-averse WF operator. The objective is to determine the optimal power and energy capacities of the ESS and optimal day-ahead JBS that maximize the expected profit in a typical year, composed of the revenue generated from participating in the day-ahead energy, SPR and FR markets, minus the annuitized investment costs. Unlike ESS investment models currently proposed in literature, minimization of exposure to low profit outcomes is actively considered in the model's objective function by means of trading-off the maximization of the expected profit and the maximization of the total CVaR for a given level of risk aversion.

The risk-averse ESS investment problem is formulated as a two-stage stochastic MILP which considers four sources of uncertainty: energy, SPR and FR prices and wind power availability. Considering the long-term assessment horizon and the number of scenarios needed to accurately represent uncertainty, achieving tractability is a complex task. One of the most common techniques to reduce problem size is to characterize the typical year through a set of typical weeks. Although problem size is greatly reduced, solving stochastic investment models for an adequate number of scenarios is impractical due to the resulting long execution times. This chapter proposes a model which combines the characterization of the typical year through representative weeks and the PHA decomposition technique in order to achieve computational efficiency.

The case studies analysed in Sections 5.5 and 5.6 lead to the following conclusions:

- The Stochastic model is able to solve the risk-neutral investment problem with 5 typical weeks, 15 and 30 scenarios under a day's worth of simulation time in Section 5.5. However, the corresponding increase in execution time due to the consideration of a higher number of scenarios and increased risk aversion severely hinder the applicability of complete stochastic formulations, as the execution time becomes longer than a day and the investment problem becomes intractable for full risk-averse simulations with 30 scenarios and at any risk aversion level with 270 scenarios. By decomposing the stochastic problem with the PHA, besides greatly reducing execution times when compared to the complete stochastic model (from 8.5x up to 41x shorter execution times), it is possible to solve the ESS investment problem for all levels of risk aversion considering all sources of uncertainty.

- Even though the optimization of CVaR complicates the application of decomposition techniques due to the lack of separability of the risk measure, the proposed model is able to successfully

solve the ESS investment problem under increased levels of risk aversion, albeit with additional iterations and increased computational efforts required per iteration. This can be explained by the fact that the wide dispersion in the solutions for the scenario-specific VaR in the algorithm's first solution greatly complicates these variables' convergence towards a single value for all scenarios The speed of convergence can be accelerated by increasing the value of the penalty factors for each source of profit VaR. This option, however, may lead to convergence to values for the corresponding VaR that result in divergence of the first-stage variables or, in the case of the model converging, the determined values for the first-stage variables lead to infeasibility in the second run of the model to determine the value for the recourse actions.

- The case study presented in Subsection 5.6.1 analyses the profitability of the investment in a 10MW ESS for three levels of risk aversion and 270 scenarios. The results show that total profits are increased between 6.0% ($\beta = 0.0$) and 7.7% ($\beta = 1.0$) for the WF+ESS configuration and the CVaR is increased between 13.6% ($\beta = 0.5$) and 16.2% ($\beta = 0.0$). The increased profits are shown to mainly arise from the provision of FR services, as total imbalance costs are reduced between 8.6% ($\beta = 0.0$) and 19.9% ($\beta = 0.5$) and are comparatively lower to the results presented in previous chapters. Despite lower imbalance costs reductions, the increased profits are able to achieve payback periods between 4.0 ($\beta = 1.0$) and 4.4 ($\beta = 0.0$) years, which is significantly lower than the 10 year lifetime assumed for the ESS. The IRR of the ESS investment varies between 22.5% ($\beta = 0.0$) and 25.4% ($\beta = 1.0$) and the ROI varies between 159% ($\beta = 0.0$) and 184% ($\beta = 1.0$), which clearly indicate the profitability of these investments. However, it should be noted that the considered capital costs for the power and energy capacities are assumed low. When the power capacity cost is set to £109.15/kW, these investments become unprofitable if the energy capacity costs take values between £901.16/kWh ($\beta = 0.0$) and £996.02/kWh ($\beta = 1.0$). For an energy capacity cost set at £395.25/kWh, power capacity costs between £613.41/kW ($\beta = 0.0$) and £708.37/kW ($\beta = 1.0$) make the WF+ESS operation unprofitable.

- Allowing larger ESS to be sized in the case study presented in Subsection 5.6.2 shows that the increased profit achieved with a 25MW/20.013MWh ESS mainly results from providing AS. Optimizing the operation of the ESS to prioritize the provision of FR services over the management of imbalances is mainly due to this service's lower energy requirements and price forecasts. Consequently, the model shows that there is a greater focus in sizing the ESS's charging/discharging power to the maximum value than the ability to store large quantities of energy. Even with higher investment costs, recovering investment costs can be achieved in approximately 7 years with a ROI of 68.7% and an IRR of 10.8%. Finally, this case study shows that expected profit increases from combining WF and ESS vary linearly with the sum of the power and energy capacities (2.25x in the conditions under analysis).

Q4: Considering the proliferation of low carbon generation technologies in the residential sector, how can the procurement of flexibility be extended to end-users? Which type of services can be provided to network operators by coordinated households with ESS and how can the community itself benefit from these technologies?

In order to assess the value of coordinating the operation of renewable generation and ESS and the provision of AS at the distribution level, Chapter 6 proposes a coordinated operation strategy for low-

carbon residential communities to make use of the flexibility of households equipped with rooftop PV and ESS technologies to trade energy with their neighbours in a P2P arrangement to reduce energy procurement costs and to procure additional sources of revenue by providing AS to the system operator and DNO. In order to incentivize energy trading within the community, households are able to procure energy from their neighbours with generation technologies at prices that are at the same time more beneficial to both parties than the prices for energy imports and exports offered by the energy supplier.

In terms of the model's mathematical formulation, the objective is to minimize energy procurement costs for the entire community associated with either through importing energy from the supplier or other households with PV and ESS installations, minus the revenue generated from selling energy to the supplier or other households. Additional revenue can be generated through PV generation and the provision of reserve and FR services. Peak power flows at the primary substation are charged in order to incentivize the minimization of the maximum power flow throughout of the assessment horizon, while maximizing the revenue from the provision of AS.

The following conclusions were made from case studies in Section 6.4 :

- In Subsection 6.4.2 it is shown that energy procurement costs can be reduced by approximately 16.8% for the whole community considering a coordinated energy trading strategy without the provision of AS. This benefit is achieved by flexibly storing excess PV generation for export during peak demand periods to households without generation technologies. When the provision of AS is considered, total costs are reduced by approximately 53%, mainly due to the provision of FR services. The results also show that energy traded within the community also increases and the minimization of peak power flows at the primary substation does not provide as much value as providing AS. Comparing the results achieved with the proposed residential coordination strategy to the results achieved without coordination, a value of £211/annum/household can be achieved for the whole community.

- The provision of AS from the ESS fundamentally changes the energy trading within the community. The potential revenue generated from providing these services leads to excess PV generation being exported to other neighbours, while the ESS is used exclusively to provide reserve and FR.

- The first case study assumes a 50% penetration of households with PV and ESS installations. Subsection 6.4.3 shows that the value of the proposed coordination strategy increases along with the penetration of low-carbon households, potentially achieving operating profits of up to £303/week with 100 % penetration.

7.1.2 Contributions of this research

The work presented in this Thesis has lead to the following original contributions:

- The development of an optimization framework for Wind Farms and Energy Storage Systems to coordinate their operation for the provision of energy and ancillary services. Resource availability, stored energy limitations and the provision of ancillary services through the full set of storage operation modes are incorporated in the formulation of the bidding strategy.

- The proposal of a stochastic formulation in order to represent how generation and provision of ancillary services are affected by day-ahead wind generation and prices uncertainty. This has allowed to better understand how wind imbalance management impacts the revenue generated from providing ancillary services, and vice-versa. It is also shown how the proposed coordinated bidding strategy mitigates the conflict between imbalance management and provision of services.

- The development of a novel two-stage stochastic mathematical programming model that allows considering different degrees of risk aversion when optimising the day-ahead energy and ancillary services bidding strategy of a Wind Farm with an on-site Energy Storage System. As a result, risk-averse wind producers will have an improved position in the day-ahead markets due to the reduced offer uncertainty.

- The linearization of absolute value functions through a tight formulation using Special Ordered-Set Type 1 and integer variables to dynamically enforce bounds for positive and negative values of energy and ancillary services imbalances that allows reducing the solutions' searching space and computational time.

- The development of a model that allows considering additional pump-turbine unit start-up and shut-down costs of a Pumped-Hydro Storage Plant due to the provision of SPR. The modelling of these additional costs allowed for, on the one hand, more informed Pumped-Hydro Storage Plant commitment decisions to be made which improve the operational lifespan of the pump-turbine units. On the other hand, it provides better insight into how wind generation variability impacts the benefit of variable-speed over fixed-speed pump-turbine technology.

- The development of a risk-averse formulation for the Energy Storage System investment problem for wind coordination and provision of ancillary services and the successful application of the Progressive Hedging Algorithm to this formulation in order to achieve computational tractability.

- Establishing a MILP model to minimize energy procurement costs through a coordinated intra-neighbourhood energy trading and multi-service business model.

7.2 Future Work

7.2.1 Impact of a risk-averse WF-ESS participant in market outcomes

The work proposed in this research has assumed several uncorrelated uncertainty sources, namely pricing and wind uncertainty, which were then superimposed for all time periods in order to ensure that the scenarios used in the stochastic models would cover all possible outcomes. Although this assumption is valid in conjunction with the price-taker approach of the combined WF and ESS (the added capacity of both facilities is assumed to not affect market prices), the same cannot be applied for larger capacities. In fact, energy and AS prices are directly influenced by renewable generation, and ESS are seen to have the potential to determine market outcomes through strategic bidding. As such, a more precise modelling of the dependencies between the uncertainties considered for the model is needed. Furthermore, for larger capacities of the WF and the ESS, a new modelling framework is needed to assess the impact of the risk-averse WF-ESS participant in the markets' outcomes. Concretely, the JBS would need to be

reformulated into a bi-level model where the proposed risk-averse JBS is determined with its impact on the energy and AS is properly taken into account in order to maximize expected profit.

7.2.2 Optimize the participation of a risk-averse WF-ESS operator in the energy and AS markets considering competition from other strategic WF-ESS participants

It is assumed that a single WF-ESS operator is considered as a risk-averse market participant. This assumption can be seen as limited given the increased interest in coordinating renewables and ESS. Furthermore, considering the potential market-wide impact of several WF-ESS participants, further research should be conducted in order to determine tools that allow a risk-averse WF-ESS operator to anticipate the impact of strategic bidding strategies from other similar participants with the potential to directly influence market outcomes, in order to minimize exposure undesirable market outcomes. This is of particular interest for market operators to address the potential for market power abuse from strategic WF-ESS operators and its impact on social welfare.

7.2.3 The maximization of the benefit of the ESS for a WF that participates in intra-day trading

One of the main components of the benefit of an ESS for a WF is the management of imbalances between bids submitted to the day-ahead markets and real-time delivery of energy and availability for the provision of AS. However, the increasing popularity of intra-day markets which are cleared within one hour ahead of delivery (in some markets, 15 minutes- or 30 minutes-ahead) allow for more informed decisions to be taken in order to minimize exposure to uncertainty. Therefore, further work needs to be carried out to understand how the proposed JBS benefits a WF participating in an hour-ahead market in which the offering uncertainty is significantly reduced when compared to a day-ahead offering. Furthermore, if the benefit of the JBS is reduced when compared to participating in an intra-day market, how can the business model be reformulated in order to maximize the profit that the ESS can bring to the WF and the system operator. While the intra-day market reduces uncertainty regarding the WF's offering, the same cannot be said regarding generation volatility which translates into the procurement of additional resources to reduce net-demand mismatches.

7.2.4 Decentralized approach to the coordinated residential energy trading and service provision strategy

The coordinated energy trading and service provision strategy proposed in Chapter 6 adopts a centralized approach by setting the prices for intra-neighbourhood trading. This approach, despite leading to significant reductions in energy procurement costs for the entire community, might, in fact, lead to undesirable cost increases for low-carbon households. Furthermore, the individual interests of certain households (maximizing revenue generated from the energy sales and provision of services) might conflict with the objective of the aggregator in charge of coordinating the operation of the low-carbon community. Hence, in order to safeguard the consumers' interests, a decentralized approach using agent-based modelling needs to be taken into account when optimizing the coordination of distributed ESS and PV to minimize energy costs and maximize revenue from the provision of services. The value of the flexibility provided by coordinated EV operation has been widely studied in literature. Considering that is likely

that households that have rooftop PV and ESS installations might also own an EV, the potential benefit of coordinating EV charging within the community must also be addressed. New research should also focus on maximizing the services that the low-carbon community provides, seeking capacity payments, voltage support and considering the flexibility of demand response.

Bibliography

[1] R. Moreira, "Business Models for Energy Storage Systems," PhD Thesis, Imperial College London, 2015. (Cited on pages 19, 28, 29, and 38)

[2] D. Cameron, N. Clegg, and C. Huhne, "Carbon Plan," HM Government, London, Tech. Rep., 2011. [Online]. Available: http://www.decc.gov.uk/en/content/cms/what_we_do/lc_uk/carbon_plan/carbon_plan.aspx (Cited on page 27)

[3] M. Bell, O. Bellamy, A. Gault, M. Hemsley, S. Smith, M. Thompson, J. Barrett, N. Pawar, P. Seera, S. Taylor, S. Westlake, and S. Wildeshaus, "UK climate change following the Paris Agreement," Committee on Climate Change, Tech. Rep., 2016. [Online]. Available: https://www.theccc.org.uk/wp-content/uploads/2016/10/UK-climate-action-following-the-Paris-Agreement-Committee-on-Climate-Change-October-2016.pdf (Cited on page 27)

[4] T. J. Foxon and P. J. G. Pearson, "The UK low carbon energy transition: prospects and challenges," *Realising Transition Pathways Working Paper*, pp. 1–19, 2013. [Online]. Available: http://www.realisingtransitionpathways.org.uk/realisingtransitionpathways/publications/Working_papers/RTP_WP_2013_3_Foxon_x_Pearson_UK_low_carbon_energy_transition.pdf (Cited on page 27)

[5] ECCC, "2020 Renewable Heat and Transport Targets," Tech. Rep., 2016. (Cited on page 27)

[6] European Commission, "Electrification of the Transport System Studies and reports," Tech. Rep., 2017. (Cited on page 27)

[7] G. Corbetta, A. Ho, I. Pineda, K. Ruby, L. Van de Velde, and J. Bickley, "Wind energy scenarios for 2030 - A report by the European Wind Energy Association," The European Wind Energy Association, Tech. Rep. August, 2015. (Cited on page 27)

[8] IRENA, "Renewable Power Generation Costs in 2017," International Renewable Energy Agency, Abu Dhabi, Tech. Rep., 2018. [Online]. Available: https://www.irena.org/publications/2018/Jan/Renewable-power-generation-costs-in-2017 (Cited on page 27)

[9] E. Ela, M. Milligan, A. Bloom, A. Botterud, A. Townsend, and T. Levin, "Evolution of Wholesale Electricity Market Design with Increasing Levels of Renewable Generation," National Renewable Energy Laboratory, Golden, CO, USA, Tech. Rep. NREL/TP-5D00-61765, 2014. (Cited on page 27)

[10] P. Ramírez, "The Role of Flexibility In Generation Expansion Planning of Power Systems With a High Degree of Renewables & Vehicle Electrification," Ph.D. dissertation, Imperial College London, 2014. (Cited on pages 28 and 115)

[11] J. M. Morales, A. J. Conejo, H. Madsen, P. Pinson, and M. Zugno, *Integrating Renewables in Electricity Markets - Operational Problems*, 2010, vol. 139. (Cited on page 28)

[12] L. Bird, J. Cochran, and X. Wang, "Wind and solar energy curtailment: experience and practices in the United States," National Renewable Energy Laboratory, Denver, Tech. Rep. NREL/TP-6A20-60983, 2014. [Online]. Available: https://www.nrel.gov/docs/fy14osti/60983.pdf (Cited on page 28)

[13] DOE, "The Importance of Flexible Electricity Supply," *Solar Integration Series. 1 of 3*, pp. 1–4, may 2011. (Cited on page 28)

[14] N. Phuangpornpitak and S. Tia, "Opportunities and challenges of integrating renewable energy in smart grid system," *Energy Procedia*, vol. 34, pp. 282–290, 2013. (Cited on page 28)

[15] T. Drees, N. V. Bracht, and A. Moser, "Reserve Providing in Future Generation Systems Considering Renewable Energy Sources," in *11th Intern. Conf. European Energy Market*. Krakow: IEEE, may 2014, pp. 1–6. [Online]. Available: http://ieeexplore.ieee.org/document/6861301/ (Cited on pages 28, 54, 55, and 57)

[16] A. J. Gesino, "Power reserve provision with wind farms," PhD, University of Kassel, 2010. (Cited on page 28)

[17] F. Teng and G. Strbac, "Assessment of the Role and Value of Frequency Response Support from Wind Plants," *IEEE Transactions on Sustainable Energy*, vol. 7, no. 2, pp. 586–595, 2016. (Cited on page 28)

[18] M. Black and G. Strbac, "Value of bulk energy storage for managing wind power fluctuations," *IEEE Transactions on Energy Conversion*, vol. 22, no. 1, pp. 197–205, 2007. (Cited on pages 28 and 37)

[19] G. N. Bathurst and G. Strbac, "Value of combining energy storage and wind in short-term energy and balancing markets," *Electric Power Systems Research*, vol. 67, no. 1, pp. 1–8, 2003. (Cited on page 28)

[20] A. Lever, D. Sanders, and N. Lehmann, "Can storage help reduce the cost of a future UK electricity system?" Carbon Trust, Imperial College London, London, Tech. Rep., 2016. (Cited on pages 28, 37, and 105)

[21] G. Strbac, M. Aunedi, D. Pudjianto, P. Djapic, F. Teng, A. Sturt, D. Jackravut, R. Sansom, V. Yufit, and N. Brandon, "Strategic Assessment of the Role and Value of Energy Storage Systems in the UK Low Carbon Energy Future," Energy Futures Lab, Imperial College London, London, Tech. Rep. June, 2012. (Cited on page 28)

[22] a. M. A. K. Abeygunawardana and G. Ledwich, "Estimating benefits of energy storage for aggregate storage applications in electricity distribution networks in Queensland," in *2013 IEEE Power & Energy Society General Meeting*. Vancouver: IEEE, jul 2013, pp. 1–5. (Cited on pages 28, 37, and 54)

[23] J. F. Bolado, H. L. Ferreira, and W. Kling, "Energy storage market value - A Netherlands case study," in *2014 49th International Universities Power Engineering Conference (UPEC)*. Cluj-Napoca: IEEE, sep 2014, pp. 1–6. (Cited on pages 28 and 54)

[24] J. Aguado, S. de la Torre, and A. Triviño, "Battery energy storage systems in transmission network expansion planning," *Electric Power Systems Research*, vol. 145, pp. 63–72, 2017. (Cited on pages 29 and 37)

[25] S. F. Santos, D. Z. Fitiwi, M. R. Cruz, C. M. Cabrita, and J. P. Catalão, "Impacts of optimal energy storage deployment and network reconfiguration on renewable integration level in distribution systems," *Applied Energy*, vol. 185, pp. 44–55, 2017. (Cited on page 29)

[26] J. García-González, R. M. R. de la Muela, L. M. Santos, A. M. Gonzalez, J. Garcia-Gonzalez, R. M. R. de la Muela, L. M. Santos, and A. M. Gonzalez, "Stochastic joint optimization of wind generation and pumped-storage units in an electricity market," *IEEE Transactions on Power Systems*, vol. 23, no. 2, pp. 460–468, 2008. (Cited on pages 29, 55, 89, and 90)

[27] A. S. A. Awad, J. D. Fuller, T. H. M. EL-Fouly, and M. M. A. Salama, "Impact of Energy Storage Systems on Electricity Market Equilibrium," *IEEE Transactions on Sustainable Energy*, vol. 5, no. 3, pp. 875–885, 2014. (Cited on page 29)

[28] R. Sioshansi, P. Denholm, T. Jenkin, and J. Weiss, "Estimating the value of electricity storage in PJM: Arbitrage and some welfare effects," *Energy Economics*, vol. 31, no. 2, pp. 269–277, 2009. (Cited on page 29)

[29] E. Drury, P. Denholm, and R. Sioshansi, "The value of compressed air energy storage in energy and reserve markets," *Energy*, vol. 36, no. 8, pp. 4959–4973, 2011. (Cited on page 29)

[30] B. Nyamdash and E. Denny, "The impact of electricity storage on wholesale electricity prices," *Energy Policy*, vol. 58, pp. 6–16, 2013. (Cited on page 29)

[31] D. Pudjianto, M. Aunedi, P. Djapic, and G. Strbac, "Whole-Systems Assessment of the Value of Energy Storage in Low-Carbon Electricity Systems," *IEEE Transactions on Smart Grid*, vol. 5, no. 2, pp. 1098–1109, 2014. (Cited on pages 29 and 37)

[32] R. Karki and S. Thapa, "Reliability benefit of energy storage in wind integrated power system operation," *IET Generation, Transmission & Distribution*, vol. 10, no. 3, pp. 807–814, 2016. (Cited on pages 29, 37, 55, and 90)

[33] X. Shen, M. Shahidehpour, Y. Han, S. Zhu, and J. Zheng, "Expansion Planning of Active Distribution Networks With Centralized and Distributed Energy Storage Systems," *IEEE Transactions on Sustainable Energy*, vol. 8, no. 1, pp. 126–134, 2017. (Cited on page 29)

[34] G. Sharp, P. Ramirez, M. Rowe, and T. Leonard, "Electricity Storage - Comparative Case Studies," DNV GL, London, Tech. Rep., 2016. [Online]. Available: https://www.ofgem.gov.uk/publications-and-updates/electricity-storage-comparative-case-studies-dnv-gl (Cited on pages 29 and 30)

[35] P. Ramirez, "The Benefits of Pumped Storage Hydro to the UK," DNV GL, London, Tech. Rep., 2016. [Online]. Available: http://scottishrenewables.com/publications/benefits-pumped-storage-hydro-uk/ (Cited on pages 29 and 30)

[36] D. Connolly, H. Lund, P. Finn, B. Mathiesen, and M. Leahy, "Practical operation strategies for pumped hydroelectric energy storage (PHES) utilising electricity price arbitrage," *Energy Policy*, vol. 39, no. 7, pp. 4189–4196, 2011. (Cited on page 29)

[37] B. Steffen, "Prospects for pumped-hydro storage in Germany," *Energy Policy*, vol. 45, pp. 420–429, 2012. (Cited on page 29)

[38] Ofgem, "A smart, flexible energy system: A call for evidence," London, Tech. Rep. November, 2016. [Online]. Available: https://www.ofgem.gov.uk/system/files/docs/2016/12/smart_flexible_energy_system_a_call_for_evidence.pdf (Cited on page 29)

[39] BEIS and Ofgem, "Upgrading Our Energy System, Smart Systems and Flexibility Plan - Call for Evidence Question Summaries and Response from the Government and Ofgem," London, Tech. Rep. July, 2017. [Online]. Available: https://www.gov.uk/government/uploads/system/uploads/attachment_data/file/631656/smart-energy-systems-summaries-responses.pdf (Cited on page 29)

[40] R. Moreno, R. Moreira, and G. Strbac, "A MILP model for optimising multi-service portfolios of distributed energy storage," *Applied Energy*, vol. 137, pp. 554–566, 2014. (Cited on pages 29, 37, and 41)

[41] X. He, E. Delarue, W. D'haeseleer, and J. M. Glachant, "A novel business model for aggregating the values of electricity storage," *Energy Policy*, vol. 39, no. 3, pp. 1575–1585, 2011. (Cited on pages 29 and 37)

[42] H. Pandzic, Y. Wang, T. Qiu, Y. Dvorkin, and D. S. Kirschen, "Near-Optimal Method for Siting and Sizing of Distributed Storage in a Transmission Network," *IEEE Transactions on Power Systems*, vol. 30, no. 5, pp. 2288–2300, 2015. (Cited on page 29)

[43] R. B. Bass, J. Carr, J. Aguilar, and K. Whitener, "Determining the Power and Energy Capacities of a Battery Energy Storage System to Accommodate High Photovoltaic Penetration on a Distribution Feeder," *IEEE Power and Energy Technology Systems Journal*, vol. 3, no. 3, pp. 119–127, 2016. (Cited on page 29)

[44] M. Samper, D. Flores, and A. Vargas, "Investment Valuation of Energy Storage Systems in Distribution Networks considering Distributed Solar Generation," *IEEE Latin America Transactions*, vol. 14, no. 4, pp. 1774–1779, 2016. (Cited on page 29)

[45] E. Nasrolahpour, S. J. Kazempour, H. Zareipour, and W. D. Rosehart, "Strategic Sizing of Energy Storage Facilities in Electricity Markets," *IEEE Transactions on Sustainable Energy*, vol. 7, no. 4, pp. 1462–1472, 2016. (Cited on page 29)

[46] J. R. Birge and F. Louveaux, *Introduction to Stochastic Programming*, 2nd ed., ser. Springer Series in Operations Research and Financial Engineering. New York, NY: Springer New York, 2011. (Cited on pages 32 and 56)

[47] P. Kall and S. W. Wallace, *Stochastic Programming*, 2nd ed. Chichester: John Wiley & Sons, 1994. (Cited on pages 32 and 56)

[48] R. T. Rockafellar and R. J.-B. Wets, "Scenarios and Policy Aggregation in Optimization Under Uncertainty," *Mathematics of Operations Research*, vol. 16, no. 1, pp. 119–147, 1991. (Cited on pages 32 and 117)

[49] J.-P. Watson, D. L. Woodruff, and D. R. Strip, "Progressive Hedging Innovations for a Class of Stochastic Resource Allocation Problems," *SSRN Electronic Journal*, pp. 1–27, 2008. (Cited on pages 32 and 118)

[50] R. Walawalkar, J. Apt, and R. Mancini, "Economics of electric energy storage for energy arbitrage and regulation in New York," *Energy Policy*, vol. 35, no. 4, pp. 2558–2568, 2007. (Cited on page 37)

[51] K. Bradbury, L. Pratson, and D. Patiño-Echeverri, "Economic viability of energy storage systems based on price arbitrage potential in real-time U.S. electricity markets," *Applied Energy*, vol. 114, pp. 512–519, 2014. (Cited on page 37)

[52] T. Das, V. Krishnan, and J. D. McCalley, "Assessing the benefits and economics of bulk energy storage technologies in the power grid," *Applied Energy*, vol. 139, pp. 104–118, 2015. (Cited on page 37)

[53] H. Chen, Z. Liu, A. K. Coskun, and A. Wierman, "Optimizing energy storage participation in emerging power markets," in *2015 Sixth International Green and Sustainable Computing Conference (IGSC)*. Las Vegas, NV: IEEE, dec 2015, pp. 1–6. (Cited on pages 37 and 137)

[54] S. J. Kazempour, M. Hosseinpour, and M. P. Moghaddam, "Self-scheduling of a joint hydro and pumped-storage plants in energy, spinning reserve and regulation markets," in *2009 IEEE Power & Energy Society General Meeting*. Calgary, AB, Canada: IEEE, oct 2009, pp. 1–8. (Cited on page 37)

[55] J. Kumano and A. Yokoyama, "Optimal weekly operation scheduling on pumped storage hydro power plant and storage battery considering reserve margin with a large penetration of renewable energy," in *2014 Inter. Conf. Power System Technology*, Chengdu, 2014, pp. 1120–1126. (Cited on page 37)

[56] M. Chazarra, J. I. Perez-Diaz, and J. Garcia-Gonzalez, "Optimal operation of variable speed pumped storage hydropower plants participating in secondary regulation reserve markets," in *11th International Conference on the European Energy Market (EEM14)*, vol. i. IEEE, 2014, pp. 1–5. (Cited on pages 37 and 54)

[57] R. Moreno, R. Moreira, and G. Strbac, "Value of corrective network security for distributed energy storage applications," *IET Generation, Transmission & Distribution*, vol. 10, no. 7, pp. 1758–1767, 2016. (Cited on pages 37 and 137)

[58] C. Suazo-Martinez, E. Pereira-Bonvallet, R. Palma-Behnke, and X.-P. Zhang, "Impacts of Energy Storage on Short Term Operation Planning Under Centralized Spot Markets," *IEEE Transactions on Smart Grid*, vol. 5, no. 2, pp. 1110–1118, mar 2014. (Cited on page 37)

[59] Forward Market Operations, "PJM Manual 11 : Energy & Ancillary Services Market Operations," PJM, Tech. Rep., 2015. (Cited on page 38)

[60] Entidade Reguladora dos Serviços Energéticos, "Manual de procedimentos da gestão global do sistema do setor elétrico," Entidade Reguladora do Sector Eléctrico Energéticos, Lisbon, Tech. Rep., 2014. (Cited on pages 38 and 40)

[61] National Grid, "Short Term Operating Reserve (STOR)," 2018. [Online]. Available: https://www.nationalgrid.com/uk/electricity/balancing-services/reserve-services/short-term-operating-reserve-stor?overview (Cited on page 40)

[62] Elexon, "Elexon Portal." [Online]. Available: https://www.elexonportal.co.uk (Cited on page 42)

[63] REN, "MIBEL - Market Results." [Online]. Available: http://www.mercado.ren.pt/EN/Electr/MarketInfo/MarketResults/OMIE/Pages/default.aspx (Cited on page 42)

[64] FICO, "FICO Xpress Optimization," 2016. [Online]. Available: http://www.fico.com/en/products/fico-xpress-optimization (Cited on pages 42, 68, and 139)

[65] G. Papaefthymiou, J. van Doorn, A. Kakorin, M. van der Meijden, L. Laurisch, J.-W. Meulenbroeks, and C. Nabe, "Future provision of control reserve from offshore wind farms: An analysis of benefits and barriers," in *2015 12th International Conference on the European Energy Market (EEM)*. Lisbon: IEEE, may 2015, pp. 1–5. (Cited on page 54)

[66] B. Zakeri and S. Syri, "Economy of electricity storage in the Nordic electricity market: The case for Finland," in *11th International Conference on the European Energy Market (EEM14)*. Krakow: IEEE, may 2014, pp. 1–6. (Cited on page 54)

[67] J. Pinto, J. de Sousa, and M. V. Neves, "The value of a pumping-hydro generator in a system with increasing integration of wind power," in *2011 8th International Conference on the European Energy Market (EEM)*, no. May. Zagreb, Croatia: IEEE, jul 2011, pp. 306–311. (Cited on page 54)

[68] J. Lagarto, F. Fernandes, J. A. M. Sousa, J. Santana, and B. Martins, "Optimal scheduling of a pumped storage hydro unit in the day-ahead and secondary reserve electricity market," in *2015 12th International Conference on the European Energy Market (EEM)*. Lisbon: IEEE, may 2015, pp. 1–5. (Cited on page 54)

[69] H. Akhavan-Hejazi and H. Mohsenian-Rad, "Optimal Operation of Independent Storage Systems in Energy and Reserve Markets With High Wind Penetration," *IEEE Transactions on Smart Grid*, vol. 5, no. 2, pp. 1088–1097, 2014. (Cited on page 54)

[70] S.-E. Fleten and T. K. Kristoffersen, "Stochastic programming for optimizing bidding strategies of a Nordic hydropower producer," *European Journal of Operational Research*, vol. 181, no. 2, pp. 916–928, 2007. (Cited on page 54)

[71] E. Nasrolahpour, J. Kazempour, H. Zareipour, and W. D. Rosehart, "A Bilevel Model for Participation of a Storage System in Energy and Reserve Markets," *IEEE Transactions on Sustainable Energy*, vol. 9, no. 2, pp. 582–598, 2018. (Cited on page 55)

[72] K. Bruninx, Y. Dvorkin, E. Delarue, H. Pandzic, W. Dhaeseleer, and D. S. Kirschen, "Coupling Pumped Hydro Energy Storage With Unit Commitment," *IEEE Transactions on Sustainable Energy*, vol. 7, no. 2, pp. 786–796, 2016. (Cited on pages 55 and 90)

[73] P. Denholm and R. Sioshansi, "The value of compressed air energy storage with wind in transmission-constrained electric power systems," *Energy Policy*, vol. 37, no. 8, pp. 3149–3158, 2009. (Cited on pages 55, 89, and 90)

[74] H. Ding, P. Pinson, Z. Hu, J. Wang, and Y. Song, "Optimal Offering and Operating Strategy for a Large Wind-Storage System as a Price Maker," *IEEE Transactions on Power Systems*, vol. 32, no. 6, pp. 4904–4913, nov 2017. (Cited on pages 55 and 90)

[75] T. Rodrigues, P. Ramírez, and G. Strbac, "The value of storage for a wind farm offering energy and spinning reserve," in *5th IET International Conference on Renewable Power Generation (RPG) 2016*. London: Institution of Engineering and Technology, 2016, p. 22(6). (Cited on pages 55 and 90)

[76] M. A. Ortega-Vazuqez, D. S. Kirschen, and Y. Dvorkin, "Wind generation as a reserve provider," *IET Generation, Transmission & Distribution*, vol. 9, no. 8, pp. 779–787, 2015. (Cited on pages 55 and 57)

[77] D. Bertsimas and M. Sim, "Robust discrete optimization and network flows," *Mathematical Programming*, vol. 98, no. 1-3, pp. 49–71, 2003. (Cited on page 56)

[78] ——, "The Price of Robustness," *Operations Research*, vol. 52, no. 1, pp. 35–53, 2004. (Cited on page 56)

[79] S. Takriti, J. Birge, and E. Long, "A stochastic model for the unit commitment problem," *IEEE Trans. Power Syst.*, vol. 11, no. 3, pp. 1497–1508, 1996. (Cited on page 56)

[80] P. a. Ruiz, C. R. Philbrick, E. Zak, K. W. Cheung, and P. W. Sauer, "Uncertainty Management in the Unit Commitment Problem," *IEEE Transactions on Power Systems*, vol. 24, no. 2, pp. 642–651, may 2009. (Cited on page 56)

[81] Y. Yuan, Q. Li, and W. Wang, "Optimal operation strategy of energy storage unit in wind power integration based on stochastic programming," *IET Renewable Power Generation*, vol. 5, no. 2, p. 194, 2011. (Cited on page 56)

[82] M. Wei and J. Zhong, "Optimal bidding strategy for demand response aggregator in day-ahead markets via stochastic programming and robust optimization," in *2015 12th International Conference on the European Energy Market (EEM)*. IEEE, may 2015, pp. 1–5. (Cited on page 56)

[83] R. A. Jabr, I. Dzafic, and B. C. Pal, "Robust Optimization of Storage Investment on Transmission Networks," *IEEE Transactions on Power Systems*, vol. 30, no. 1, pp. 531–539, 2015. (Cited on page 56)

[84] N. G. Cobos, J. M. Arroyo, N. Alguacil-Conde, and J. Wang, "Robust Energy and Reserve Scheduling Considering Bulk Energy Storage Units and Wind Uncertainty," *IEEE Transactions on Power Systems*, vol. 8950, no. c, pp. 1–1, 2018. (Cited on page 56)

[85] A. Shapiro, D. Dentcheva, and A. Ruszczynski, *Lectures on Stochastic Programming: Modelling and Theory*. Society for Industrial and Applied Mathematics and Mathematical Programming Society, 2009. (Cited on page 57)

[86] A. J. Conejo, M. Carrión, and J. M. Morales, *Decision Making Under Uncertainty in Electricity Markets*, ser. International Series in Operations Research & Management Science, F. S. Hillier, Ed. Boston, MA: Springer US, 2010, vol. 153. (Cited on pages 57, 89, 90, and 91)

[87] ELEXON, "Imbalance Pricing." [Online]. Available: https://www.elexon.co.uk/operations-settlement/imbalance-pricing/ (Cited on page 57)

[88] P. Belotti, C. Kirches, S. Leyffer, J. Linderoth, J. Luedtke, and A. Mahajan, "Mixed-integer nonlinear optimization," *Acta Numerica*, vol. 22, no. 2013, pp. 1–131, may 2013. (Cited on page 57)

[89] J. Bisschop, *AIMMS - Optimization Modeling*. Paragon Decision Technology, 2015. (Cited on page 57)

[90] G. Cavazzinni and J. I. Perez-Diaz, "Technological developments for pumped-hydro energy storage," Mechanical Storage Subprogramme, Joint Programme on Energy Storage, European Energy Research Alliance, Tech. Rep., may 2014. [Online]. Available: http://www.eera-set.eu/wp-content/uploads/Technological-Developments-for-Pumped-Hydro-Energy-Storage_EERA-report-2014.pdf (Cited on page 62)

[91] O. Nilsson and D. Sjelvgren, "Hydro unit start-up costs and their impact on the short term scheduling strategies of Swedish power producers," *IEEE Transactions on Power Systems*, vol. 12, no. 1, pp. 38–44, 1997. (Cited on page 74)

[92] ——, "Variable splitting applied to modelling of start-up costs in short term hydro generation scheduling," *IEEE Transactions on Power Systems*, vol. 12, no. 2, pp. 770–775, 1997. (Cited on page 74)

[93] EPIS LLC, "AURORAxmp," 2016. [Online]. Available: http://epis.com/aurora_xmp/ (Cited on page 74)

[94] H. Pousinho, V. Mendes, and J. Catalão, "A risk-averse optimization model for trading wind energy in a market environment under uncertainty," *Energy*, vol. 36, no. 8, pp. 4935–4942, 2011. (Cited on pages 89 and 90)

[95] L. Baringo and A. J. Conejo, "Offering Strategy of Wind-Power Producer: A Multi-Stage Risk-Constrained Approach," *IEEE Transactions on Power Systems*, vol. 31, no. 2, pp. 1420–1429, 2016. (Cited on pages 89 and 90)

[96] E. Moiseeva and M. R. Hesamzadeh, "Strategic bidding by a risk-averse firm with a portfolio of renewable resources," in *2015 IEEE Eindhoven PowerTech*. Eindhoven, Netherlands: IEEE, jun 2015, pp. 1–6. (Cited on page 89)

[97] Y. Zhang, J. Wang, T. Ding, and X. Wang, "Conditional value at risk-based stochastic unit commitment considering the uncertainty of wind power generation," *IET Generation, Transmission & Distribution*, vol. 12, no. 2, pp. 482–489, 2018. (Cited on page 89)

[98] N. G. Paterakis, A. A. S. de la Nieta, A. G. Bakirtzis, J. Contreras, and J. P. S. Catalao, "Effect of risk aversion on reserve procurement with flexible demand side resources from the ISO point of view," *IEEE Transactions on Sustainable Energy*, vol. 8, no. 3, pp. 1040–1050, 2017. (Cited on page 89)

[99] P. Ilak, S. Krajcar, I. Rajšl, and M. Delimar, "Pricing Energy and Ancillary Services in a Day-Ahead Market for a Price-Taker Hydro Generating Company Using a Risk-Constrained Approach," *Energies*, vol. 7, no. 4, pp. 2317–2342, 2014. (Cited on pages 89 and 90)

[100] S. Moazeni, W. B. Powell, and A. H. Hajimiragha, "Mean-Conditional Value-at-Risk Optimal Energy Storage Operation in the Presence of Transaction Costs," *IEEE Transactions on Power Systems*, vol. 30, no. 3, pp. 1222–1232, 2015. (Cited on pages 89 and 90)

[101] S. Moazeni, B. Defourny, and A. H. Hajimiragha, "Risk-sensitive stochastic optimization for storage operation management," in *2015 IEEE International Conference on Smart Energy Grid Engineering (SEGE)*. Oshawa, ON: IEEE, aug 2015, pp. 1–6. (Cited on page 89)

[102] M. Chazarra, J. I. Perez-Diaz, and J. Garcia-Gonzalez, "Optimal Joint Energy and Secondary Regulation Reserve Hourly Scheduling of Variable Speed Pumped Storage Hydropower Plants," *IEEE Transactions on Power Systems*, vol. 33, no. 1, pp. 103–115, 2018. (Cited on page 89)

[103] I. G. Moghaddam, M. Nick, F. Fallahi, M. Sanei, and S. Mortazavi, "Risk-averse profit-based optimal operation strategy of a combined wind farm-cascade hydro system in an electricity market," *Renewable Energy*, vol. 55, pp. 252–259, 2013. (Cited on page 89)

[104] T. Rodrigues, P. J. Ramírez, and G. Strbac, "Risk-averse bidding of energy and spinning reserve by wind farms with on-site energy storage," *IET Renewable Power Generation*, vol. 12, no. 2, pp. 165–173, feb 2018. (Cited on pages 90 and 137)

[105] R. T. Rockafellar and S. Uryasev, "Optimization of conditional value-at-risk," *The Journal of Risk*, vol. 2, no. 3, pp. 21–41, 2000. (Cited on page 90)

[106] P. Artzner, F. Delbaen, J.-M. Eber, and D. Heath, "Coherent Measures of Risk," *Mathematical Finance*, vol. 9, no. 3, pp. 203–228, 1999. (Cited on page 90)

[107] K. Pavlikov and S. Uryasev, "Cvar norm and applications in optimization," *Optimization Letters*, vol. 8, no. 7, pp. 1999–2020, Oct 2014. [Online]. Available: https://doi.org/10.1007/s11590-013-0713-7 (Cited on page 91)

[108] IRENA, "Electricity Storage and Renewables: Costs and Markets To 2030," International Renewable Energy Agency, Abu Dhabi, Tech. Rep. October, 2017. [Online]. Available: http://www.irena.org/publications/2017/Oct/Electricity-storage-and-renewables-costs-and-markets (Cited on page 105)

[109] F. J. de Sisternes, J. D. Jenkins, and A. Botterud, "The value of energy storage in decarbonizing the electricity sector," *Applied Energy*, vol. 175, pp. 368–379, 2016. (Cited on page 105)

[110] S. B. Peterson, J. Apt, and J. Whitacre, "Lithium-ion battery cell degradation resulting from realistic vehicle and vehicle-to-grid utilization," *Journal of Power Sources*, vol. 195, no. 8, pp. 2385–2392, 2010. (Cited on page 106)

[111] C. Zhou, K. Qian, M. Allan, and W. Zhou, "Modeling of the Cost of EV Battery Wear Due to V2G Application in Power Systems," *IEEE Transactions on Energy Conversion*, vol. 26, no. 4, pp. 1041–1050, 2011. (Cited on page 106)

[112] B. Xu, A. Oudalov, A. Ulbig, G. Andersson, and D. S. Kirschen, "Modeling of Lithium-Ion Battery Degradation for Cell Life Assessment," *IEEE Transactions on Smart Grid*, vol. 9, no. 2, pp. 1131–1140, 2018. (Cited on pages 106 and 111)

[113] A. Perez, R. Moreno, R. Moreira, M. Orchard, and G. Strbac, "Effect of Battery Degradation on Multi-Service Portfolios of Energy Storage," *IEEE Transactions on Sustainable Energy*, vol. 7, no. 4, pp. 1718–1729, 2016. (Cited on pages 106 and 111)

[114] M. Ouyang, X. Feng, X. Han, L. Lu, Z. Li, and X. He, "A dynamic capacity degradation model and its applications considering varying load for a large format Li-ion battery," *Applied Energy*, vol. 165, pp. 48–59, 2016. (Cited on pages 106 and 111)

[115] M. Martinez, M. G. Molina, and P. E. Mercado, "Optimal Storage Technology Selection and Sizing for Providing Reserve to Power Systems with High Penetration of Wind Generation," *IEEE Latin America Transactions*, vol. 13, no. 9, pp. 2983–2990, 2015. (Cited on page 106)

[116] T. Brijs, A. van Stiphout, S. Siddiqui, and R. Belmans, "Evaluating the role of electricity storage by considering short-term operation in long-term planning," *Sustainable Energy, Grids and Networks*, vol. 10, pp. 104–117, 2017. (Cited on page 106)

[117] Y. Dvorkin, R. Fernandez-Blanco, D. S. Kirschen, H. Pandzic, J.-P. Watson, and C. A. Silva-Monroy, "Ensuring Profitability of Energy Storage," *IEEE Transactions on Power Systems*, vol. 32, no. 1, pp. 611–623, 2017. (Cited on pages 106 and 115)

[118] R. Fernandez-Blanco, Y. Dvorkin, B. Xu, Y. Wang, and D. S. Kirschen, "Optimal Energy Storage Siting and Sizing: A WECC Case Study," *IEEE Transactions on Sustainable Energy*, vol. 8, no. 2, pp. 733–743, 2017. (Cited on pages 106 and 115)

[119] Y. Dvorkin, R. Fernandez-Blanco, Y. Wang, B. Xu, D. S. Kirschen, H. Pandzic, J.-P. Watson, and C. A. Silva-Monroy, "Co-Planning of Investments in Transmission and Merchant Energy Storage," *IEEE Transactions on Power Systems*, vol. 33, no. 1, pp. 245–256, 2018. (Cited on pages 106 and 115)

[120] M. Weibelzahl and A. Martz, "Optimal storage and transmission investments in a bilevel electricity market model," *Optimization Online*, 2017. [Online]. Available: http://www.optimization-online.org/DB_FILE/2017/03/5937.pdf (Cited on page 106)

[121] P. Xiong and C. Singh, "Optimal Planning of Storage in Power Systems Integrated With Wind Power Generation," *IEEE Transactions on Sustainable Energy*, vol. 7, no. 1, pp. 232–240, 2016. (Cited on pages 106 and 108)

[122] K. W. Chan, X. Luo, M. Qin, T. Wu, and C. Y. Chung, "Optimal planning and operation of energy storage systems in radial networks for wind power integration with reserve support," *IET Generation, Transmission & Distribution*, vol. 10, no. 8, pp. 2019–2025, 2016. (Cited on pages 106 and 108)

[123] Y. Zhang, K. Meng, F. Luo, Z. Y. Dong, K. P. Wong, and Y. Zheng, "Optimal allocation of battery energy storage systems in distribution networks with high wind power penetration," *IET Renewable Power Generation*, vol. 10, no. 8, pp. 1105–1113, 2016. (Cited on pages 106 and 108)

[124] A. Kargarian, G. Hug, and J. Mohammadi, "A Multi-Time Scale Co-Optimization Method for Sizing of Energy Storage and Fast-Ramping Generation," *IEEE Transactions on Sustainable Energy*, vol. 7, no. 4, pp. 1351–1361, 2016. (Cited on pages 106 and 108)

[125] S. J. Kazempour and A. J. Conejo, "Strategic Generation Investment Under Uncertainty Via Benders Decomposition," *IEEE Transactions on Power Systems*, vol. 27, no. 1, pp. 424–432, 2012. (Cited on page 106)

[126] V. Dvorkin, "Multi-stage Strategic Investment in CCGTs and Wind Power Units via Progressive Hedging," MSc, Technical University of Denmark, 2017. (Cited on pages 106 and 117)

[127] P. Falugi, I. Konstantelos, and G. Strbac, "Planning with Multiple Transmission and Storage Investment Options under Uncertainty: A Nested Decomposition Approach," *IEEE Transactions on Power Systems*, vol. 8950, no. c, pp. 1–1, 2017. (Cited on page 106)

[128] J. Qiu, J. Zhao, D. Wang, and Z. Y. Dong, "Decomposition-based approach to risk-averse transmission expansion planning considering wind power integration," *IET Generation, Transmission & Distribution*, vol. 11, no. 14, pp. 3458–3466, 2017. (Cited on pages 106 and 108)

[129] Y. Tohidi, M. R. Hesamzadeh, and F. Regairaz, "Modified Benders Decomposition for Solving Transmission Investment Game With Risk Measure," *IEEE Transactions on Power Systems*, vol. 33, no. 2, pp. 1936–1947, 2018. (Cited on pages 106 and 108)

[130] R. T. Rockafellar, "Solving Stochastic Programming Problems with Risk Measures by Progressive Hedging," *Set-Valued and Variational Analysis*, pp. 1–10, 2017. (Cited on pages 107 and 118)

[131] J. Sumaili, H. Keko, V. Miranda, Z. Zhou, A. Botterud, and J. Wang, "Finding representative wind power scenarios and their probabilities for stochastic models," *2011 16th International Conference on Intelligent System Applications to Power Systems, ISAP 2011*, 2011. (Cited on page 116)

[132] S. Pineda and A. Conejo, "Scenario reduction for risk-averse electricity trading," *IET Generation, Transmission & Distribution*, vol. 4, no. October 2009, pp. 694–705, 2010. (Cited on page 116)

[133] T. Rodrigues, V. Miranda, and J. Sumaili, "Finding Representative Scenarios in Wind Power or Load Forecast," Ph.D. dissertation, Faculty of Engineering of the University of Porto, 2013. (Cited on page 116)

[134] J. F. Benders, "Partitioning procedures for solving mixed-variables programming problems," *Numerische Mathematik*, vol. 4, no. 1, pp. 238–252, dec 1962. (Cited on page 117)

[135] S. M. Ryan, R. J. Wets, D. L. Woodruff, C. Silva-Monroy, and J.-P. Watson, "Toward scalable, parallel progressive hedging for stochastic unit commitment," in *2013 IEEE Power & Energy Society General Meeting*. Vancouver, BC, Canada: IEEE, jul 2013, pp. 1–5. (Cited on page 117)

[136] C. Ordoudis, P. Pinson, M. Zugno, and J. M. Morales, "Stochastic unit commitment via Progressive Hedging - extensive analysis of solution methods," in *2015 IEEE Eindhoven PowerTech*. Eindhoven, Netherlands: IEEE, jun 2015, pp. 1–6. (Cited on pages 117, 118, and 120)

[137] M. Majidi-Qadikolai and R. Baldick, "A Generalized Decomposition Framework for Large-Scale Transmission Expansion Planning," *IEEE Transactions on Power Systems*, vol. 33, no. 2, pp. 1635–1649, 2018. (Cited on page 117)

[138] J.-P. Watson and D. L. Woodruff, "Progressive hedging innovations for a class of stochastic mixed-integer resource allocation problems," *Computational Management Science*, vol. 8, no. 4, pp. 355–370, 2011. (Cited on pages 118 and 120)

[139] I. Atzeni, L. G. Ordonez, G. Scutari, D. P. Palomar, and J. R. Fonollosa, "Demand-Side Management via Distributed Energy Generation and Storage Optimization," *IEEE Transactions on Smart Grid*, vol. 4, no. 2, pp. 866–876, 2013. (Cited on page 137)

[140] N. G. Paterakis, S. F. Santos, J. P. S. Catalao, O. Erdinc, and A. G. Bakirtzis, "Coordination of smart-household activities for the efficient operation of intelligent distribution systems," in *IEEE PES Innovative Smart Grid Technologies, Europe*. IEEE, oct 2014, pp. 1–6. (Cited on page 137)

[141] N. G. Paterakis, O. Erdinc, I. N. Pappi, A. G. Bakirtzis, and J. P. S. Catalao, "Coordinated Operation of a Neighborhood of Smart Households Comprising Electric Vehicles, Energy Storage and Distributed Generation," *IEEE Transactions on Smart Grid*, vol. 7, no. 6, pp. 2736–2747, 2016. (Cited on page 137)

[142] J. Rajasekharan and V. Koivunen, "Optimal Energy Consumption Model for Smart Grid Households With Energy Storage," *IEEE Journal of Selected Topics in Signal Processing*, vol. 8, no. 6, pp. 1154–1166, 2014. (Cited on page 137)

[143] A. A. Hasib, N. Nikitin, and L. Natvig, "Cost-comfort balancing in a smart residential building with bidirectional energy trading," in *2015 Sustainable Internet and ICT for Sustainability (SustainIT)*, no. 7491. IEEE, apr 2015, pp. 1–6. (Cited on page 137)

[144] M. Castillo-Cagigal, E. Caamano-Martin, E. Matallanas, D. Masa-Bote, A. Gutierrez, F. Monasterio-Huelin, and J. Jimenez-Leube, "PV self-consumption optimization with storage and Active DSM for the residential sector," *Solar Energy*, vol. 85, no. 9, pp. 2338–2348, 2011. (Cited on page 137)

[145] J. Hoppmann, J. Volland, T. S. Schmidt, and V. H. Hoffmann, "The economic viability of battery storage for residential solar photovoltaic systems - A review and a simulation model," *Renewable and Sustainable Energy Reviews*, vol. 39, pp. 1101–1118, 2014. (Cited on page 137)

[146] E. L. Ratnam, S. R. Weller, and C. M. Kellett, "An optimization-based approach to scheduling residential battery storage with solar PV: Assessing customer benefit," *Renewable Energy*, vol. 75, pp. 123–134, 2015. (Cited on page 137)

[147] B.-G. Kim, S. Ren, M. van der Schaar, and J.-w. Lee, "Bidirectional Energy Trading and Residential Load Scheduling with Electric Vehicles in the Smart Grid," *IEEE Journal on Selected Areas in Communications*, vol. 31, no. 7, pp. 1219–1234, 2013. (Cited on page 137)

[148] M. R. Sarker, Y. Dvorkin, and M. A. Ortega-Vazquez, "Optimal participation of an electric vehicle aggregator in day-ahead energy and reserve markets," *IEEE Transactions on Power Systems*, vol. 31, no. 5, pp. 3506–3515, 2016. (Cited on page 137)

[149] N. G. Paterakis, M. F. Medeiros, J. P. S. Catalao, and O. Erdinc, "Distribution system operation enhancement through household consumption coordination in a dynamic pricing environment," in *2015 IEEE Eindhoven PowerTech*. Eindhoven, Netherlands: IEEE, jun 2015, pp. 1–6. (Cited on pages 137 and 138)

[150] B. Celik, R. Roche, D. Bouquain, and A. Miraoui, "Coordinated energy management using agents in neighborhood areas with RES and storage," in *2016 IEEE International Energy Conference (ENERGYCON)*. IEEE, apr 2016, pp. 1–6. (Cited on page 138)

[151] N. Yaagoubi and H. T. Mouftah, "A distributed game theoretic approach to energy trading in the smart grid," in *2015 IEEE Electrical Power and Energy Conference (EPEC)*. IEEE, oct 2015, pp. 203–208. (Cited on page 138)

[152] M. Juelsgaard, A. Teixeira, M. Johansson, R. Wisniewski, and J. Bendtsen, "Distributed coordination of household electricity consumption," in *2014 IEEE Conf. on Control Applications (CCA)*. IEEE, oct 2014, pp. 33–40. (Cited on page 138)

[153] T. Rodrigues, R. Moreira, and G. Strbac, "Coordinated operation of distributed energy storage in low carbon networks," in *2017 IEEE Power & Energy Society General Meeting*, no. July. Chicago, IL: IEEE, jul 2017, pp. 1–5. (Cited on page 138)

Appendix A

Assessment Model for Deterministic Bids

Chapter 2 presents a deterministic model to determine the day-ahead energy and AS bids for the independent operation of ESS and WF. In this model, uncertain parameters such as prices and wind generation forecasts were characterized by their expected value. However, it is widely documented in current literature that deterministic models are inadequate for optimizing against uncertainty as it may lead to undesirable outcomes and, consequently, lower profits than originally expected.

This appendix presents a stochastic equivalent for the model presented in Section 2.3 in order to assess the performance of the deterministic bids calculated in Section 2.4, which were solely based on the expected values for the uncertainty parameters (energy and AS prices, and wind power availability), when exposed to uncertainty when calculating the expected profits.

A.1 Nomenclature

A.1.1 Indices, Sets and Sub-Sets

$e \in S^{\mathrm{E}}$	Day-ahead energy price forecasts.
$a \in S^{\mathrm{A}}$	Day-ahead AS price forecasts.
$w \in S^{\mathrm{W}}$	Day-ahead available wind power forecasts.
$h \in H$	Time periods.
Ω^{BV}	Set of all binary decision variables.
$\Omega^{\mathrm{CV}^{+}}$	Set of all positive continuous decision variables.
Ω^{CV}	Set of all continuous decision variables.

A.1.2 Parameters

K^{W}	WF generation capacity [MW].
$\mathrm{P}^{\mathrm{AV}}_{w,h}$	Wind power available at forecast w and time period h [p.u.].
η	Roundtrip efficiency of the conversion unit [p.u.].
$\overline{\mathrm{P}}$	Maximum charge/discharge rate of the ESS [MW].
$\overline{\mathrm{E}}$	Energy capacity of the ESS [MWh].

$\pi^{\text{En}}_{e,h}$ Energy market price at forecast e and time period h [£/MWh].

$\pi^{\text{AS-Up}}_{a,h}$ Upward AS market price at forecast a and time period h [£/MW/h].

$\pi^{\text{AS-Dw}}_{a,h}$ Downward AS market price at forecast a and time period h [£/MW/h].

τ^{AS} Maximum duration of ancillary service requirement [h].

$\underline{\text{AS}}^{\text{Up/Dw}}$ Minimum level for upward/downward ancillary service provision [MW].

ρ_e, ρ_a, ρ_w Probability of each forecast e, a and w [p.u.].

$\omega^{\text{En}^{+/-}}_{e,h}$ Price Penalty factor for positive/negative energy imbalances at forecast e and time period h [p.u.].

$\omega^{\text{AS}^{+/-}}_{a,h}$ Price Penalty factor for positive/negative ancillary service imbalances at forecast a and time period h [p.u.].

$\text{X}^{\text{En,ESS}}_{h}$ Deterministic day-ahead energy bid for the ESS [MWh].

$\text{X}^{\text{AS,Up,ESS}}_{h}$ Deterministic day-ahead upward BS bid for the ESS [MW].

$\text{X}^{\text{AS,Dw,ESS}}_{h}$ Deterministic day-ahead downward BS bid for the ESS [MW].

$\text{X}^{\text{En,W}}_{h}$ Deterministic day-ahead energy bid for the WF [MWh].

$\text{X}^{\text{AS,Up,W}}_{h}$ Deterministic day-ahead upward BS bid for the WF [MW].

$\text{X}^{\text{AS,Dw,W}}_{h}$ Deterministic day-ahead downward BS bid for the WF [MW].

M Large number for constraint relaxation.

A.1.3 Binary Variables

$Q^{\text{Up,D/C}}_{e,a,w,h}$ Commitment of upward AS in discharging/charging mode for scenario e,a,w at time period h.

$Q^{\text{Dw,D/C}}_{e,a,w,h}$ Commitment of downward AS in discharging/charging mode for scenario e,a,w at time period h.

A.1.4 Continuous Variables

$e_{e,a,w,h}$ Energy stored in the ESS at time period h [MWh].

$p^{\text{C}}_{e,a,w,h}$ Power consumed by the ESS for scenario e,a,w at time period h [MW].

$p^{\text{D}}_{e,a,w,h}$ Power generated by the ESS for scenario e,a,w at time period h [MW].

$p^{\text{W}}_{e,a,w,h}$ Power output of the WF for scenario e,a,w at time period h [MW].

$r^{\text{Up,D}}_{e,a,w,h}$ Upward AS contribution by the ESS during discharging for scenario e,a,w at time period h [MW].

$r^{\text{Dw,D}}_{e,a,w,h}$ Downward AS contribution by the ESS during discharging for scenario e,a,w at time period h [MW].

$r^{\text{Up,C}}_{e,a,w,h}$ Upward AS contribution by the ESS during charging for scenario e,a,w at time period h [MW].

$r^{\text{Dw,C}}_{e,a,w,h}$ Downward AS contribution by the ESS during charging for scenario e,a,w at time period h [MW].

$r^{\text{Up,ESS}}_{e,a,w,h}$ Total Upward AS contribution by the ESS for scenario e,a,w at time period h [MW].

$r^{\text{Dw,ESS}}_{e,a,w,h}$ Total Downward AS contribution by the ESS for scenario e,a,w at time period h [MW].

$r^{\text{Up,W}}_{e,a,w,h}$ Upward AS contribution of the WF for scenario e,a,w at time period h [MW].

$r^{\text{Dw,W}}_{e,a,w,h}$ Downward AS contribution of the WF for scenario e,a,w at time period h [MW].

$i^{\text{En,ESS}^{+/-}}_{e,a,w,h}$ Positive/Negative ESS energy deviation from the day-ahead bid at scenario e,a,w, and time period h [MW].

$i^{\text{AS,Up,ESS}^{+/-}}_{e,a,w,h}$ Positive/Negative ESS upward AS deviation from the day-ahead bid at scenario e,a,w, and time period h [MW].

$i^{\text{AS,Dw,ESS}^{+/-}}_{e,a,w,h}$ Positive/Negative ESS downward AS deviation from the day-ahead bid at scenario e,a,w, and time period h [MW].

$i^{\text{En,W}^{+/-}}_{e,a,w,h}$ Positive/Negative WF energy deviation from the day-ahead bid at scenario e,a,w, and time period h [MW].

$i^{\text{AS,Up,W}^{+/-}}_{e,a,w,h}$ Positive/Negative AS upward AS deviation from the day-ahead bid at scenario e,a,w, and time period h [MW].

$i^{\text{AS,Dw,W}^{+/-}}_{e,a,w,h}$ Positive/Negative AS downward AS deviation from the day-ahead bid at scenario e,a,w, and time period h [MW].

A.2 Mathematical Formulation

A.2.1 Keys properties and assumptions

The underlying assumption for this model is that, despite the bids not being optimized against uncertainty, the operators of the WF and ESS are given the opportunity to correct deviations from the day-ahead bids through the balancing market. This settlement schemes allows either party to sell excess energy or pay for energy not delivered by using a pair of cash-out prices similar to the System-Buy-Price/System-Sell-Prices in the UK. For simplicity's sake, these are assumed to be directly related to the day-ahead energy market prices through positive and negative penalty factors $\left(\omega^{\text{En/AS}^{+/-}}_{e/a,h}\right)$. The same concept is applied to AS bids, in which failure to provide the volume in the day-ahead bid is penalized over the market price.

This model looks to optimize the recourse stage in which both facilities seek to mitigate the exposure to uncertainty. In order to achieve such objective, a single-stage stochastic model is constructed. Considering the different sources of uncertainty (prices and wind power availability), a scenario for this model is constructed by superimposing all possible values for each energy price e, ancillary service price a and wind power availability w and calculating the respective scenario probability $(\rho_e \times \rho_a \times \rho_w)$.

A.2.2 Objective function

$$
\begin{aligned}
\underset{\substack{\Omega^{\mathrm{BV}},\Omega^{\mathrm{CV}^+},\\ \Omega^{\mathrm{SCV}^+},\Omega^{\mathrm{CV}^{\mathrm{SOS1}}}}}{\text{Maximize}} \Bigg\{ & \sum_{e\in S^{\mathrm{E}}}\sum_{a\in S^{\mathrm{A}}}\sum_{w\in S^{\mathrm{W}}} \rho_e\,\rho_a\,\rho_w \Bigg[\sum_{h\in H} \Big(\pi^{\mathrm{En}}_{e,h} \mathrm{X}^{\mathrm{En,ESS}}_{h} + \omega^{\mathrm{En}^+}_{e,h}\,\pi^{\mathrm{En}}_{e,h}\,i^{\mathrm{En,ESS}^+}_{e,a,w,h} - \omega^{\mathrm{En}^-}_{e,h}\,\pi^{\mathrm{En}}_{e,h}\,i^{\mathrm{En,ESS}^-}_{e,a,w,h} \\
& + \pi^{\mathrm{AS,Up}}_{a,h} \mathrm{X}^{\mathrm{AS,Up,ESS}}_{h} + \omega^{\mathrm{AS}^+}_{a,h}\,\pi^{\mathrm{AS,Up}}_{a,h}\,i^{\mathrm{AS,Up,ESS}^+}_{e,a,w,h} - \omega^{\mathrm{AS}^-}_{a,h}\,\pi^{\mathrm{AS,Up}}_{a,h}\,i^{\mathrm{AS,Up,ESS}^-}_{e,a,w,h} \\
& + \pi^{\mathrm{AS,Dw}}_{a,h} \mathrm{X}^{\mathrm{AS,Dw,ESS}}_{h} + \omega^{\mathrm{AS}^+}_{a,h}\,\pi^{\mathrm{AS,Dw}}_{a,h}\,i^{\mathrm{AS,Dw,ESS}^+}_{e,a,w,h} - \omega^{\mathrm{AS}^-}_{a,h}\,\pi^{\mathrm{AS,Dw}}_{a,h}\,i^{\mathrm{AS,Dw,ESS}^-}_{e,a,w,h} \Big) \\
& + \sum_{h\in H} \Big(\pi_{e,h}{}^{\mathrm{En}} \mathrm{X}^{\mathrm{En,WF}}_{h} + \omega^{\mathrm{En}^+}_{e,h}\,\pi^{\mathrm{En}}_{e,h}\,i^{\mathrm{En,WF}^+}_{e,a,w,h} - \omega^{\mathrm{En}^-}_{e,h}\,\pi^{\mathrm{En}}_{e,h}\,i^{\mathrm{En,WF}^-}_{e,a,w,h} \\
& + \pi^{\mathrm{AS,Up}}_{a,h} \mathrm{X}^{\mathrm{AS,Up,WF}}_{h} + \omega^{\mathrm{AS}^+}_{a,h}\,\pi^{\mathrm{AS,Up}}_{a,h}\,i^{\mathrm{AS,Up,WF}^+}_{e,a,w,h} - \omega^{\mathrm{AS}^-}_{a,h}\,\pi^{\mathrm{AS,Up}}_{a,h}\,i^{\mathrm{AS,Up,WF}^-}_{e,a,w,h} \\
& + \pi^{\mathrm{AS,Dw}}_{a,h} \mathrm{X}^{\mathrm{AS,Dw,WF}}_{h} + \omega^{\mathrm{AS}^+}_{a,h}\,\pi^{\mathrm{AS,Dw}}_{a,h}\,i^{\mathrm{AS,Dw,WF}^+}_{e,a,w,h} - \omega^{\mathrm{AS}^-}_{a,h}\,\pi^{\mathrm{AS,Dw}}_{a,h}\,i^{\mathrm{AS,Dw,WF}^-}_{e,a,w,h} \Big) \Bigg] \Bigg\}.
\end{aligned}
\tag{A.1}
$$

The objective function (A.1) seeks to maximize the expected market's profit for both facilities using the bids determined by the model presented in Section 2.3 $\left(\mathrm{X}^{\mathrm{En,ESS/WF}}_{h}, \mathrm{X}^{\mathrm{AS\text{-}Up,ESS/WF}}_{h} \text{ and } \mathrm{X}^{\mathrm{AS\text{-}Dw,ESS/WF}}_{h}\right)$ for all scenarios, given the probability for each forecast (ρ_e, ρ_a, ρ_w). The ESS's profit is calculated in lines 1 through 3, while the WF's profit is calculated in lines 4 to 6. Each facility's profit is calculated as the sum of the day-ahead market revenue $(1^{\mathrm{st}}\,\text{term})$ and the revenue from excess generation/provided ancillary service $\left(2^{\mathrm{nd}}\,\text{term}\right)$ minus the shortage cost $\left(3^{\mathrm{rd}}\,\text{term}\right)$.

A.2.3 Model Constraints

A.2.3.1 Energy and AS market operation

Given the stochastic nature of this model, all constraints in the previous model are now scenario dependent. Constraints (2.5) to (2.31) are transformed to their scenario-dependent counterparts in constraints (A.2) to (A.28). Wind power generation this time, is limited the available wind power for each forecast w in constraints (A.6) for all scenarios.

$$p^{\mathrm{C}}_{e,a,w,h} \le \overline{\mathrm{P}}, \quad \forall e,a,w,h, \tag{A.2}$$

$$p^{\mathrm{D}}_{e,a,w,h} \le \overline{\mathrm{P}}, \quad \forall e,a,w,h, \tag{A.3}$$

$$e_{e,a,w,h} = e_{e,a,w,h-1} + \eta\, p^{\mathrm{C}}_{e,a,w,h} - p^{D}_{e,a,w,h}, \quad \forall e,a,w,h, \tag{A.4}$$

$$e_{e,a,w,h} \le \overline{\mathrm{E}}, \quad \forall e,a,w,h, \tag{A.5}$$

$$p^{\mathrm{W}}_{e,a,w,h} \le \mathrm{P}^{\mathrm{AV}}_{w,h}\mathrm{K}^{\mathrm{W}}, \quad \forall e,a,w,h. \tag{A.6}$$

$$p^{\mathrm{C}}_{e,a,w,h} + r^{\mathrm{Dw,C}}_{e,a,w,h} \le \overline{\mathrm{P}}, \quad \forall e,a,w,h, \tag{A.7}$$

$$r^{\mathrm{Up,C}}_{e,a,w,h} \le p^{\mathrm{C}}_{e,a,w,h}, \quad \forall e,a,w,h, \tag{A.8}$$

$$p^{\mathrm{D}}_{e,a,w,h} + r^{\mathrm{Up,D}}_{e,a,w,h} \le \overline{\mathrm{P}}, \quad \forall e,a,w,h, \tag{A.9}$$

$$r^{\mathrm{Dw,D}}_{e,a,w,h} \le p^{\mathrm{D}}_{e,a,w,h}, \quad \forall e,a,w,h, \tag{A.10}$$

$$r_{e,a,w,h}^{\mathrm{Up,ESS}} = r_{e,a,w,h}^{\mathrm{Up,C}} + r_{e,a,w,h}^{\mathrm{Up,D}}, \quad \forall e,a,w,h, \tag{A.11}$$

$$r_{e,a,w,h}^{\mathrm{Up,ESS}} \leq \begin{cases} 2\overline{\mathrm{P}} & , r_{e,a,w,h}^{\mathrm{Up,C}} + r_{e,a,w,h}^{\mathrm{Up,D}} \geq \underline{\mathrm{AS}}^{\mathrm{Up}} \\ 0 & , r_{e,a,w,h}^{\mathrm{Up,C}} + r_{e,a,w,h}^{\mathrm{Up,D}} < \underline{\mathrm{AS}}^{\mathrm{Up}} \end{cases}, \quad \forall e,a,w,h, \tag{A.12}$$

$$r_{e,a,w,h}^{\mathrm{Dw,ESS}} = r_{e,a,w,h}^{\mathrm{Dw,C}} + r_{e,a,w,h}^{\mathrm{Dw,D}}, \quad \forall e,a,w,h, \tag{A.13}$$

$$r_{e,a,w,h}^{\mathrm{Dw,ESS}} \leq \begin{cases} 2\overline{\mathrm{P}} & , r_{e,a,w,h}^{\mathrm{Dw,C}} + r_{e,a,w,h}^{\mathrm{Dw,D}} \geq \underline{\mathrm{AS}}^{\mathrm{Dw}} \\ 0 & , r_{e,a,w,h}^{\mathrm{Dw,C}} + r_{e,a,w,h}^{\mathrm{Dw,D}} < \underline{\mathrm{AS}}^{\mathrm{Dw}} \end{cases}, \quad \forall e,a,w,h, \tag{A.14}$$

$$p_{e,a,w,h}^{\mathrm{W}} + r_{e,a,w,h}^{\mathrm{Up,W}} \leq \mathrm{P}_{w,h}^{\mathrm{AV}} \mathrm{K}^{\mathrm{W}}, \quad \forall e,a,w,h, \tag{A.15}$$

$$r_{e,a,w,h}^{\mathrm{Up,W}} \leq \begin{cases} \mathrm{K}^{\mathrm{W}} & , r_{e,a,w,h}^{\mathrm{Up,W}} \geq \underline{\mathrm{AS}}^{\mathrm{Up}} \\ 0 & , r_{e,a,w,h}^{\mathrm{Up,W}} < \underline{\mathrm{AS}}^{\mathrm{Up}} \end{cases}, \quad \forall e,a,w,h, \tag{A.16}$$

$$r_{e,a,w,h}^{\mathrm{Dw,W}} \leq p_{e,a,w,h}^{\mathrm{W}}, \quad \forall e,a,w,h. \tag{A.17}$$

$$r_{e,a,w,h}^{\mathrm{Dw,W}} \leq \begin{cases} \mathrm{K}^{\mathrm{W}} & , r_{e,a,w,h}^{\mathrm{Dw,W}} \geq \underline{\mathrm{AS}}^{\mathrm{Dw}} \\ 0 & , r_{e,a,w,h}^{\mathrm{Dw,W}} < \underline{\mathrm{AS}}^{\mathrm{Dw}} \end{cases}, \quad \forall e,a,w,h, \tag{A.18}$$

$$-\mathrm{M}\left(1 - Q_{e,a,w,h}^{\mathrm{Up,D}}\right) \leq e_{e,a,w,h-1} + \eta\, p_{e,a,w,h}^{\mathrm{C}} - \left(p_{e,a,w,h}^{\mathrm{D}} + r_{e,a,w,h}^{\mathrm{Up,D}}\right)\tau^{\mathrm{AS}} \leq \overline{\mathrm{E}} + \mathrm{M}\left(1 - Q_{e,a,w,h}^{\mathrm{Up,D}}\right), \quad \forall e,a,w,h, \tag{A.19}$$

$$-\mathrm{M}\left(1 - Q_{e,a,w,h}^{\mathrm{Dw,D}}\right) \leq e_{e,a,w,h-1} + \eta\, p_{e,a,w,h}^{\mathrm{C}} - \left(p_{e,a,w,h}^{\mathrm{D}} - r_{e,a,w,h}^{\mathrm{Dw,D}}\right)\tau^{\mathrm{AS}} \leq \overline{\mathrm{E}} + \mathrm{M}\left(1 - Q_{e,a,w,h}^{\mathrm{Dw,D}}\right), \quad \forall e,a,w,h, \tag{A.20}$$

$$-\mathrm{M}\left(1 - Q_{e,a,w,h}^{\mathrm{Up,C}}\right) \leq e_{e,a,w,h-1} + \eta\left(p_{e,a,w,h}^{\mathrm{C}} - r_{e,a,w,h}^{\mathrm{Up,C}}\right)\tau^{\mathrm{AS}} - p_{e,a,w,h}^{\mathrm{D}} \leq \overline{\mathrm{E}} + \mathrm{M}\left(1 - Q_{e,a,w,h}^{\mathrm{Up,C}}\right), \quad \forall e,a,w,h, \tag{A.21}$$

$$-\mathrm{M}\left(1 - Q_{e,a,w,h}^{\mathrm{Dw,C}}\right) \leq e_{e,a,w,h-1} + \eta\left(p_{e,a,w,h}^{\mathrm{C}} + r_{e,a,w,h}^{\mathrm{Dw,C}}\right)\tau^{\mathrm{AS}} - p_{e,a,w,h}^{\mathrm{D}} \leq \overline{\mathrm{E}} + \mathrm{M}\left(1 - Q_{e,a,w,h}^{\mathrm{Dw,C}}\right), \quad \forall e,a,w,h, \tag{A.22}$$

$$r_{e,a,w,h}^{\mathrm{Up,D}} \leq \mathrm{M}\, Q_{e,a,w,h}^{\mathrm{Up,D}}, \quad \forall e,a,w,h, \tag{A.23}$$

$$r_{e,a,w,h}^{\mathrm{Dw,D}} \leq \mathrm{M}\, Q_{e,a,w,h}^{\mathrm{Dw,D}}, \quad \forall e,a,w,h, \tag{A.24}$$

$$r_{e,a,w,h}^{\mathrm{Up,C}} \leq \mathrm{M}\, Q_{e,a,w,h}^{\mathrm{Up,C}}, \quad \forall e,a,w,h, \tag{A.25}$$

$$r_{e,a,w,h}^{\mathrm{Dw,C}} \leq \mathrm{M}\, Q_{e,a,w,h}^{\mathrm{Dw,C}}, \quad \forall e,a,w,h, \tag{A.26}$$

$$p^{\mathrm{W}}_{e,a,w,t} + r^{\mathrm{Up,W}}_{e,a,w,h} \leq \mathrm{P}^{\mathrm{AV}}_{w,t}\mathrm{K}^{\mathrm{W}} + \overline{\mathrm{P}}, \quad \forall e,a,w,h,\, h \leq t < h + \tau^{\mathrm{AS}}, \tag{A.27}$$

$$p^{\mathrm{W}}_{e,a,w,t} - r^{\mathrm{Dw,W}}_{e,a,w,h} \leq 0, \quad \forall e,a,w,h,\, h \leq t < h + \tau^{\mathrm{AS}}. \tag{A.28}$$

A.2.3.2 Energy and AS Bids

As the energy and AS bids are pre-determined in this case, the objective of constraints (A.29) to (A.34) is to calculate excess $\left(i^{\mathrm{En/AS,ESS/WF^{+}}}_{e,a,w,h}\right)$ and shortage $\left(i^{\mathrm{En/AS,ESS/WF^{-}}}_{e,a,w,h}\right)$ quantities for both facilities and respective markets. It should be noted that these quantities represent recourse actions taken once the outcome of the uncertain parameters is revealed. Considering that each of these variables is non-negative, it must ensured that only one variable is positive for each facility, market and time period. This can be achieved by defining each imbalance related variables $\left(\text{e.g., } i^{\mathrm{En,ESS^{+}}}_{e,a,w,h} \text{ and } i^{\mathrm{En,ESS^{-}}}_{e,a,w,h}\right)$ as SOS1 variables.

$$p^{\mathrm{D}}_{e,a,w,h} - p^{\mathrm{C}}_{e,a,w,h} - \mathrm{X}^{\mathrm{En,ESS}}_{h} = i^{\mathrm{En,ESS^{+}}}_{e,a,w,h} - i^{\mathrm{En,ESS^{-}}}_{e,a,w,h}, \quad \forall e,a,w,h. \tag{A.29}$$

$$r^{\mathrm{Up,D}}_{e,a,w,h} + r^{\mathrm{Up,C}}_{e,a,w,h} - \mathrm{X}^{\mathrm{AS\text{-}Up,ESS}}_{h} = i^{\mathrm{AS,Up,ESS^{+}}}_{e,a,w,h} - i^{\mathrm{AS,Up,ESS^{-}}}_{e,a,w,h}, \quad \forall e,a,w,h. \tag{A.30}$$

$$r^{\mathrm{Dw,D}}_{e,a,w,h} + r^{\mathrm{Dw,C}}_{e,a,w,h} - \mathrm{X}^{\mathrm{AS,Dw,ESS}}_{h} = i^{\mathrm{AS,Dw,ESS^{+}}}_{e,a,w,h} - i^{\mathrm{AS,Dw,ESS^{-}}}_{e,a,w,h}, \quad \forall e,a,w,h. \tag{A.31}$$

$$p^{\mathrm{W}}_{e,a,w,h} - \mathrm{X}^{\mathrm{En,WF}}_{h} = i^{\mathrm{En,WF^{+}}}_{e,a,w,h} - i^{\mathrm{En,WF^{-}}}_{e,a,w,h}, \quad \forall e,a,w,h. \tag{A.32}$$

$$r^{\mathrm{Up,W}}_{e,a,w,h} - \mathrm{X}^{\mathrm{AS,Up,WF}}_{h} = i^{\mathrm{AS,Up,WF^{+}}}_{e,a,w,h} - i^{\mathrm{AS,Up,WF^{-}}}_{e,a,w,h}, \quad \forall e,a,w,h. \tag{A.33}$$

$$r^{\mathrm{Dw,D}}_{e,a,w,h} + r^{\mathrm{Dw,C}}_{e,a,w,h} - \mathrm{X}^{\mathrm{AS\text{-}Dw,WF}}_{h} = i^{\mathrm{AS,Dw,WF^{+}}}_{e,a,w,h} - i^{\mathrm{AS,Dw,WF^{-}}}_{e,a,w,h}, \quad \forall e,a,w,h. \tag{A.34}$$

A.2.3.3 Variables types

Lastly, variables types are defined in constraints (A.35) to (A.38).

$$\Omega^{\mathrm{BV}} = \left\{ Q^{\mathrm{Up,D}}_{e,a,w,h}, Q^{\mathrm{Dw,D}}_{e,a,w,h}, Q^{\mathrm{Up,C}}_{e,a,w,h}, Q^{\mathrm{Dw,C}}_{e,a,w,h} \right\} \in \{0,1\}, \quad \forall h, \tag{A.35}$$

$$\Omega^{\mathrm{SCV^{+}}} = \left\{ r^{\mathrm{Up,ESS}}_{e,a,w,h}, r^{\mathrm{Dw,ESS}}_{e,a,w,h}, r^{\mathrm{Up,W}}_{e,a,w,h}, r^{\mathrm{Dw,W}}_{e,a,w,h} \right\} \in \mathbb{R}_{\geq 0}, \quad \forall e,a,w,h, \tag{A.36}$$

$$\Omega^{\mathrm{CV^{+}}} = \left\{ p^{\mathrm{W}}_{e,a,w,h}, e_{e,a,w,h}, r^{\mathrm{Up,D}}_{e,a,w,h}, r^{\mathrm{Up,C}}_{e,a,w,h}, r^{\mathrm{Dw,D}}_{e,a,w,h}, r^{\mathrm{Dw,C}}_{e,a,w,h}, \right\} \in \mathbb{R}_{\geq 0}, \quad \forall e,a,w,h. \tag{A.37}$$

$$\begin{aligned} \Omega^{\mathrm{CV^{SOS1}}} = \Big\{ & p^{\mathrm{D}}_{e,a,w,h}, p^{\mathrm{C}}_{e,a,w,h}, i^{\mathrm{En,ESS^{+}}}_{e,a,w,h}, i^{\mathrm{En,ESS^{-}}}_{e,a,w,h}, i^{\mathrm{AS\text{-}Up,ESS^{+}}}_{e,a,w,h}, i^{\mathrm{AS\text{-}Up,ESS^{-}}}_{e,a,w,h}, i^{\mathrm{AS\text{-}Dw,ESS^{+}}}_{e,a,w,h}, i^{\mathrm{AS\text{-}Dw,ESS^{-}}}_{e,a,w,h}, \\ & i^{\mathrm{En,WF^{+}}}_{e,a,w,h}, i^{\mathrm{En,WF^{-}}}_{e,a,w,h}, i^{\mathrm{AS\text{-}Up,WF^{+}}}_{e,a,w,h}, i^{\mathrm{AS\text{-}Up,WF^{-}}}_{e,a,w,h}, i^{\mathrm{AS\text{-}Dw,WF^{+}}}_{e,a,w,h}, i^{\mathrm{AS\text{-}Dw,WF^{-}}}_{e,a,w,h} \Big\} \in \mathbb{R}_{\geq 0}, \quad \forall e,a,w,h. \end{aligned} \tag{A.38}$$

Appendix B

Full List of Expressions used in the Progressive Hedging Algorithm

This appendix presents a complete description of the generalized equations (5.83) through (5.94) in Subsection 5.4.2 for the power and energy capacities of the ESS, day-ahead Energy, SPR-Up, SPR-Dw, FR-Up and FR-Dw bids and associated profit VaR.

Section B.5 presents a generalized piecewise linear approximation for the proximal terms in objective function (5.82) for the day-ahead bids, power and energy capacities of the ESS and each source of profit VaR.

B.1 Aggregation of Decision Variables

$$\hat{x}^{\mathrm{En(i)}}_{d,h} = \sum_{e\in S^{\mathrm{E}}}\sum_{r\in S^{\mathrm{R}}}\sum_{f\in S^{\mathrm{F}}}\sum_{w\in S^{\mathrm{W}}} \rho_e \rho_r \rho_f \rho_w x^{\mathrm{En(i)}}_{d,e,r,f,w,h}, \quad \forall i,d,h, \tag{B.1}$$

$$\hat{x}^{\mathrm{SPR,Up(i)}}_{d,h} = \sum_{e\in S^{\mathrm{E}}}\sum_{r\in S^{\mathrm{R}}}\sum_{f\in S^{\mathrm{F}}}\sum_{w\in S^{\mathrm{W}}} \rho_e \rho_r \rho_f \rho_w x^{\mathrm{SPR,Up(i)}}_{d,e,r,f,w,h}, \quad \forall i,d,h, \tag{B.2}$$

$$\hat{x}^{\mathrm{SPR,Dw(i)}}_{d,h} = \sum_{e\in S^{\mathrm{E}}}\sum_{r\in S^{\mathrm{R}}}\sum_{f\in S^{\mathrm{F}}}\sum_{w\in S^{\mathrm{W}}} \rho_e \rho_r \rho_f \rho_w x^{\mathrm{SPR,Dw(i)}}_{d,e,r,f,w,h}, \quad \forall i,d,h, \tag{B.3}$$

$$\hat{x}^{\mathrm{FR,Up(i)}}_{d,h} = \sum_{e\in S^{\mathrm{E}}}\sum_{r\in S^{\mathrm{R}}}\sum_{f\in S^{\mathrm{F}}}\sum_{w\in S^{\mathrm{W}}} \rho_e \rho_r \rho_f \rho_w x^{\mathrm{FR,Up(i)}}_{d,e,r,f,w,h}, \quad \forall i,d,h, \tag{B.4}$$

$$\hat{x}^{\mathrm{FR,Dw(i)}}_{d,h} = \sum_{e\in S^{\mathrm{E}}}\sum_{r\in S^{\mathrm{R}}}\sum_{f\in S^{\mathrm{F}}}\sum_{w\in S^{\mathrm{W}}} \rho_e \rho_r \rho_f \rho_w x^{\mathrm{FR,Dw(i)}}_{d,e,r,f,w,h}, \quad \forall i,d,h, \tag{B.5}$$

$$\hat{K}^{\mathrm{P(i)}} = \sum_{e\in S^{\mathrm{E}}}\sum_{r\in S^{\mathrm{R}}}\sum_{f\in S^{\mathrm{F}}}\sum_{w\in S^{\mathrm{W}}} \rho_e \rho_r \rho_f \rho_w K^{\mathrm{P(i)}}_{e,r,f,w}, \quad \forall i, \tag{B.6}$$

$$\hat{K}^{\mathrm{E(i)}} = \sum_{e\in S^{\mathrm{E}}}\sum_{r\in S^{\mathrm{R}}}\sum_{f\in S^{\mathrm{F}}}\sum_{w\in S^{\mathrm{W}}} \rho_e \rho_r \rho_f \rho_w K^{\mathrm{E(i)}}_{e,r,f,w}, \quad \forall i, \tag{B.7}$$

$$\hat{\zeta}^{\mathrm{En(i)}} = \sum_{e\in S^{\mathrm{E}}}\sum_{r\in S^{\mathrm{R}}}\sum_{f\in S^{\mathrm{F}}}\sum_{w\in S^{\mathrm{W}}} \rho_e \rho_r \rho_f \rho_w \zeta^{\mathrm{En(i)}}_{e,r,f,w}, \quad \forall i, \tag{B.8}$$

$$\hat{\zeta}^{\text{SPR,Up(i)}} = \sum_{e\in S^{\text{E}}}\sum_{r\in S^{\text{R}}}\sum_{f\in S^{\text{F}}}\sum_{w\in S^{\text{W}}} \rho_e \rho_r \rho_f \rho_w \zeta^{\text{SPR,Up(i)}}_{e,r,f,w}, \quad \forall i, \tag{B.9}$$

$$\hat{\zeta}^{\text{SPR,Dw(i)}} = \sum_{e\in S^{\text{E}}}\sum_{r\in S^{\text{R}}}\sum_{f\in S^{\text{F}}}\sum_{w\in S^{\text{W}}} \rho_e \rho_r \rho_f \rho_w \zeta^{\text{SPR,Dw(i)}}_{e,r,f,w}, \quad \forall i, \tag{B.10}$$

$$\hat{\zeta}^{\text{FR,Up(i)}} = \sum_{e\in S^{\text{E}}}\sum_{r\in S^{\text{R}}}\sum_{f\in S^{\text{F}}}\sum_{w\in S^{\text{W}}} \rho_e \rho_r \rho_f \rho_w \zeta^{\text{FR,Up(i)}}_{e,r,f,w}, \quad \forall i, \tag{B.11}$$

$$\hat{\zeta}^{\text{FR,Dw(i)}} = \sum_{e\in S^{\text{E}}}\sum_{r\in S^{\text{R}}}\sum_{f\in S^{\text{F}}}\sum_{w\in S^{\text{W}}} \rho_e \rho_r \rho_f \rho_w \zeta^{\text{FR,Dw(i)}}_{e,r,f,w}, \quad \forall i, \tag{B.12}$$

B.2 Calculation of Lagrange multipliers

$$m^{\text{En(i)}}_{d,e,r,f,w,h} = m^{\text{En(i-1)}}_{d,e,r,f,w,h} + \lambda^{\text{En(i)}}_{d,h}\left(x^{\text{En(i)}}_{d,e,r,f,w,h} - \hat{x}^{\text{En(i)}}_{d,h}\right), \quad \forall d,e,r,f,w,h,i>0 \tag{B.13}$$

$$m^{\text{SPR,Up(i)}}_{d,e,r,f,w,h} = m^{\text{SPR,Up(i-1)}}_{d,e,r,f,w,h} + \lambda^{\text{SPR,Up(i)}}_{d,h}\left(x^{\text{SPR,Up(i)}}_{d,e,r,f,w,h} - \hat{x}^{\text{SPR,Up(i)}}_{d,h}\right), \quad \forall d,e,r,f,w,h,i>0 \tag{B.14}$$

$$m^{\text{SPR,Dw(i)}}_{d,e,r,f,w,h} = m^{\text{SPR,Dw(i-1)}}_{d,e,r,f,w,h} + \lambda^{\text{SPR,Dw(i)}}_{d,h}\left(x^{\text{SPR,Dw(i)}}_{d,e,r,f,w,h} - \hat{x}^{\text{SPR,Dw(i)}}_{d,h}\right), \quad \forall d,e,r,f,w,h,i>0 \tag{B.15}$$

$$m^{\text{FR,Up(i)}}_{d,e,r,f,w,h} = m^{\text{FR,Up(i-1)}}_{d,e,r,f,w,h} + \lambda^{\text{FR,Up(i)}}_{d,h}\left(x^{\text{FR,Up(i)}}_{d,e,r,f,w,h} - \hat{x}^{\text{FR,Up(i)}}_{d,h}\right), \quad \forall d,e,r,f,w,h,i>0 \tag{B.16}$$

$$m^{\text{FR,Dw(i)}}_{d,e,r,f,w,h} = m^{\text{FR,Dw(i-1)}}_{d,e,r,f,w,h} + \lambda^{\text{FR,Dw(i)}}_{d,h}\left(x^{\text{FR,Dw(i)}}_{d,e,r,f,w,h} - \hat{x}^{\text{FR,Dw(i)}}_{d,h}\right), \quad \forall d,e,r,f,w,h,i>0 \tag{B.17}$$

$$m^{\text{K,P(i)}}_{e,r,f,w} = m^{\text{K,P(i-1)}}_{e,r,f,w} + \lambda^{\text{K,P(i)}}\left(K^{\text{P(i)}}_{e,r,f,w} - \hat{K}^{\text{P(i)}}\right), \quad \forall e,r,f,w,i>0 \tag{B.18}$$

$$m^{\text{K,E(i)}}_{e,r,f,w} = m^{\text{K,E(i-1)}}_{e,r,f,w} + \lambda^{\text{K,E(i)}}\left(K^{\text{E(i)}}_{e,r,f,w} - \hat{K}^{\text{E(i)}}\right), \quad \forall e,r,f,w,i>0 \tag{B.19}$$

$$m^{\zeta,\text{En(i)}}_{e,r,f,w} = m^{\zeta,\text{En(i-1)}}_{e,r,f,w} + \lambda^{\zeta,\text{En(i)}}\left(\zeta^{\text{En(i)}}_{e,r,f,w} - \hat{\zeta}^{\text{En(i)}}\right), \quad \forall e,r,f,w,i>0 \tag{B.20}$$

$$m^{\zeta,\text{SPR,Up(i)}}_{e,r,f,w} = m^{\text{SPR,Up(i-1)}}_{e,r,f,w} + \lambda^{\zeta,\text{SPR,Up(i)}}\left(\zeta^{\text{SPR,Up(i)}}_{e,r,f,w} - \hat{\zeta}^{\text{SPR,Up(i)}}\right), \quad \forall e,r,f,w,i>0 \tag{B.21}$$

$$m^{\zeta,\text{SPR,Dw(i)}}_{e,r,f,w} = m^{\zeta,\text{SPR,Dw(i-1)}}_{e,r,f,w} + \lambda^{\zeta,\text{SPR,Dw(i)}}\left(\zeta^{\text{SPR,Dw(i)}}_{e,r,f,w} - \hat{\zeta}^{\text{SPR,Dw(i)}}\right), \quad \forall e,r,f,w,i>0 \tag{B.22}$$

$$m^{\zeta,\text{FR,Up(i)}}_{e,r,f,w} = m^{\zeta,\text{FR,Up(i-1)}}_{e,r,f,w} + \lambda^{\zeta,\text{FR,Up(i)}}\left(\zeta^{\text{FR,Up(i)}}_{e,r,f,w} - \hat{\zeta}^{\text{FR,Up(i)}}\right), \quad \forall e,r,f,w,i>0 \tag{B.23}$$

$$m_{e,r,f,w}^{\zeta,\mathrm{FR,Dw(i)}} = m_{e,r,f,w}^{\zeta,\mathrm{FR,Dw(i-1)}} + \lambda^{\zeta,\mathrm{FR,Dw(i)}} \left(\zeta_{e,r,f,w}^{\mathrm{FR,Dw(i)}} - \hat{\zeta}^{\mathrm{FR,Dw(i)}} \right), \quad \forall e,r,f,w,i>0 \tag{B.24}$$

B.3 Choice of Penalty factors $\lambda_{d,h}^{(.)(i)}$, $\lambda^{K,P/E(i)}$ and $\lambda^{\zeta,(.)(i)}$

$$\lambda_{d,h}^{\mathrm{En(i)}} = \frac{\sum_{e\in S^{\mathrm{E}}} \rho_e \pi_{d,e,h}^{\mathrm{En}}}{\max\left[\sum_{e\in S^{\mathrm{E}}} \sum_{r\in S^{\mathrm{R}}} \sum_{r\in S^{\mathrm{F}}} \sum_{w\in S^{\mathrm{W}}} \rho_e \rho_r \rho_f \rho_w \left(x_{d,e,r,f,w,h}^{\mathrm{En(i)}} - \hat{x}_{d,h}^{\mathrm{En(0)}} \right), 1 \right]}, \quad \forall d,h,i>0 \tag{B.25}$$

$$\lambda_{d,h}^{\mathrm{SPR,Up(i)}} = \frac{\sum_{r\in S^{\mathrm{R}}} \rho_r \pi_{d,r,h}^{\mathrm{SPR,Up}}}{\max\left[\sum_{e\in S^{\mathrm{E}}} \sum_{r\in S^{\mathrm{R}}} \sum_{r\in S^{\mathrm{F}}} \sum_{w\in S^{\mathrm{W}}} \rho_e \rho_r \rho_f \rho_w \left(x_{d,e,r,f,w,h}^{\mathrm{SPR,Up(i)}} - \hat{x}_{d,h}^{\mathrm{SPR,Up(0)}} \right), 1 \right]}, \quad \forall d,h,i>0 \tag{B.26}$$

$$\lambda_{d,h}^{\mathrm{SPR,Dw(i)}} = \frac{\sum_{r\in S^{\mathrm{R}}} \rho_r \pi_{d,er,h}^{\mathrm{SPR,Dw}}}{\max\left[\sum_{e\in S^{\mathrm{E}}} \sum_{r\in S^{\mathrm{R}}} \sum_{r\in S^{\mathrm{F}}} \sum_{w\in S^{\mathrm{W}}} \rho_e \rho_r \rho_f \rho_w \left(x_{d,e,r,f,w,h}^{\mathrm{SPR,Dw(i)}} - \hat{x}_{d,h}^{\mathrm{SPR,Dw(0)}} \right), 1 \right]}, \quad \forall d,h,i>0 \tag{B.27}$$

$$\lambda_{d,h}^{\mathrm{FR,Up(i)}} = \frac{\sum_{f\in S^{\mathrm{F}}} \rho_f \pi_{d,f,h}^{\mathrm{FR,Up}}}{\max\left[\sum_{e\in S^{\mathrm{E}}} \sum_{r\in S^{\mathrm{R}}} \sum_{r\in S^{\mathrm{F}}} \sum_{w\in S^{\mathrm{W}}} \rho_e \rho_r \rho_f \rho_w \left(x_{d,e,r,f,w,h}^{\mathrm{FR,Up(i)}} - \hat{x}_{d,h}^{\mathrm{FR,Up(0)}} \right), 1 \right]}, \quad \forall d,h,i>0 \tag{B.28}$$

$$\lambda_{d,h}^{\mathrm{FR,Dw(i)}} = \frac{\sum_{f\in S^{\mathrm{F}}} \rho_f \pi_{d,f,h}^{\mathrm{FR,Dw}}}{\max\left[\sum_{e\in S^{\mathrm{E}}} \sum_{r\in S^{\mathrm{R}}} \sum_{r\in S^{\mathrm{F}}} \sum_{w\in S^{\mathrm{W}}} \rho_e \rho_r \rho_f \rho_w \left(x_{d,e,r,f,w,h}^{\mathrm{FR,Dw(i)}} - \hat{x}_{d,h}^{\mathrm{FR,Dw(0)}} \right), 1 \right]}, \quad \forall d,h,i>0 \tag{B.29}$$

$$\lambda^{\mathrm{K,P(i)}} = \frac{\mathrm{C^P} \frac{\delta(1+\delta)^{\gamma}}{(1+\delta)^{\gamma}-1}}{\max\left[\sum_{e\in S^{\mathrm{E}}} \sum_{r\in S^{\mathrm{R}}} \sum_{r\in S^{\mathrm{F}}} \sum_{w\in S^{\mathrm{W}}} \rho_e \rho_r \rho_f \rho_w \left(K_{e,r,f,w}^{\mathrm{P(i)}} - \hat{K}^{\mathrm{P(0)}} \right), 1 \right]}, \quad \forall i>0 \tag{B.30}$$

$$\lambda^{\mathrm{K,E(i)}} = \frac{\mathrm{C^E} \frac{\delta(1+\delta)^{\gamma}}{(1+\delta)^{\gamma}-1}}{\max\left[\sum_{e\in S^{\mathrm{E}}} \sum_{r\in S^{\mathrm{R}}} \sum_{r\in S^{\mathrm{F}}} \sum_{w\in S^{\mathrm{W}}} \rho_e \rho_r \rho_f \rho_w \left(K_{e,r,f,w}^{\mathrm{E(i)}} - \hat{K}^{\mathrm{E(0)}} \right), 1 \right]}, \quad \forall i>0 \tag{B.31}$$

$$\lambda^{\zeta,\mathrm{En(i)}} = \frac{\mathrm{k}}{\max\left[\left(\zeta_{max}^{\mathrm{En(i)}} - \zeta_{min}^{\mathrm{En(i)}} \right), 1 \right]}, \quad \forall i>0 \tag{B.32}$$

$$\lambda^{\zeta,\mathrm{SPR,Up(i)}} = \frac{\mathrm{k}}{\max\left[\left(\zeta_{max}^{\mathrm{SPR,Up(i)}} - \zeta_{min}^{\mathrm{SPR,Up(i)}} \right), 1 \right]}, \quad \forall i>0 \tag{B.33}$$

$$\lambda^{\zeta,\mathrm{SPR,Dw(i)}} = \frac{\mathrm{k}}{\max\left[\left(\zeta_{max}^{\mathrm{SPR,Dw(i)}} - \zeta_{min}^{\mathrm{SPR,Dw(i)}} \right), 1 \right]}, \quad \forall i>0 \tag{B.34}$$

$$\lambda^{\zeta,\mathrm{FR,Up(i)}} = \frac{\mathrm{k}}{\max\left[\left(\zeta_{max}^{\mathrm{FR,Up(i)}} - \zeta_{min}^{\mathrm{FR,Up(i)}} \right), 1 \right]}, \quad \forall i>0 \tag{B.35}$$

$$\lambda^{\zeta,\mathrm{FR,Dw(i)}} = \frac{\mathrm{k}}{\max\left[\left(\zeta_{max}^{\mathrm{FR,Dw(i)}} - \zeta_{min}^{\mathrm{FR,Dw(i)}} \right), 1 \right]}, \quad \forall i>0 \tag{B.36}$$

B.4 Stopping Criteria

$$g^{\mathrm{En(i)}} = \sum_{e\in S^{\mathrm{E}}}\sum_{r\in S^{\mathrm{R}}}\sum_{r\in S^{\mathrm{F}}}\sum_{w\in S^{\mathrm{W}}} \rho_e\rho_r\rho_f\rho_w \frac{\sum_{d\in D}\sum_{h\in H}\left|x^{\mathrm{En(i)}}_{d,e,r,f,w,h} - \hat{x}^{\mathrm{En(i)}}_{d,h}\right|}{\mathrm{N^D N^H}}, \quad \forall i \tag{B.37}$$

$$g^{\mathrm{SPR,Up(i)}} = \sum_{e\in S^{\mathrm{E}}}\sum_{r\in S^{\mathrm{R}}}\sum_{r\in S^{\mathrm{F}}}\sum_{w\in S^{\mathrm{W}}} \rho_e\rho_r\rho_f\rho_w \frac{\sum_{d\in D}\sum_{h\in H}\left|x^{\mathrm{SPR,Up(i)}}_{d,e,r,f,w,h} - \hat{x}^{\mathrm{SPR,Up(i)}}_{d,h}\right|}{\mathrm{N^D N^H}}, \quad \forall i \tag{B.38}$$

$$g^{\mathrm{SPR,Dw(i)}} = \sum_{e\in S^{\mathrm{E}}}\sum_{r\in S^{\mathrm{R}}}\sum_{r\in S^{\mathrm{F}}}\sum_{w\in S^{\mathrm{W}}} \rho_e\rho_r\rho_f\rho_w \frac{\sum_{d\in D}\sum_{h\in H}\left|x^{\mathrm{SPR,Dw(i)}}_{d,e,r,f,w,h} - \hat{x}^{\mathrm{SPR,Dw(i)}}_{d,h}\right|}{\mathrm{N^D N^H}}, \quad \forall i \tag{B.39}$$

$$g^{\mathrm{FR,Up(i)}} = \sum_{e\in S^{\mathrm{E}}}\sum_{r\in S^{\mathrm{R}}}\sum_{r\in S^{\mathrm{F}}}\sum_{w\in S^{\mathrm{W}}} \rho_e\rho_r\rho_f\rho_w \frac{\sum_{d\in D}\sum_{h\in H}\left|x^{\mathrm{FR,Up(i)}}_{d,e,r,f,w,h} - \hat{x}^{\mathrm{FR,Up(i)}}_{d,h}\right|}{\mathrm{N^D N^H}}, \quad \forall i \tag{B.40}$$

$$g^{\mathrm{FR,Dw(i)}} = \sum_{e\in S^{\mathrm{E}}}\sum_{r\in S^{\mathrm{R}}}\sum_{r\in S^{\mathrm{F}}}\sum_{w\in S^{\mathrm{W}}} \rho_e\rho_r\rho_f\rho_w \frac{\sum_{d\in D}\sum_{h\in H}\left|x^{\mathrm{FR,Dw(i)}}_{d,e,r,f,w,h} - \hat{x}^{\mathrm{FR,Dw(i)}}_{d,h}\right|}{\mathrm{N^D N^H}}, \quad \forall i \tag{B.41}$$

$$g^{\mathrm{K,P(i)}} = \sum_{e\in S^{\mathrm{E}}}\sum_{r\in S^{\mathrm{R}}}\sum_{r\in S^{\mathrm{F}}}\sum_{w\in S^{\mathrm{W}}} \rho_e\rho_r\rho_f\rho_w \left|K^{\mathrm{P(i)}}_{e,r,f,w} - \hat{K}^{\mathrm{P(i)}}\right|, \quad \forall i \tag{B.42}$$

$$g^{\mathrm{K,E(i)}} = \sum_{e\in S^{\mathrm{E}}}\sum_{r\in S^{\mathrm{R}}}\sum_{r\in S^{\mathrm{F}}}\sum_{w\in S^{\mathrm{W}}} \rho_e\rho_r\rho_f\rho_w \left|K^{\mathrm{E(i)}}_{e,r,f,w} - \hat{K}^{\mathrm{E(i)}}\right|, \quad \forall i \tag{B.43}$$

$$g^{\zeta,\mathrm{En(i)}} = \sum_{e\in S^{\mathrm{E}}}\sum_{r\in S^{\mathrm{R}}}\sum_{r\in S^{\mathrm{F}}}\sum_{w\in S^{\mathrm{W}}} \rho_e\rho_r\rho_f\rho_w \left|\zeta^{\mathrm{En(i)}}_{e,r,f,w} - \hat{\zeta}^{\mathrm{En(i)}}\right|, \quad \forall i \tag{B.44}$$

$$g^{\zeta,\mathrm{SPR,Up(i)}} = \sum_{e\in S^{\mathrm{E}}}\sum_{r\in S^{\mathrm{R}}}\sum_{r\in S^{\mathrm{F}}}\sum_{w\in S^{\mathrm{W}}} \rho_e\rho_r\rho_f\rho_w \left|\zeta^{\mathrm{SPR,Up(i)}}_{e,r,f,w} - \hat{\zeta}^{\mathrm{SPR,Up(i)}}\right|, \quad \forall i \tag{B.45}$$

$$g^{\zeta,\mathrm{SPR,Dw(i)}} = \sum_{e\in S^{\mathrm{E}}}\sum_{r\in S^{\mathrm{R}}}\sum_{r\in S^{\mathrm{F}}}\sum_{w\in S^{\mathrm{W}}} \rho_e\rho_r\rho_f\rho_w \left|\zeta^{\mathrm{SPR,Dw(i)}}_{e,r,f,w} - \hat{\zeta}^{\mathrm{SPR,Dw(i)}}\right|, \quad \forall i \tag{B.46}$$

$$g^{\zeta,\mathrm{FR,Up(i)}} = \sum_{e\in S^{\mathrm{E}}}\sum_{r\in S^{\mathrm{R}}}\sum_{r\in S^{\mathrm{F}}}\sum_{w\in S^{\mathrm{W}}} \rho_e\rho_r\rho_f\rho_w \left|\zeta^{\mathrm{FR,Up(i)}}_{e,r,f,w} - \hat{\zeta}^{\mathrm{FR,Up(i)}}\right|, \quad \forall i \tag{B.47}$$

$$g^{\zeta,\mathrm{FR,Dw(i)}} = \sum_{e\in S^{\mathrm{E}}}\sum_{r\in S^{\mathrm{R}}}\sum_{r\in S^{\mathrm{F}}}\sum_{w\in S^{\mathrm{W}}} \rho_e\rho_r\rho_f\rho_w \left|\zeta^{\mathrm{FR,Dw(i)}}_{e,r,f,w} - \hat{\zeta}^{\mathrm{FR,Dw(i)}}\right|, \quad \forall i \tag{B.48}$$

B.5 Piecewise Linear Approximation for the Square Proximal Term

B.5.1 Day-ahead bids

As stated in Subsection 5.4.2.4, the square proximal terms in objective function (5.82) are approximated using three segments. The piecewise linear approximation is exemplified for the day-ahead bids in the following equations using the additional variables for positive $\left(\Delta x^{(.)(\mathrm{i})^+}_{d,e,r,f,w,h}\right)$ and negative $\left(\Delta x^{(.)(\mathrm{i})^-}_{d,e,r,f,w,h}\right)$ deviations between the bids $\left(x^{(.)(\mathrm{i})}_{d,e,r,f,w,h}\right)$ and the previous iteration's probability-weighted average of the respective bid $\left(\hat{x}^{(.)(\mathrm{i\text{-}1})}_{d,h}\right)$. These auxiliary variables are defined as a SOS1 variable pair to ensure that only

one set of variables is positive.

$$x^{(.)(\mathrm{i})}_{d,e,r,f,w,h} - \hat{x}^{(.)(\mathrm{i}\text{-}1)}_{d,h} = \Delta x^{(.)(\mathrm{i})^{+}}_{d,e,r,f,w,h} - \Delta x^{(.)(\mathrm{i})^{-}}_{d,e,r,f,w,h}, \quad \forall i,d,e,r,f,w,h \tag{B.49}$$

Then, each auxiliary variable is divided in 3 segments in equations (B.50) and, which are bounded with constraints (B.51) to (B.53).

$$\Delta x^{(.)(\mathrm{i})^{+/-}}_{d,e,r,f,w,h} = \Delta x^{(.)(\mathrm{i})1^{+/-}}_{d,e,r,f,w,h} + \Delta x^{(.)(\mathrm{i})2^{+/-}}_{d,e,r,f,w,h} + \Delta x^{(.)(\mathrm{i})3^{+/-}}_{d,e,r,f,w,h}, \quad \forall i,d,e,r,f,w,h \tag{B.50}$$

$$0 \leq \Delta x^{(.)(\mathrm{i})1^{+/-}}_{d,e,r,f,w,h} \leq 1 \quad \forall i,d,e,r,f,w,h \tag{B.51}$$

$$1 \leq \Delta x^{(.)(\mathrm{i})2^{+/-}}_{d,e,r,f,w,h} \leq \frac{\mathrm{K}^{\mathrm{W}} + \overline{\mathrm{P}} + \overline{\mathrm{E}}}{2}, \quad \forall i,d,e,r,f,w,h \tag{B.52}$$

$$\frac{\mathrm{K}^{\mathrm{W}} + \overline{\mathrm{P}} + \overline{\mathrm{E}}}{2} \leq \Delta x^{(.)(\mathrm{i})3^{+/-}}_{d,e,r,f,w,h} \leq \mathrm{K}^{\mathrm{W}} + \overline{\mathrm{P}} + \overline{\mathrm{E}}, \quad \forall i,d,e,r,f,w,h \tag{B.53}$$

The slopes for each segment are calculated with equations (B.54) to (B.56) based on the bounds defined earlier.

$$y^{(.)(\mathrm{i})1}_{d,e,r,f,w,h} = 1, \quad \forall i,d,e,r,f,w,h \tag{B.54}$$

$$y^{(.)(\mathrm{i})2}_{d,e,r,f,w,h} = \frac{\left(\frac{\mathrm{K}^{\mathrm{W}} + \overline{\mathrm{P}} + \overline{\mathrm{E}}}{2}\right)^2 - 1^2}{\frac{\mathrm{K}^{\mathrm{W}} + \overline{\mathrm{P}} + \overline{\mathrm{E}}}{2} - 1}, \quad \forall i,d,e,r,f,w,h \tag{B.55}$$

$$y^{(.)(\mathrm{i})3}_{d,e,r,f,w,h} = \frac{\left(\mathrm{K}^{\mathrm{W}} + \overline{\mathrm{P}} + \overline{\mathrm{E}}\right)^2 - \left(\frac{\mathrm{K}^{\mathrm{W}} + \overline{\mathrm{P}} + \overline{\mathrm{E}}}{2}\right)^2}{\frac{\mathrm{K}^{\mathrm{W}} + \overline{\mathrm{P}} + \overline{\mathrm{E}}}{2}}, \quad \forall i,d,e,r,f,w,h \tag{B.56}$$

The generic square proximal term for the day-ahead (Energy/SPR-Up/SPR-Dw/FR-Up/FR-Dw) bids is approximated through equation (B.57).

$$\begin{aligned}\left(x^{(.)(\mathrm{i})}_{d,e,r,f,w,h} - \hat{x}^{(.)(\mathrm{i}\text{-}1)}_{d,h}\right)^2 = &\left(\Delta x^{(.)(\mathrm{i})1^{+}}_{d,e,r,f,w,h} + \Delta x^{(.)(\mathrm{i})1^{-}}_{d,e,r,f,w,h}\right) y^{(.)(\mathrm{i})1}_{d,e,r,f,w,h} + \\ &\left(\Delta x^{(.)(\mathrm{i})2^{+}}_{d,e,r,f,w,h} + \Delta x^{(.)(\mathrm{i})2^{-}}_{d,e,r,f,w,h}\right) y^{(.)(\mathrm{i})2}_{d,e,r,f,w,h} + \\ &\left(\Delta x^{(.)(\mathrm{i})3^{+}}_{d,e,r,f,w,h} + \Delta x^{(.)(\mathrm{i})3^{-}}_{d,e,r,f,w,h}\right) y^{(.)(\mathrm{i})3}_{d,e,r,f,w,h}, \quad \forall i,d,e,r,f,w,h\end{aligned} \tag{B.57}$$

B.5.2 Power and Energy Capacities of the ESS

The linear approximation for the power and energy capacities of the ESS is achieved in a similar fashion with equations and constraints (B.58) through (B.70).

$$K^{\mathrm{P/E(i)}}_{e,r,f,w} - \hat{K}^{\mathrm{P/E(i-1)}} = \Delta K^{\mathrm{P/E(i)}^{+}}_{e,r,f,w} - \Delta K^{\mathrm{P/E(i)}^{-}}_{e,r,f,w}, \quad \forall i,e,r,f,w \tag{B.58}$$

$$\Delta K^{\mathrm{P/E(i)}^{+/-}}_{e,r,f,w} = \Delta K^{\mathrm{P/E(i)1}^{+/-}}_{e,r,f,w} + \Delta K^{\mathrm{P/E(i)2}^{+/-}}_{e,r,f,w} + \Delta K^{\mathrm{P/E(i)3}^{+/-}}_{e,r,f,w}, \quad \forall i,e,r,f,w \tag{B.59}$$

$$0 \leq \Delta K_{e,r,f,w}^{\mathrm{P/E(i)1}^{+/-}} \leq 1 \quad \forall i,e,r,f,w \tag{B.60}$$

$$1 \leq \Delta K_{e,r,f,w}^{\mathrm{P(i)2}^{+/-}} \leq \frac{\overline{\mathrm{P}}}{2}, \quad \forall i,e,r,f,w \tag{B.61}$$

$$1 \leq \Delta K_{e,r,f,w}^{\mathrm{E(i)2}^{+/-}} \leq \frac{\overline{\mathrm{E}}}{2}, \quad \forall i,e,r,f,w \tag{B.62}$$

$$\frac{\overline{\mathrm{P}}}{2} \leq \Delta K_{e,r,f,w}^{\mathrm{P(i)3}^{+/-}} \leq \overline{\mathrm{P}}, \quad \forall i,e,r,f,w \tag{B.63}$$

$$\frac{\overline{\mathrm{E}}}{2} \leq \Delta K_{e,r,f,w}^{\mathrm{P(i)3}^{+/-}} \leq \overline{\mathrm{E}}, \quad \forall i,e,r,f,w \tag{B.64}$$

$$y_{e,r,f,w}^{\mathrm{K,P/E(i)1}} = 1, \quad \forall i,e,r,f,w \tag{B.65}$$

$$y_{e,r,f,w}^{\mathrm{K,P(i)2}} = \frac{\left(\frac{\overline{\mathrm{P}}}{2}\right)^2 - 1^2}{\frac{\overline{\mathrm{P}}}{2} - 1}, \quad \forall i,e,r,f,w \tag{B.66}$$

$$y_{e,r,f,w}^{\mathrm{K,E(i)2}} = \frac{\left(\frac{\overline{\mathrm{E}}}{2}\right)^2 - 1^2}{\frac{\overline{\mathrm{E}}}{2} - 1}, \quad \forall i,e,r,f,w \tag{B.67}$$

$$y_{e,r,f,w}^{\mathrm{K,P(i)3}} = \frac{\left(\overline{\mathrm{P}}\right)^2 - \left(\frac{\overline{\mathrm{P}}}{2}\right)^2}{\frac{\overline{\mathrm{P}}}{2}}, \quad \forall i,e,r,f,w \tag{B.68}$$

$$y_{e,r,f,w}^{\mathrm{K,E(i)3}} = \frac{\left(\overline{\mathrm{E}}\right)^2 - \left(\frac{\overline{\mathrm{E}}}{2}\right)^2}{\frac{\overline{\mathrm{E}}}{2}}, \quad \forall i,e,r,f,w \tag{B.69}$$

$$\begin{aligned}\left(K_{e,r,f,w}^{\mathrm{P/E(i)}} - \hat{K}^{\mathrm{P/E(i-1)}}\right)^2 = &\left(\Delta K_{e,r,f,w}^{\mathrm{P/E(i)1}^{+}} + \Delta K_{e,r,f,w}^{\mathrm{P/E(i)1}^{-}}\right) y_{e,r,f,w}^{\mathrm{K,P/E(i)1}} + \\ &\left(\Delta K_{e,r,f,w}^{\mathrm{P/E(i)2}^{+}} + \Delta K_{e,r,f,w}^{\mathrm{P/E(i)2}^{-}}\right) y_{e,r,f,w}^{\mathrm{K,P/E(i)2}} + \\ &\left(\Delta K_{e,r,f,w}^{\mathrm{P/E(i)3}^{+}} + \Delta K_{e,r,f,w}^{\mathrm{P/E(i)3}^{-}}\right) y_{e,r,f,w}^{\mathrm{K,P/E(i)3}}, \quad \forall i,e,r,f,w\end{aligned} \tag{B.70}$$

B.5.3 Profit VaR

Approximating the square proximal term for each type of profit (Energy/SPR-Up/SPR-Dw/FR-Up/FR-Dw) VaR is a more complicated task considering the unbounded nature of these variables. In other words, wrongly choosing a bound for each VaR might lead to convergence problems or unnecessarily expanding the size of the sub-problem and, consequently, increasing computational times. However, as iteration 0 of the PHA does not feature the square proximal terms in the objective function and provides a range of optimal values for each VaR with the scenario-dependent solutions $\zeta_{e,r,f,w}^{(.)(\mathrm{i})}$, it is possible to estimate a parameter-free value for the upper bound of the deviation $\zeta_{e,r,f,w}^{(.)(\mathrm{i})} - \hat{\zeta}^{(.)(\mathrm{i})}$ as the maximum value for this

deviation occurs at iteration 0, $\overline{\Delta\zeta}^{(.)}$, as calculated in (B.71).

$$\overline{\Delta\zeta}^{(.)} = \max_{e\in S^{\mathrm{E}} r\in S^{\mathrm{R}} f\in S^{\mathrm{F}} w\in S^{\mathrm{W}}} \left|\zeta^{(.)(0)}_{e,r,f,w} - \hat{\zeta}^{(.)(0)}\right| \tag{B.71}$$

As such, the square proximal terms for each type of profit VaR can be approximated with equations and constraints (B.72) through (B.80).

$$\zeta^{(.)(\mathrm{i})}_{e,r,f,w} - \hat{\zeta}^{(.)(\mathrm{i}\text{-}1)} = \Delta\zeta^{(.)(\mathrm{i})^{+}}_{e,r,f,w} - \Delta\zeta^{(.)(\mathrm{i})^{-}}_{e,r,f,w}, \quad \forall i,e,r,f,w \tag{B.72}$$

$$\Delta\zeta^{(.)(\mathrm{i})^{+/-}}_{e,r,f,w} = \Delta\zeta^{(.)(\mathrm{i})1^{+/-}}_{e,r,f,w} + \Delta\zeta^{(.)(\mathrm{i})2^{+/-}}_{e,r,f,w} + \Delta\zeta^{(.)(\mathrm{i})3^{+/-}}_{e,r,f,w}, \quad \forall i,e,r,f,w \tag{B.73}$$

$$0 \le \Delta\zeta^{(.)(\mathrm{i})1^{+/-}}_{e,r,f,w} \le \frac{\overline{\Delta\zeta}^{(.)}}{3} \quad \forall i,e,r,f,w \tag{B.74}$$

$$\frac{\overline{\Delta\zeta}^{(.)}}{3} \le \Delta\zeta^{(.)(\mathrm{i})2^{+/-}}_{e,r,f,w} \le 2\cdot\frac{\overline{\Delta\zeta}^{(.)}}{3}, \quad \forall i,e,r,f,w \tag{B.75}$$

$$2\cdot\frac{\overline{\Delta\zeta}^{(.)}}{3} \le \Delta\zeta^{(.)(\mathrm{i})3^{+/-}}_{e,r,f,w} \le \overline{\Delta\zeta}^{(.)}, \quad \forall i,e,r,f,w \tag{B.76}$$

$$y^{\zeta,(.)(\mathrm{i})1}_{e,r,f,w} = \frac{\overline{\Delta\zeta}^{(.)}}{3}, \quad \forall i,e,r,f,w \tag{B.77}$$

$$y^{\zeta,(.)(\mathrm{i})2}_{e,r,f,w} = \frac{\left(2\cdot\frac{\overline{\Delta\zeta}^{(.)}}{3}\right)^2 - \left(\frac{\overline{\Delta\zeta}^{(.)}}{3}\right)^2}{\frac{\overline{\Delta\zeta}^{(.)}}{3}}, \quad \forall i,e,r,f,w \tag{B.78}$$

$$y^{\zeta,(.)(\mathrm{i})3}_{e,r,f,w} = \frac{\left(\overline{\Delta\zeta}^{(.)}\right)^2 - \left(2\cdot\frac{\overline{\Delta\zeta}^{(.)}}{3}\right)^2}{\frac{\overline{\Delta\zeta}^{(.)}}{3}}, \quad \forall i,e,r,f,w \tag{B.79}$$

$$\begin{aligned}\left(\zeta^{(.)(\mathrm{i})}_{e,r,f,w} - \hat{\zeta}^{(.)(\mathrm{i}\text{-}1)}\right)^2 = &\left(\Delta\zeta^{(.)(\mathrm{i})1^{+}}_{e,r,f,w} + \Delta\zeta^{(.)(\mathrm{i})1^{-}}_{e,r,f,w}\right) y^{\zeta,(.)(\mathrm{i})1}_{e,r,f,w} + \\ &\left(\Delta\zeta^{(.)(\mathrm{i})2^{+}}_{e,r,f,w} + \Delta\zeta^{(.)(\mathrm{i})2^{-}}_{e,r,f,w}\right) y^{\zeta,(.)(\mathrm{i})2}_{e,r,f,w} + \\ &\left(\Delta\zeta^{(.)(\mathrm{i})3^{+}}_{e,r,f,w} + \Delta\zeta^{(.)(\mathrm{i})3^{-}}_{e,r,f,w}\right) y^{\zeta,(.)(\mathrm{i})3}_{e,r,f,w}, \quad \forall i,e,r,f,w\end{aligned} \tag{B.80}$$

Appendix C

Pricing and Wind Power Availability Scenarios for Case Studies in Chapter 5

The energy, SPR and FR price and wind power availability forecasts used in Section 5.5 to test the proposed risk-averse ESS investment problem solved with Stochastic and PHA models are presented in this Appendix.

C.1 Energy Price Forecasts

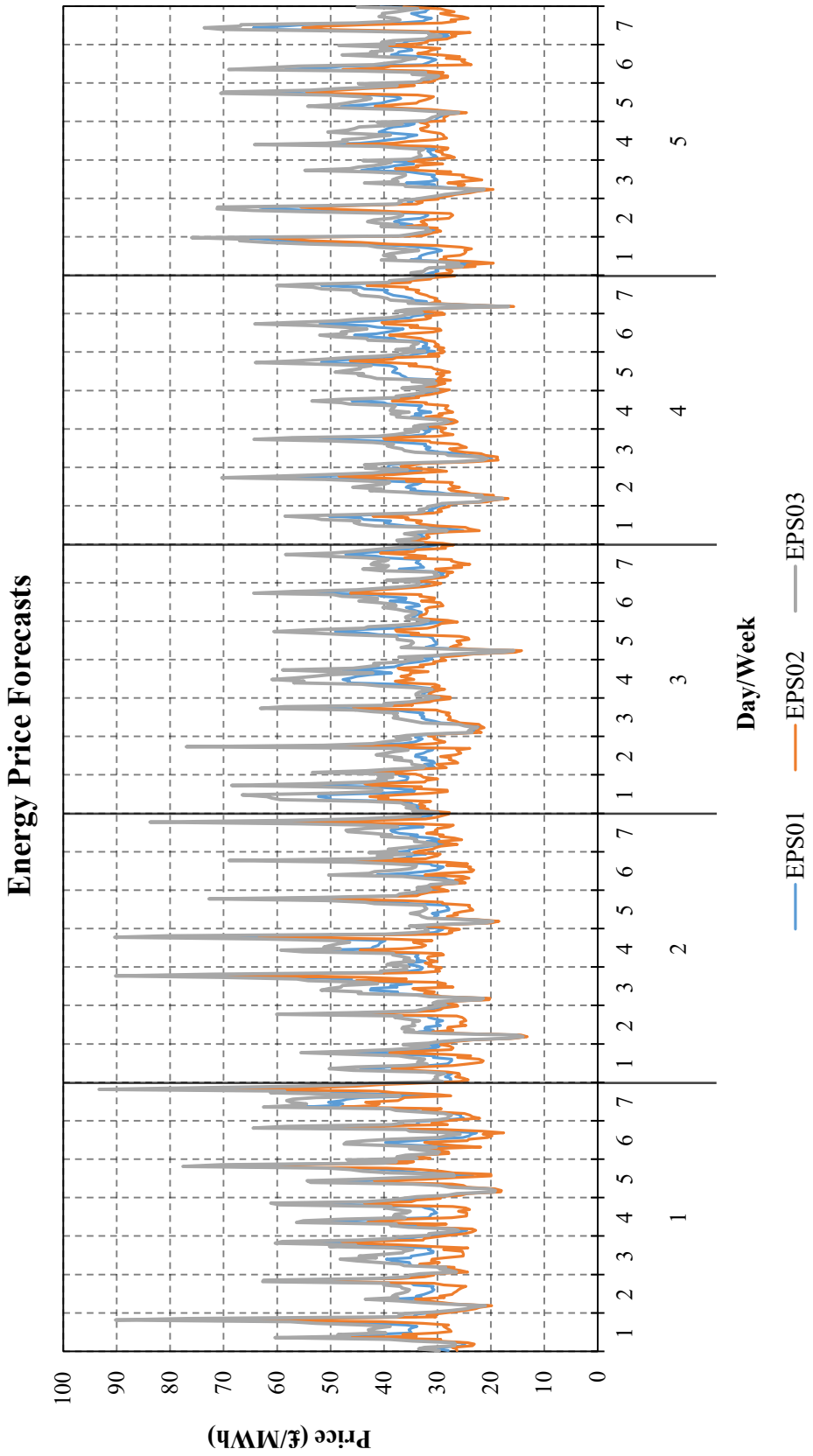


Fig. C.1: Energy price forecasts for the 5 representative weeks (24 hour resolution).

C.2 SPR Price Forecasts

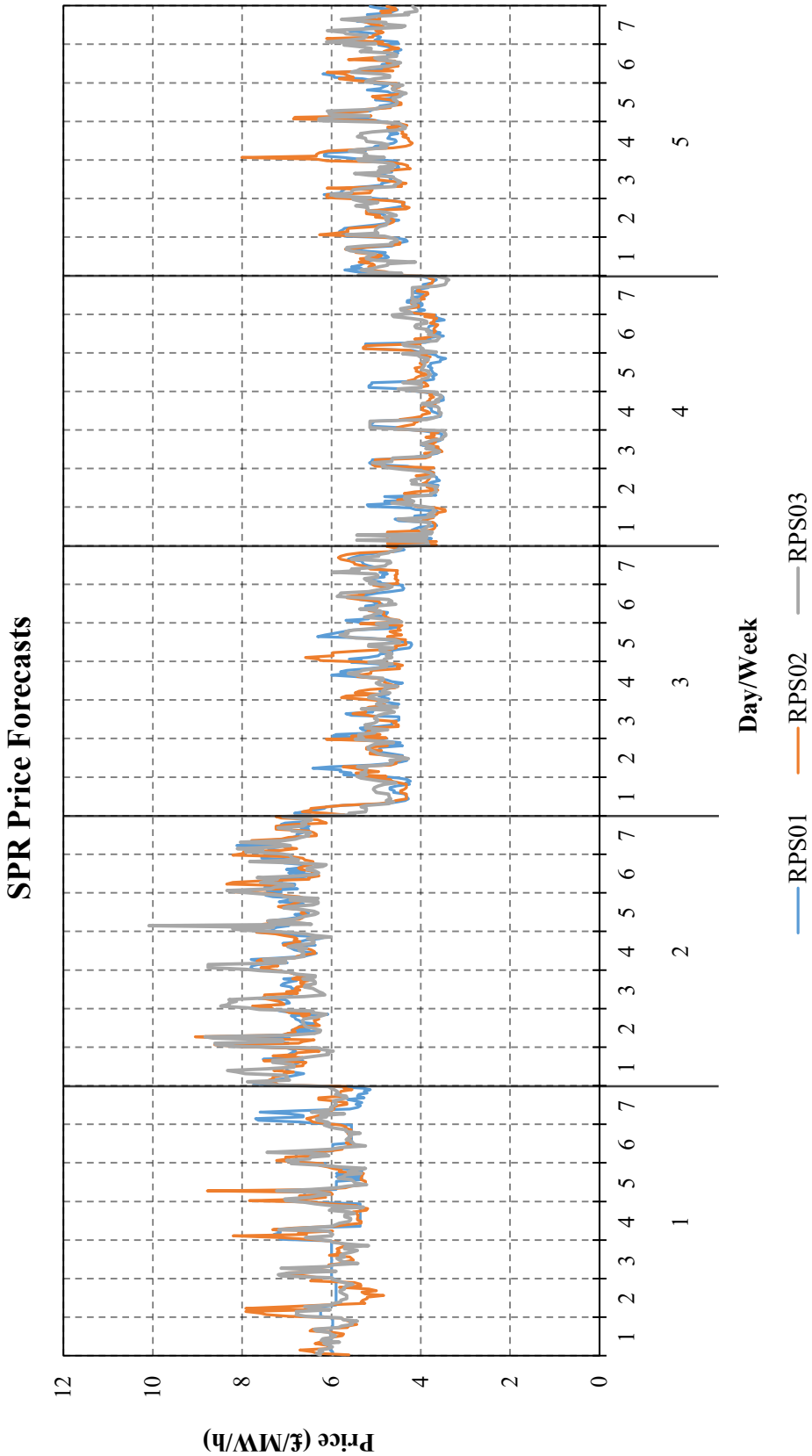


Fig. C.2: SPR price forecasts for the 5 representative weeks (24 hour resolution).

C.3 FR Price Forecasts

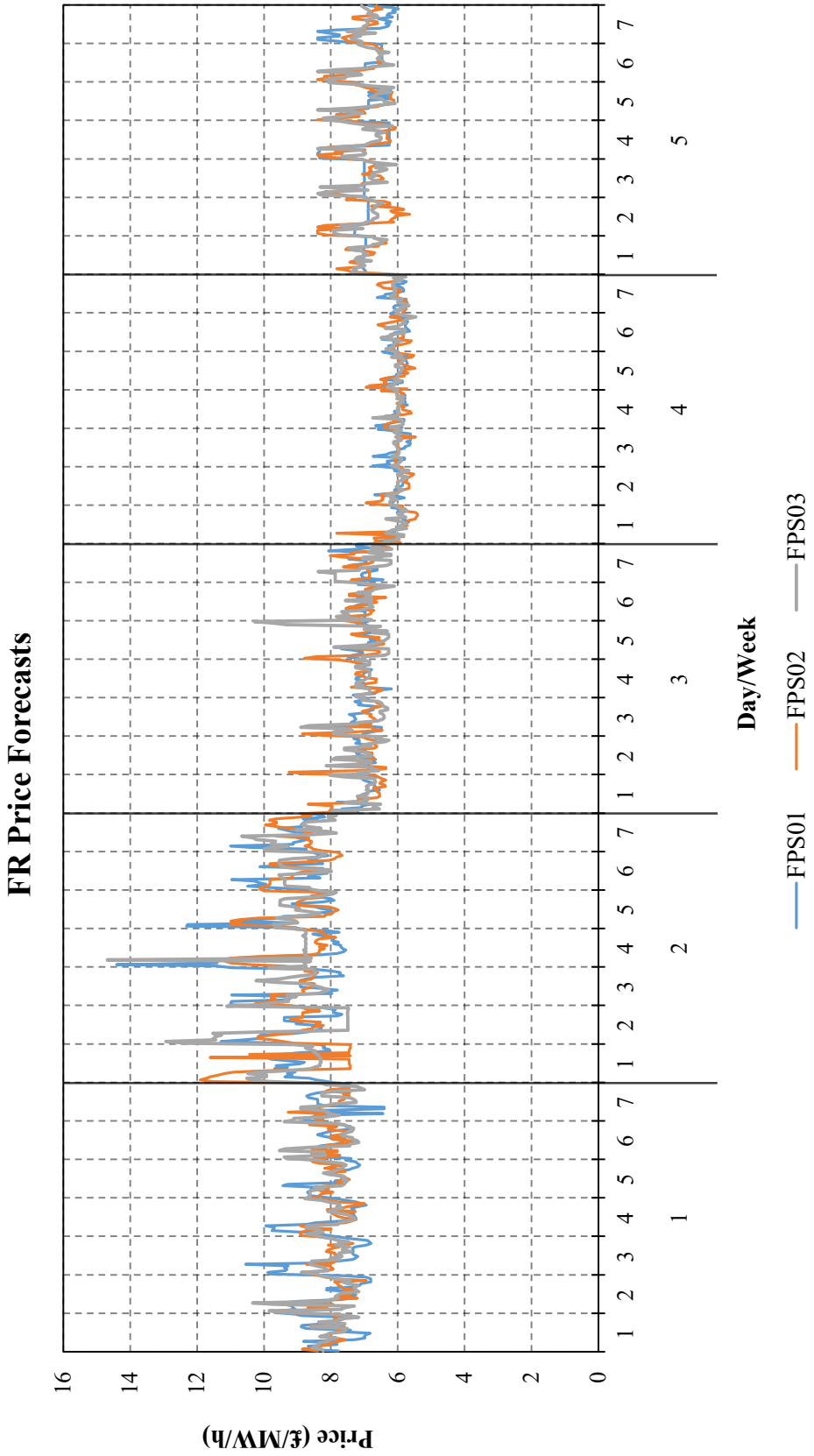


Fig. C.3: FR price forecasts for the 5 representative weeks (24 hour resolution).

C.4 Wind Power Availability Forecasts

C.4.1 5 Forecasts

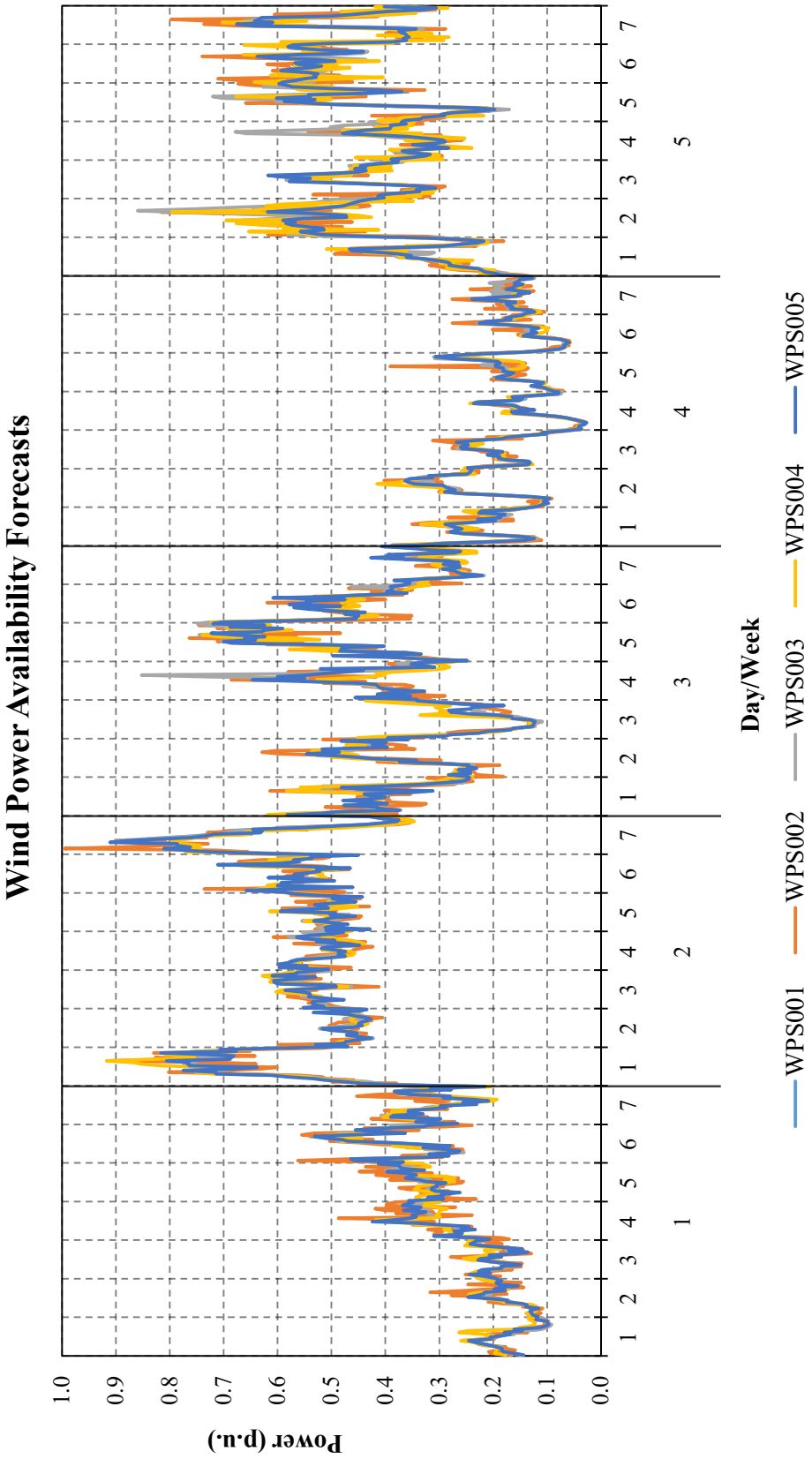


Fig. C.4: 5 Wind power availability forecasts for the 5 representative weeks (24 hour resolution).

C.4.2 10 Forecasts

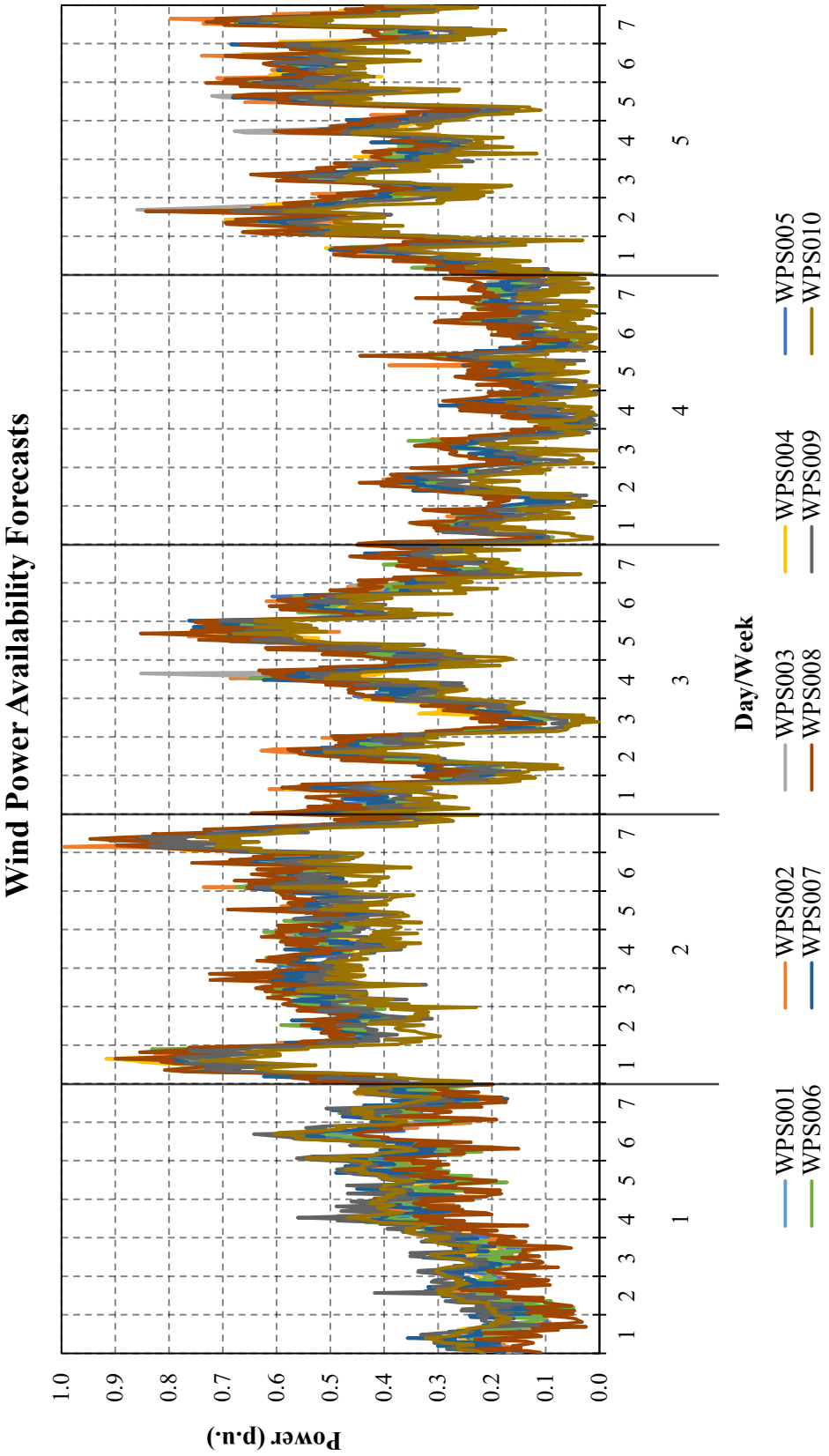


Fig. C.5: 10 Wind power availability forecasts for the 5 representative weeks (24 hour resolution).